# Amphibious Vehicle Propulsion System Design Report

For a Propulsion System
Demonstrator (PSD) Vehicle

July 8 , 1988



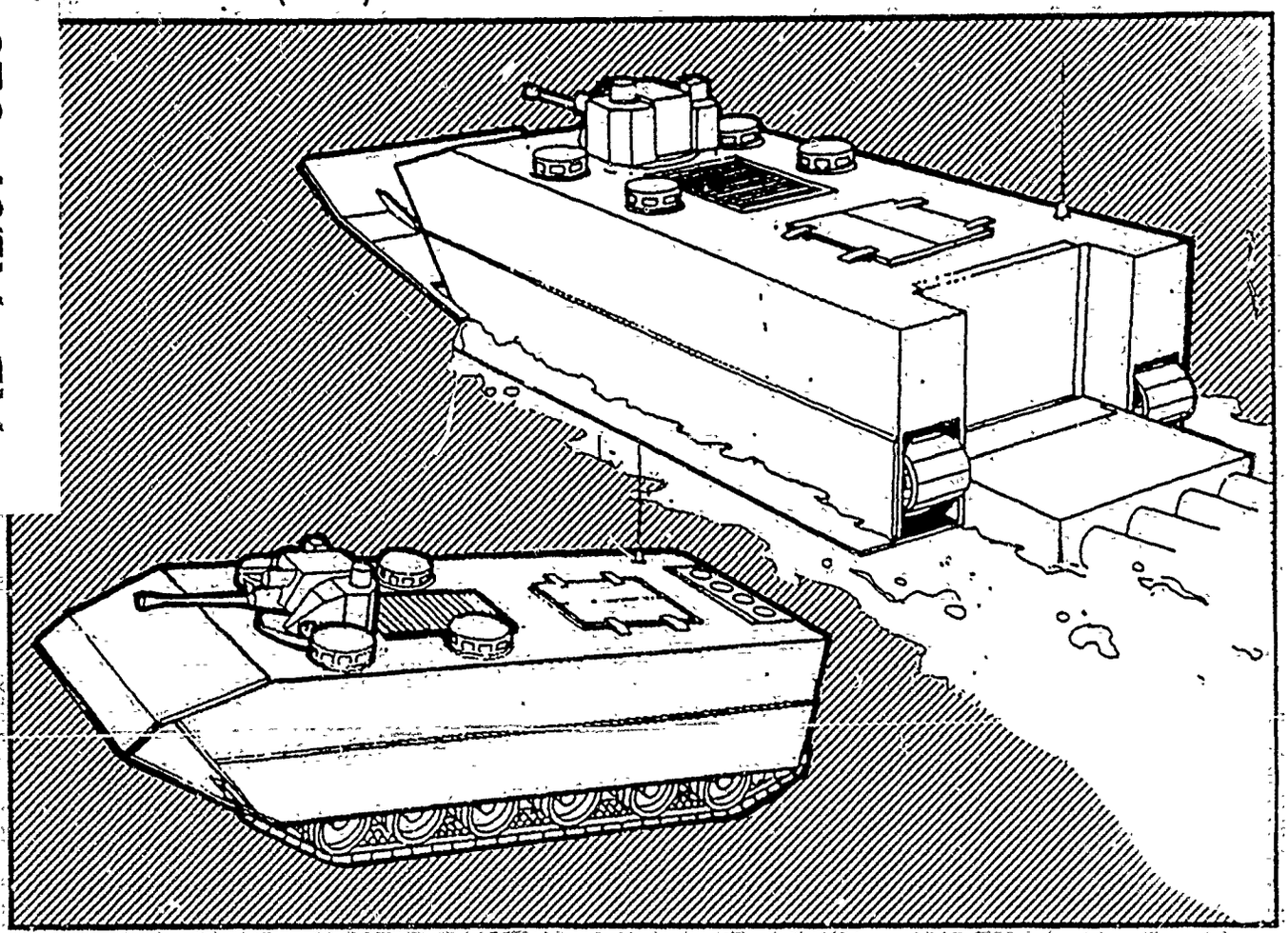

Prepared Under
Contract No. N00167-86-C-0158
for
David Taylor Research Center
Bethesda, Maryland

Westinghouse

Westinghouse Inc.
Oceanic Division - Cleveland Operation
18901 Euclid Avenue
Cleveland, Ohio 44117

05/204/88/081-c

# DISCLAIMER NOTICE

THIS DOCUMENT IS BEST QUALITY PRACTICABLE. THE COPY FURNISHED TO DTIC CONTAINED A SIGNIFICANT NUMBER OF PAGES WHICH DO NOT REPRODUCE LEGIBLY.

SECURITY CLASSIFICATION OF THIS PAGE

# REPORT DOCUMENTATION PAGE

| | |
|---|---|
| 1a REPORT SECURITY CLASSIFICATION<br>UNCLASSIFIED | 1b. RESTRICTIVE MARKINGS |
| 2a. SECURITY CLASSIFICATION AUTHORITY | 3 DISTRIBUTION / AVAILABILITY OF REPORT<br>APPROVED FOR PUBLIC RELEASE:<br>DISTRIBUTION IS UNLIMITED |
| 2b. DECLASSIFICATION / DOWNGRADING SCHEDULE | |
| 4 PERFORMING ORGANIZATION REPORT NUMBER(S) | 5. MONITORING ORGANIZATION REPORT NUMBER(S)<br>DTRC - SSID - CR - 3 - 89 |
| 6a. NAME OF PERFORMING ORGANIZATION<br>WESTINGHOUSE INC.<br>6b OFFICE SYMBOL (If applicable) | 7a NAME OF MONITORING ORGANIZATION<br>DAVID TAYLOR RESEARCH CENTER |
| 6c ADDRESS (City, State, and ZIP Code)<br>Ocean Division - Cleveland Operation<br>18901 Euclid Avenue<br>Cleveland, Ohio 44117 | 7b. ADDRESS (City, State, and ZIP Code)<br>Code 1240<br>Bethesda, MD 20084-5000 |
| 8a. NAME OF FUNDING / SPONSORING ORGANIZATION<br>DAVID TAYLOR RESEARCH CENTER<br>8b. OFFICE SYMBOL (If applicable)<br>1240 | 9. PROCUREMENT INSTRUMENT IDENTIFICATION NUMBER<br>N00167 - 86 - C - 0158 |
| 8c ADDRESS (City, State, and ZIP Code) | 10 SOURCE OF FUNDING NUMBERS<br>PROGRAM ELEMENT NO. ~~266-23M~~ / PROJECT NO C0021 / TASK NO. / WORK UNIT ACCESSION NO. DN479001 |

11 TITLE (Include Security Classification)
AMPHIBIOUS VEHICLE PROPULSION SYSTEM DESIGN REPORT FOR A PROPULSION SYSTEM DEMONSTRATOR (PSD) VEHICLE

12 PERSONAL AUTHOR(S)

| 13a. TYPE OF REPORT | 13b TIME COVERED | 14. DATE OF REPORT (Year, Month, Day) | 15 PAGE COUNT |
|---|---|---|---|
| FINAL DESIGN | FROM 10/86 TO 7/88 | 1988 July 8 | 270 |

16 SUPPLEMENTARY NOTATION

| 17 COSATI CODES | | | 18. SUBJECT TERMS (Continue on reverse if necessary and identify by block number) |
|---|---|---|---|
| FIELD | GROUP | SUB-GROUP | Electric Drive<br>Military Vehicle |
| | | | |
| | | | |

19 ABSTRACT (Continue on reverse if necessary and identify by block number)

The David Taylor Research Center has funded the development of an electric drive train for a waterjet propulsion system to demonstrate high water speed in a Marine Corps propulsion system demonstrator vehicle. In the water, this vehicle will be propelled by four waterjets, each rated at 400hp, to provide the required thrust. The task was to design and develop a system that would be compact, lightweight, efficient and available to support vehicle demonstration testing.

A system trade-off study resulted in selection of an approach which uses four identical electric water propulsion modules, consisting of: an AC alternator and alternator controller, an AC induction motor with integral speed decreasing gearbox and a coupling that connects the motor/gearbox to the waterjet. This Report documents the hardware Design Effort and provided hardware characteristics.

| | |
|---|---|
| 20 DISTRIBUTION / AVAILABILITY OF ABSTRACT<br>☒ UNCLASSIFIED/UNLIMITED ☐ SAME AS RPT ☐ DTIC USERS | 21. ABSTRACT SECURITY CLASSIFICATION<br>UNCLASSIFIED |
| 22a NAME OF RESPONSIBLE INDIVIDUAL<br>Michael Gallagher | 22b. TELEPHONE (Include Area Code) (301) 227-1852 / 22c. OFFICE SYMBOL 1240 |

DD FORM 1473, 84 MAR 83 APR edition may be used until exhausted

SECURITY CLASSIFICATION OF THIS PAGE

CDRL A001

# Amphibious Vehicle Propulsion System Design Report

July 8 1988

Prepared under
Contract No. N00167-86-C-0158
for David Taylor Research Center
Bethesda, Maryland

Westinghouse Inc.
Oceanic Division- Cleveland Operation
18901 Euclid Avenue
Cleveland Ohio 44117

16

*John Witkowski,* Technical Director

*James Triner,* Program Director

05/204/88/082-g

ABSTRACT

The Marine Corps Program Office at the David Taylor Research Center has funded the development of an electric drive train for a waterjet propulsion system to demonstrate high water speed in a Marine Corps propulsion system demonstrator (PSD) vehicle. In the water, this vehicle will be propelled by four waterjets, each rated at 400 hp, to provide the required thrust. The task was to design and develop a system that would be compact, lightweight, efficient and available to support vehicle demonstration testing in June of 1989.

Due to schedule and cost constraints a decision was made to design the propulsion motor around an existing alternator. A system trade-off study was embarked upon in October of 1986, to identify a system configuration. The study resulted in selection of an approach which uses four identical electric water propulsion modules, consisting of: an AC alternator and alternator controller, an AC induction motor with integral speed decreasing gearbox and a coupling that connects the motor/gearbox to the waterjet.

The alternator selected is a Westinghouse air cooled machine with the following output characteristics at nominal operating conditions:

322 kW nominal continuous power rating
520 volts line-to-line rms, 3-phase
450 Hz

Westinghouse has designed an AC induction motor to be compatible with the alternator and waterjet requirements. The motor has the following characteristics:

Water cooled exterior
Oil cooled/lubricated interior
7:1 single stage, speed decreasing gearbox (SDG)
Size: 16 inches O.D. X 24 inches long
Weight: 329 lb.
Efficiency (motor/SDG): 92%

# DESIGN REPORT
# FOR
# ELECTRIC WATER PROPULSION SYSTEM
# FOR A HIGH SPEED TRACKED AMPHIBIOUS VEHICLE

## TABLE OF CONTENTS

TABLE OF CONTENTS (cont'd)

# LIST OF FIGURES

## LIST OF FIGURES (cont'd)

## LIST OF FIGURES (cont'd)

## LIST OF FIGURES (cont'd)

# LIST OF TABLES

## APPENDICES

# 1. Introduction

This report discusses the design of an Electric Water Propulsion System (EWPS) used to drive the primary waterjets of the Propulsion System Demonstrator (PSD) vehicle. The EWPS was designed to meet stringent size, weight and efficiency requirements that would demonstrate improved performance over an existing hydraulically operated propulsion system.

The EWPS is comprised of four parallel drives known as Electric Water Propulsion Modules (EWPM). Each EWPM has a continuous rated shaft horsepower of 400, for a total shaft horsepower rating of 1600 for the system. A dual primary power source is used to drive four alternators. A rotary engine/ gearbox is used to drive one alternator and a turbine will be used to drive the other three alternators from a splitter gearbox.

The EWPM consists of three main components; the first is an AC alternator which converts the mechanical energy available from the primary power sources to electrical energy; the second component is a Motor/Speed Decreasing Gearbox (M/SDG) which converts the electrical energy back to mechanical energy to drive a waterjet; and the last major component is the Propulsion System Controller (PSC) which regulates the power flow between the alternator and the M/SDG in response to the speed of the prime movers. A flexible coupling connects the M/SDG output shaft to the waterjet driveshaft.

A pictorial of the PSD vehicle electric high water speed powertrain is shown in Figure 1. Note that the waterjets which propel the vehicle have been shown simply as propellers in the figure.

## 1.1 Technical Requirements

The technical requirements for the EWPS were specified by DTRC. These requirements were derived from the goal of accelerating a 55,570 pound (28T) amphibious vehicle to a final speed greater than 20 knots. The key requirements are listed in Table 1.

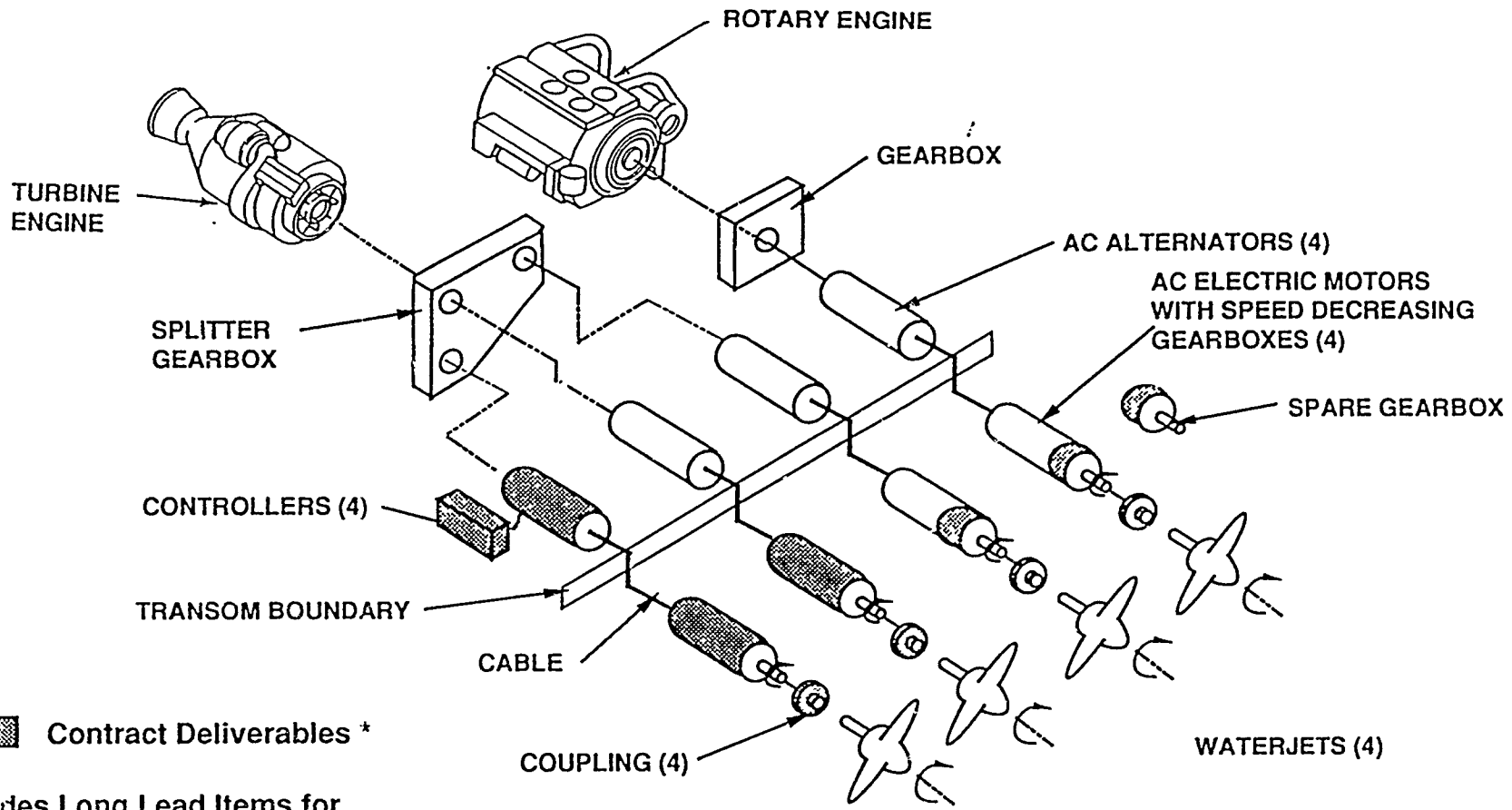


Figure 1. Electric Water Propulsion System

| Table 1. EWPS Technical Requirements | |
|---|---|
| Weight | 3200 lb. |
| Shaft Power (continuous) | 1600 hp |
| Shaft Power (60s rating) | 2080 hp |
| Shaft Speed Range, Operational | 615-1,250 RPM |
| Power Source 1<br>Gearbox operational output speed range | Rotary Engine/Gearbox<br>4,306-9,000 rpm (±100 RPM) |
| Power Source 2<br>Gearbox operational output speed range | Turbine/Splitter Gearbox<br>4,306-9,000 rpm (±100 RPM) |

As discussed Westinghouse's design features four identical parallel EWPM's. Each EWPM is one-fourth of the ratings in Table 1. The ratings for an individual EWPM are shown in Table 2.

| Table 2. Individual EWPM Technical Requirements | |
|---|---|
| Weight | 800 lb. |
| Shaft Power (continuous) | 400 hp |
| Shaft Power (60 second rating) | 520 hp |
| Shaft Speed Range, Operational | 615-1,250 RPM |

A detailed description of all system requirements is contained in Appendix I, Interface Specification.

## 1.2 System Study

After Westinghouse was contracted to design and fabricate the induction motors, DTRC requested Westinghouse assistance in determining an appropriate EWPS configuration for the PSD vehicle. A study was performed to identify an EWPS configuration that would preferably use an existing alternator design. Three system concepts, outlined in Figure 2, were examined. In addition to technical trade-offs, program issues including hardware availability, schedule, and cost were considered for each concept.

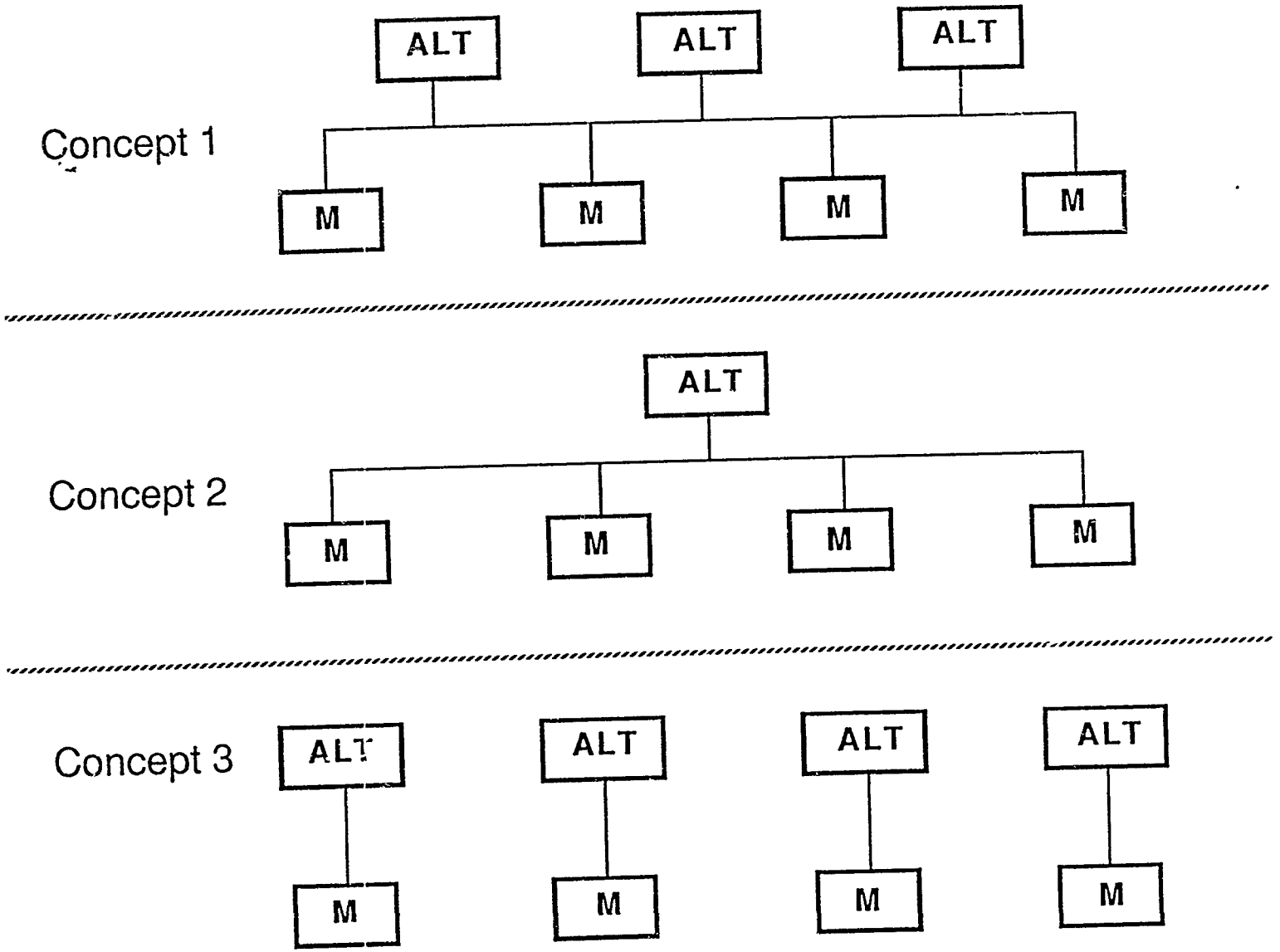


Figure 2. Electric Water Propulsion System Configurations.

Design Concept 1 uses multiple alternators, and motors on a common bus. This was an extension of the electric propulsion design concept for the High Water Speed Technology Demonstrator (HWSTD) vehicle. The advantage of using this approach is having multiple electrical power sources. Should one alternator go offline for any reason, the vehicle could still operate at reduced power.

However, there are several disadvantages to this concept: 1) There is a severe switchgear penalty (size and weight) imposed on the system; 2) The motors are operating from a common bus, therefore, each alternator must have the same phase sequence and exact voltage (magnitude and phase) for parallel operation and load sharing. Any difference of voltage between the alternators will cause large circulating currents to flow and overheat the alternators; 3) The alternators must be mechanically indexed so that the poles are oriented exactly; and 4) Each alternator must have a power rating of approximately 430kW for which an existing design of that rating could not be identified.

Design Concept 2 uses a single Government Furnished Equipment (GFE) alternator rated at 1.193 MW (1600 hp). The alternator would supply power directly, or through switchgear, to four parallel M/SDG units, each rated at 298.3 kW (400 hp). The alternator powering the M/SDG units directly, as shown in Figure 2, has the advantage of simplicity; however, in the event of a M/SDG failure, the entire system could fail. A variation to this approach is shown in Figure 3. This system is similar to the one shown in Figure 2, with the exception that switchgear has been added between the alternator and each M/SDG. The weight and volume of the switchgear and high current requirements for the alternator and cabling are major disadvantages with this design approach.

Since the weight and volume of the switchgear is a function of the system voltage, two classes of switchgear were investigated for the above applications. The impact of including motor starters was also examined. The typical weights and volumes are shown in Table 3.

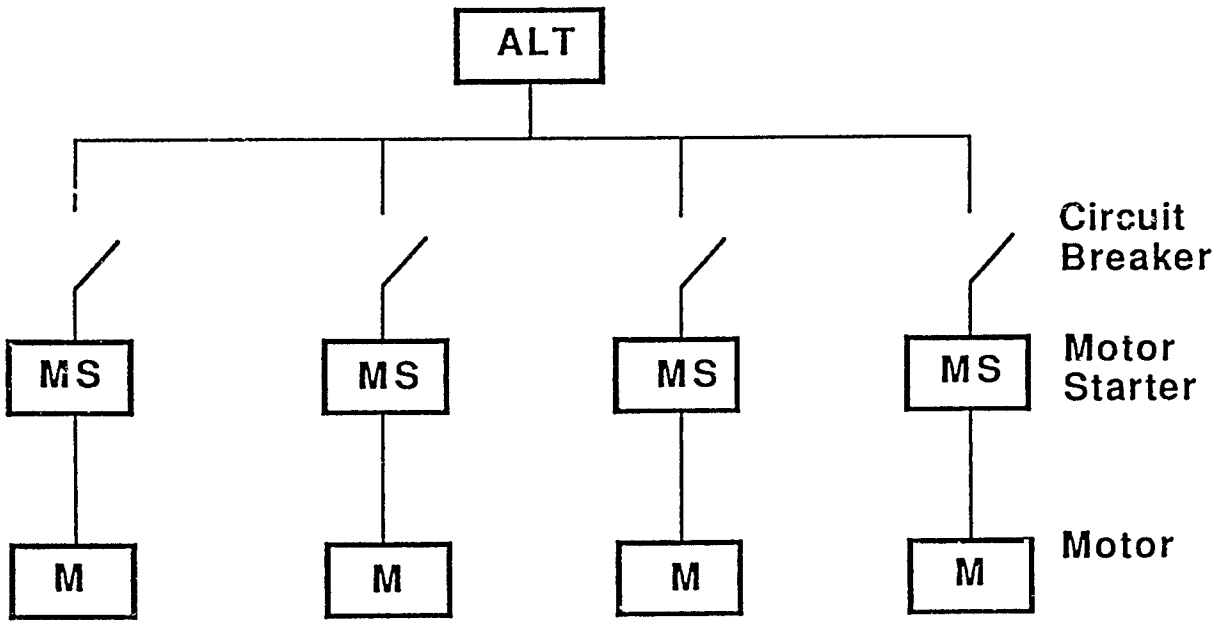


Figure 3. Typical Electric Water Propulsion System with Switchgear

Table 3. Physical Characteristics, Off-The-Shelf Switchgear

| Item | Low Voltage 600 V | High Voltage 5 kV |
|---|---|---|
| Circuit Breakers | | |
| Weight | 75 lb. | 2850 lb. |
| Volume | 0.42 $ft^3$ | 188 $ft^3$ |
| Motor Starters | | |
| Weight | 3160 lb. | 4800 lb. |
| Volume | 120 $ft^3$ | 135 $ft^3$ |

The significant weights and volumes of off-the-shelf switchgear were determined to be unacceptable. The development of custom switchgear was beyond the schedule constraints of this contract.

Design Concept 3 depicts four identical, independent, drives. Each drive has an alternator which powers an AC induction motor. The vehicle prime movers provide variable speed input power to the four alternators. Each alternator has a voltage controller which maintains the appropriate field excitation to the alternator to produce a required volts/hertz output to the motor. The voltage and frequency of the alternator varies proportionally with the prime mover speed which results in varying the speed of the motor accordingly. The controllers provide the ability to start and stop each motor independently, thereby eliminating the need for switchgear. The disadvantages of this approach are: 1) four power takeoffs must be provided to drive the alternators; 2) the available alternator is air cooled and requires intake/discharge ducting which adds vehicle complexity; and 3) the available alternator exceeds noise goals.

The system study concluded that design Concepts 1 and 2, and their described variations, were rejected for the following disadvantages:

1. Switchgear weight and volume penalties
2. Alternator unavailability; an alternator having desired ratings and an acceptable delivery schedule could not be identified
3. Lower mission reliability than could be achieved with four independent drives

The study concluded that Concept 3 should be pursued as a result of the following advantages:

1. Lowest overall system weight and volume
2. Alternator availability; an existing design of a Westinghouse 322 kW, air cooled alternator would provide the required output power and could be procured in time to support program schedules
3. Mission reliability is improved; the vehicle can operate at reduced power if a drive component failure does occur.

## 2. EWPS Description

The design approach resulted from the system study described above. The goal of maximizing overall system efficiency while staying within the propulsion system weight budget influenced the design of the hardware. The design intent was to minimize both technical and developmental risks. The three major EWPS components are 1) Alternator; 2) Motor/SDG; and 3) Propulsion System Controller. A brief description follows. A more detailed discussion of each of the above components is described later in this report.

The power source is a three phase, brushless alternator. The specification weight requirements dictated a high power density design. This led to the selection of a military type (400 Hz) alternator. The alternator was modified to maximize the induction motor starting and steady state performance. The alternator full load speed was increased to 9000 rpm and the exciter field pole and armature material was changed to a Cobalt-Iron alloy to enhance starting performance. The performance compatibility of the air cooled alternator and the availability guided the selection process.

Each EWPM consists of an AC induction motor, a speed decreasing gear box, and a shaft coupling to connect to the waterjet. In order to fit within the envelope of the transom, an integrated motor/SDG assembly was designed. A single stage speed decreaser was selected minimizing the axial length of the SDG. The coupling connecting the motor/SDG to the waterjet is designed to take angular and parallel misalignment. The waterjet thrust is not absorbed by the EWPM.

The propulsion system controller (PSC) provides start/run/off control for the vehicle and provides the required power conditioning and excitation to the alternator during starting and full power operation. The PSC provides the interface to the vehicle controller via an RS-232 serial link. The microprocessor monitors the motor and alternator warning and fault conditions. The PSC has software programmable setpoints for motor start limits, motor run limits, and motor voltage limits.

The weight of each of the major components was a key consideration in the design process. The selected alternator satisfies the weight goal. The integrated motor/SDG assembly is oil cooled to minimize both its size and weight. The motor also uses high magnetic permeability steel for its stator and rotor cores to minimize its weight.

## 2.1 Operational Requirements

The operational requirements of the vehicle establish the operational requirements of the EWPS. The detailed Interface Specification is included in Appendix I. The shaft horsepower ($HP_{shaft}$) requirements are illustrated in Figure 4 as a function of shaft speed. The actual shaft speed based on the design of record speed decreasing gear is discussed in Section 2.3.1. The shaft horsepower varies as a cube function of shaft speed and is approximated by the following equation, where $k = 2.048 \times 10^{-7}$:

$$HP_{shaft} = k \times RPM^3$$

The overload capability of the propulsion system is defined as 1.3 times $HP_{shaft}$, at 1,250 RPM for 60 seconds maximum. The propulsion system overload condition is to be demonstrated once during acceptance testing. Currently, there are no operating requirements for the overload condition after the initial demonstration.

Efficient delivery of the required shaft horsepower is an important goal of the EWPS. The system efficiency goal is 80%. The efficiency goal allocated to each of the components is shown in Table 4.

Table 4 Propulsion System Efficiency

| Component | Efficiency Goal, % |
|---|---|
| Alternator | 88 |
| Alternator-M/SDG Cable | 99 |
| M/SDG<br>Motor 96<br>Speed Reducing Gear 96 | 92 |
| System Efficiency | 80 |

Note: Efficiencies are only expressed at the full load operating point of 400 $HP_{shaft}$ at 1,250 rpm.

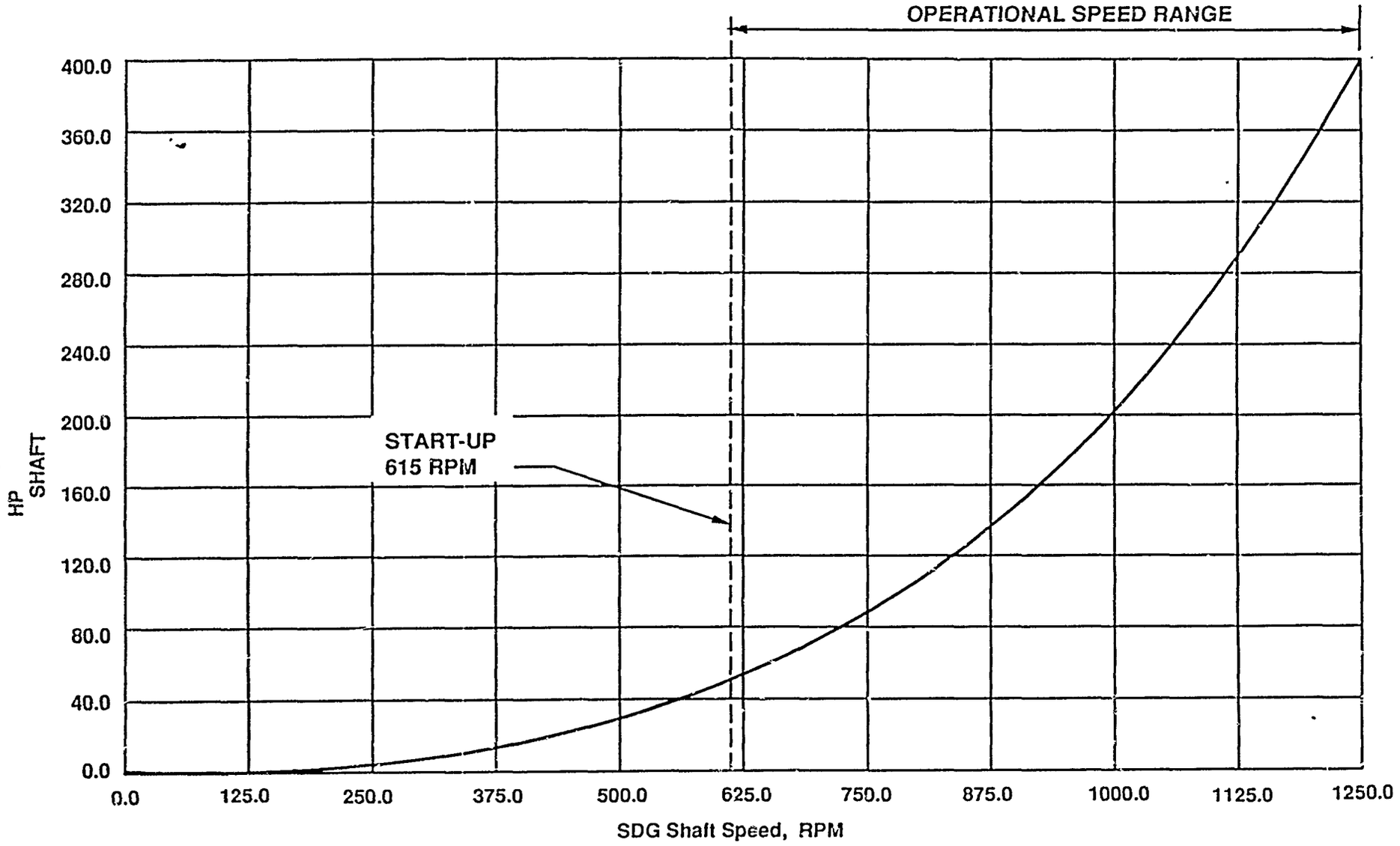


Figure 4. Motor/SDG Power/Speed Requirements

## 2.2 Alternator

Program constraints dictated the selection of an existing alternator. An industry wide survey of military style alternators was conducted and is summarized in Appendix II. This study resulted in the selection of the Westinghouse alternator, shown in Figure 5. This machine was designed to deliver 250 kW at 8,000 RPM. The original application of this machine required a conservative design. Consequently, the alternator is capable of producing the required rating of 322 kW by increasing the RPM to 9,000. A summary of the machine rating is contained in Table 5.

Table 5. Alternator Summary

| Design Type | Separately-Excited Rotating Rectifier |
|---|---|
| Continuous Rating | 322 kW (432 hp) |
| Transient Rating (1 minute) | 418 kW (561 hp) |
| Phases | 3 |
| Voltage | 520 Vac Line to Line |
| Frequency | 450 Hz |
| Number of Poles | 6 |
| Efficiency | 0.88 Minimum |
| Min. Starting Current @215.3 Hz (4306 rpm) | 900 amps for 3 sec. |
| Weight | 373 lb |
| Cooling Method | Air cooled (Integral Fan) |
| Cooling Flow | 1,100 CFM at 9,000 RPM |
| Shaft Speed @ 322 KW | 9,000 RPM |
| Shock/Vibration | 10 G (all axes) |
| Dimensions | See Interface Control Dwg., Alternator (E77497) |

The alternator subsystem consists of a main alternator, an exciter, permanent magnetic generator (PMG) and a power system controller (PSC).

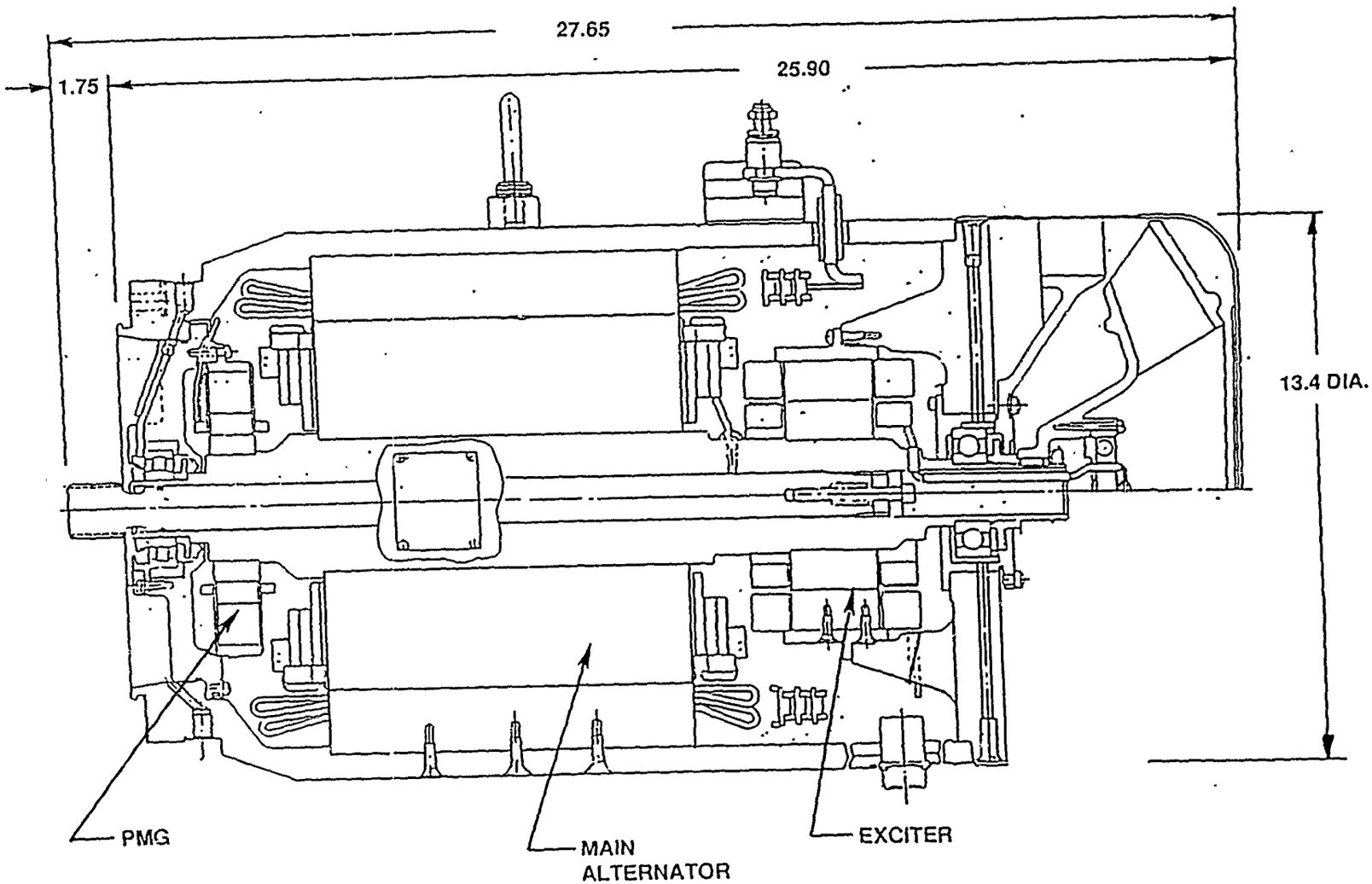




05/204/88/022

Figure 5. Alternator, Westinghouse Model 977J031-6

The alternator has demonstrated an overspeed condition of 10,500 RPM. Based upon the design margin continuous operation at 9000 rpm is reasonable. The conservative thermal design of the machine permits operation at continuous power levels exceeding the original design specification.

One minor design modification was performed on the alternator. The M-15 magnetic steel originally used to construct the exciter, was upgraded to Permendur V to enhance exciter performance. This change will enable the main machine to deliver starting currents in excess of 900 $A_{rms}$. The Westinghouse part number for this modified alternator is Model 977J031-6. A detailed description of the alternator is contained in Appendix III.

The turbine and rotary engines, through the appropriate gearboxes, will drive each of four identical alternators. The induction motor has been designed to operate with the three phase alternator voltage and frequency values shown in Table 5.

The turbine and rotary engine will be brought up to an idle speed of approximately 4300 RPM with no exciter field excitation applied. (The alternators are producing no electrical power.)

The PMG provides a voltage reference to the exciter field regulator. The PSC initiates the field excitation (during vehicle starting) providing an induction motor starting current in excess of 900 amperes. Later, the PSC provides the necessary field excitation to maintain constant volts/hertz to the induction motor as the alternator loading reaches steady state conditions. The design of the exciter field regulator and PSC is described in Section 2.5 of this report. The Power Sensing Box, which will mount on top of the alternator power terminal block, is described in Section 2.5.12 of this report.

In order to cool the alternator 1100 cfm of air is required at 9000 RPM. It is brought in at the anti-drive end through an expanded metal screen by a unidirectional fan. The air flows axially through the alternator and is exhausted at the drive end.

The schematic diagram of the alternator is shown in Figure 6. The electrical power flow through the alternator is as follows:

The single phase ac output of the PMG to the exciter field regulator is brought out at connector pins B and C. The output of the voltage regulator is brought into the exciter field through connector pins A and F. The three phases of the alternator are terminals T1, T2, and T3. Terminals T4, T5, and T6 together form the neutral connections.

The installation requirements for the alternator are shown in Figure 7, 322 kW Alternator Installation Requirements and are as follows:

a. Bearing Lubrication
b. Cooling Air
c. Mechanical Interface Data

The bearings require 230 cc/minute (.061 GPM) at .5 to 1.5 psi of MIL-L-7808 oil. The drive end oil outlet line only needs to be evacuated to 1.0 +/-.5 PSIG vacuum to prevent oil from flowing into the drive end bearing cavity. The oil flow through the anti-drive end is by gravity.

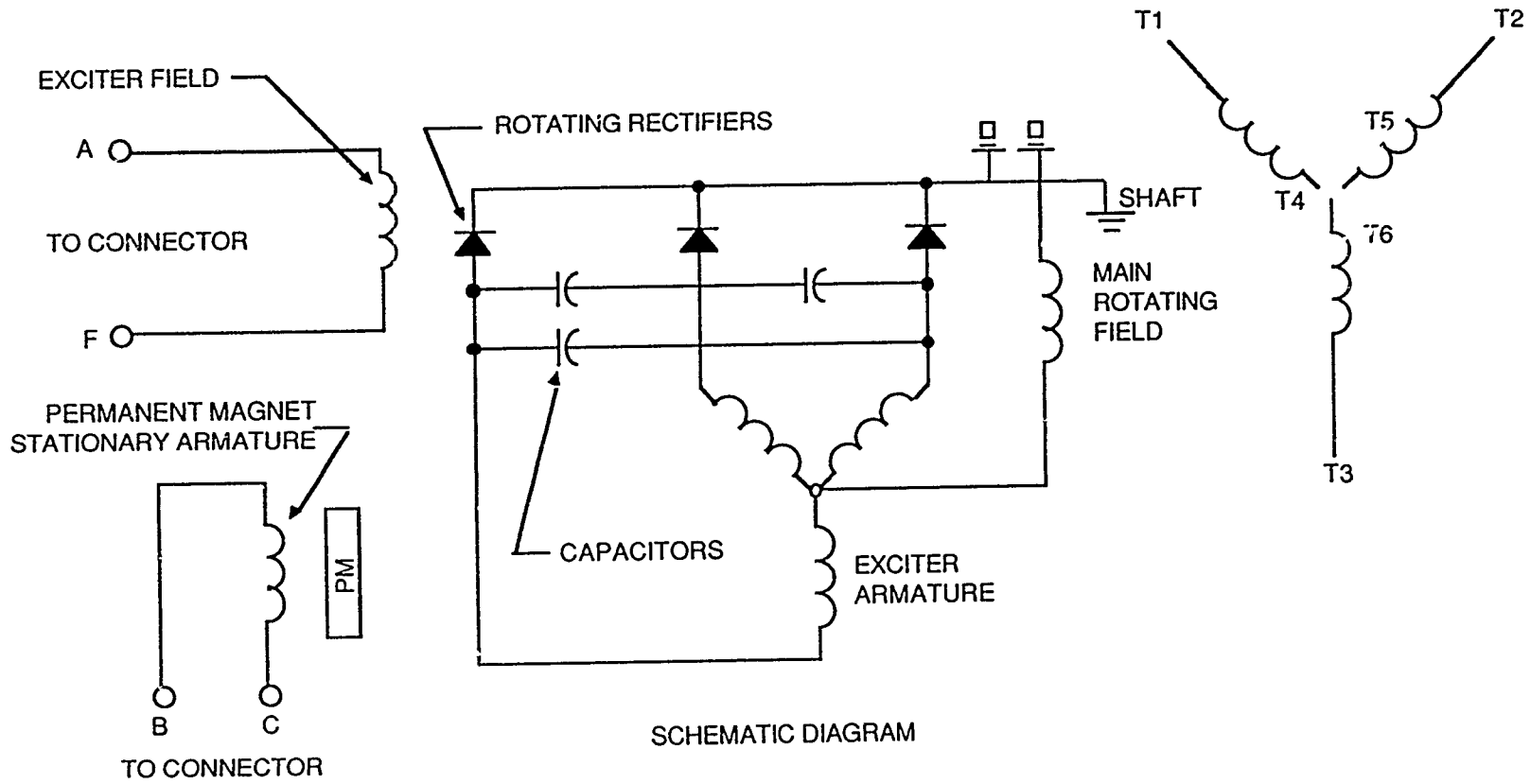


05/204/88/023-K

Figure 6. 322 kW Alternator-Electrical Interface

| | |
|---|---|
| o BEARING OIL | |
| TYPE | MIL-L-7808 |
| FLOW RATE @ 1.0 ±.5 | .0615 GAL/MIN. |
| TEMPERATURE (MAX) | 212°F |
| SPECIAL INSTRUCTIONS: DRIVE END OIL OUTLET LINE TO BE EVACUATED TO 1.0 ±.5 PSIG VACUUM MEASURED AT THE BEARING CAVITY OUTLET | |
| o COOLING AIR SUPPLY | |
| VOLUME | 1100 CFM |
| SPECIAL AIR SUPPLY INSTRUCTIONS: COMBINED AIR INLET DROP AND EXHAUST BACK PRESSURE MUST NOT EXCEED 6.0" $H_2O$ | |
| o SPLINE DATA | |
| NUMBER OF TEETH | 24 |
| PITCH | 20/30 PITCH |
| PRESSURE ANGLE | 30° |
| MAJOR DIAMETER | 1.262"/1.267" |
| SPLINE LENGTH | 1.250" |
| o MOUNTING FLANGE | |
| BOLT CIRCLE | 10" DIAMETER |

Figure 7. 322 KW Alternator Installation Requirements

The alternator cooling fan draws 1100 CFM at 9000 RPM. The combined air inlet drop and exhaust back pressure must not exceed 6.0" $H_2O$. A shroud must be provided at the drive end of the alternator frame to create a negative pressure drop in the bearing cavity of at least 3.0 inches $H_2O$ below the exhaust back pressure measured at air outlet.

The alternator will mate to the appropriate gear box via the 10" bolt circle and spline on the drive shaft end. The alternator interface information is described on Westinghouse ICD, Dwg. No. E77497.

## 2.3 Motor/Speed Decreasing Gear/Coupling Design Overview

The motor/SDG is an integral design to minimize weight and volume. The design is totally enclosed with a self contained oil system for lubrication and cooling. Heat from the oil is transferred through an integral heat exchanger to water which flows over the exterior of the motor. The coupling provides for angular and parallel misalignment between the motor and pump jet. All surfaces which are exposed to seawater are corrosion resistant. All parts fabricated from aluminum are electroless nickel plated. All other parts are either corrosion resistant stainless steel or bronze. The overall dimensions of the motor/SDG and coupling are given in Figure 8 and additional detail is found on the ICD drawing number J77496. The weights of the various components are given in Figure 9.

The coupling is illustrated in Figure 10. A double flex gear type has been selected to provide for parallel and angular misalignment and to minimize size and weight. The coupling is constructed of stainless steel and sealed to retain the lubricant.

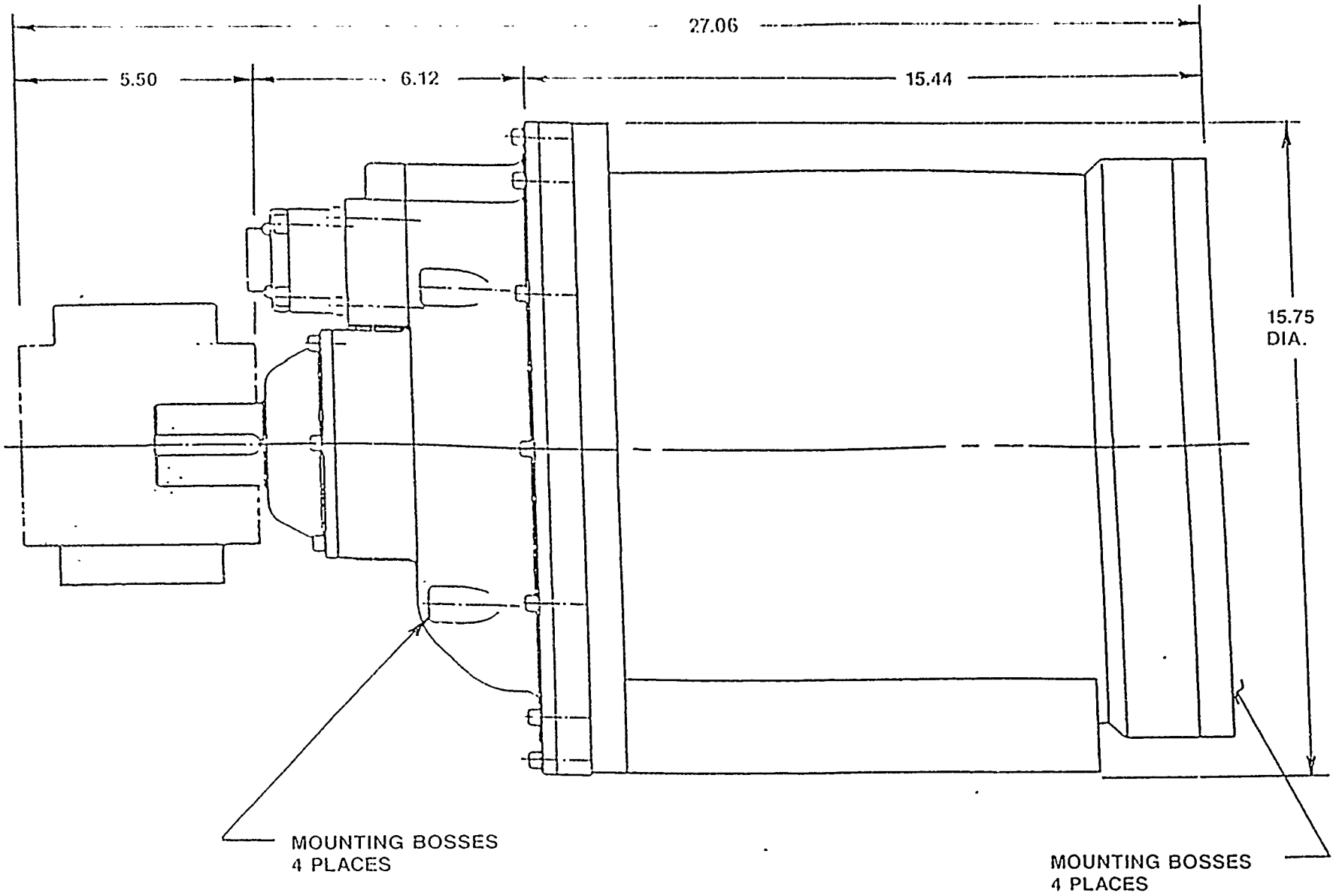


Figure 8. Waterjet Propulsion System - Transom Mounting Dimensions

| Item | Weight, LBM |
|---|---|
| Motor Assembly | 224 |
| Gearbox | 67 |
| Coupling | 33 |
| Oil | 5 |
| **Total** | **329** |

Figure 9. Weights Summary

Sier Bath
Size C-3

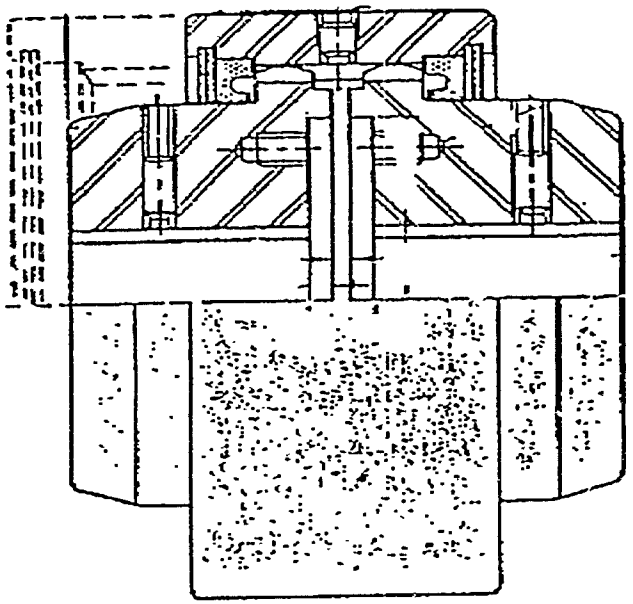

| | |
|---|---|
| Weight | 33 lbm |
| Size (inches) | 6.625 dia. x 6.875 lg. |
| Misalignment | |
| Parallel | .010 in. |
| Angular | .2° |
| Torque | 5180 ft-lbf Max |
| Material | 316 SS |

Figure 10 Coupling

### 2.3.1 Motor/Speed Decreasing Gear Constraints

The design of the motor was driven by the power and speed requirements of the waterjet and the need to be compatible with an existing 400 Hz alternator. An initial electromagnetic design sensitivity study indicated maximum frequency with the above constraints to be 600 Hz. In order to keep the size of the SDG at a minimum, a single stage reducer was desired. A single stage planetary gear reducer has a gear ratio upper limit of approximately 10:1. With a waterjet speed of 1250 RPM and a gear ratio of 10:1, the maximum motor speed is 12,500 RPM. During the design iterations a motor frequency of 500 hertz was selected to minimize the stator core losses and mechanical stresses in the rotor. The laminated rotor core and fabricated copper bar and end ring structure set an upper bound relative to the maximum operating speed that could be obtained. The maximum number of poles was determined to be six resulting in a motor speed of 10,000 RPM while still staying within the SDG constraints. Any lower number of poles (4 or 2) at 500 Hz results in increased weight of the motor and/or exceeds the available envelope.

Discussions with the alternator vendor established the upper speed limit for continuous operation at 9,000 RPM. Therefore the resulting design of record frequency is 450 hertz, which provides a motor synchronous speed of 9,000 RPM.

The full load operating point of 3,000 RPM prime mover/9,000 RPM alternator speeds and 1,250 RPM waterjet speed results in a 7.2:1 motor/SDG speed reduction ratio. The ideal ratio of 7.2:1 was used to perform initial design calculations. Based upon calculated motor slip (8,919 motor RPM), and a practical, achievable SDG ratio of 7:1, the resulting waterjet speed is 1,274 RPM. By adjusting prime mover speed the system will operate at the desired 1,250 RPM waterjet speed. The alternator and motor/SDG will provide the required 400 HP at the adjusted speed without incurring additional losses, as the efficiency is constant over minor speed variations around the full load operating point.

### 2.3.2 Induction Motor

The motor consists of the motor housing and stator assembly, forward bulkhead assembly, and shaft assembly. The motor housing, stator assembly and forward bulkhead assembly are shown in Figure 11.

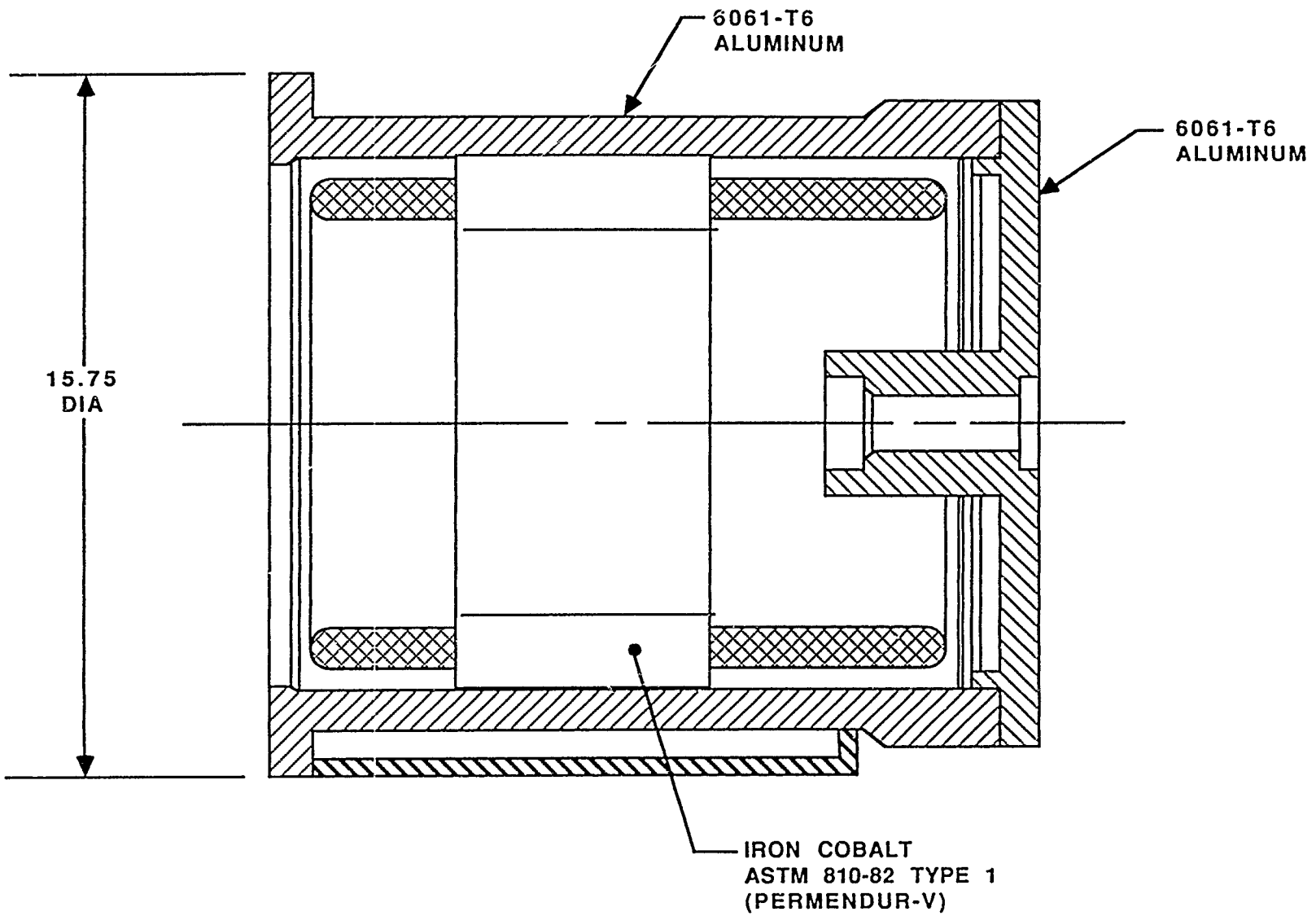


Figure 11. Motor Housing, Stator Assembly and Forward Bulkhead Assembly

2.3.2.1 Construction

The motor housing consists of 6061 aluminum inner and outer shells and sump which are welded together to function as a heat exchanger and oil reservoir. After the oil lubricates/cools the gearbox/motor it gravity drains into the sump. Fins made of 3003 aluminum are brazed into the outer shell to provide adequate heat transfer from the oil to the outer shell. The motor housing mounts the stator, which is shrunk into the bore, and mates up with the SDG and the forward bulkhead.

The stator assembly consists of 50% cobalt iron laminations which are bonded together with epoxy resin. The slots are lined with nomex-kapton-nomex insulation and the stator is wound with rectangular cross section oxygen free copper wire with ml insulation. The top and bottom turns in each slot are insulated from each other with G-30 mid sticks. Windings are retained in the slots with injection molded Torlon top sticks. End turns, jumpers, neutrals and feedthroughs are copper brazed. After brazing the stator assembly is vacuum pressure impregnated with an epoxy varnish.

The forward bulkhead assembly includes the forward bulkhead, the oil spray manifold and nozzles, and the speed pickup housing. The nozzles are made of brass and the bearing insert is made of 17-4PH stainless steel; the remaining parts are made from 6061-T6 aluminum.

The rotor assembly, Figure 12, can be further broken down into the shaft subassembly and the rotor. The shaft subassembly is illustrated in Figure 13. The stub shafts are rough machined, shrunk into the end plates and welded. These units are then shrunk into the drum which has been rough machined and the final welding is completed. The shaft subassembly is then rough turned and ground. At this point the first balancing operation is completed. The material selected for use in the stub shafts is PH13-8MO stainless steel which has the strength necessary to carry the torsional load and can be readily welded to the end plates. The drum and end plates are made of high strength ANSI 4130 alloy steel which combines high strength with availability and low cost.

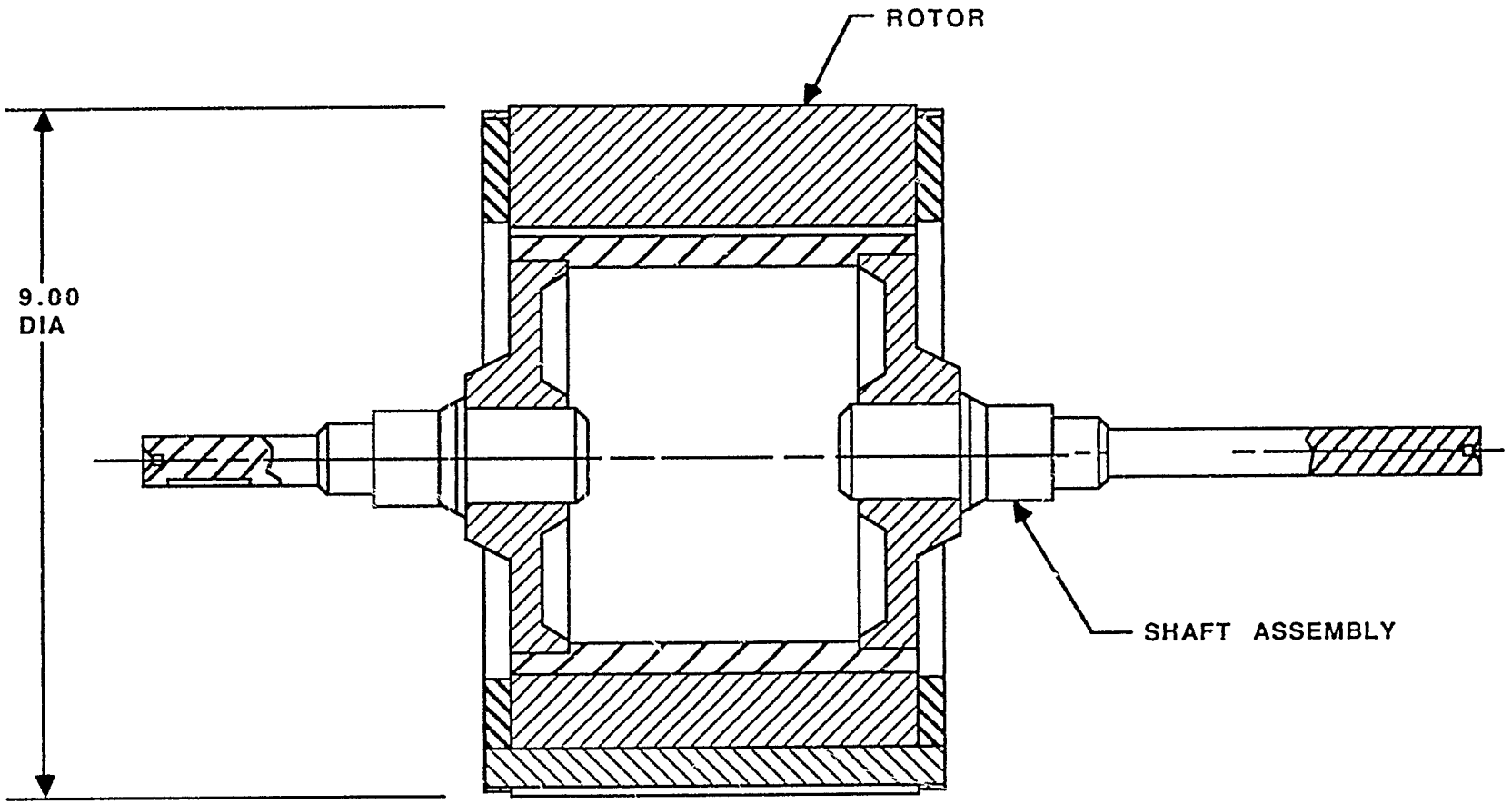


Figure 12. Rotor Assembly

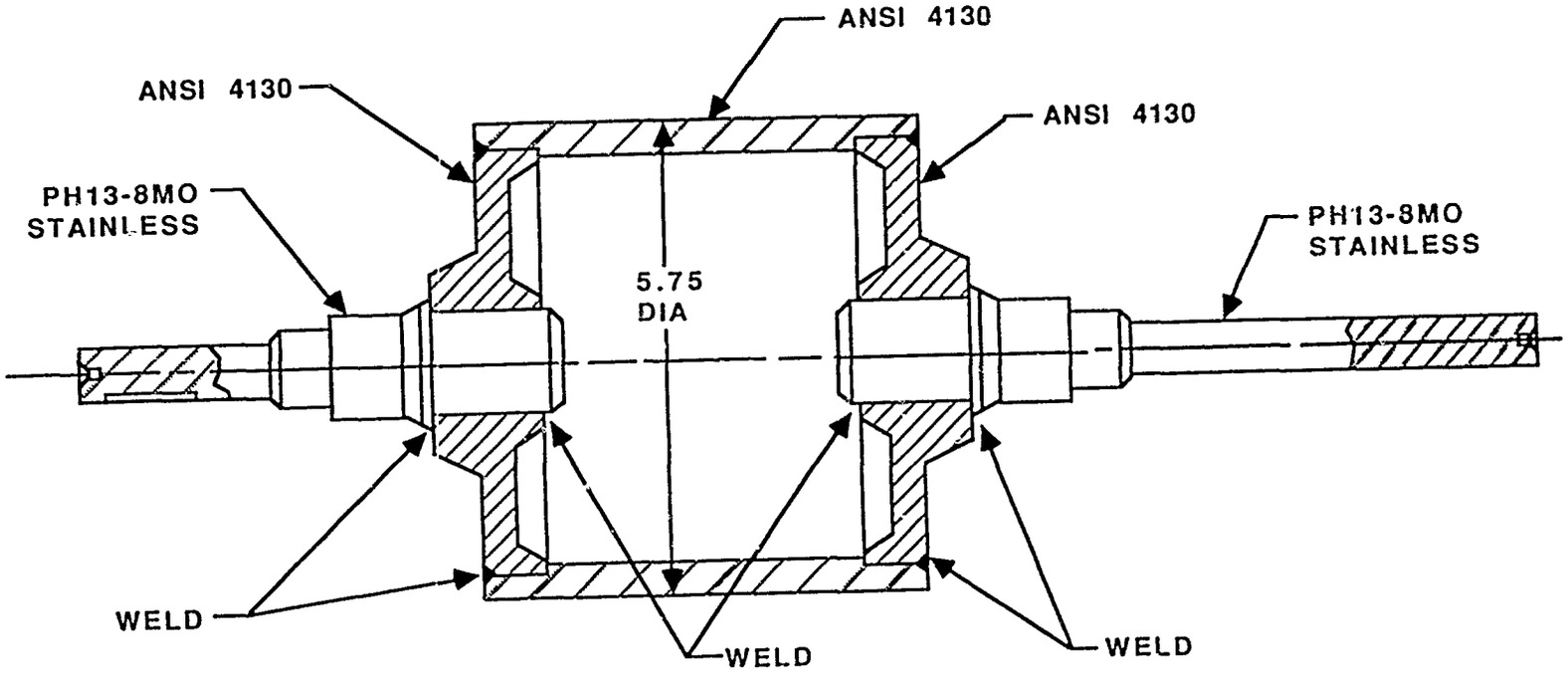


Figure 13. Shaft Subassembly

The rotor is shown in Figure 14. It consists of iron cobalt ASTM 801-82 Type 1 steel laminations, zirconium copper CDA 15000 bars and end rings, and Inconel 625 shrink rings. The laminations are stacked and clamped in an alignment fixture. The inside diameter is then ground and the shaft subassembly shrunk in place. The end plates are then welded to the shaft subassembly and the entire unit removed from the fixture. The rotor bars and end rings are then installed and brazed. The shaft is then finish ground and the end rings are machined for assembly of the shrink rings. Final balancing of the rotor assembly is done at this time. The lamination steel is selected for its magnetic properties and the zirconium copper for its combination of electrical and mechanical properties. The shrink ring provides support for the end rings and bars when they are subjected to centrifugal force.

All parts which are subjected to the salt water environment are either electroless nickel plated or made from stainless steel to protect from corrosion. Insulation materials have been selected to meet the life requirements over the range of operating temperatures and to be compatible with the MIL-L-7808 lubricating and cooling oil.

Many features of this design were incorporated to minimize weight. Among these are the hollow shaft construction, the selection of cobalt iron for the laminations which allows the use of higher flux densities and the selection of high strength aluminum alloys for the housing and bulkhead. A breakdown of the motor weights is given in Figure 15.

The oil system for the motor and SDG is shown in Figure 16. The oil is collected in the sump and after passing through a filter, flows through passages in the motor housing and SDG assembly to the oil pump which is driven by a gear on the planet carrier. A relief valve limits the pump discharge pressure to 200 psi during a cold start when the resistance to flow in the heat exchanger is high. At steady state operating temperature the oil pressure drops to about 50 psi. From the pump the oil flows into the heat exchanger which is built into the motor housing. Here the heat in the oil is transferred into the fins in the outer shell and conducted out to the surrounding water.

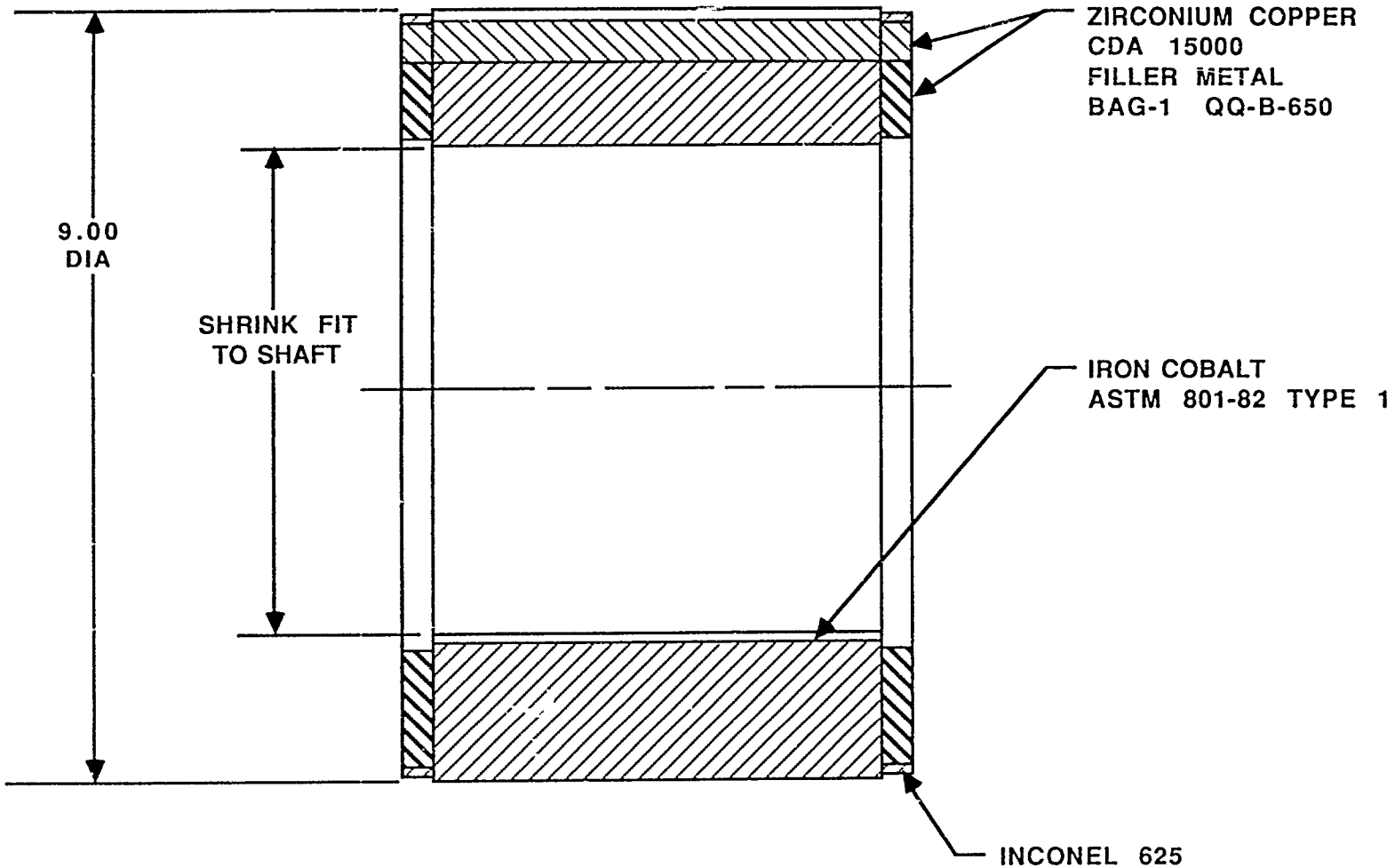


Figure 14. Rotor

| | | |
|---|---|---|
| **Housing Assembly** | | **76.36** |
| Housing | (52.4) | |
| Fwd Bracket | (14.8) | |
| Misc. | (9.16) | |
| **Stator** | | **71.53** |
| Laminations | (47.24) | |
| Copper | (24.29) | |
| **Rotor** | | **76.21** |
| Shaft | (18.39) | |
| Laminations | (46.10) | |
| Copper | (11.72) | |
| **TOTAL** | | **224.15** |

Figure 15. Motor Weights (LBM)

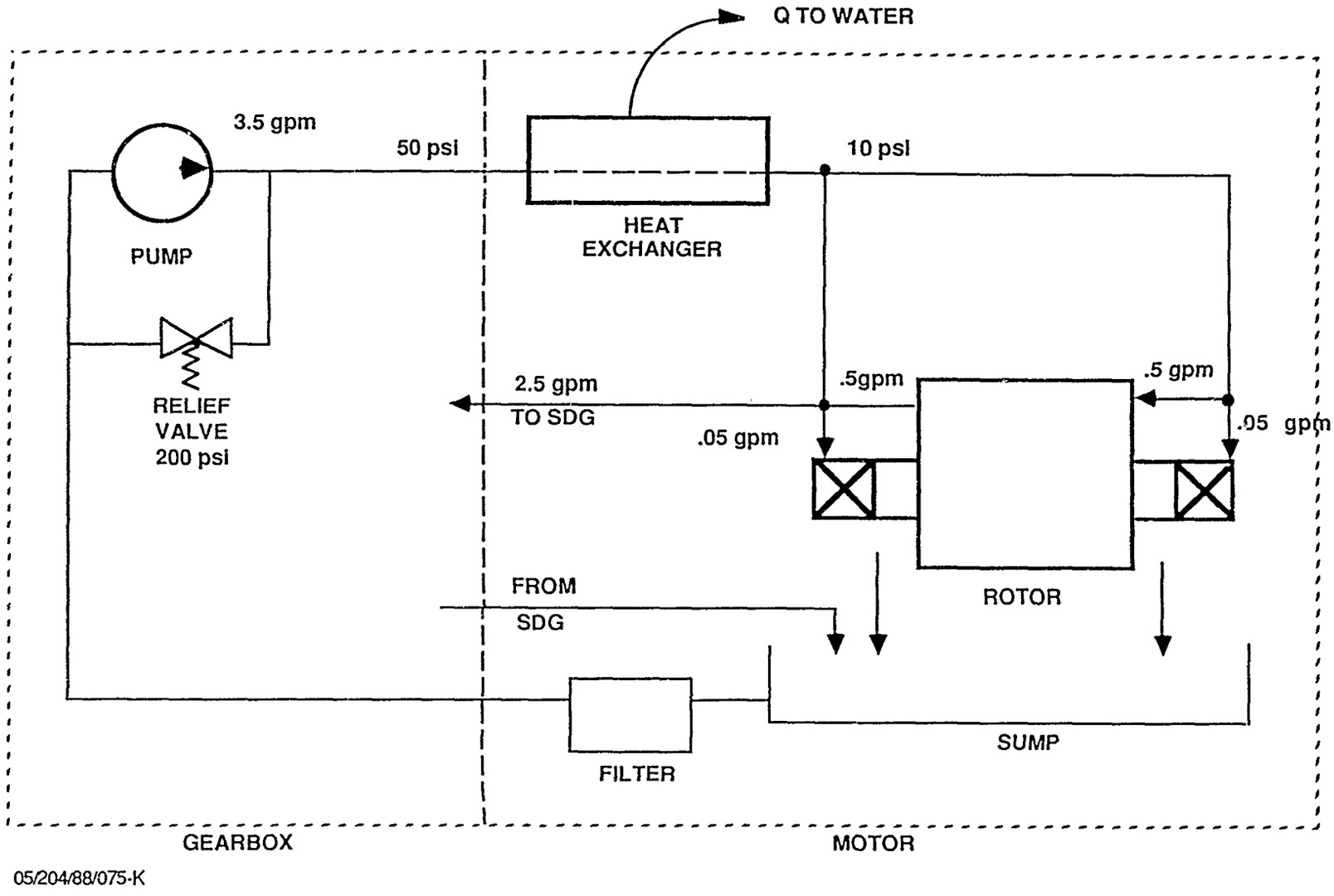


Figure 16. Oil Coolant and Lubrication System.

After leaving the heat exchanger the flow is split between the motor bearings and rotor and the SDG. A pressure transducer monitors the pressure at the discharge of the heat exchanger to ensure that oil flow is maintained.

The motor has been designed so that when the maximum combined vehicle/transom pitch angle of 18.5 degrees is established the oil continues to cover the oil inlet and does not flow into the air gap between the rotor and stator. The drain from the SDG has been designed to deliver the oil directly to the sump so that it is filtered prior to entering the motor.

2.3.2.2 Electrical Performance

The nominal load condition: (400 HP) is dictated by the single operating vehicle point that corresponds to the highest drag/power value that the vehicle may see when it reaches hydroplanning speed. The motor electrical performance was bounded by: steady state operation under nominal load conditions and starting behavior. A design compromise was achieved to meet the required efficiency level and still provide for satisfactory starting performance. Specification requirements call for a combined motor-SDG efficiency of 92% which dictates a high efficiency motor design at nominal conditions. The final motor size, weight and material selections are dominated primarily by the required motor design efficiency. The motor design must provide adequate starting torque with manageable starting phase currents. This was accomplished by utilizing rotor cage "deep bar" effect to enhance motor starting torque. This approach uses the skin effect phenomena present in the rotor bars during starting conditions to achieve increased rotor cage resistance and therefore increased torque during the starting interval. In addition to the above requirements the drive system must be capable of a 30% overload for 60 seconds. Sufficient thermal storage capability exists in the stator and rotor to meet this requirement.

A comparison of the nominal, overload and starting performance parameters is shown in Figure 17. The motor nominal HP is based on the assumption that the SDG efficiency will be 96% and the power delivered to the waterjet is 400 HP. The motor electromagnetic weight consists of those components that carry either electrical current or magnetic flux. The calculated starting time for these conditions is approximately three seconds based upon steady state performance data. More refined data is shown by the systems simulation model (see Section 2.5, Propulsion System Controller).

| Parameter | Nominal Condition | Overload Condition | Starting (15°C) |
|---|---|---|---|
| Motor Terminal Voltage | 300.22 Vrms (L-N) | 300.22 Vrms (L-N) | 87 Vrms (L-N) |
| System Frequency | 450 Hz | 450 Hz | 215.3 Hz |
| Motor Horsepower Out | 416.67 | 541.67 | – |
| SDG Output Horsepower | 400 | 520 | – |
| Motor Phase Current | 391 Amp | 531 Amp | 940 Amp |
| Motor Input Power | 322 kW | 424 kW | 42 kW |
| Motor Speed | 8919 rpm | 8885 rpm | 0 rpm |
| Motor Input P.F. | .914 | .886 | .169 |
| Motor Efficiency | .962 | .953 | – |
| Motor Torque | 245.2 Lb•ft | 320 Lb•ft | 40.6 Lb•ft |
| Breakdown Torque | 444.8 Lb•ft | 444.8 Lb•ft | 148.4 Lb•ft |
| Acceleration Time | – | – | 3 sec |
| Electromagnetic Weight | 129 Lb | | |

Figure 17. Motor Electrical Design Summary

Figure 18 shows how the motor HP and predicted efficiency vary as a function of motor speed. Figure 19 illustrates the predicted motor power factor and phase current as a function of motor speed. These figures show that maximum efficiency is obtained near nominal conditions and that it is relatively insensitive to load up to the overload point.

2.3.2.3 Equivalent Circuit

The per phase equivalent circuit model of the induction motor is shown in Figure 20. The parameters shown are given at nominal conditions (322 kW, 8919 RPM, 450 Hz). The saturation factor used in the determination of the motor's magnetizing inductance is 1.054. The value of the stator winding phase resistance was evaluated at 150°C and includes the effect of stator coil cross slot eddy losses.

2.3.2.4 Electromagnetic Design

The stator and rotor cores are fabricated from .010 inch thick 50% cobalt-iron alloy laminations. This material was selected to minimize stator core losses and provide high permeability for the magnetic flux path. The stator laminations will be bonded together using an epoxy based adhesive. The adhesive serves to both electrically insulate the laminations from each other and to bond the core mechanically. This process reduces core losses. Figure 21 shows the details of the stator lamination design. The lamination has 54 partially closed slots which contain the stator winding. Both rotor and stator cores are 5.05 inches in axial (air gap) length.

The rotor lamination slot detail is shown in Figure 21. The rotor lamination has 63 partially closed slots within which the rotor bars will be placed. No bonding adhesive will be used between the rotor core laminations. The rotor will be constrained mechanically by axial welds in three circumferential positions on the rotor core I.D.. The welding procedure is used instead of epoxy adhesive since the rotor has low slip and does require insulation between laminations.

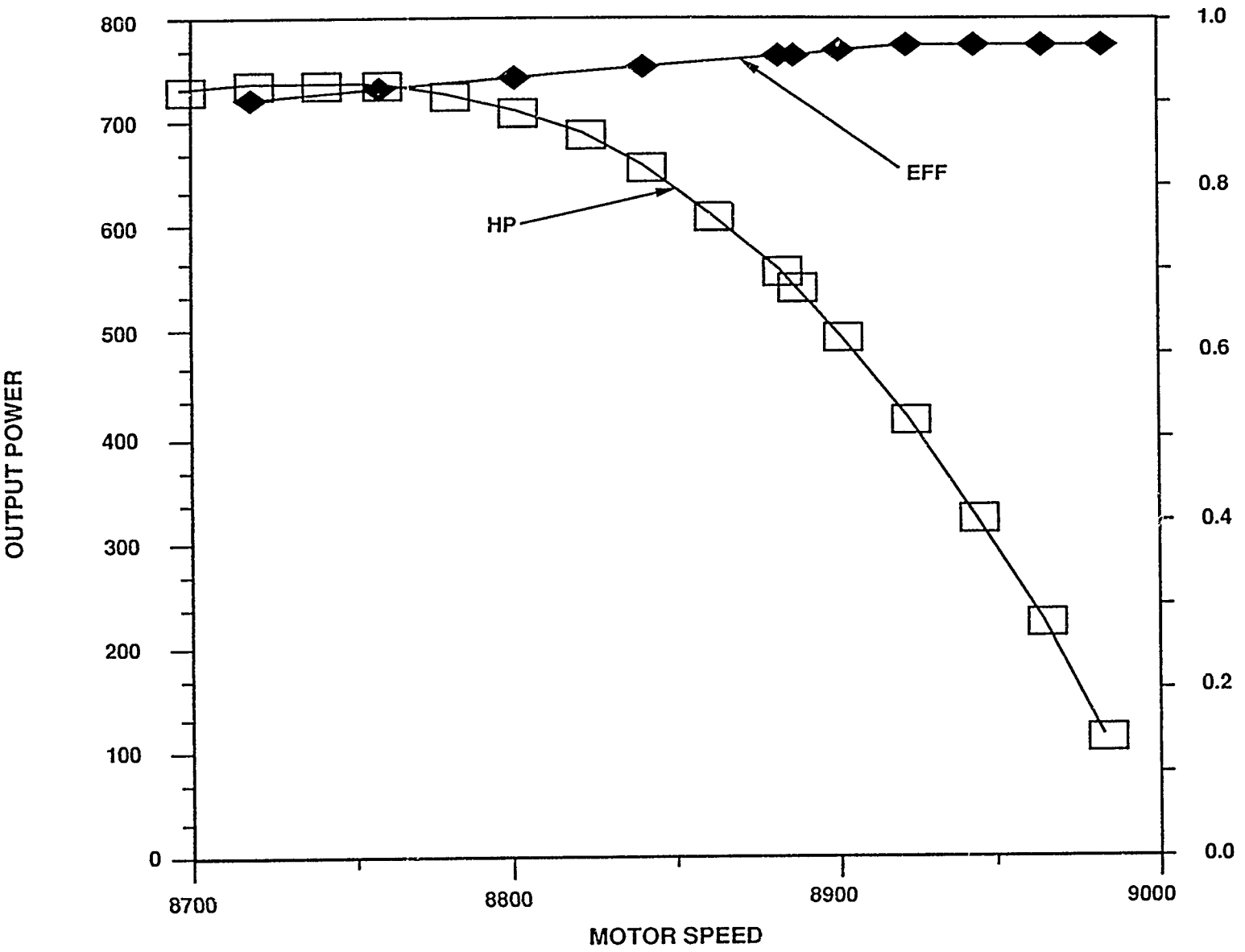


| | Nominal | Overload |
|---|---|---|
| HP | 416.67 | 541.67 |
| EFF | .962 | .953 |
| PF | .914 | .886 |
| RPM | 8919 | 8885 |
| AMP | 392 | 531 |

Figure 18. Predicted Induction Motor Performance - Power/Efficiency

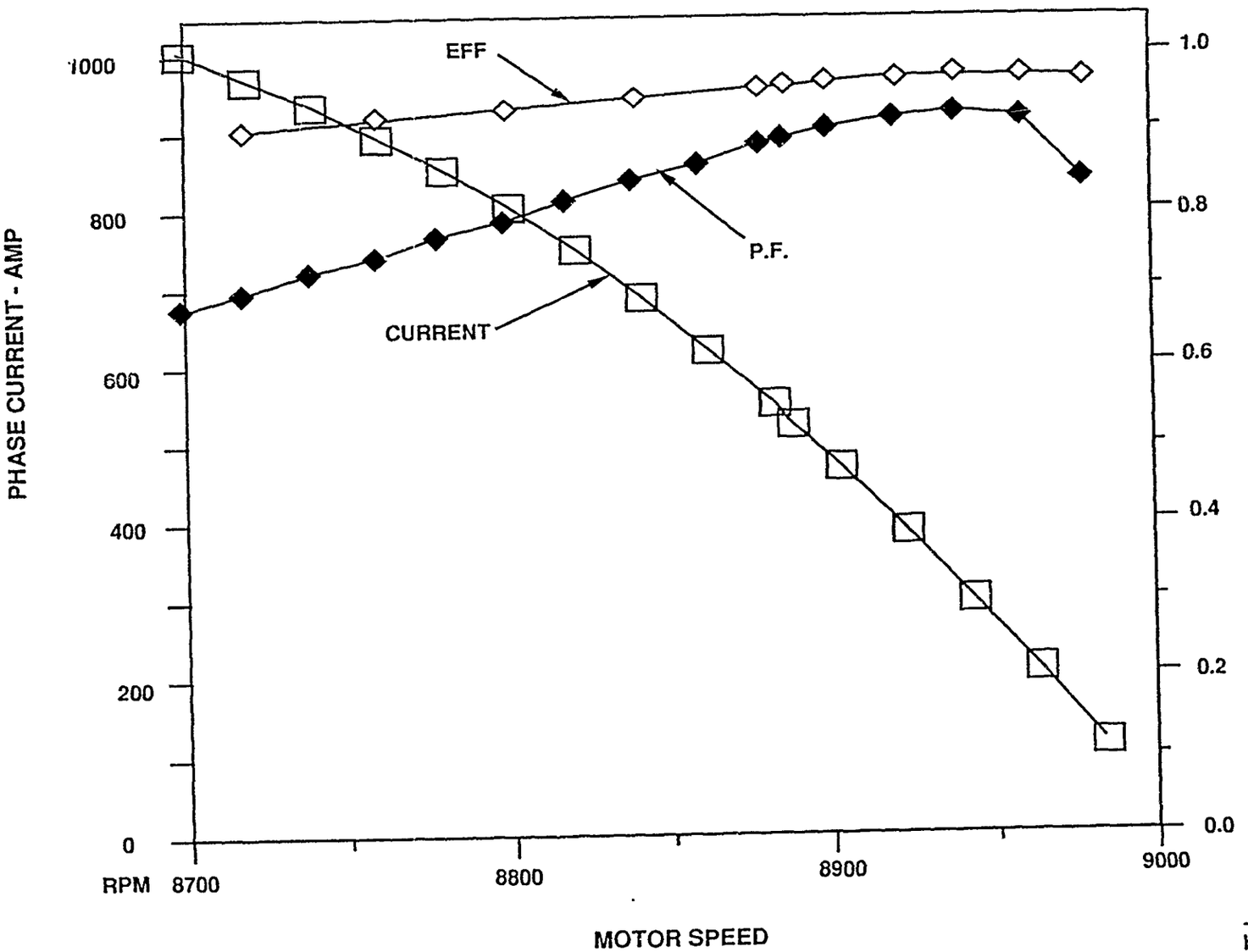


| | Nominal Overload | |
|---|---|---|
| HP | 416.67 | 541.67 |
| EFF | .962 | .953 |
| PF | .914 | .886 |
| RPM | 8919 | 8885 |
| AMP | 392 | 531 |

Figure 19. Predicted Induction Motor Performance - 450 Hz (Line Current/Power Factor)

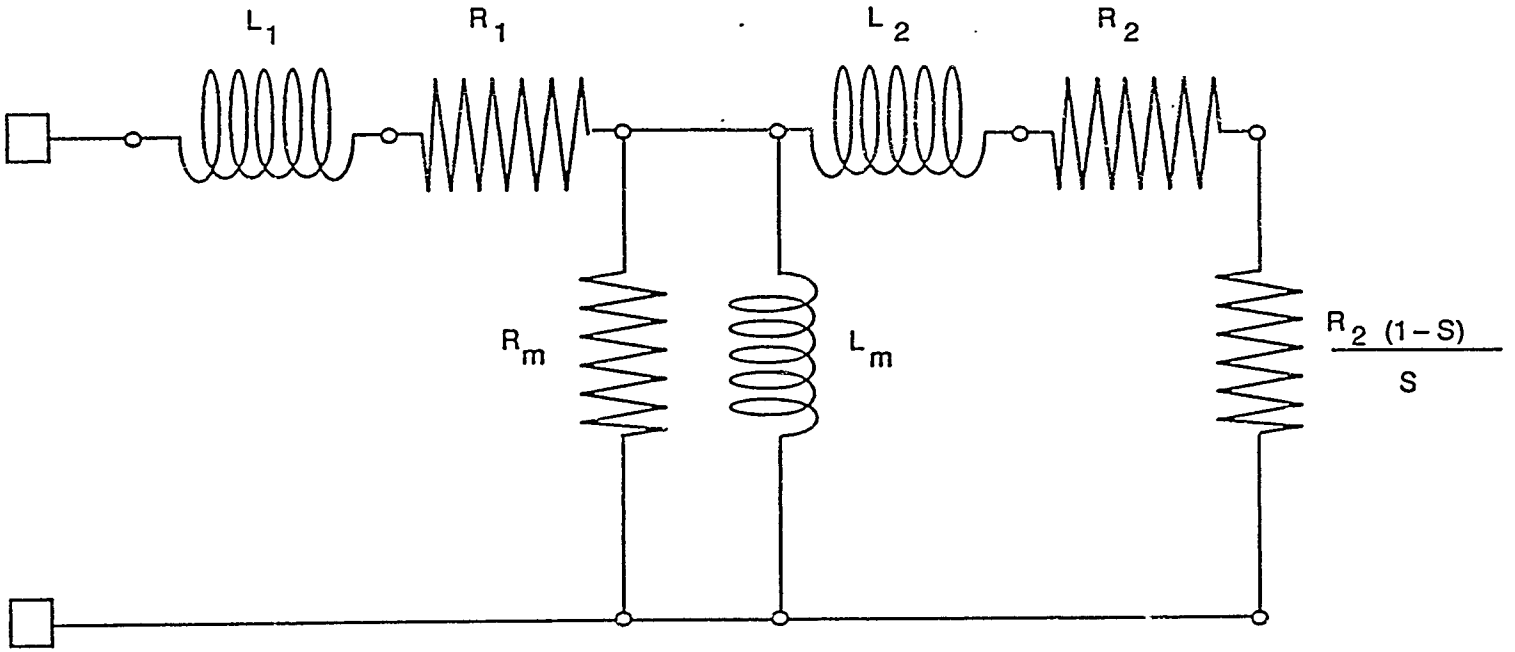


$L_1 = 4.35 \times 10^{-5}$ H

$R_1 = 1.27 \times 10^{-2}\ \Omega$

$R_m = 211.9\ \Omega$

$L_m = 1.79 \times 10^{-3}$ H

$L_2 = 3.27 \times 10^{-5}$ H

$R_2 = 6.53 \times 10^{-3}\ \Omega$

$S$ = Per Unit Slip

Figure 20. Induction Motor Per Phase Equivalent Circuit

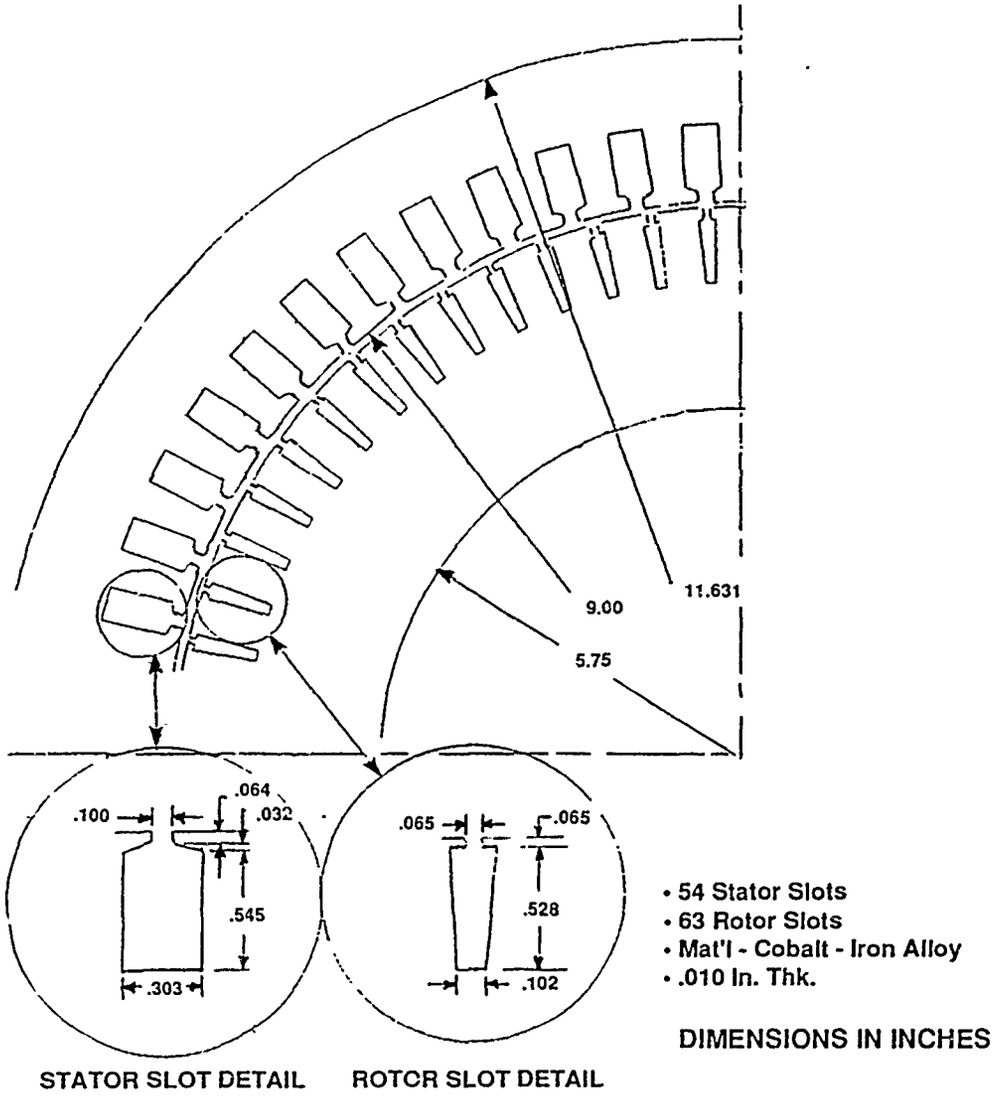


Figure 21. Stator and Rotor Laminations

The type of stator winding selected is a single circuit wave winding which provides the minimum number of internal connections. The end result of this selection is a winding which minimizes the axial length of the wound stator core. The winding diagram is shown in Figure 22. It is described as a three-phase, six-pole, three-lead, single turn full pitch winding. The stator conductors are rectangular in cross section. The coils are partially preformed then inserted in the stator core slots. Following coil insertion, coil end turn forming is completed. Each coil side has two conductors in parallel for a total of four conductors per slot.

The slot insulation system shown in Figure 23 is rated for a 180°C, 600 volt, 450 hertz design. All insulation materials are compatible with the internal oil system coolant (MIL-L-7808). The slot ground wall insulation is a Nomex-Kapton-Nomex composite which has a high tear and cut-through resistance. The ground wall provides a 6600 volt dielectric strength to ground and has long life at elevated temperatures. The film insulation on the winding conductors is a heavy polyamide-imide which is compatible with MIL-L-7808. It has a nominal temperature rating of 200°C. In addition to long thermal life, the cut-through and heat shock tolerance are superior to other types of magnet wire insulation. The wound stator is vacuum pressure impregnated with an epoxy resin which provides resistance to contaminates, seals the winding against moisture absorption and facilitates heat transfer by eliminating air voids in the ground wall system. In addition to the conductor film insulation the stator winding end turn area is insulated with an epoxy resin coating to enhance the heat transfer in this region from the conductor to the oil (MIL-L-7808).

2.3.2.5 Starting and Acceleration Characteristics, Initial Design

The ability of the motor to accelerate the waterjet commensurate with the alternator characteristics was initially analyzed using steady state performance data. The motor voltage and power factor were held constant during the acceleration time period. Figure 24 shows the predicted electrical system voltages and currents under both hot (15°C) and cold (150°C) starting conditions. During starting the alternator will be at 4306 ±RPM and the

## STATOR WINDING FEATURES

- Winding Type: Three-Phase Six-Pole Wave Wound WYE Connected Series Winding
- Rectangular Conductors, Form Tunnel Wound
- Full Pitch, 54 Slots, 2-Layer
- Advantages:
  Minimizes Axial Length
  All Internal Connections in Common Location
- Common Winding Arrangement for Motor and Alternator

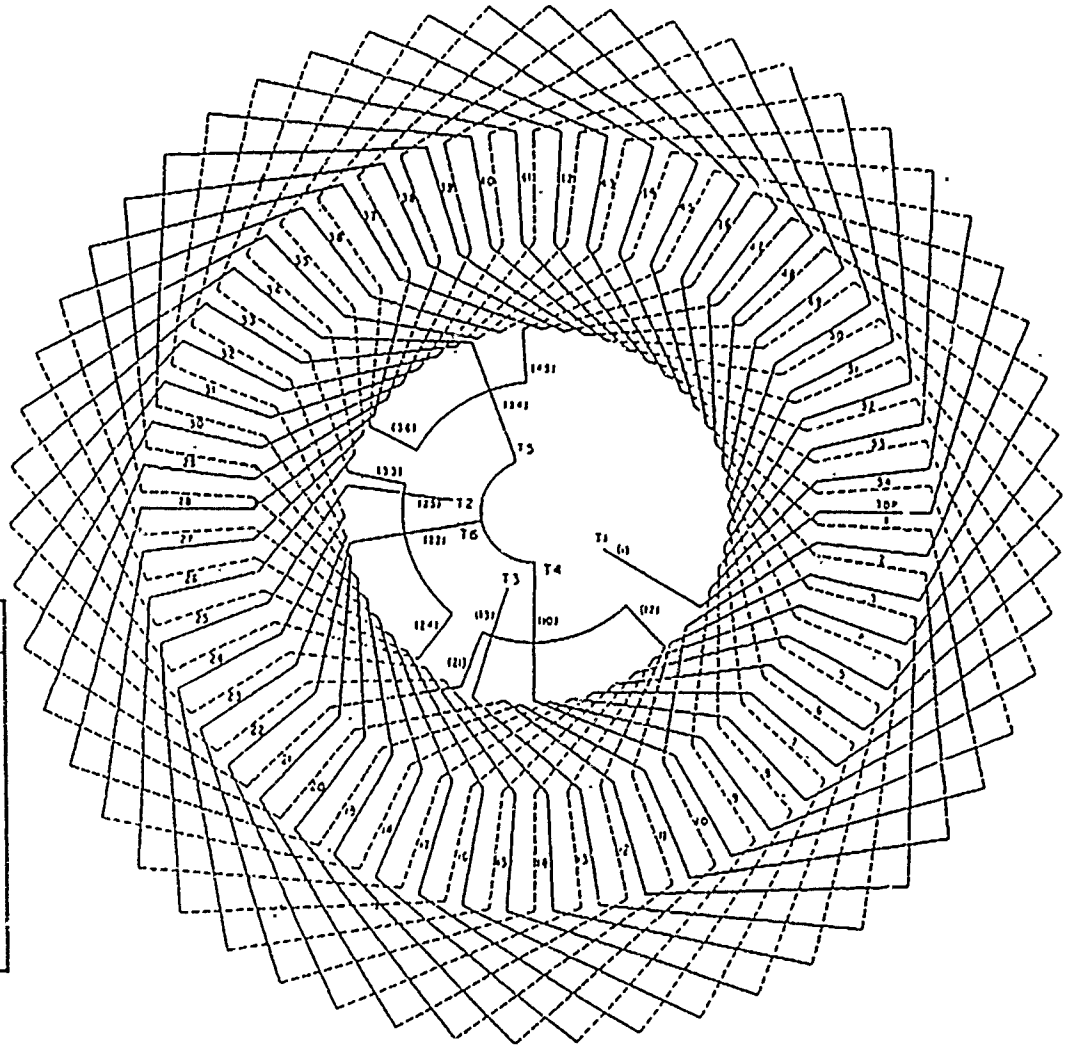


05/204/88/019

Figure 22. Motor Stator Winding Design

## SLOT INSULATION SYSTEM

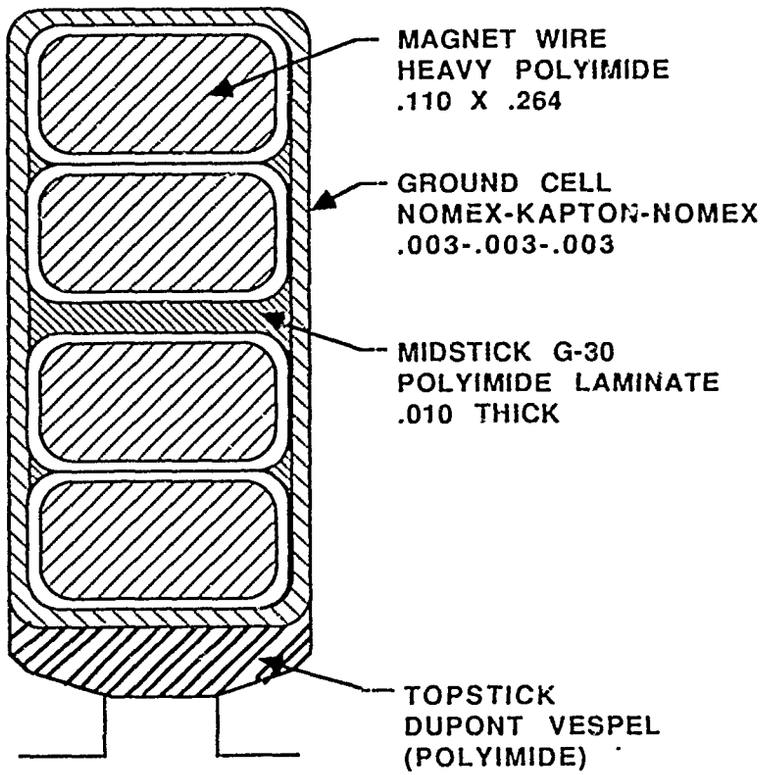


## DESIGN REQUIREMENTS

- Insulation - 180°C
- Voltage - 520 Volt RMS Continuous
  2040 Volt Dielectric Withstand
- Frequency - 450 Hz
- Life - 500 Hrs. Operating
  10 Yrs. Storage (-40C to + 125C)
  Oil Resistant (Mil-L-7808)

## KEY FEATURES

- Voltage Breakdown >4000 V/Mil
- Vacuum Pressure Impregnated with Epoxy Resin
- Excellent Heat Transfer Characteristics

05/204/88/020-F

Figure 23. Stator Insulation System

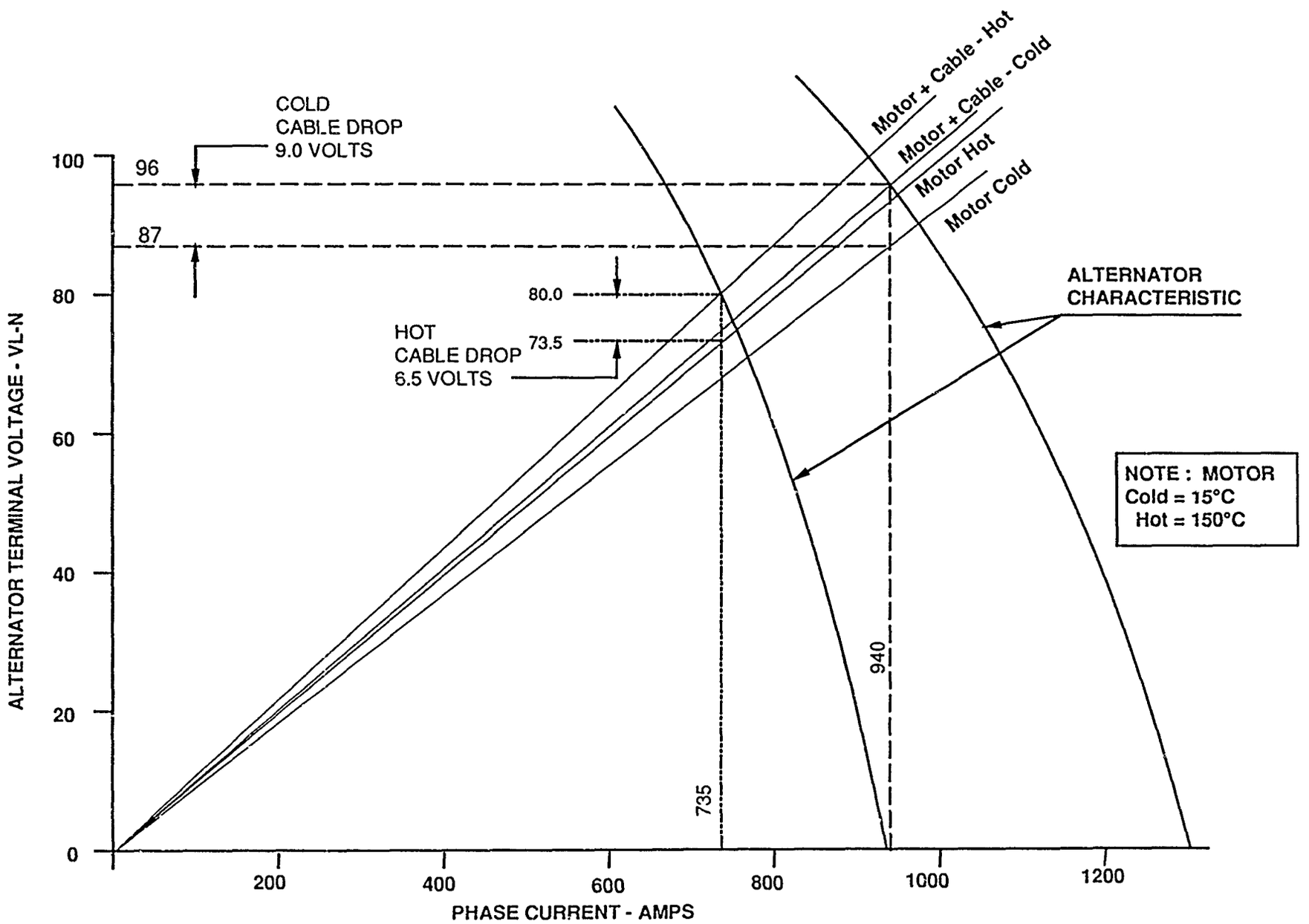


Figure 24. Operating Point Starting Conditions ( 0 Motor Speed, 215.3 Hz)

system frequency at 215.3 hertz. Alternator no-load voltage at this frequency should be 143.6 volts (L-N) corresponding to rated volts/hz; but, due to the large currents drawn during starting, the motor terminal voltage drops to 87.0 volts for a cold start and 73.5 volts for a hot start. The intersection of the alternator and motor starting characteristics determines the motor starting conditions. The power cable voltage drop (assuming a 4/0 cable of 25 feet in length) for hot and cold conditions are shown.

Once the motor terminal voltage has been determined under starting conditions, the motor speed-torque curve can be calculated (Figure 25). This curve is calculated assuming the motor is at 15 degrees C temperature. The developed motor torque includes the fundamental as well as additional harmonic torques that exist primarily at lower motor speeds. The expected load-torque (reflected to the motor shaft) curve and its associated break-away torque is below the motor torque. The difference between these two curves is the torque available for accelerating the load. Given the accelerating torque and the system inertia, the drive system acceleration time is calculated (Figure 26). The dynamic performance during starting is simulated using the system model. The motor voltage and power factor vary during acceleration and are taken into account in the system model. (Refer to section 2.5, Propulsion System Controller, for a more detailed discussion.)

The worst case starting condition occurs when the drive system is at temperatures corresponding to nominal load conditions. This condition may occur should a restart of the vehicle be required immediately after a full load run. The capability of the drive system to start at elevated temperatures was investigated. The motor terminal voltage was determined from the alternator characteristic to be 73.5 volts (Figure 24). The motor's terminal voltage at elevated temperatures is lower than ambient conditions which provides decreased motor starting torques with an accompanying decrease in starting current. The motor torque (including fundamental and harmonics) and load torque during a hot start are shown in Figure 27. From this, the time for a hot start (restart) was calculated to be approximately four seconds (Figure 28) using the steady state approach. (Refer to the section 2.5, Propulsion System Controller, for the simulated starting conditions using the system model.)

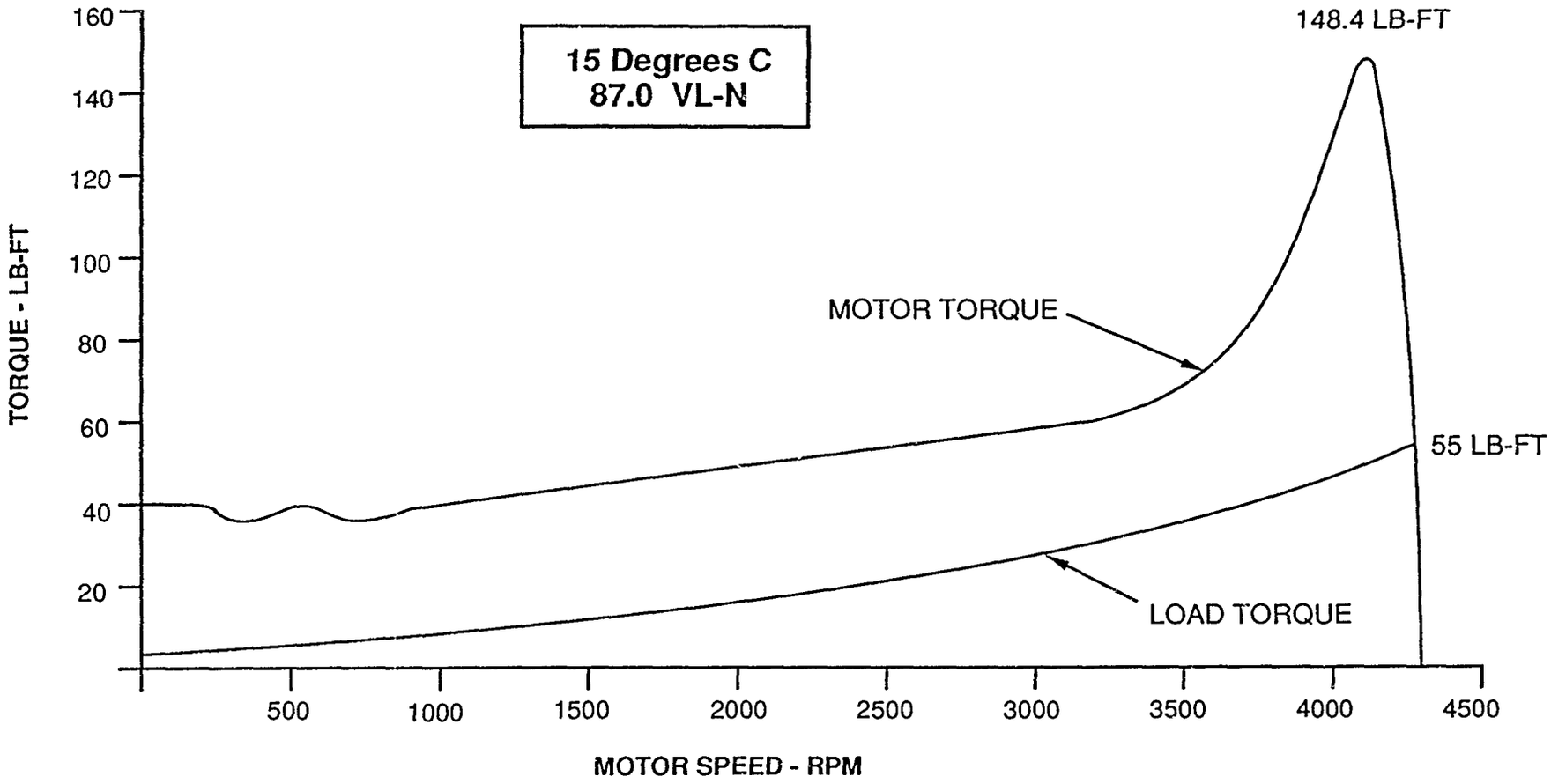


Figure 25. Speed Torque Curves (Cold Starting Condition)

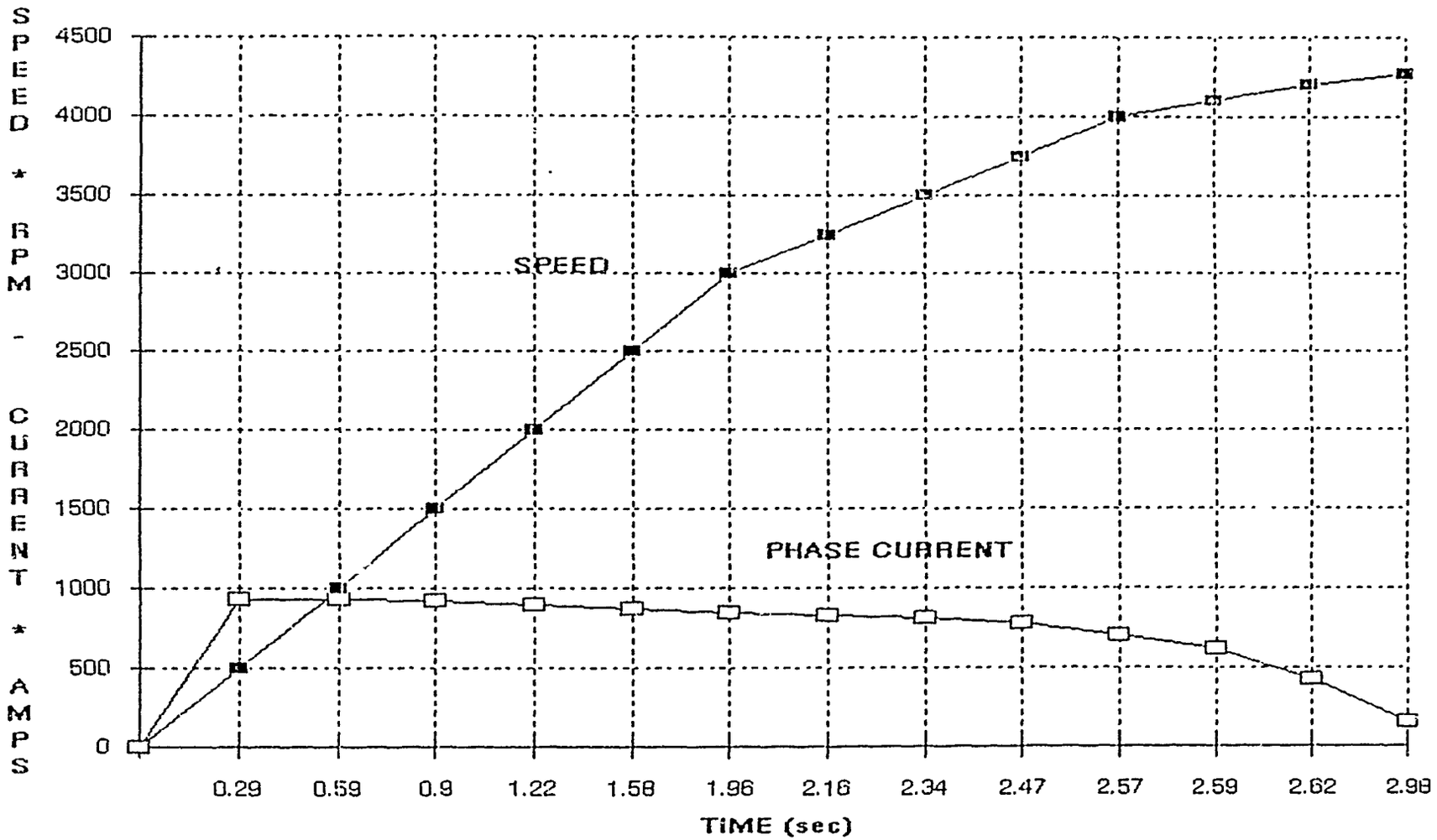


Figure 26. Motor Acceleration (15C)

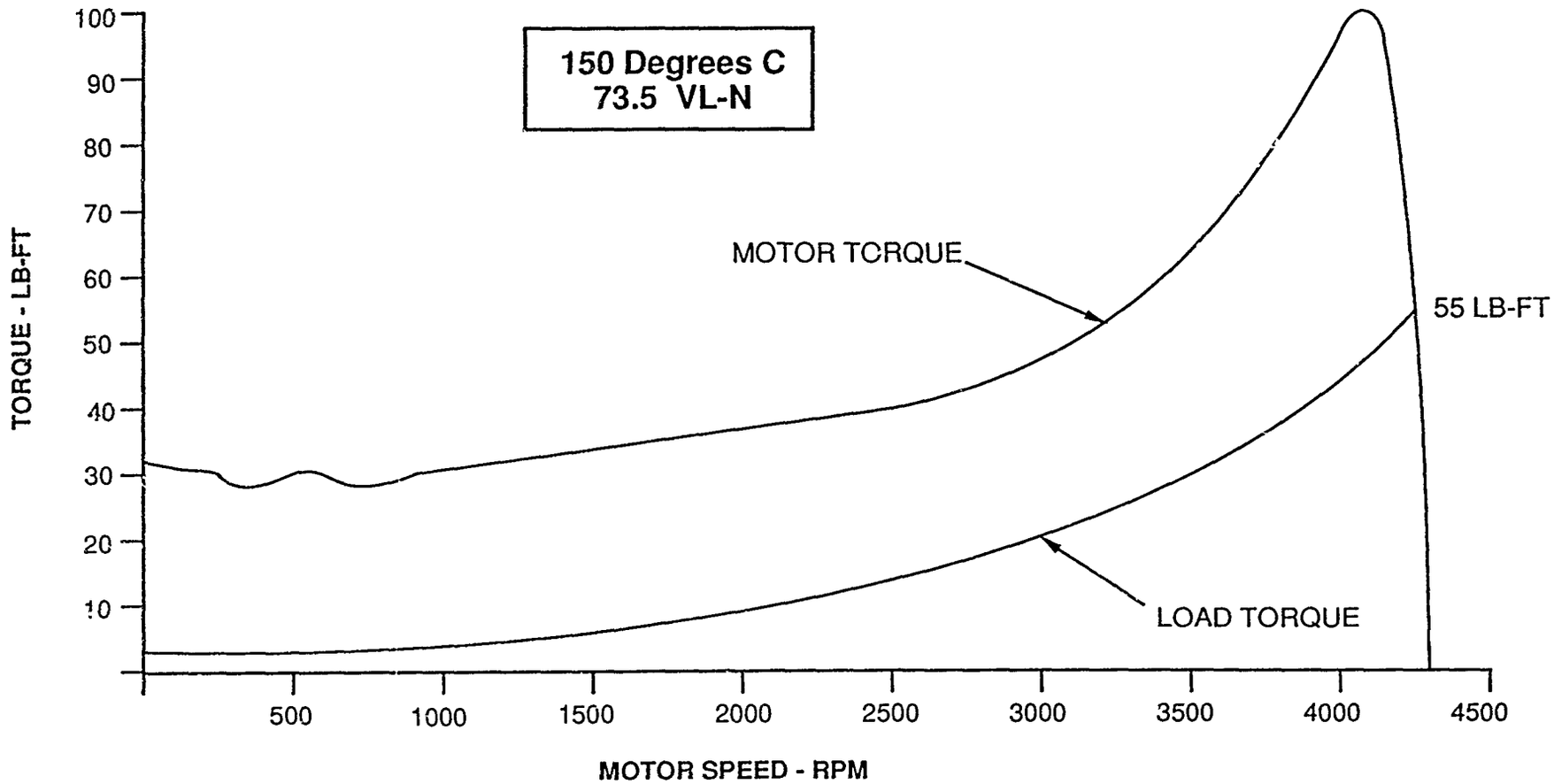


Figure 27. Speed Torque Curves ( Hot Starting Condition)

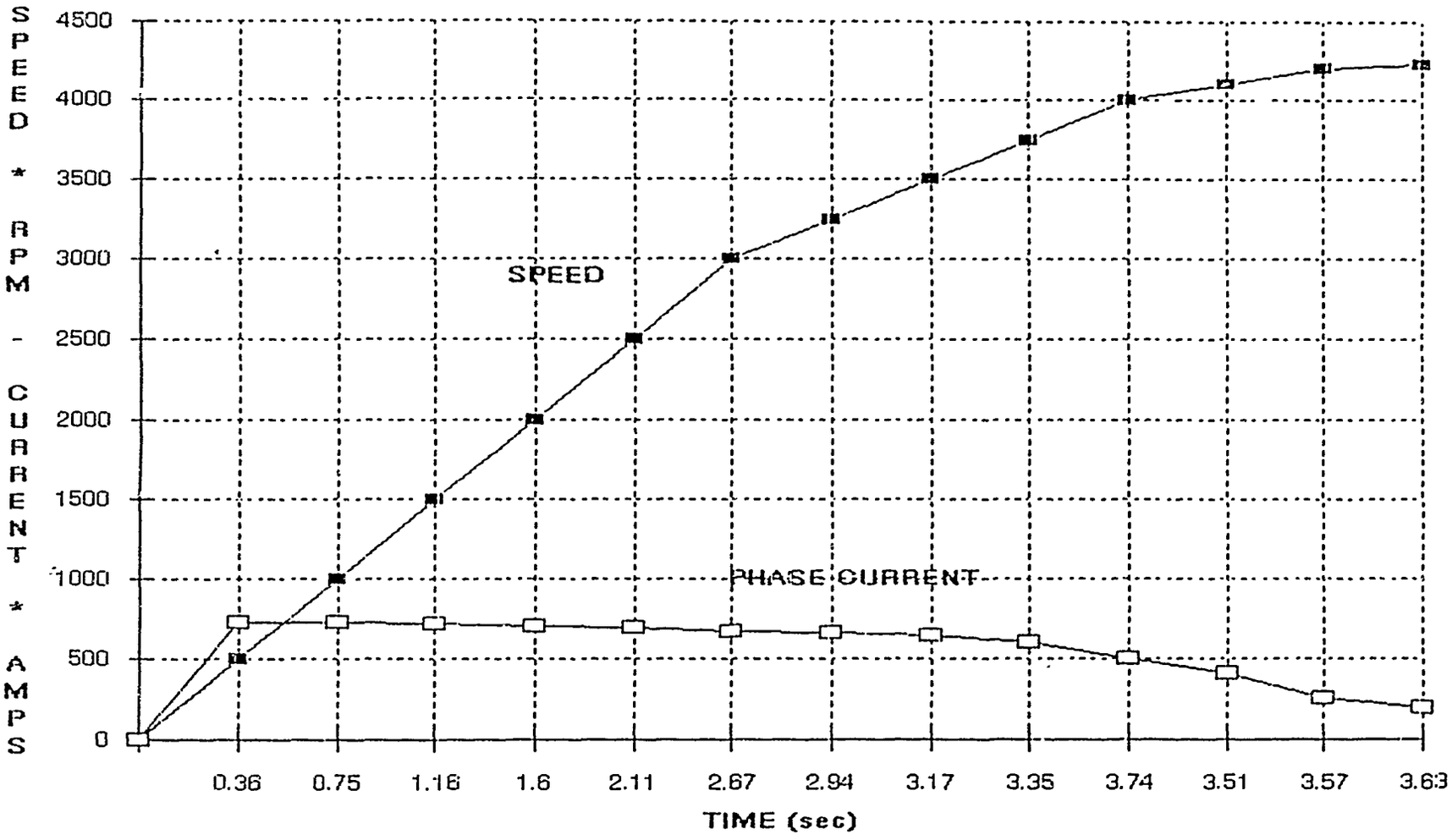


Figure 28. Motor Acceleration (150C)

2.3.2.6 Mechanical Stresses

The mechanical design requirements are summarized in Figure 29. The torque requirements result in shear stress in the stub shaft. The speed requirements result in centrifugal forces which create stresses in many of the shaft components. The shock loads create bending stresses in the stub shafts and bending stresses in the forward bulkhead. The life requirement has an impact on the working stresses in the shaft components.

The rotor assembly (Figure 12) was modeled with finite element analysis. The ANSYS model is shown in Figure 30. Numbers on the diagram represent node and element numbers. The centerline of the shaft runs through nodes 54 and 56.

Shaft stresses due to centrifugal force at 9000 rpm are shown in Figure 31. The safe working stresses in this figure are adjusted for cyclic and temperature effects. The rotor lamination stress is a hoop stress located at the inside diameter of the rotor lamination. The assembly stress in the lamination is not superimposed since the safety factor is quite large and the superposition process adds substantial complexity to the model. The copper end ring stress is also a hoop stress located at the inside diameter of the end ring. The end ring and bar stress is a hoop stress which occurs at the braze joint between the bars and end rings. Assembly stresses due to the shrink ring are superimposed on the end rings since the shrink rings are installed specifically to keep the end ring stresses at an acceptable level.

The shrink ring stress is a hoop stress which is the combined effect of assembly, thermal and centrifugal forces. The safe tensile stress for the shrink ring is not adjusted for cyclic loading because the cyclic stress is small relative to the average stress and the number of stress cycles is at the threshold at which no correction is needed. The shaft stress is a hoop stress located at the point where the stub shafts are welded to the end plates.

The centrifugal stresses of 10500 rpm are shown in Figure 32. Since this speed only occurs in the overspeed test the material properties are not adjusted for cyclic or temperature effects. All stresses are located as described above.

- 250 Ft. Lb. Torque at 9000 RPM Nominal
- 10,500 RPM Overspeed
- Shock Load - 7G All Directions
- 500 Hr. Life

Figure 29. Mechanical Design Requirements

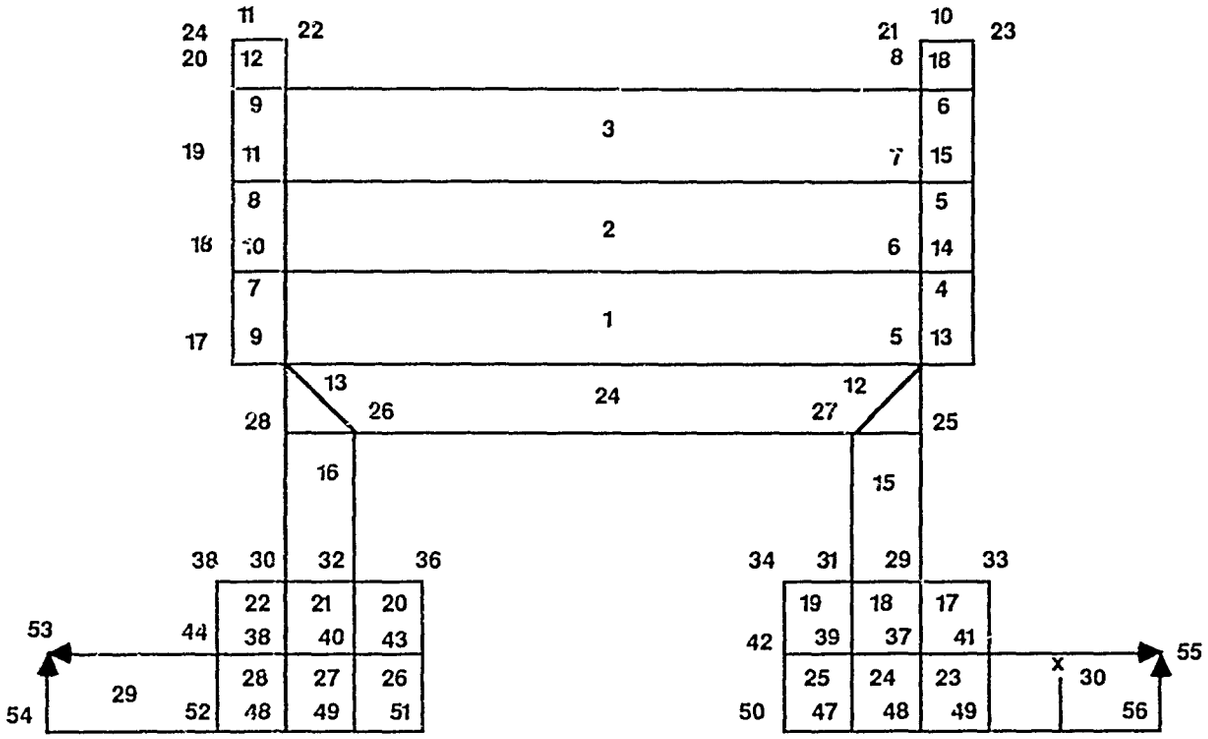


Figure 30. Rotor Ansys Model

| Item | Material | Material Properties | | Design-Operating | |
|---|---|---|---|---|---|
| | | Minimum Tensile Yield PSI | * Safe Tensile Stress PSI | Maximum Tensile Stress PSI | Factor of Safety |
| Rotor Lamination | Iron-Cobalt ASTM801-82 Type 1 | 30,000 | 20,000 | 9,900 | 2.02 |
| Copper End Ring | Zirconium-Copper CDA15000 | 32,000 | 16,000 | 9,900 | 1.616 |
| Copper End Ring & Bars | Zirconium-Copper CDA15000<br>Filler Metal Bag-1 QQ-B-650 | 32,000 | 16,000<br>10,500 | 6,350 | 1.653 |
| Shrink Ring | Inconel 625 | 60,000 | 51,600+ | 49,000 | 1.05 |
| Shaft/End Plate Joint | ANSI 4130 Steel | 40,000 | 35,000 | 25,200 | 1.389 |

* Adjusted for Temperature and Cyclic Effects
+ Adjusted for Temeprature Only (See Text)

Figure 31. Centrifugal Stresses (9000 RPM)

| Item | Material | Material Properties | Design-Operating | |
|---|---|---|---|---|
| | | Minimum Tensile Yield PSI | Maximum Tensile Stress PSI | Factor of Safety |
| Rotor Lamination | Iron-Cobalt ASTM801-82 Type 1 | 30,000 | 13,500 | 2.22 |
| Copper End Ring | Zirconium-Copper CDA15000 | 32,000 | 13,500 | 2.37 |
| Copper End Ring & Bars | Zirconium-Copper CDA15000<br>Filler Metal Bag-1 QQ-B-650 | 32,000<br>40,000 | 8,600 | 3.72 |
| Shrink Ring | Inconel 625 | 60,000 | 41,600 | 1.44 |
| Shaft/End Plate Joint | ANSI 4130 Steel | 40,000 | 34,000 | 1.18 |

Figure 32. Centrifugal Stresses (10500 RPM)

Bending and torsional stress in the shaft end assembly are shown in Figure 33. The shaft working stresses are adjusted for operating temperature.

The stress and deflection in the forward bulkhead are shown in Figure 34. The working stress is not adjusted since the operating temperature is low and the number of repetitions is not expected to be large.

The assembly stresses in the housing and stator are shown in Figure 35. The worst case stress condition occurs at the low temperature limit since the external housing has a larger coefficient of thermal expansion than the stator. The resultant interference at operating temperature is also shown to demonstrate that the stator does not become loose in the housing under this condition.

Bearing life and shock handling capability are shown in Figure 36. Safety factors are large because bearing size was made large to fit over the shaft which was sized to carry the torque.

The critical speeds are shown in Figure 37. As can be seen, the first critical speed is well above the maximum operating speed of the motor.

Stress calculations are found in Appendix IV.

2.3.2.7 Rotor/Stator Thermal Predictions

A summary of the motor losses at nominal conditions is shown in Figure 38. The rotor losses and a portion of the stator winding end turn losses are rejected to the internal oil cooling system which in turn rejects these losses to seawater via the oil-to-water heat exchanger implemented in the outer motor housing. The remaining motor losses are rejected to seawater by radial conduction through the stator core to the outer motor housing.

Finite difference models were used to predict temperature distribution in the motor wound stator core and rotor cage. The analysis is based on 26.6°C (80°F) seawater flowing past the motor housing at a velocity of 10 ft./sec. The rotor temperature analysis indicates that 904 watts will be transferred across the motor air gap from the rotor O.D. to the I.D. of the stator core under nominal steady state load conditions. The remaining rotor loss is conducted axially along the rotor bars to the rotor cage end rings where it is rejected to the internal oil coolant.

| Load | Type of Stress | Point of Maximum Stress | Material | Safe Working Stress PSI | Actual Stress PSI | Factor of Safety |
|---|---|---|---|---|---|---|
| 7G Shock | Bending | Stub Shaft Adjacent to Hub | PH13-8 MO Stainless Steel | 190,500 | 2,040 | 93 |
| 1.3 Nominal Torque | Torsional Shear | Stub Shaft Adjacent to Coupling | PH15-8 MO Stainless Steel | 75,000 | 22,600 | 3.32 |
| Assembly | Tangential | Inside Diameter of Lamination | Permendur V 50% Cobalt Steel | 30,000 | 12,000 | 2.5 |

Figure 33. Shaft Stresses

| | |
|---|---|
| Load | 7G Shock = 525/LBF |
| Type of Stress | Bending |
| Material | Aluminum 6061-T6 |
| Safe Working Stress | 40,000 PSI |
| Actual Stress | 1700 PSI |
| Factor of Safety | 23.5 |
| Deflection | .002 in. |

Figure 34. Forward Bulkhead Stress

## Maximum Interference

Operating Point = 50°F

Assumptions: Max Interference at Room Temp (.014 in.)

Interference at Operating Point = .016 in.

| Item | Material | Safe Stress PSI | Actual Stress PSI | Factor of Safety |
|---|---|---|---|---|
| Housing | Aluminum 6061-T6 | 40,000 | 10,400 | 3.84 |
| Stator | Permendur - V<br>50% Cobalt Steel | 30,000 | 10,400 | 2.88 |



## Minimum Interference

Operating Point: Steady State Full Load
Average Housing Temp 136°F
Average Stator Temp 170°F

Assumptions: Min Interference at Room Temp (.008 in.)

Interference at Operating Point = .004 in.

Figure 35. Housing and Stator Assembly

## LIFE

| Load Mechanism | Rotor Weight | Spring Washer | |
|---|---|---|---|
| Load LBF. | 37.5 | 39.0 | |
| **Oper Speed RPM** | **Expected Life Hrs.** | **Required Life Hrs.** | **Safety Factor** |
| 9000 | 42,800 | 500 | 85.6 |

## SHOCK

| Load Direction | Shock Load LBF | Brg Cap LBF | Safety Factor |
|---|---|---|---|
| Axial | 525 | 1,772 | 3.38 |
| Radial | 263 | 1,136 | 4.33 |

Figure 36. Bearing Loads

Shaft Weight: 76 LBM

Bearing Stiffness: 400,000 lb/in

Model Lumped-Mass Modal Analysis Program, CRTSPDM

Results:

1st Critical Speed 16,900 RPM

2nd Critical Speed 40,700 RPM

Figure 37. Critical Speed

416.67 HP
G/Box Eff = 96%

**Motor Loss Segregation (Watts)**

| Stator | | | Rotor |
|---|---|---|---|
| **Heat Generated** | | | |
| Sta $I^2R$ | 5856 | Bar $I^2R$ | 2246 |
| Core | 1104 | E/R $I^2R$ | 581 |
| SLL (Stray Load Loss) | 777 | SLL | 777 |
| Windage (Drum) | 131 | Oil Drag | 150 |
| | 7868 | | 3754 |
| **Heat Transfer** | | | |
| Rot → Sta (Gap Path) | +904 | Rot → Sta | -904 |
| To Housing Conduction Path | 8772 | To Oil System | 2850 |

Figure 38. Motor Losses/Heat Transfer

The predicted results of the stator analysis are shown in Figure 39 for nominal load conditions. The model used assumed that no heat was transferred from the stator end turns to the internal oil coolant. This assumption produces the worst case stator coil temperature distribution. Winding top coil temperatures are found to be the highest since the losses are larger in this coil and it is further from the cooling jacket than the bottom coil. Since the model assumes that the top and bottom coils are physically disconnected in the end turn area, the temperature difference between coils is higher than anticipated. This is due to the fact that every top coil is physically connected to a bottom coil in the actual winding.

A minor modification to the above model was made to determine the effect of oil cooling of the end turns. The modification consisted of the removal of 1,040 watts from the end turns of the top coils via convection to the cooling oil. This is equivalent to conducting away all the heat generated in this portion of the end turns and is based on a conservative estimate of the amount of heat transferred to the oil via convection.

The results of this modified model are shown in Figure 40. The highest temperature (180°C) is located at the end of the top coil. The insulation system selected for this design will withstand this environment for 500 hours as required.

Steady state rotor cage temperatures at nominal load conditions are shown in Figure 41. The rotor model assumes that no rotor losses flow from the rotor core to the rotor shaft and hub assembly. The only paths permitted for heat flow in the model consist of the motor air gap and the axial route along the rotor cage bars to the cage end rings. This assumption yields a worst case model for the rotor temperature analysis. The primary concern is that no rotor component temperature be in excess of the oil coolant temperature limit which is 180°C (356°F) for nominal conditions and 204°C (400°F) for the overload condition. A radial temperature profile for a rotor end ring is also shown indicating a maximum temperature of 120°C (248°F) at the ring O.D.

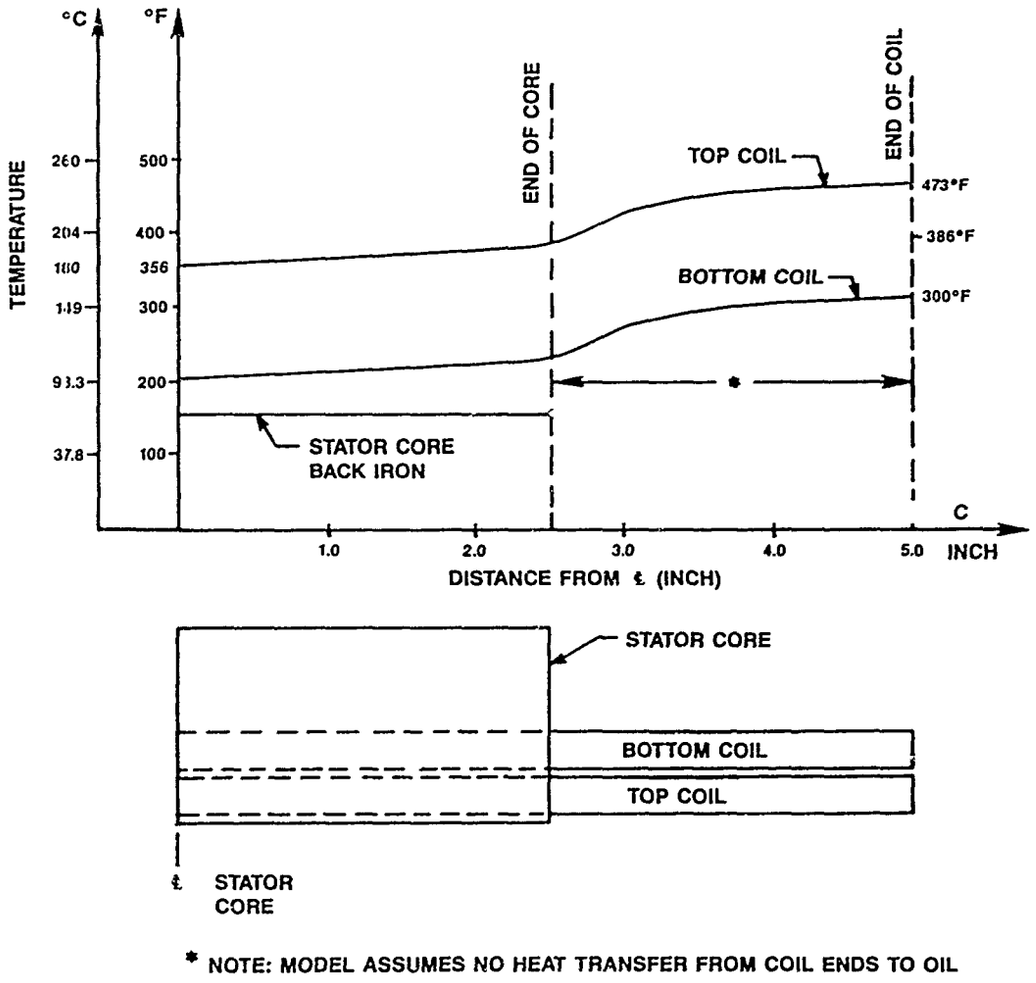


Figure 39. Predicted Steady State Stator Temperatures (Nominal Conditions); Original Model

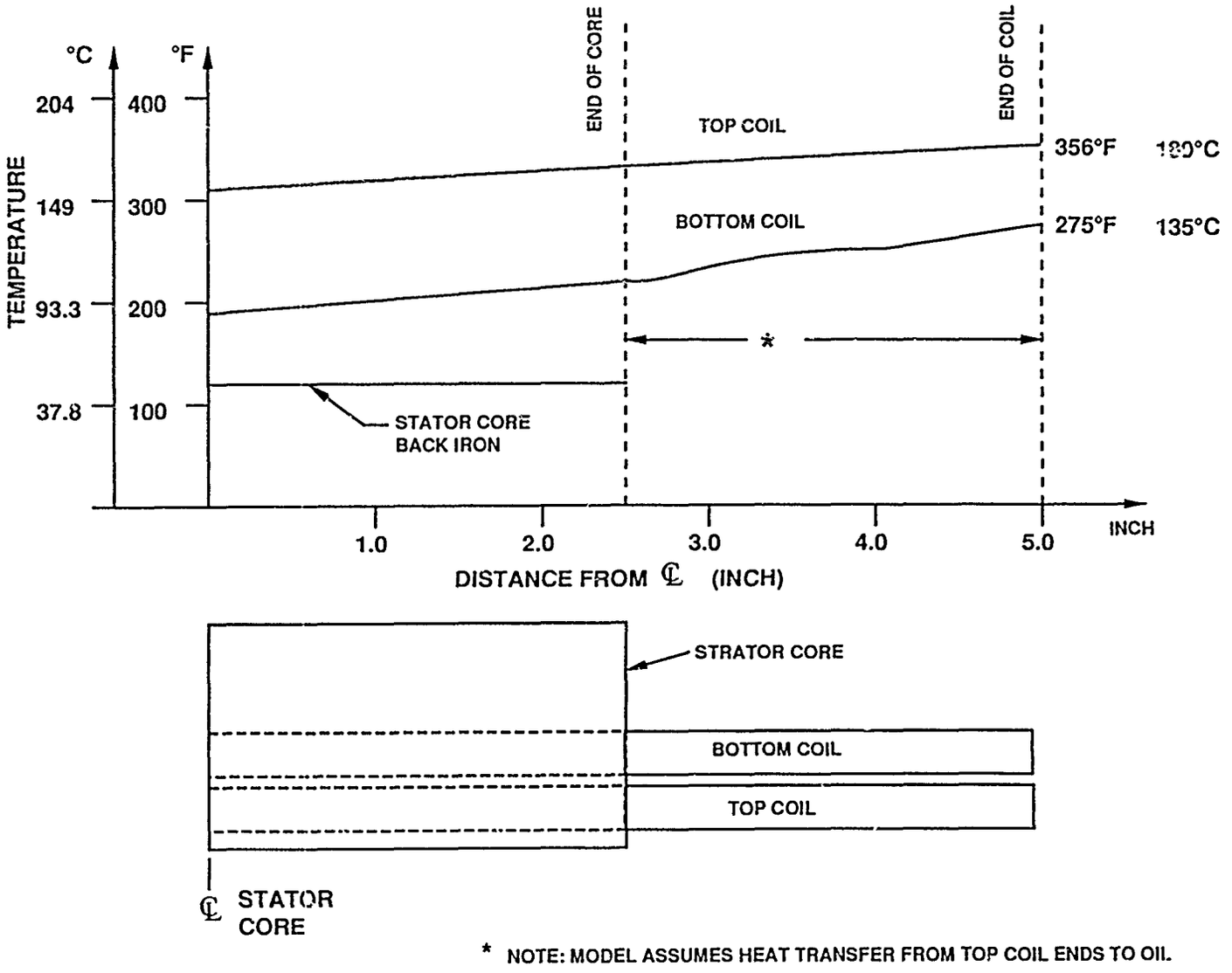


Figure 40. Predicted Steady State Stator Temperatures (Nominal Conditions); Modified Model

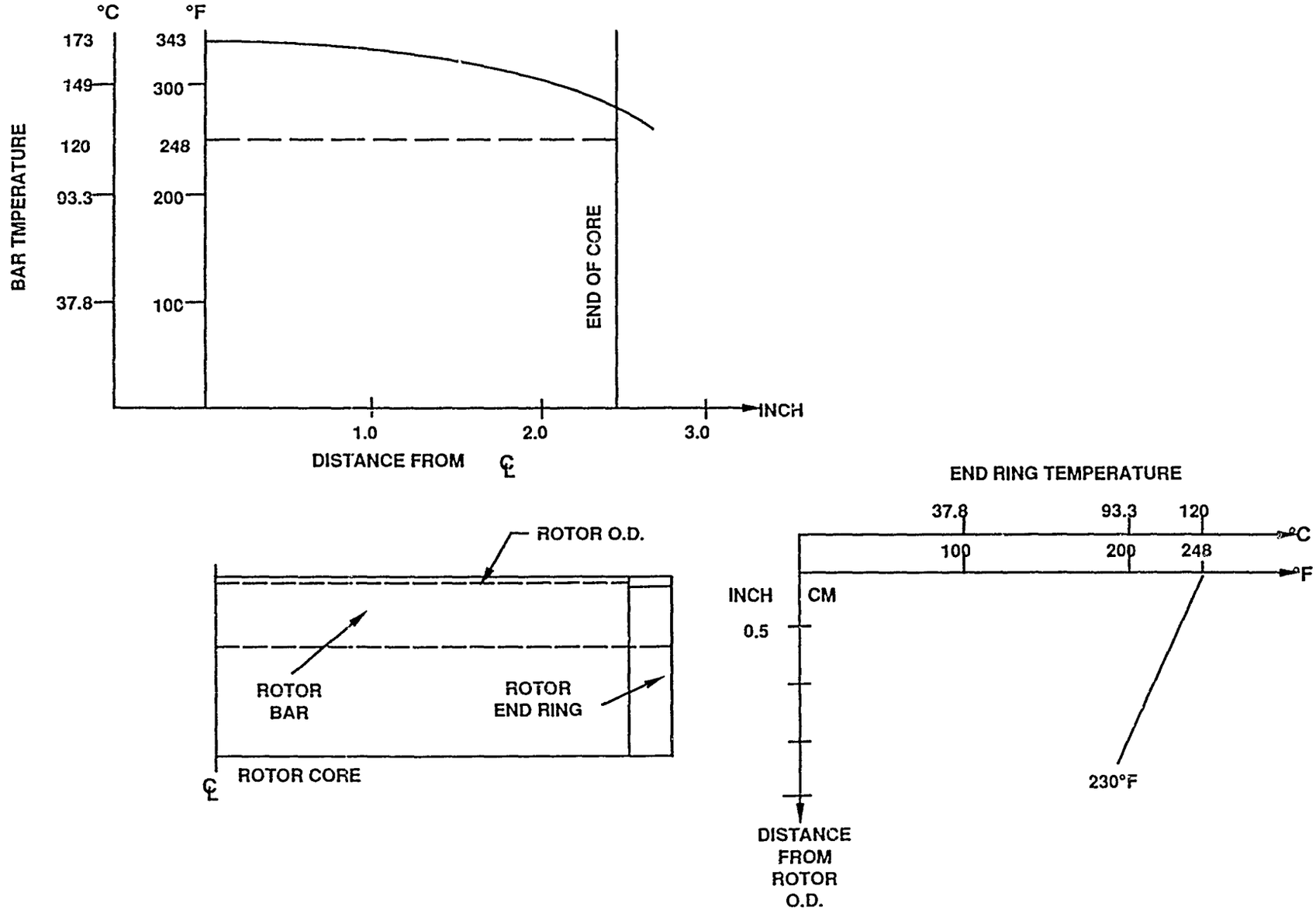


Figure 41. Predicted Steady State Rotor Cage Temperatures (Nominal Conditions)

Rotor bar thermal transient response is depicted in Figure 42. These results indicate the rotor bar thermal response to the 60 second 30% overload condition. The maximum rotor bar temperature after one minute reached 195°C (383°F) and is located at the axial centerline of the rotor. The rotor cage, therefore, has adequate thermal storage to meet the overload requirement. Continued operation at 1.3 overload will result in steady state rotor bar temperatures of 306°C (583°F). This temperature exceeds the maximum allowed oil temperature of 204°C. Therefore, continuous operation at 1.3 overload is not permitted.

2.3.2.8 Motor/SDG Thermal Analysis

A schematic of the oil system is shown in Figure 16. Oil is drawn from the sump in the bottom of the motor through the 20 micron filter into the lubrication pump located in the SDG. The filter is located in the sump and can be removed for cleaning or replacement through an access port in the bottom of the sump. From the pump the oil flows into the heat exchanger surrounding the motor and on into passages which feed lubricating oil to bearings and gears and cooling oil to the rotor. A relief valve at the outlet of the pump prevents excessive pressure from developing.

The assumptions used in the thermal analysis are shown in Figure 43. These assumptions lead to a worst case analysis for the system. The required oil flow rate was established through an iterative process. A safe hot oil temperature was selected based on the SDG manufacturer's recommendation and an estimate was made at the cold oil temperature that could be produced with the heat exchanger. The required oil flow rate was then calculated from the temperature difference and the total heat flow into the oil.

The temperature drop in the heat exchanger was then calculated to verify the cold oil temperature used. The new cold oil temperature was then used to adjust the required oil flow rate and the entire process repeated.

The thermal model is shown in Figure 44. In this model the heat exchanger is treated as two separate units. The first unit surrounds the stator and transfers heat from the stator through its walls to the water outside as well. In addition to this, heat from the oil is transferred to the fins in the outer shell and into the water.

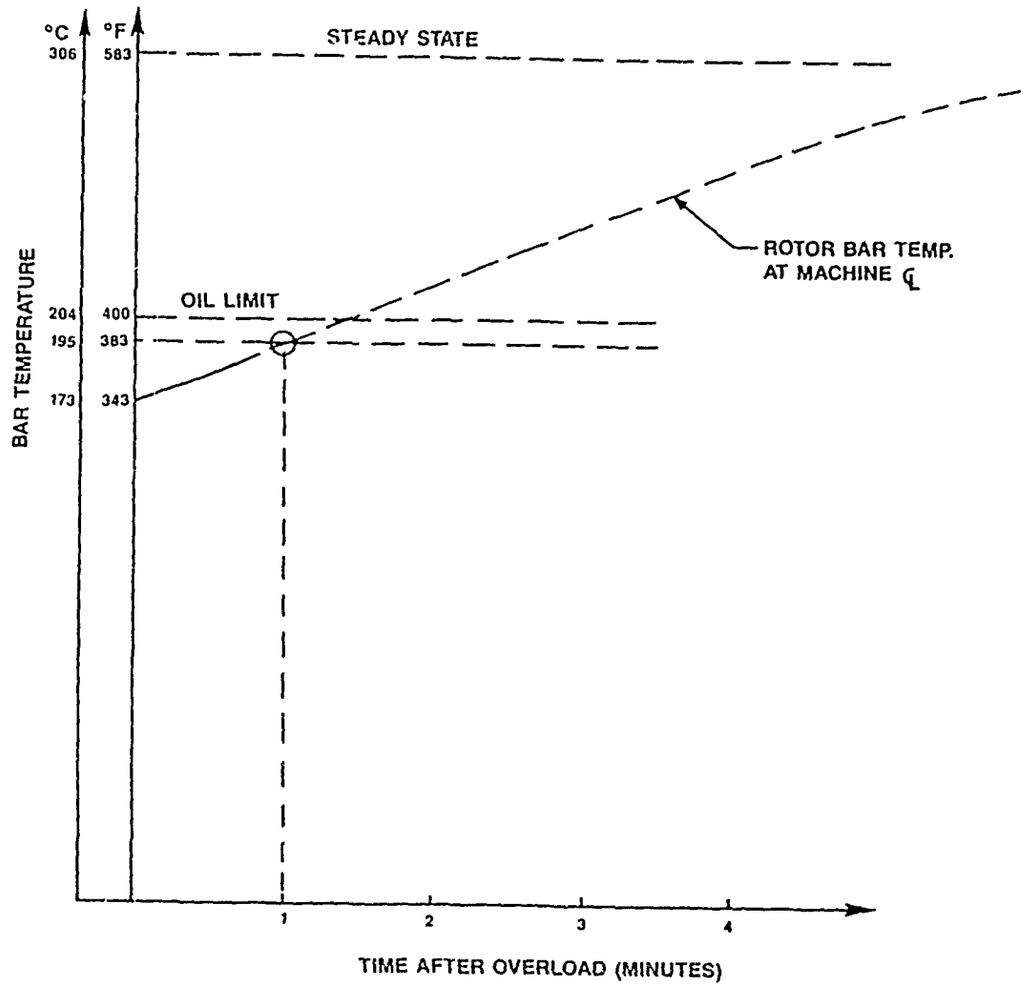


NOTE: MAGNITUDE OF OVERLOAD IS 1.3X NOMINAL



05/204/88/026

Figure 42. Thermal Transient Response of Rotor Cage Bar (1.3 Per Unit Overload)

- Steady State
- 400 HP
- 80 F Water Temperature
- 10 FPS Water Velocity
- Efficiency
  - 96% Gearbox
  - 96.2% Motor

Figure 43. Thermal Design Assumptions (Oil Temperature)

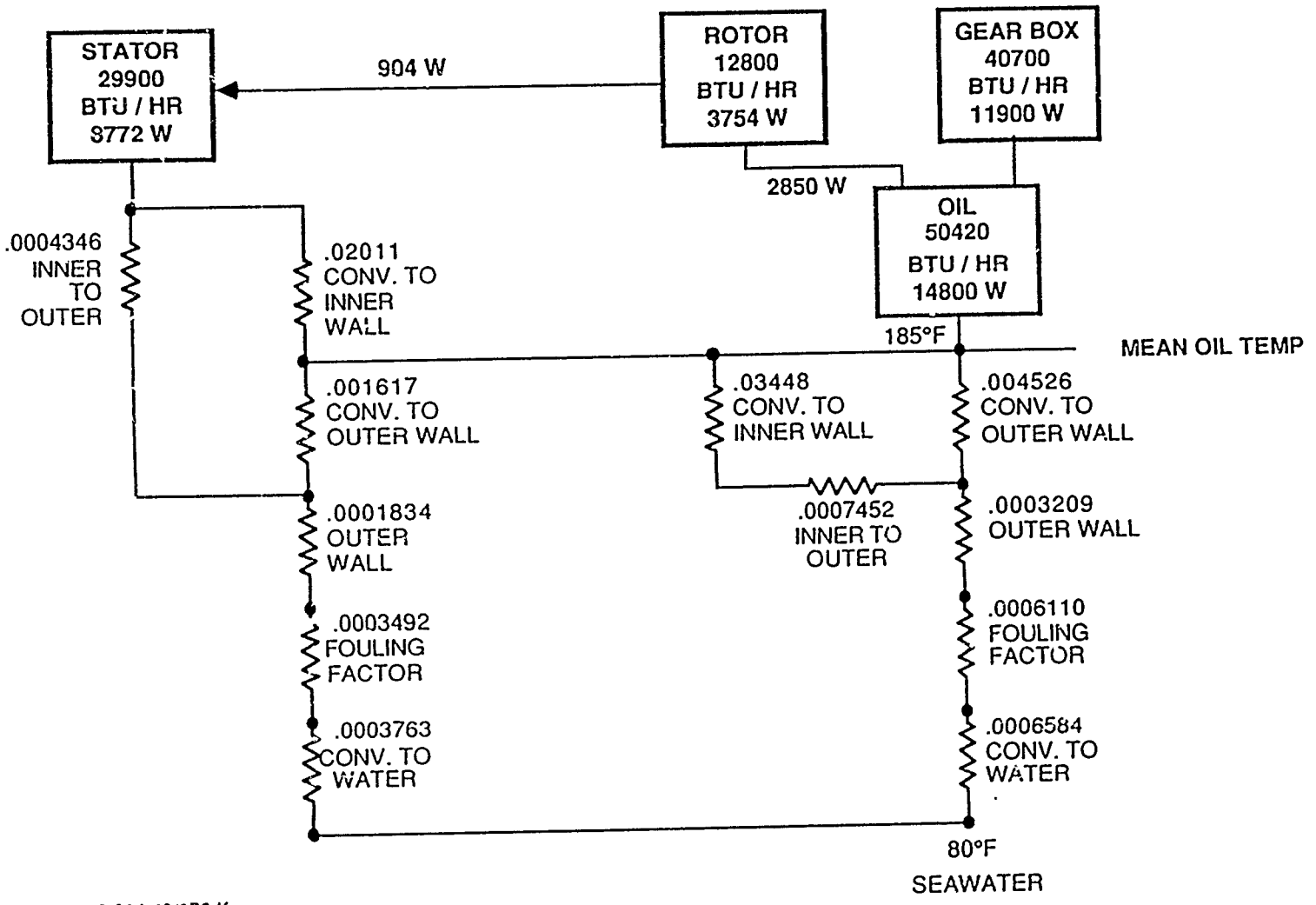


Figure 44 Thermal Model (No End Turn Cooling)

The second unit represents the section of heat exchanger between the stator and SDG and the section between the stator and forward bulkhead combined. This unit transfers heat from the oil to the fins and outer shell to the water but does not carry heat from the stator.

After all thermal resistances were calculated, node equations were written and solved simultaneously with a matrix algorithm. To verify the analytical results an experimental heat exchanger similar in design to that used in the motor was fabricated and tested. The test results are shown in Figure 45.

The thermal model was modified as shown in Figure 45 to include the 1040 watts transferred from the end turns to the oil in the modified stator model. This resulted in a 6 degree F rise in the mean oil temperature prediction. This is offset by the higher than predicted heat flow observed in the experimental heat exchanger and is not expected to occur in the actual design.

The thermal calculations are shown in Appendix V.

### 2.3.3 Speed Decreasing Gear

#### 2.3.3.1 Design Description

The SDG is a single stage planetary type reducer with three planets and floating sun and ring gears. The general features of the speed decreasing gear are listed in Figure 47. All gears are fabricated from Alloy steel (AISI 9310 in the sun and planet gears and AISI 4150 in the ring gear) and the housing and bulkhead are cast aluminum alloy (A-356) as shown in Figure 48. The planet carrier is made from 17-4PH stainless steel which combines high strength with the corrosion resistance it needs since the output end will be exposed to seawater. The gear teeth are a proprietary spiroid (ITW) design and are ground to a special tooth form which makes it possible to manufacture a sun gear with a small number of teeth without undercutting. This permits a large speed reduction in a single stage.

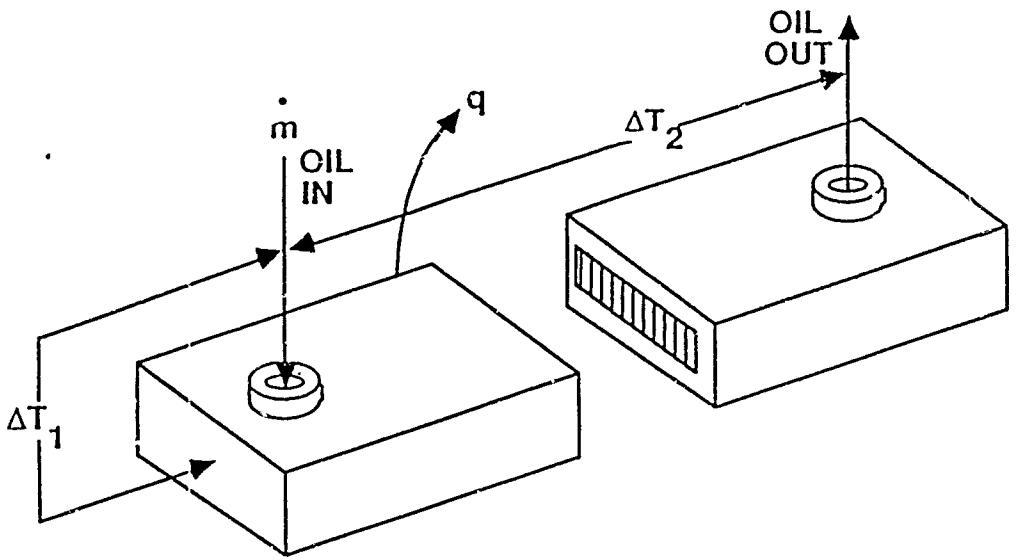


HEAT FLOW PREDICTED BY MODEL

q = 6110 BTU/HR

HEAT FLOW MEASURED

q = 8041 BTU/HR (32% GREATER THAN PREDICTED)

MEASURED DATA:

$\Delta T_1$ TEMPERATURE DIFFERENCE (OIL TO EXCHANGER)

$\Delta T_2$ TEMPERATURE DIFFERENCE (OIL IN-OIL OUT)

$\dot{m}$ MASS FLOW RATE OF OIL

05/204/88/077-k

Figure 45. Model Verification

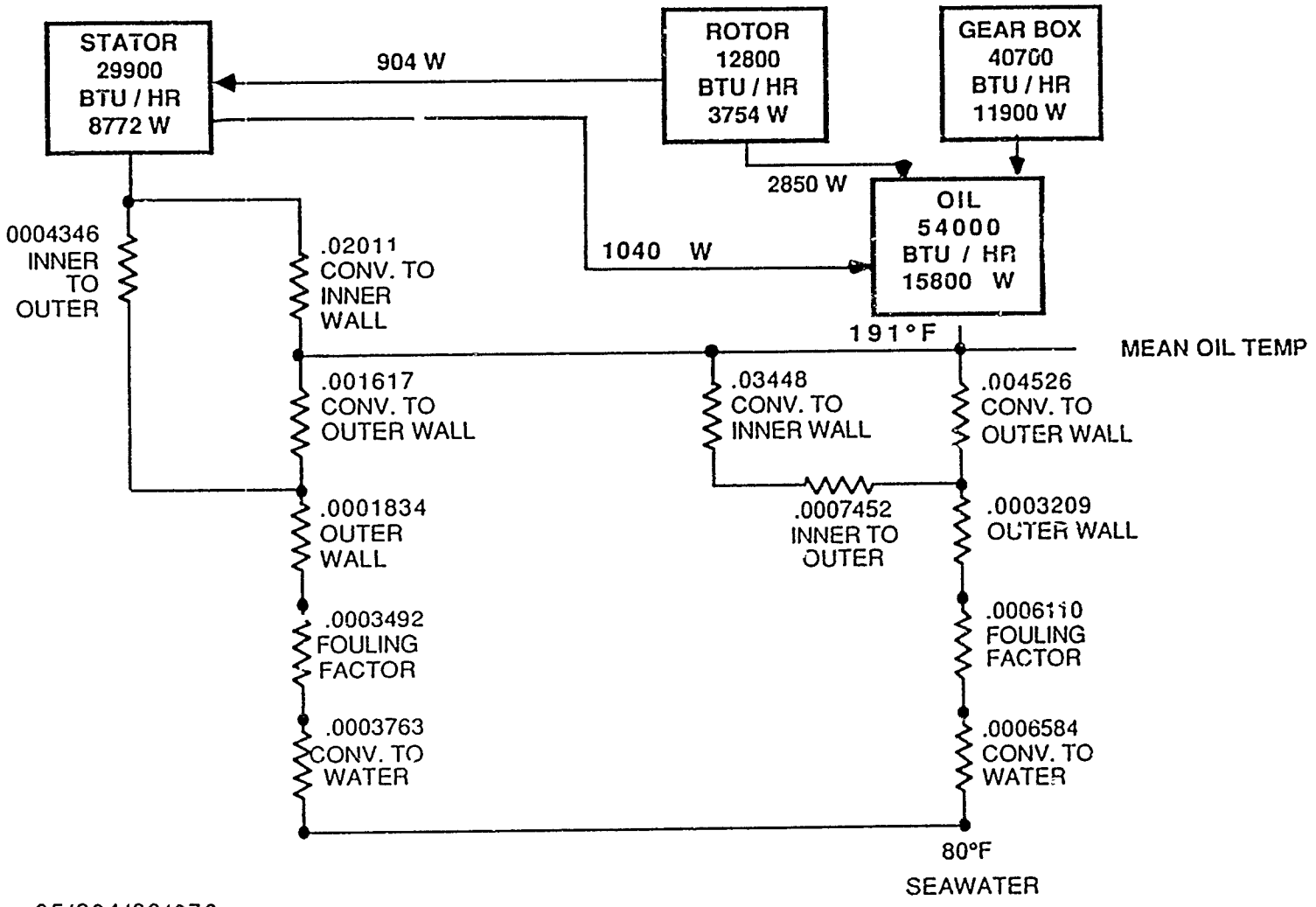


Figure 46. Thermal Model (With End Turn Cooling)

- Gear Ratio 7:1
- Gear System: Planetary with Sun Gear
- Tooth Form: Concurve
- Housing Material: Cast A-356 Aluminum
- Motor Interface: Common Bulkhead
- Oil Pump: Gear Driven



Figure 47. Speed Decreasing Gear

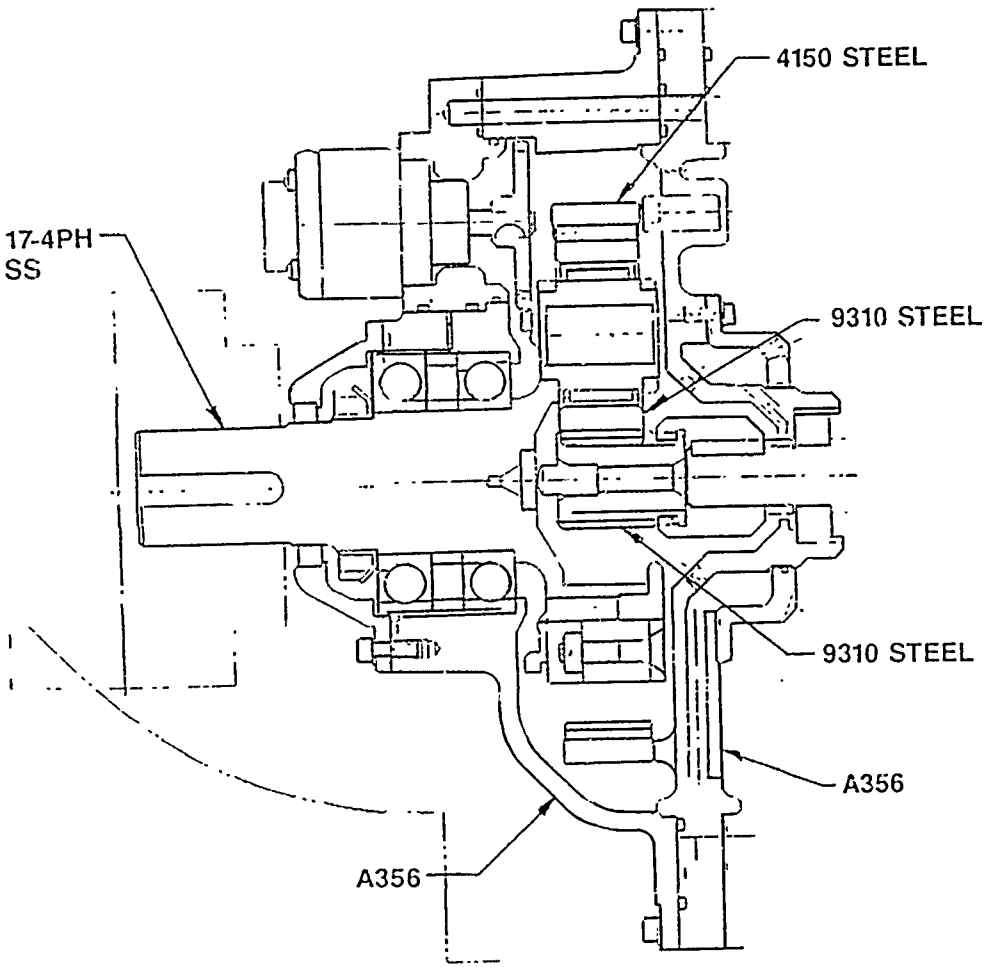


Figure 48 Speed Decreasing Gear Construction

The oil pump is a special gear pump design consisting of steel gears and shafts in a bronze case. A mechanism inside the pump causes the oil to be delivered to the same port regardless of the direction of rotation. A gear on the pump input shaft meshes with a gear on the planet carrier in the SDG. The pump runs at 3125 RPM and delivers 3.5 GPM of oil when the SDG runs at full speed.

Minimum weight and volume were major considerations in the SDG design. The floating ring gear and sun gear more evenly distributes the load among the planet gears resulting in a lighter set of gears for the required power. Weight and volume considerations were also the reasons for the selection of A-356 aluminum for the gearbox and bulkhead castings. The gearbox weight breakdown is given in Figure 49.

2.3.3.2 GEAR TOOTH STRESSES

All stress calculations for Concurve gear teeth are done by Spiroid developed computer programs. The general approach is conventional but several refinements have been made to help create a more comprehensive stress analysis.

Bending stresses are calculated for two points on both pinion (sun) and gear (planet): 1) tip load assuming only one tooth carrying the full load (actual stresses are half this value since the load is actually shared by two teeth in accurate gearing) and 2) "worst point load" (highest point of single tooth contact).

Compressive (Hertz) stresses are calculated for many points along the tooth profile from tooth tip to lowest point of contact.

The stresses in the ring gear teeth are not a factor in the gearbox design since they are much lower in value than the sun gear and planet gear stresses. Therefore only the sun and planet gear stresses are shown.

| Item | Weight, lbM |
|---|---|
| Output Shaft Carrier | 8.66 |
| Housing | 10.87 |
| Bulkhead | 11.51 |
| Planet Gears (3) | 5.81 |
| Ring Gear | 6.41 |
| Pump | 4.50 |
| Misc. | 18.74 |
| **Total** | **66.50** |

Figure 49. Speed Decreasing Gear - Weights (lbm)

Loads used for stress calculations were derived from a steady state input horsepower to the gearbox of 416 horsepower. In evaluating maximum torque overload stresses, a 1.3 factor was used. These stresses were then compared with the bending yield strength of 135,000 psi and compressive (Hertz) yield strength of 450,000 psi for 9310 alloy steel used in both gears) to determine factors of safety. Figure 50 summarizes stress analysis results.

Stresses for other components of the SDG are shown in Figure 51. The stresses in the input key and input coupling are directly due to the input shaft torque. The ring gear tang and bulkhead dowel pin prevent rotation of the ring gear. There are two dowel pins and two sets of tangs. The stresses are calculated in the basis of the entire load on one dowel pin. The calculations for the above stresses are found in Appendix IV.

### 2.3.4 Coupling

#### 2.3.4.1 Design Description

The coupling shown in Figure 10, is a double flex gear type made of 316 stainless steel. Seals at each end of the sleeve retain lubricant in the coupling. This design was selected on the basis of minimum size and weight and the capability to operate under seawater.

#### 2.3.4.2 Mechanical Stresses

The coupling was sized by derating a known design of alloy steel on the basis of the comparison of its yield strength compared to 316 stainless steel. The maximum torque rating (5180 ft-lb) provides a safety factor of 2.37 for 1.3 nominal overload condition.

#### Miscellaneous Stresses

Stresses for other components of the SDG are shown in Figure 51. The stresses in the input key and input coupling are directly due to the input shaft torque. The ring gear tang and bulkhead dowel pin prevent rotation of the ring gear. There are two dowel pins and two sets of tangs. The stresses are calculated on the basis of the entire load on one dowel pin. The calculations for the above stresses are found in Appendix IV.

## Sun/Planet Gear Tooth Stress Analysis Summary

| Gear | Torque/ Tooth Load (HP) | Root Bending Stress | Bending Stress Allowable | Safety/ Service Factor | Compressive (Hertz) Stress | Compressive Stress Allowable | Safety Service Factor |
|---|---|---|---|---|---|---|---|
| Sun | 2942 in. lb./ 1401 lb. T.L. (416 HP) | 20,404 PSI | **50,500 PSI | 2.48 | 177,320 PSI | **230,000 PSI | 1.30 |
| | 3825 in.lb./ 1821 lb. T.L. (1.3 x overload) | 26,460 PSI | 135,000 PSI | 5.10 | 202,160 PSI | 450,000 PSI | 2.22 |
| Planet | 1401 lb. T.L. (416 HP) | 20,845 PSI* | **53,000 PSI | 2.54 | 177,320 PSI | **250,000 PSI | 1.40 |
| | 1821 lb. T.L. (1.3 x overload) | 18,948 PSI | 135,000 PSI | 7.12 | 202,160 PSI | 450,000 PSI | 2.22 |

* Planet gear tooth bending fatigue stresses include a 1.43 factor to account for reverse bending of planet gear teeth.

** Adjusted for cyclic effects.

Figure 50. Gear Tooth Stresses.

| Item/Material | Type of Stress | Safe Working Stress PSI | Actual Stress PSI | Factor of Safety |
|---|---|---|---|---|
| Input Shaft Key 4140 Steel | Shear | 66,000 | 24,920 | 2.65 |
| | Compressive | 132,000 | 49,000 | 2.69 |
| Input Coupling 4150 Steel | Shear (in neck) | 72,000 | 4,320 | 16.7 |
| | Shear (in spline teeth) | 72,000 | 8,020 | 8.98 |
| | Compressive (in spline teeth) | 145,000 | 10,100 | 14.4 |
| Ring Gear Tang 4150 Steel | Bending | 145,000 | 62,400 | 2.32 |
| Bulkhead (seat for dowel pin) A356 Aluminum | Compressive | 22,000 | 11,000 | 2.00 |

Figure 51. SDG Stresses – at 1.3 Nominal Torque

## 2.4 Power Cable

As shown in Figure 1, the power cable transmits the electrical energy from the alternator to the motor/SDG. Three cables are required, one for each of the three phases of the motor. The cable was selected based upon the design requirements shown in Table 6.

TABLE 6. CABLE REQUIREMENTS

| | | | |
|---|---|---|---|
| ELECTRICAL | MOTOR CURRENT | | 392 $A_{rms}$ continuous<br>531 $A_{rms}$ 60 seconds<br>1,000 $A_{rms}$ 5 seconds |
| | DIELECTRIC VOLTAGE | | 1,000 $V_{rms}$, 450 Hz continuous<br>2,040 $V_{rms}$, 60 Hz 60 seconds |
| PHYSICAL | PRIMARY INSULATION | | 200°C |
| | SIZE | | 4/0 AWG |
| | BEND RADIUS | | 1 FT. Max |
| | WEIGHT | | .944 LB/LINEAR FT. NOMINAL |
| ENVIRONMENTAL | COMPATIBILITY | | OIL, SEAWATER AND ABRASION RESISTANT |
| | OPERATING | TEMPERATURE | 0-32°C |
| | | LIFE | 500 HR MIN |
| | STORAGE | TEMPERATURE | -40 to 125°C |
| | | LIFE | 10 YR, DAMP SALT AIR |

The selected 4/0 AWG cable results in a nominal current density of 2424 amps/in$^2$. A pictorial of the cable is shown in Figure 52. The conductor has 259 strands of 21 AWG tinned solid wire. This stranding insures that the cable can meet the bend radius requirement. The primary insulation is silicon rubber impregnated glass fiber overwrapped with mylar tape. The outer jacket is polyurethane with an internal kevlar braid. The cable has a nominal outside diameter of 1.015 in.

Power Connector

The main lead power connector is shown in Figure 53. There are three such connectors for each motor. The main lead power connector consists of the power feed through, the bolted joint and the power connector housing.

The three power feed throughs are fabricated from oxygen free copper (OFC) rod for maximum conductivity and are individually brazed to their respective phase winding connection. The current density of the power feed through at the connection is approximately the same as that of the phase winding. The power feed through is electrically insulated from the motor housing via vespel bushings and is sealed with Viton "O" rings. The vespel material and the viton o-rings were selected because of their compatibility with the coolant oil (MIL-L-7808). The viton o-rings will maintain their elasticity when subjected to the coolant oil. The power feed through and the cable assembly is silver plated at the bolted joint to improve electrical conduction with the mating parts and to eliminate oxidation of the copper feed through. The power connector housing is fabricated from aluminum bar and has a polyurethane boot at its inside diameter to provide the necessary environmental seal and ground insulation.

## 2.5 Propulsion System Controller (PSC)

The controller must provide excitation control for the AC alternator in response to the prime mover speed so that the volts/hertz ratio of the alternator output is kept essentially constant. This provides required AC power to the motor for full output torque capability and variable speed proportional to the prime mover speed. System component characteristics are presented in other portions of this report.

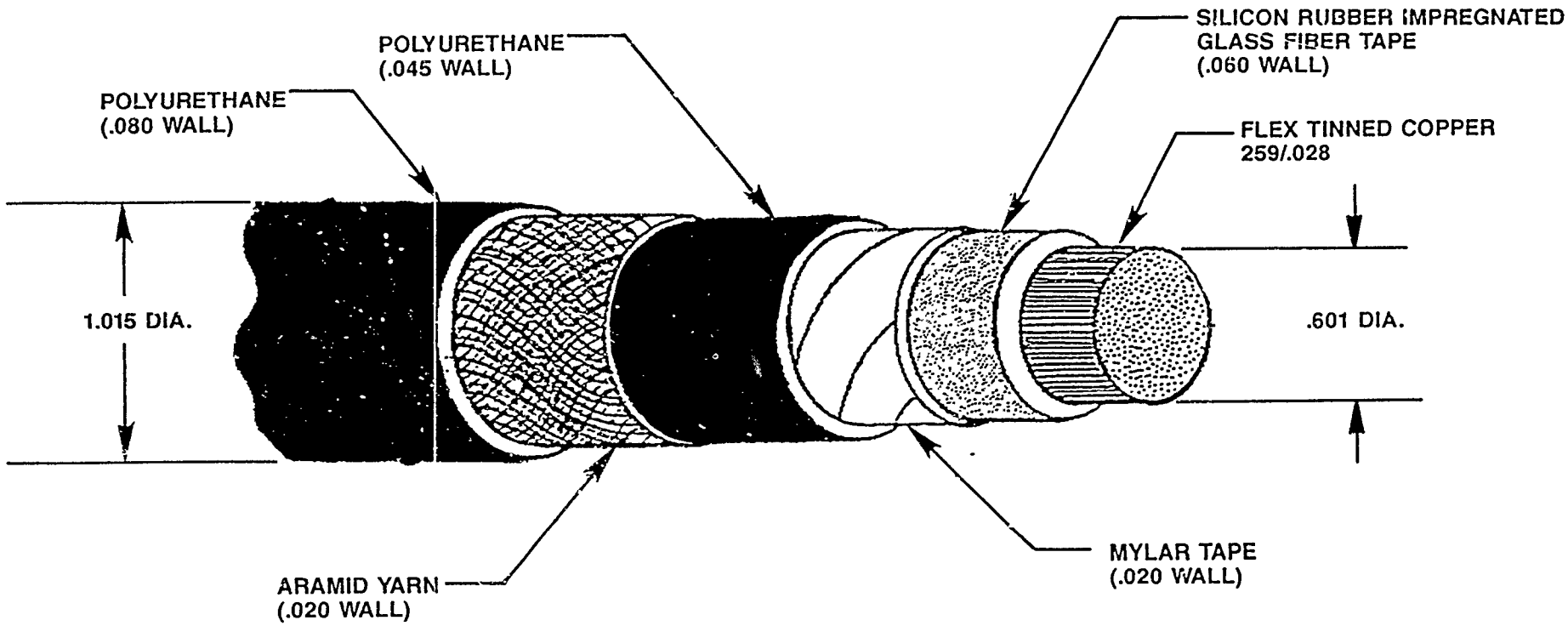


DIMENSIONS IN INCHES

Figure 52. Motor/Alternator Cable

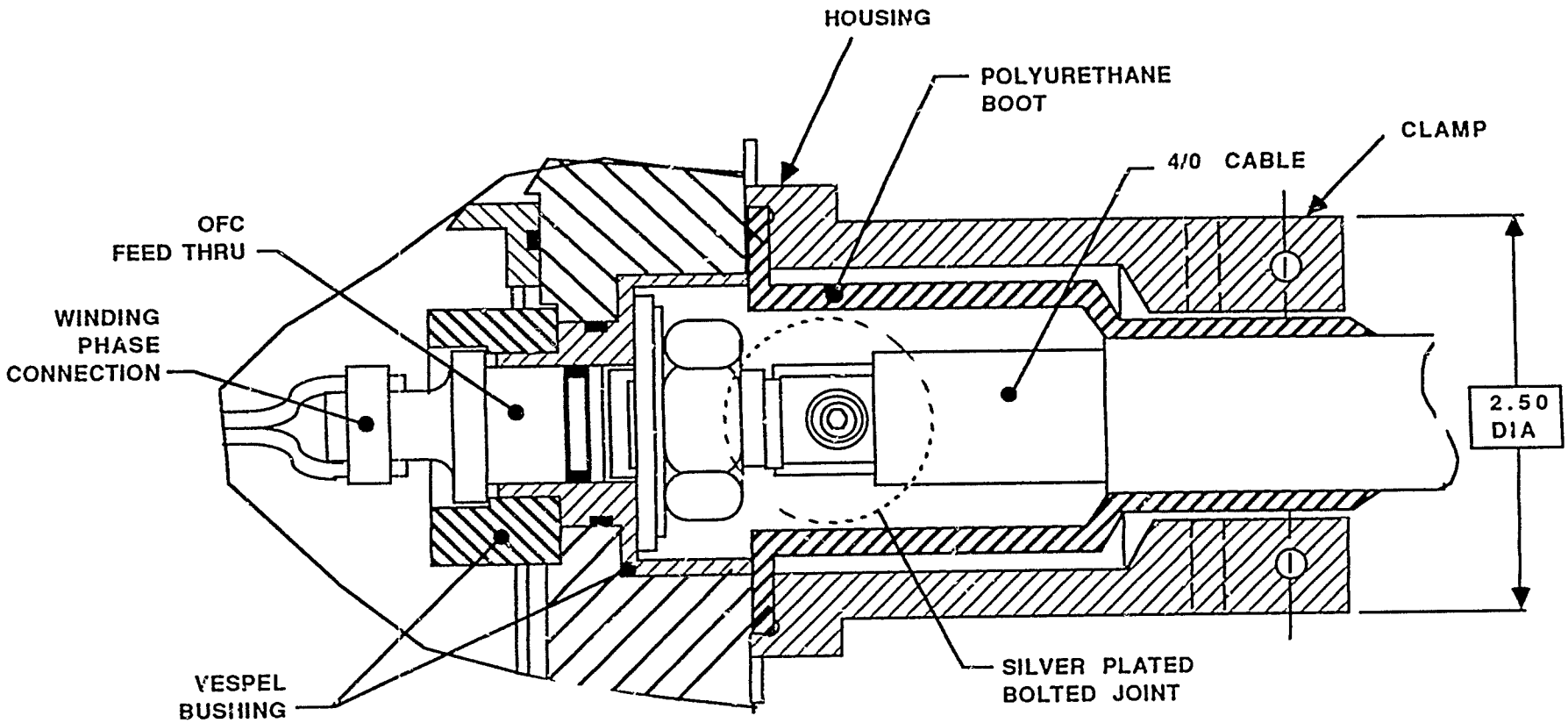


Figure 53. Main Lead Power Connector

In addition to the above requirements the controller must monitor and provide inputs to the display panel for the following parameters: component temperatures; motor RPM; start/stop or run action of this system in response to operator command; and fault indication and automatic shut-down to protect system hardware.

2.5.1 Performance Requirements

Inputs:

The controller shall have the necessary inputs to monitor the alternator and the motor/SDG critical temperatures which limit system performance. Motor RPM shall be monitored.

Provisions shall be made to start, stop and reliably safeguard the system during its operation. Multiple safeguards must be used to ensure positive system control under adverse malfunction.

The vehicle operator's actions (start, stop, speed adjust, etc.) and the automatic sequencing and control of each of the alternators and motors must be accommodated by the controller.

The alternator permanent magnet generator (PMG) shall be used as the volts/hertz reference signal for closed loop feedback control of the propulsion system.

Outputs:

The primary output of the controller shall be excitation current to the rotary exciter field located in the alternator. The current shall be an outcome of the closed loop control of the alternator output terminal voltage and the reference voltage (PMG output) representing the prime mover speed. This field excitation shall be satisfactory for system control from start-up through full load, load transient (as described below) and orderly shut-down.

The secondary outputs of the controller shall provide necessary drives to the control panel instrumentation for visual indication of temperatures, propulsor speed and operating modes as well as vehicle operator's activities.

System Stability:

The controller shall provide the above described system with alternator terminal voltage control to follow the reference signal to within +/- 3% of its linear operating range excluding transients. When load transients occur, a sightly underdamped (vs. overdamped) system response is preferable to improve response time. The prime mover accelerates the alternator from 4300 RPM to 9000 RPM in one second. The closed loop band width of this control system shall accommodate the response of the prime mover.

System Start-up:

The controller shall support the alternator operational speed range of 4300-9000 RPM as provided by the prime mover. At start up, the alternator speed shall be 4300 +/- 100 RPM. The propulsion system must start under the environmental conditions stated.

At room ambient conditions (20-25°C), the controller must provide the necessary alternator excitation to support a motor starting current of not less than 900 amperes RMS. The motor acceleration from 4300 to 9000 RPM shall be completed within five seconds to avoid thermal damage to the system components. Failure to start must be safely aborted. The start-up sequence can be repeated within the propulsion system safety protection limits.

Load Transients:

During the propulsion system's prime mover acceleration from start to full speed (corresponding alternator speeds of 4300 - 9000 RPM), the waterjet may experience transients ranging from no load to full load in 0.1 second. The controller must provide the necessary alternator excitation and subsequent output current to support the induction motor requirements resulting in continuous system operation. In addition, the instantaneous unloading of the waterjet shall not invoke a system shut-down or produce a damaging transient. A one time, one minute, 1.3 system overload must be supported by the controller hardware.

System Shut-down:

The controller shall provide an orderly shut-down of the propulsion system. It shall also provide for instantaneous operator initiated system shut-down. The controller shall have system safety/protection functions built in its hardware and shall include mechanical interrupt capability of the alternator exciter field current. This shall be accomplished with a relay having normally open contacts.

Acoustic Noise:

The controller hardware shall not emanate acoustic noise to the environment below 20 khz at intensities perceptible to the human ear 3 feet from the equipment.

Humidity and splash proof enclosure:

The controller hardware must be operational in the salt air environment and must have a splash proof enclosure as a minimum. Shelf life shall be considered in sheltered environment only.

A detailed description of the PSC requirements is contained in Appendix I, Interface Specification.

## 2.5.2 Approach

The specifications which were the key drivers of the electrical design will be reiterated along with the design impact.

The design drivers were the size/weight requirements (1 cubic foot and 20 pounds) and the requirement for safe shutdown in cases of various fault modes (overcurrent, overtemp, excessive start time, excessive motor slip). The size/weight limitations disallowed the use of conventional switchgear (circuit breakers, fuses, contactors). Monitoring of fault conditions is performed by a microprocessor interfaced to RTD's, current transformers, and tachometers. Shutdown of the regulator is done electronically with two backup modes of shutdown, the last being to physically open the 150V supply from the field regulator amplifier using a small vacuum relay.

The requirement of monitoring multiple points in the Propulsion System Controller (PSC) also drove the design to a microprocessor with a multiplexer and an analog to digital converter.

The characteristics of the alternator and field exciter and the induction motor established the starting and running power levels of the PSC. About 75 watts output is needed to run the motor at 9000 rpm with nominal load. About 800 watts is needed for starting. The controlled variable is the alternator voltage, which must follow the prime mover speed to keep constant V/Hz. The actuated variable is the exciter field current. For the motor to start in 3 seconds at a prime mover speed of 4300 rpm, the alternator/motor line current must reach 900 amps for an ambient start (25 degrees C). Exciter field current of 9 amps gives 1000A peak during ambient start and 800A peak during a hot start (150 degrees C motor). System modeling showed that for nominal alternator parameters, 7A exciter current is sufficient. A 9A current limit was used to assure a robust system with respect to system parameter variations.

The field regulator bus voltage was selected at 150V to enable the field current to be forced faster than the time constant of the exciter field (L/R=0.1 Sec). With 150V bus and 9 Ohm max field resistance, current limit can be reached in .08 second. This was selected to satisfy the worst case load transient. This transient was hypothesized to be the case of the waterjet coming out of the water (fully unloading) and then being put back into the water (fully loading). Whether this is realistic or not is not known at this time, but it is used as a design goal. If the waterjet is fully loaded instantaneously after being out of the water, the system only recovers from the transient if the waterjet was unloaded no more than 75% (25% remaining) and then full load reapplied. With a more realistic transient of going from no load to full load with a .1 second ramp time, the system can respond with a 100V bus and 6A. Since the actual worst case transient is not known, the 150V, 9A levels in the PSC will be used to assure robustness. See section on system modeling for more detail.

The available input source is 28VDC at a max power of 2KW. Since 150VDC bus is desired, some type of voltage step-up is needed. If the 28V was fairly constant and the load was fairly constant, the 28V could be chopped at a high frequency, put through a step-up transformer, rectified and filtered to obtain 150VDC. However, 28V can vary +/-4V and the 150V load can vary from 0.5A to 6A; therefore, regulation is needed. Output voltage will be sensed and compared to a reference; the error signal will be used to pulsewidth modulate the chopped AC waveform to compensate for line and load variations. The bandwidth of this boost converter should be much greater than the field regulator current loop bandwidth (50 Hz). 1 KHz open loop crossover is the design goal. The switching frequency should be at least 10X the bandwidth. Higher frequency, however, reduces the size of the magnetics and filter capacitors. 60 KHz was selected as a compromise between size and efficiency. The 2KW limitation on 28V power necessitates that the field controllers start sequentially since each requires greater than 1000W during the 3 second starting interval.

The alternator voltage must be controlled to follow the prime mover speed in order to maintain constant V/Hz in the induction motor. Since the prime mover can go from idle to full speed in about 1 second, the alternator voltage controller (field regulator) must have a bandwidth of at least 5Hz. To obtain this bandwidth for small signal perturbations, the main field pole (0.46Hz) must be cancelled with a lead network. An integrator was also used to zero the steady state error voltage. By controlling the integration constant (1/RC), the open loop crossover can be selected. The crossover is nominally 6.7 Hz. An inner current loop is utilized also to control exciter field current and limit the maximum exciter current to 9A. This inner loop crosses over at 67 Hz nominal (10X voltage loop).

In order to adequately control the field current, the regulator must be able to force current down as well as up (instead of merely freewheeling to zero with L/R time constant). A full wave, half-controlled power bridge is used (two mosfets and two diodes). The mosfets are pulsewidth modulated at a fixed frequency of 20KHz, just above the audible range.

Due to the close proximity of power circuits and low level analog and digital circuits, noise management had to be considered carefully. The following safeguards were implemented to prevent problems:

1. High current carrying conductors and their returns were run as twisted pairs to minimize radiator loop area.

2. All logic circuits are cmos technology, which has good noise immunity.

3. The logic circuitry was layed out with multilayer boards, including a ground plane and a power plane for low receptor loop area.

4. Three isolated grounds are used in the PSC to prevent ground loops and noise coupling.

5. Physical separation of power leads and harnesses from signal leads and harnesses was implemented to prevent crosstalk.

6. An LC filter was put in between the 28VDC source and the boost converter power bridge to reduce the switching frequency and its harmonics on the 28V source. This 28V source is the input for all of the DC to DC converters used on the various cards.

### 2.5.3 Boost Converter Description

The boost converter produces a constant 150VDC output voltage to be used by the field regulator. Regulation is provided against line changes of the 28VDC source (+/-4V) and load changes demanded by the field regulator (0.5A to 6A). Each block of the block diagram in Figure 54 will be described briefly.

The EMI filtering consists of an input LC filter. The inductor is 5UH at 50ADC with a resonant frequency in the megahertz region. The capacitor consists of six 1400UF aluminum electrolytics in parallel to satisfy RMS current requirements and two 30UF polypropylene capacitors (located right at the power mosfets) to offset line inductance at the high frequency components of the switching waveform. These high frequency capacitors keep the voltage overshoot at an acceptable value. A damping resistor (0.02 Ohms) is put in series with the choke to prevent oscillations due to negative input impedance of the converter. The EMI filter smooths the current in the 28 VDC source to reduce conducted and radiated emissions to other circuits within the PSC as well as other external equipment connected to the system 28V source.

The power mosfet full H-bridge consists of two power cubes, each one being a half-bridge with 72A RMS current capability. The mosfets are pulsewidth modulated at 60 KHz to provide a variable duty cycle AC square wave to the primary of the step-up transformer. The primary current is limited to 70A by the pulsewidth modulator. The transformer is a high frequency design, ferrite pot core with extremely low leakage inductance. This is necessary to push the required peak currents through the converter at the operating frequency and duty cycle. The secondary currents (as required by the field regulator) vary from 0.6A (steady state) to about 6A (motor starting). This translates to 5.4A to 54A peaks in the transformer primary.

The transformer output is rectified and filtered to obtain a smooth 150VDC output voltage. This voltage is sensed and sent to the voltage controller where it is used to generate an error signal. The error signal is used as input to the pulsewidth modulator to adjust the duty cycle.

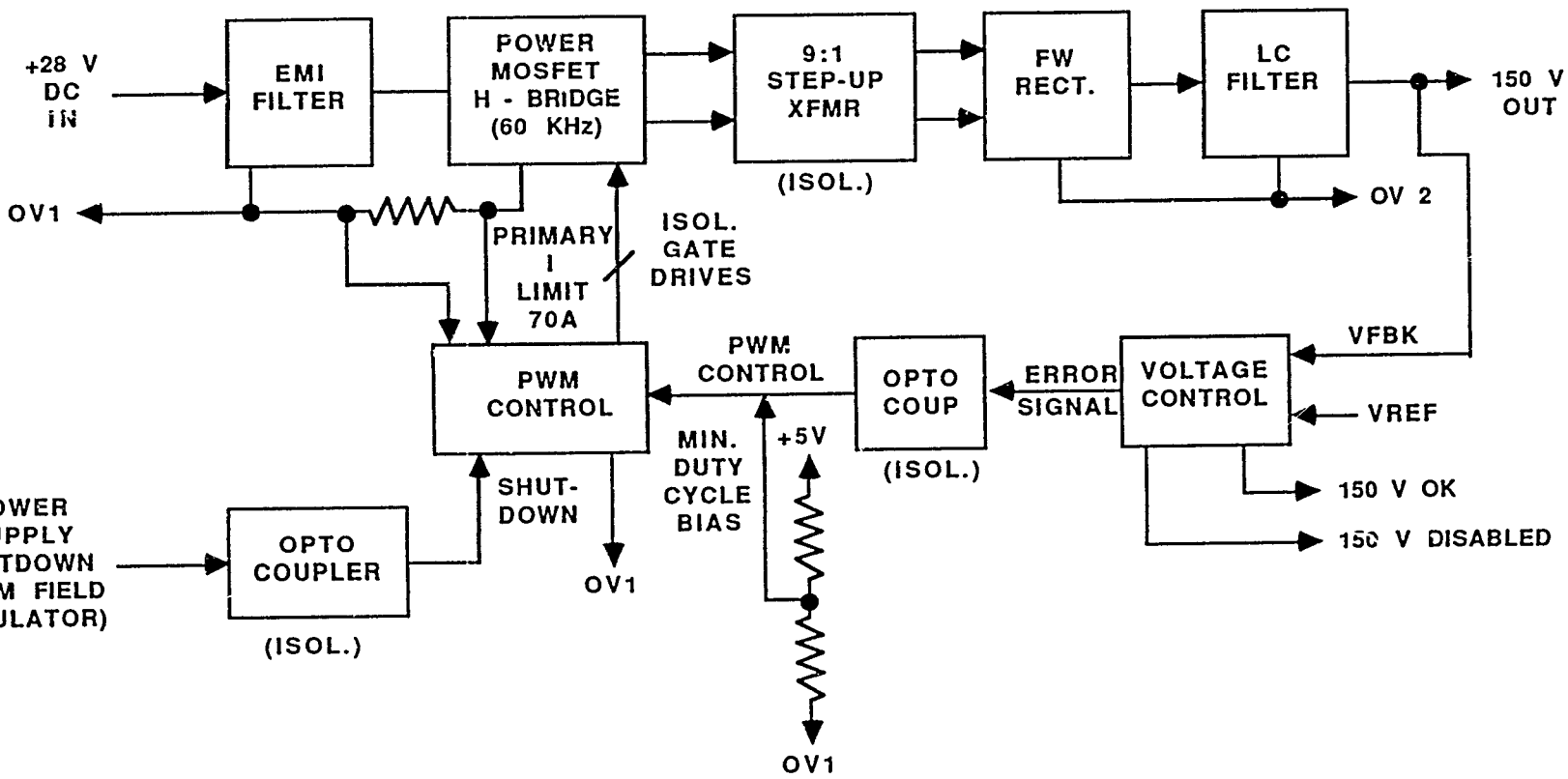


Figure 54. Boost Converter Block Diagram

It should be noted that three isolated grounds exist in the system; 0V1 is the system ground tied to the 28V source and the boost converter power bridge; 0V2 is the field regulator high voltage ground tied to the 150V bus and the exciter field; and 0V3 is the low level control and logic ground. Opto-couplers are used throughout the system to keep these grounds isolated from one another.

Three other signals, related to fault shutdown, can be seen in the block diagram. 'Power supply shutdown', from the field regulator, tells the boost converter to shutdown due to a failure in the main shutdown mode. The main shutdown mode is a regulator disable signal which turns off the current to the exciter field. When this fails, the 150V bus is instructed to shutdown by means of the 'power supply shutdown' signal previously mentioned. '150V disabled' signal tells the field regulator if this has been successful. If in a set time interval, neither the field current or the 150V have shutdown, the field regulator issues an 'abort' signal to the relay board. This opens up the 150V to the field regulator bridge by means of a vacuum relay.

The '150V OK' signal is a signal looked at by the logic card to prevent start-up of the regulator in event of low or high bus.

### 2.5.4 Field Regulator

The field regulator, see Figure 55 controls the alternator voltage by means of the exciter field current. The reference which the alternator voltage must follow is the permanent magnet generator (PMG) rectified average voltage, which is proportional to alternator and prime mover speed. The higher the required alternator voltage, the more exciter field current that must be supplied. The relationship is non-linear due to saturation of the various machines. 9A is the exciter field current limit set by the field regulator current controller.

The exciter field is pulsewidth modulated at 20 KHz by a full-wave, half-controlled mosfet bridge to obtain the requested current. The field current is sensed by a Hall effect sensor and sent to the current controller. The reference for the current controller is the error signal generated by the alternator voltage controller. The alternator voltage controller, which uses proportional plus integral control, compares the isolated voltage feedback signal from the power sensing box to the voltage reference, generated by the PMG. System shutdown, under normal and fault conditions, is controlled in the field regulator. The signal 'regulator enable', which comes from the logic card, is used to turn the field regulator on and off via the shutdown pin on the pulsewidth modulator. If the current does not decay to near zero in a set time interval, the field regulator sends a 'power supply disable' signal to the boost converter. It then waits to get a handshake ('150V off') verifying that the 150V bus has decayed to some lower voltage. If this handshake does not occur, the field regulator issues an 'abort' signal to the relay board. The relay board energizes a vacuum relay to remove the 150V from the field regulator bridge causing the alternator voltage to go to zero.

As in the boost converter, opto-couplers are used to maintain isolation between the various grounds in the system.

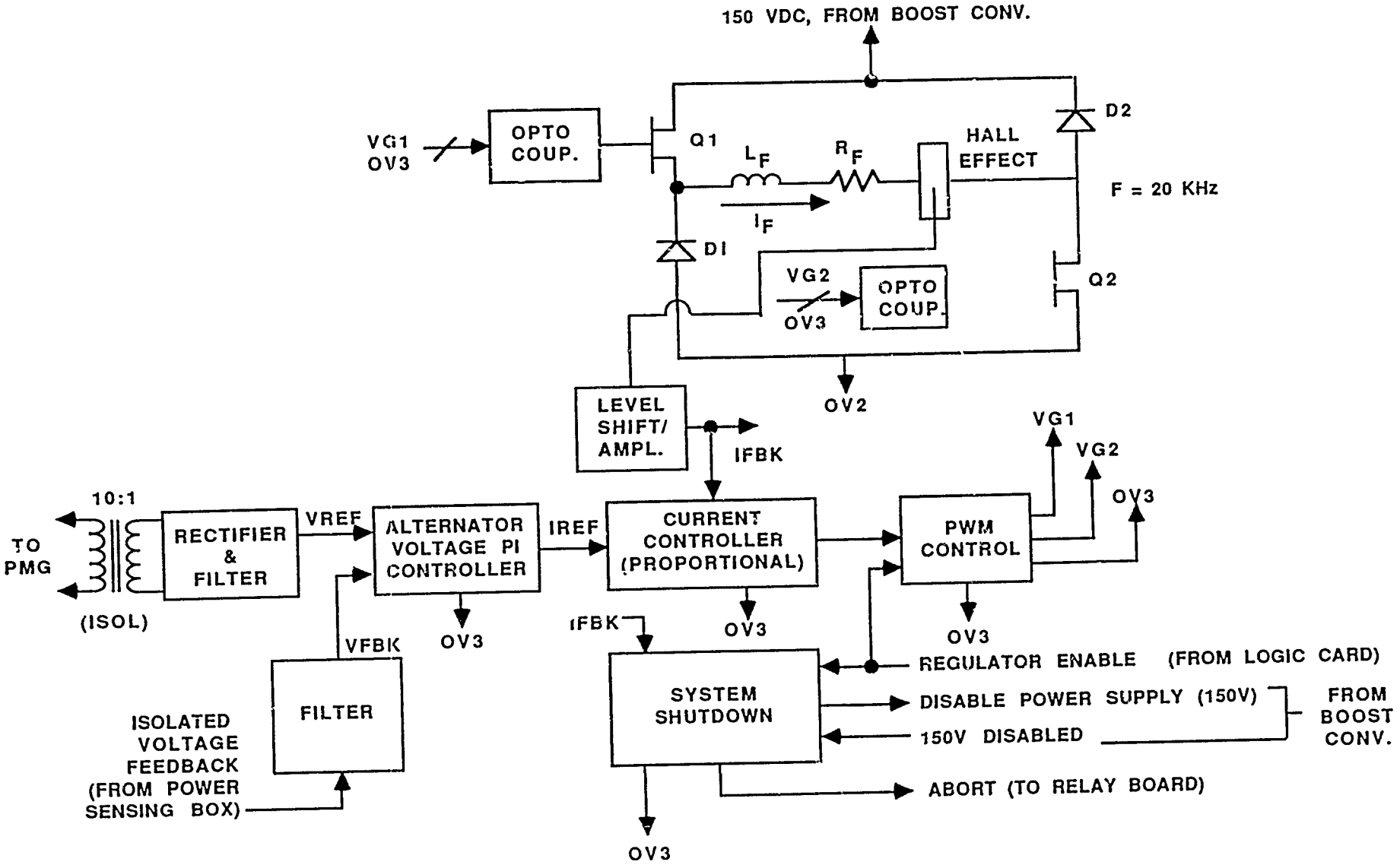


05/204/88/030-F

Figure 55. Field Regulator Block Diagram

### 2.5.5 Signal Conditioning Card

The purpose of the signal conditioning card is to provide circuitry which will condition the signal levels of the various sensors for conversion to digitai data. This card consists of:

| | |
|---|---|
| 11 | Identical RTD Circuits |
| 1 | Instrumentation Amplifier Circuit |
| 2 | RMS-to-DC Circuits, Each with a Post-Amplifier |
| 1 | 16-Channel Signal Multiplexer (MUX) |
| 1 | 1 Bridge Excitation Regulator |

A block diagram of the Signal Conditioning Card is shown in Figure 56.

The RTD circuits condition the signals from the temperature sensors. There are four alternator stator RTD's, six motor stator RTD's and one motor oil temperature RTD. Each circuit consists of a current source to excite the RTD, a filter to provide noise immunity, a differential amplifier, and a level-shift/gain stage which subtracts an offset and provides amplification. Each RTD circuit output goes to the MUX. Additionally, the output of the motor oil temperature RTD circuit leaves the card as a separate line to the logic card.

The instrumentation amplifier circuit conditions the motor oil pressure signal from a pre-amplifier embedded in the motor. It provides amplification and filtering. The output of this circuit goes to the MUX and also leaves the card as a separate line to the logic card.

The RMS-to-DC circuits convert the AC signals from the current sensors to a DC signal which can easily be digitized. These circuits, by the nature of the AC to DC conversion process, also provide signal filtering. Each circuit also has a post amplifier which provides additional signal amplification.

The 16 channel mux provides a means for one A-to-D converter to digitize up to 16 different signals. The signal to be digitized is selected by a 4-bit digital code outputted to the MUX by the logic card.

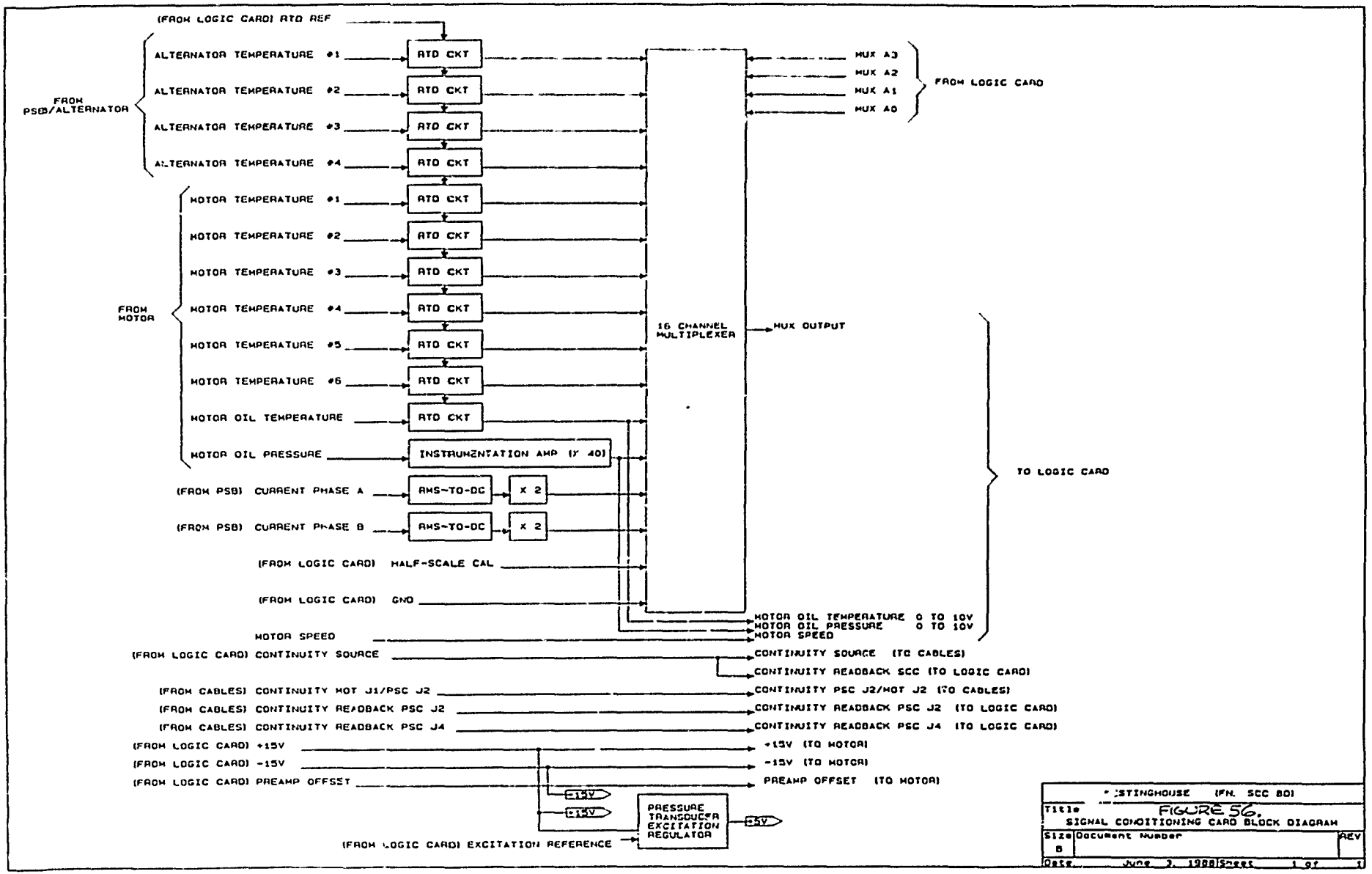




05/204/88/84

Figure 56. Signal Conditioning Card Block Diagram

The bridge excitation regulator converts +15V to +5V to provide excitation for the motor oil pressure transducer. This regulator is protected against a short circuit on its output.

### 2.5.6 Logic Card

The Logic Card provides circuitry to implement the following functions:

- Control of PSC operating modes
- Interface to vehicle controller
- Monitoring of alternator/motor system status
- Control of REGULATOR ENABLE signal
- Communication of system status to vehicle controller

A block diagram of the Logic Card is shown in FIGURE 57. A description of each block is as follows:

VEHICLE CONTROLLER INTERFACE: This interface allows the vehicle controller to control PSC operation and to receive system status. The inputs/outputs of this block are optically-isolated from the vehicle controller.

SEQUENCER: This block provides circuitry to sequence the PSC operating modes. It also generates the REGULATOR ENABLE signal based on operating modes and fault status.

WATCHDOG CIRCUIT: The purpose of this circuit is to provide fault tolerance in the event of a microcontroller hardware/software failure. If the microcontroller fails to reset this circuit within a specified time period, it will cause the sequencer to disable the regulator.

CLOCK/RESET CIRCUIT: This circuit provides 3 crystal oscillator-based clock frequencies: 6 MHz, 3 MHz, and 1 MHz; additionally, it provides a clock synchronized power-on reset circuit. The clock synchronization keeps circuitry reset until the clock has started.

MICROCONTROLLER/ADDRESS LATCH/DECODER: This block is the central element of the Logic Card. The microcontroller is responsible for executing system software and determining fault status. Additionally, it contains:

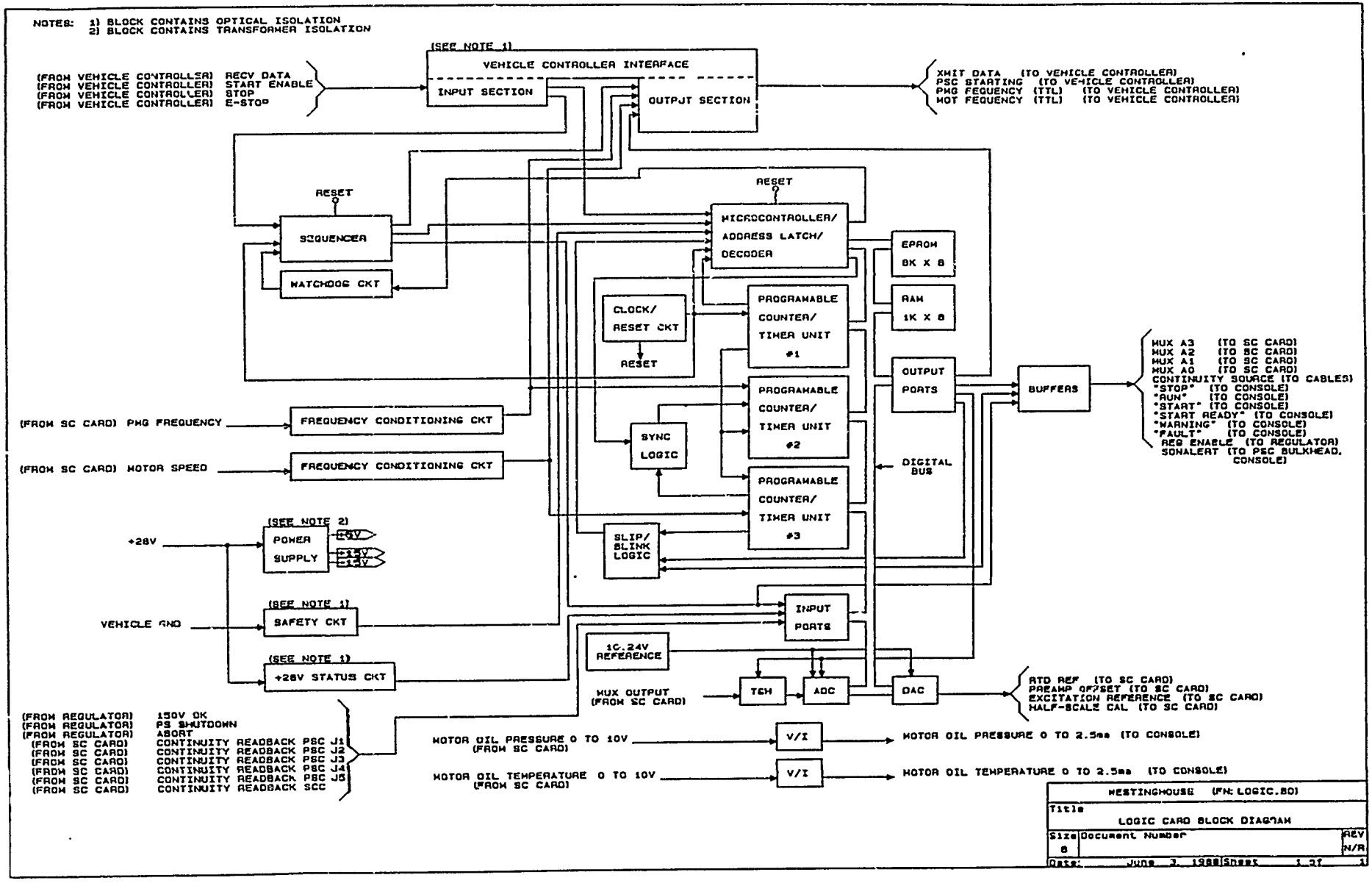


Figure 57. Logic Card Block Diagram

- o An onboard serial port with interrupt for status communication to the vehicle controller
- o A nine bit input/output port
- o Two 16 bit counter/timers, each with one interrupt
- o Two additional interrupts
- o Bus control logic
- o 128 bytes of RAM

The address latch and decoder provide the additional logic required to control activity on the digital data bus.

EPROM: This block consists of the single I.C. used to store the software program.

RAM: This block consists of the single I.C. used to store temporary data values generated during the execution of the program.

FREQUENCY CONDITIONING CIRCUIT: This block provides signal conditioning to translate the input voltage to TTL levels. It also provides filtering and hysteresis to increase noise immunity.

PROGRAMMABLE COUNTER/TIMER UNIT (PCTU) #1: Provides 300 KHz and 1 KHz clocks.

PROGRAMMABLE COUNTER/TIMER UNIT #2: Provides 1 counter to scale the PMG frequency and 1 timer to measure its period.

PROGRAMMABLE COUNTER/TIMER UNIT #3: Provides 1 counter to scale the motor frequency and 1 timer to measure its period. An additional counter is used to generate the blink frequency of the "WARNING" lamp.

SYNC LOGIC: Provides circuitry to synchronize PCTU #2 with PCTU #3 so that slip can be measured.

SLIP/BLINK LOGIC: Provides circuitry to implement slip interrupt and "WARNING" lamp blinking functions.

INPUT PORTS: Provides a means of inputting parallel digital data into microcontroller.

OUTPUT PORTS: Provides a means for the microcontroller to output parallel digital data.

BUFFERS: These circuits increase drive capability for output signals that leave the card.

T&H (TRACK AND HOLD): This circuit, when commanded, holds an analog signal value constant so that it can be digitized.

ADC (ANALOG TO DIGITAL CONVERTER): Provides a means to convert analog signal information into digital data for use by the microcontroller. The ADC has a resolution of 8 bits.

DAC (DIGITAL TO ANALOG CONVERTER): Provides a means for digital data from the microcontroller to be converted into analog signals. The DAC has a resolution of 8 bits.

10.24V REFERENCE: Provides a scaling voltage for the ADC and DAC such that each bit of digital data is equivalent to 40 mV of analog signal.

V/I: This circuit converts a signal voltage into a proportional current for use in driving an analog panel meter.

POWER SUPPLY: This is an on-card DC-to-DC converter which converts +28V to +5V, +15V, and -15V.

SAFETY CIRCUIT: This circuit alerts the microcontroller when an excessive voltage exists between VEHICLE GND and PSC GND. The microcontroller will respond by beeping an audible alarm both in the PSC and at the test console. Additionally, a warning message will be sent to the vehicle controller. The purpose of this circuit is to protect personnel during PSC service operations and to alert operators of the existence of a hardware fault.

+28V STATUS CIRCUIT: This circuit alerts the microcontroller when the primary DC voltage is outside a specified boundary. The microcontroller will respond by sending a warning message to the vehicle controller.

### 2.5.7 Microcontroller Software Description

The PSC software has two primary functions:

1. Control of the REGULATOR ENABLE signal based on the status of system sensor signals with respect to limits.

2. Communication of fault status to the vehicle controller.

The PSC has three modes of operation: PRESTART, START, and RUN. Mode control is performed by the sequencer, which is a separate hardware block from the microcontroller. The software is mode dependent, however, and the microcontroller must monitor the mode command inputs from the vehicle controller.

The rationale in having a sequencer in addition to the microcontroller (which could have easily performed the mode control directly) is that a level of hardware redundancy is provided. This redundancy provides fault tolerance to a single point failure if it occurred. If there is a software fault, mode control will not be chaotic, since it is performed in a separate hardware block. Alternately, the sequencer does not have absolute control over start-up; it is dependent on microcontroller-generated start ready and fault signals. The microcontroller provides the means to monitor the sequencer's start timer and regulator enable output. If a hardware fault occurs in the start timer, the microcontroller can provide a fault signal to the sequencer which will disable the regulator.

The software for the PSC can be partitioned into two major sections:

1. The main program, which performs the two primary functions described above.

2. The data acquisition section, which determines the status of the system sensor signals with respect to limits.

Note that both sections of the software are mode dependent.

A flowchart for the software is shown in FIGURE 58 (a), (b), (c) and (d). At the beginning of the main program, the microcontroller sets up its internal registers and peripheral devices. It then enters the PRESTART mode. Its first action in this mode is to start a 10 ms sampling timer. It then enters a data acquisition subroutine, where it samples a set of PRESTART parameters and compares them to limits appropriate for that mode. If a parameter is sampled and a WARNING limit is exceeded, a WARNING flag for that parameter is set. If, additionally, a FAULT limit is exceeded, that parameter will be sampled two more times immediately after the first. If the FAULT limit is exceeded on all three samples, then a FAULT flag is also set. The microcontroller then finishes acquiring data for the rest of the PRESTART parameters and exits the subroutine. When it re-enters the main program, it checks to see if any WARNING/FAULT flags were set. IF any FAULT flags are set, the microcontroller will jump to a shutdown routine. The shutdown routine will disable the regulator and send FAULT status to the vehicle controller/CRT. There is no great significance to this in the PRESTART mode, since the regulator remains disabled until the START mode. However, it does mean that the command to start the motor will be ignored until all faults have been cleared. If any WARNING flags are set, the WARNING lamp will be flashed.

The microcontroller will continue to execute the main program. It will exit the PRESTART mode when there are no faults and the mode-select criteria for the START mode have been met. Otherwise, it will continue to loop in the PRESTART mode, acquiring sensor data on a 10 ms interval.

The START and RUN modes operate analogously to PRESTART with these distinctions:

- The parameters samples and their limits are functions of the mode.
- Entering the shutdown routine because of a fault will cause a jump back to PRESTART.
- The non-synchronizable parameter, slip, is measured. Its sampling interval is variable in length and the beginning of this interval is random. Because of this, the microcontroller samples it on an interrupt basis.

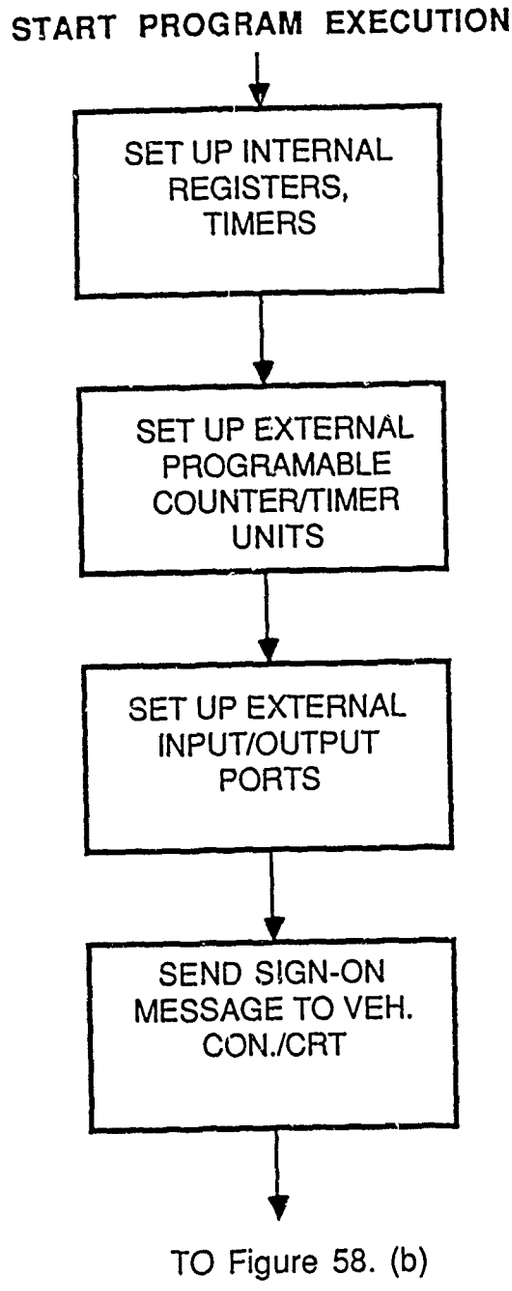


Figure 58. (a) Microcontroller Software Flow Chart

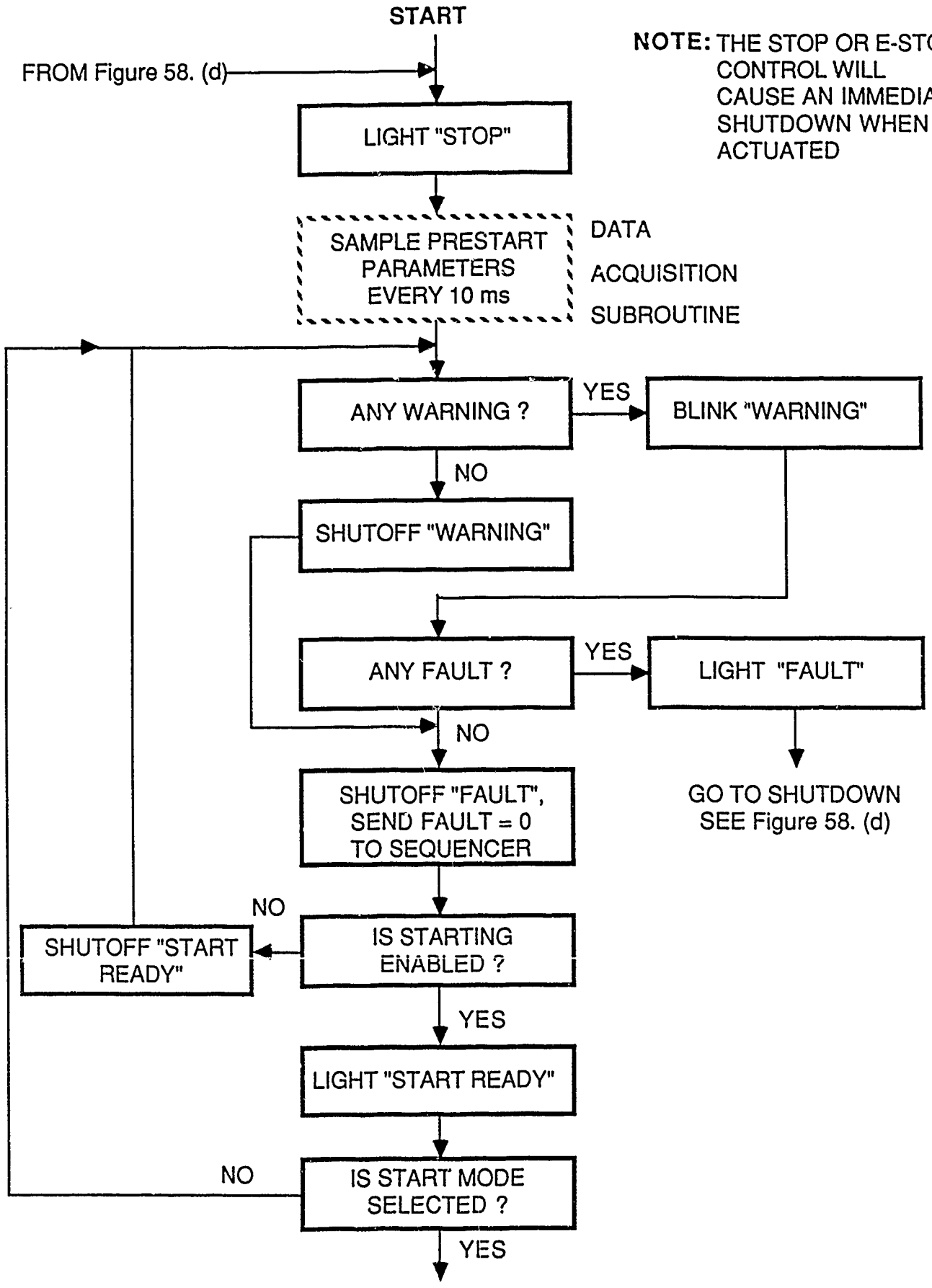


05/204/88/066-A

Figure 58. (b) Microcontroller Software Flow Chart (Prestart Mode)

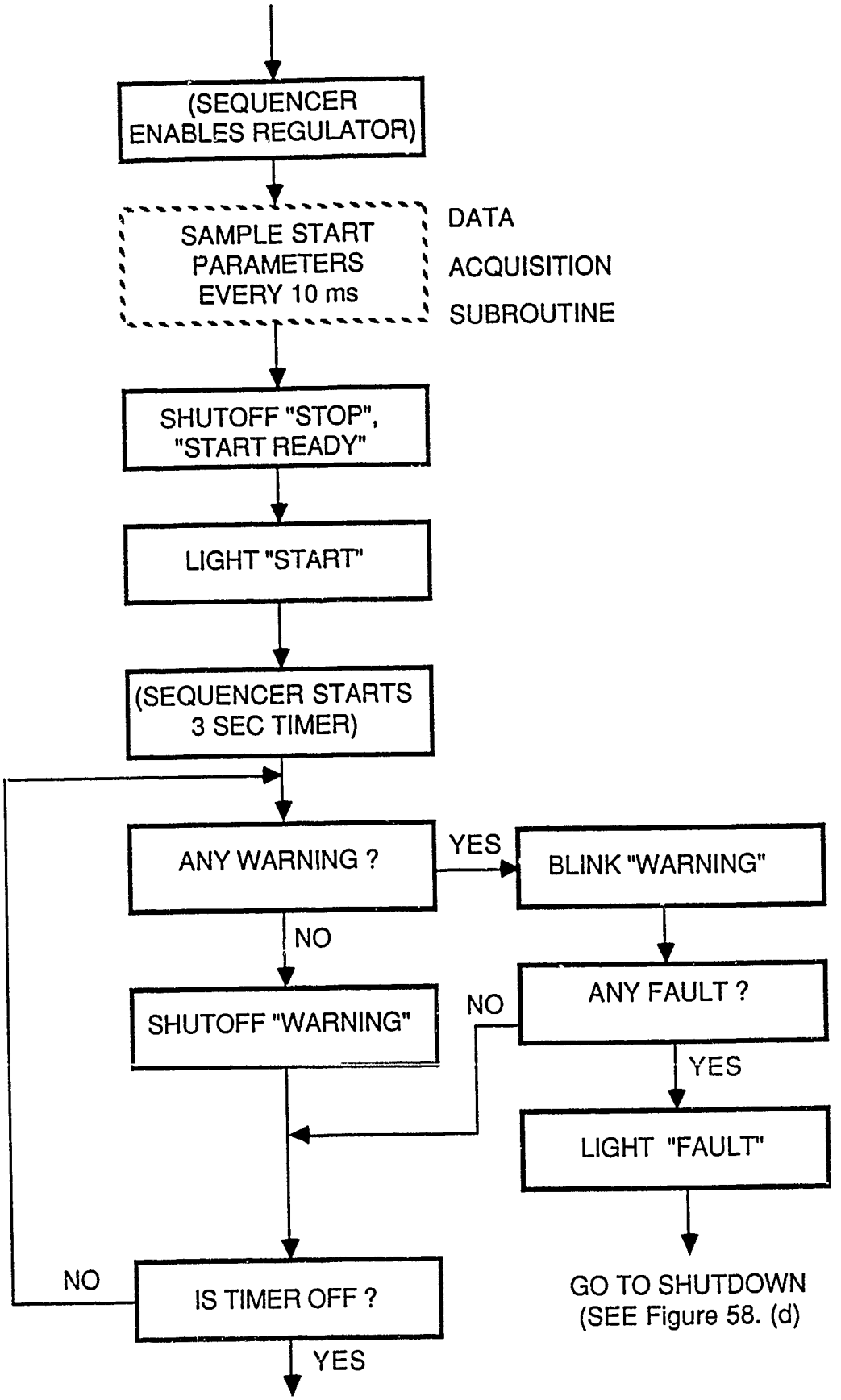


05/204/88/065-A

Figure 58.(c) Microcontroller Software Flow Chart (Start Mode)

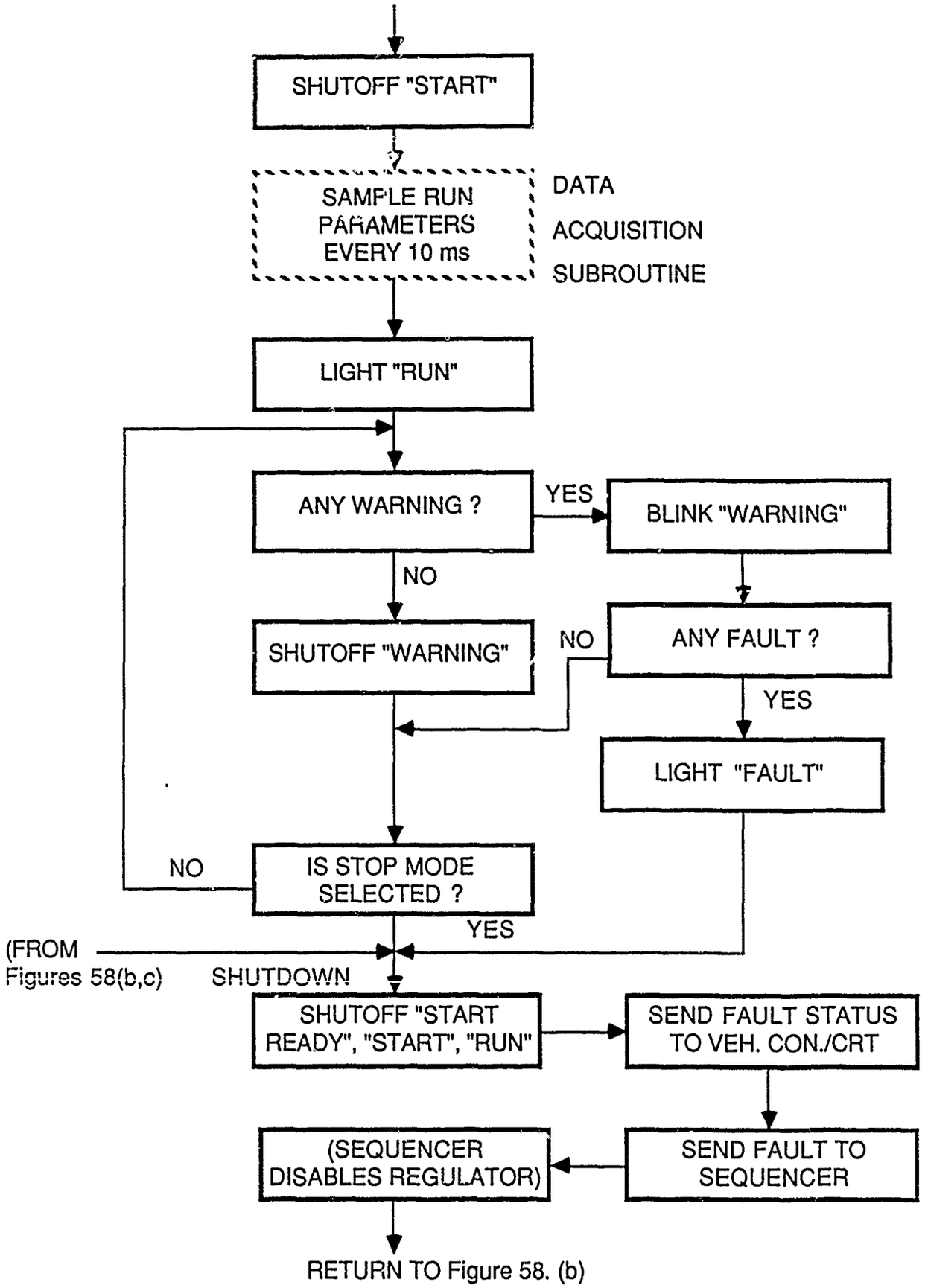


Figure 58. (d) Microcontroller Software Flow Chart (Run Mode/Shutdown Sequence)

05/204/88/064-A

### 2.5.8 Boost Converter Stability Analysis

The boost converter must be able to respond to any load demands put on it by the field regulator current loop. This loop has a bandwidth of 66 Hz. To insure response a boost converter closed loop bandwidth of 5 to 10 times 66 Hz is required, thereby minimizing interaction with the field regulator. One KHz was the design goal.

The control diagram of the converter is shown in Figure 59. The complex poles of the converter's LC filter occur at 196 Hz for nominal components (CF=1300UF,LF=500UH). This frequency moves to 160 Hz for the max tolerance on the capacitor (+50%). The control philosophy is to approximately cancel the LC filter poles with two lead networks and to use an integrator to zero steady state error. Figure 60 shows the open loop bode plot of the converter with the extremes of CF. The compensator lead networks place zeroes at 160 Hz and 190 Hz. The LC filter poles are located between 160 Hz and 196 Hz. The two extreme crossovers are shown at 828 Hz and 1.2 KHz with corresponding phase margins of 88 and 92 degrees. Sufficient bandwidth and stability have been realized.

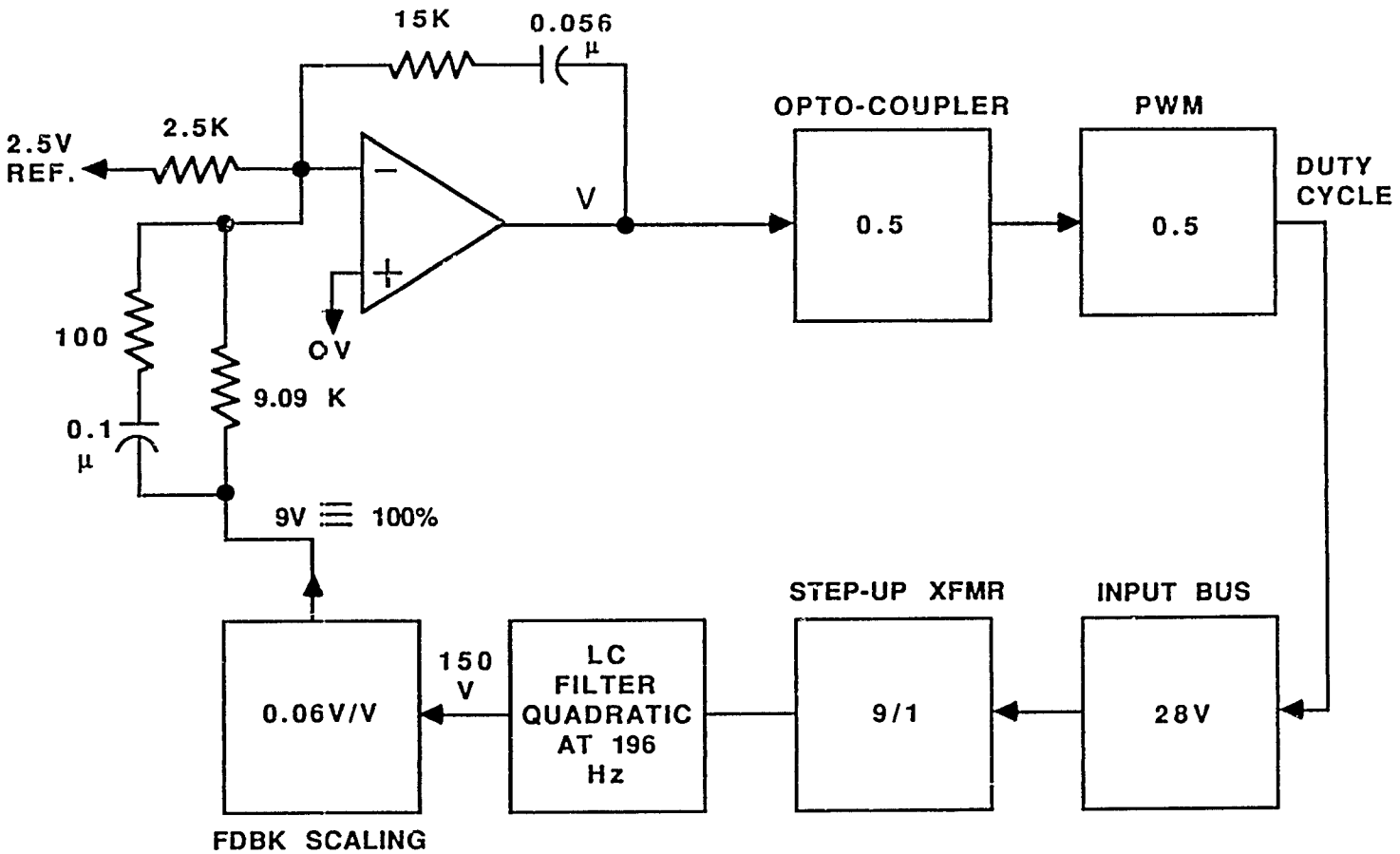


$$\text{T.F.}_{\text{Open Loop}} = \frac{\overbrace{[\,(9.09\text{k} \times 0.056\mu)^{-1} \times 0.5 \times 0.5 \times 28 \times 9 \times 0.06\,]}^{6187} \times \left(1+\frac{S}{2\pi \times 255}\right)\left(1+\frac{S}{2\pi \times 190}\right)}{S \times (\text{Quadratic at } 196 \text{ Hz})}$$

$$F_{co} \simeq 1 \text{ KHz}$$

Figure 59. Boost Converter Voltage Loop Control Diagram

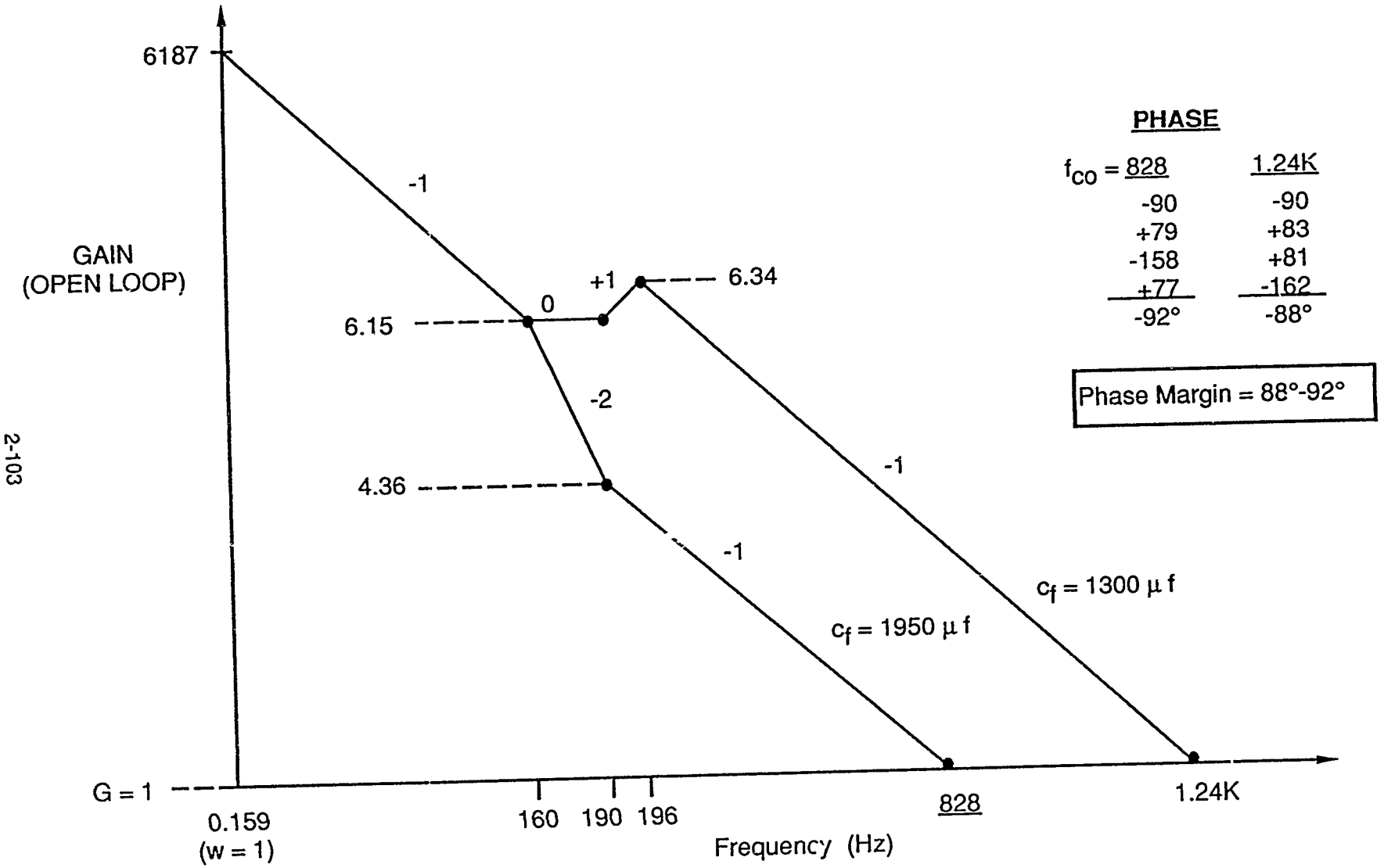


Figure 60. Boost Converter Bode Plot

### 2.5.9 Field Regulator Small Signal Stability Analysis

The alternator voltage controller (field regulator) must respond to prime mover changes on the order of 1 Hz frequency. Five to ten times this frequency is therefore required as a closed loop bandwidth of the controller. Figure 61 shows the control diagram. The current loop pole and the voltage filter pole are both located more than 10 times the open loop crossover frequency and thus can be ignored for the analysis. The only time constant which affects the response is the main field time constant (2.88 RAD/SEC or .46 Hz). The control philosophy is to cancel this pole with a lead network at 2.8 RAD/SEC, and to use an integrator to zero steady state error. The required crossover can be obtained by adjusting the integration constant (1/RC) of the controller. Figure 62 shows the bode plot of the resultant system with an open loop crossover of 6.7 Hz. The final compensated system looks like a simple integrator with phase margin of 90 degrees.

The inner loop (current controller) control diagram is shown in Figure 63. The single time constant of the system is the exciter field L/R time constant. Proportional control is used since some current error is acceptable. The gain of the current error amplifier is adjusted to obtain the required bandwidth of 66 Hz. This can be seen in Figure 62.

### 2.5.10 Mechanical Packaging

The propulsion system controller, see Figure 64, is assembled in an aluminum box with a removable heat sink on one side. The overall dimensions of the box are 10.06 wide by 13.00 high by 12.00 deep. Further dimensional information can be found on the ICD drawing E77857.

The high power elements of the circuit are mounted directly on the heat sink. Boost converter and field regulator PWB's are also mounted on the heat sink to minimize lead lengths in these circuits. Heavy components are mounted to the heat sink or walls of the box keeping the PWB's light and capable of enduring the shock loads. This arrangement is also convenient for testing the boost converter and field regulator circuits since the entire unit can be removed from the box giving easy access to all components.

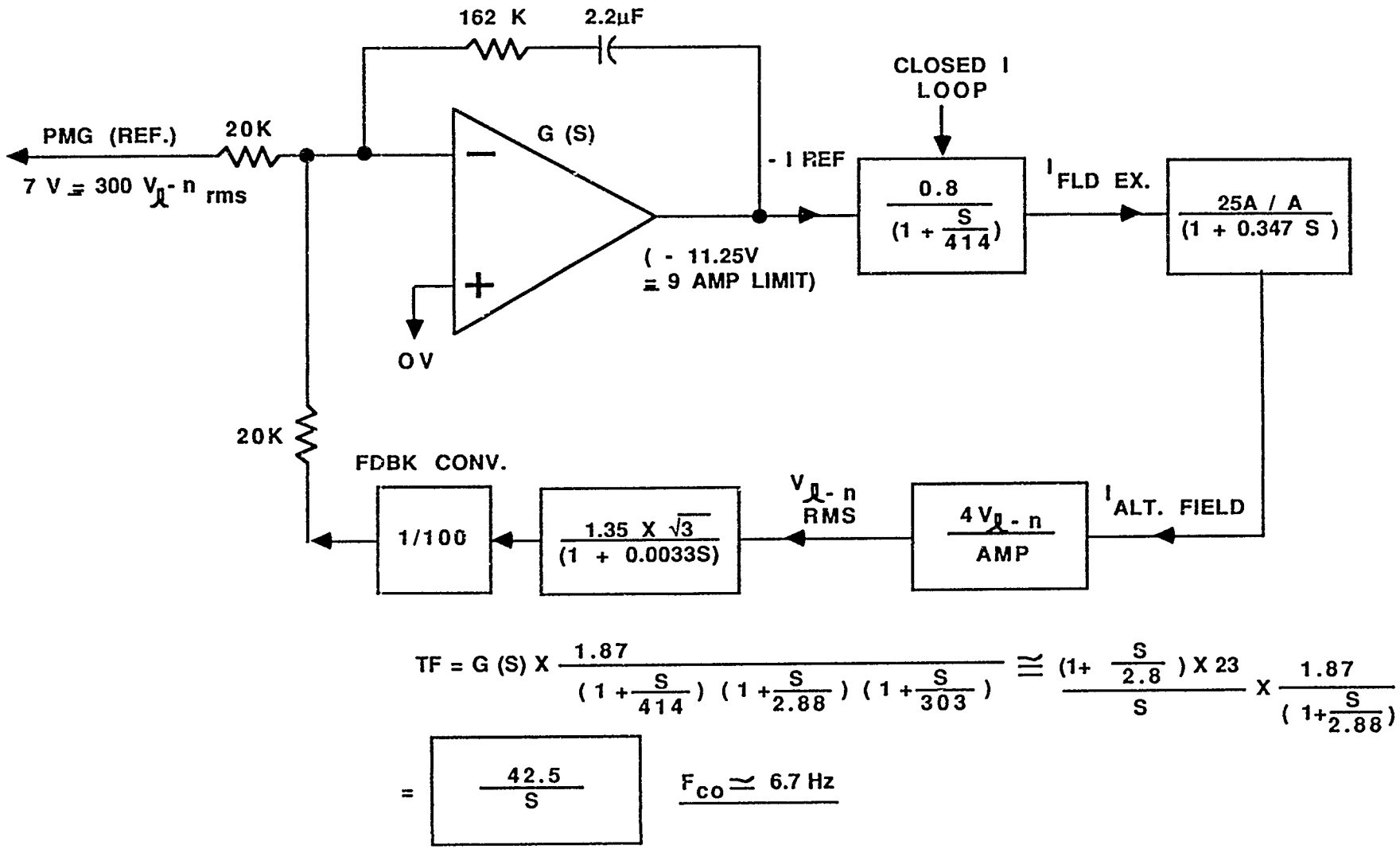


Figure 61. Alternator Voltage Loop Control Diagram

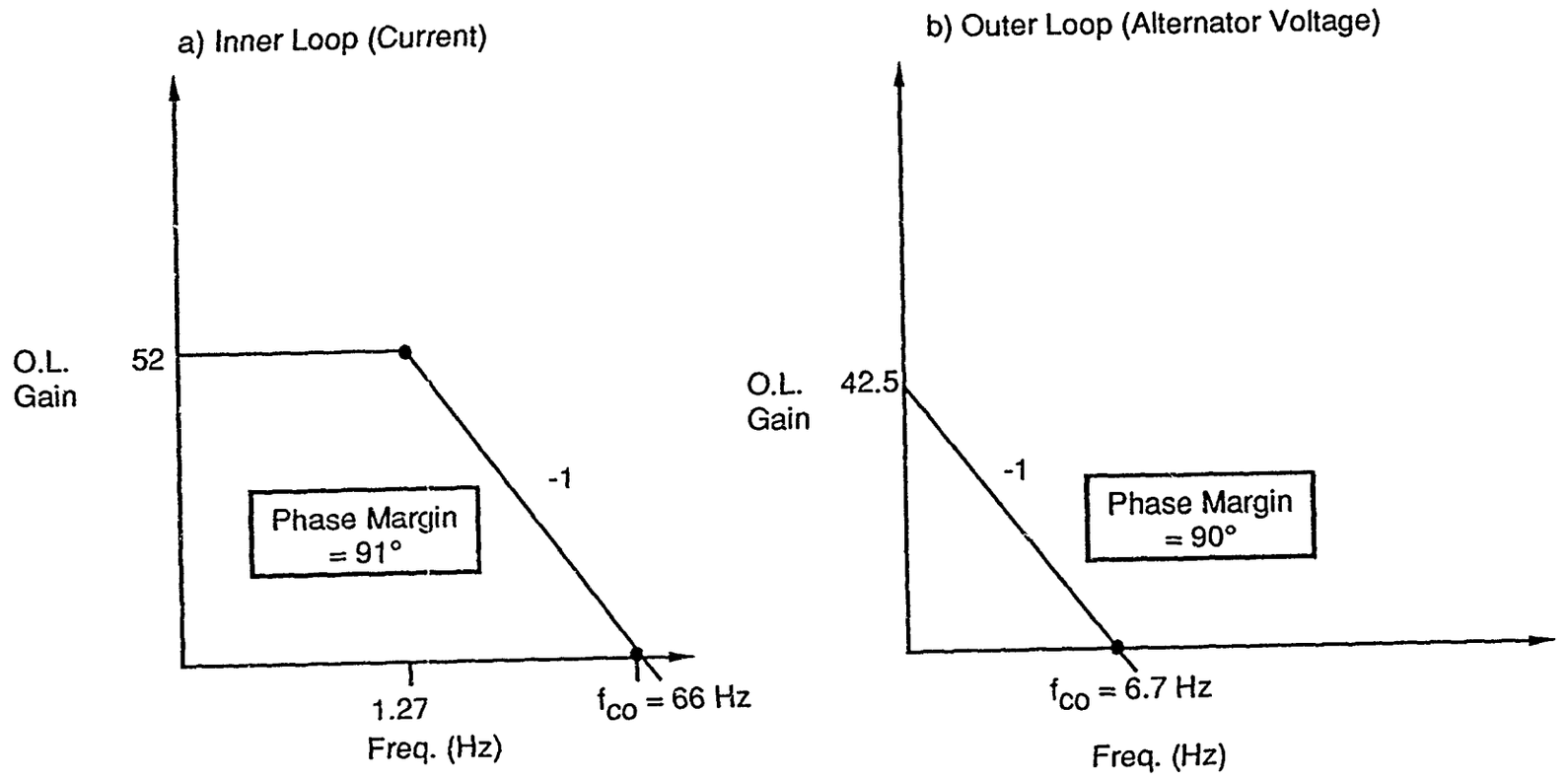


Figure 62. Field Regulator Bode Plots

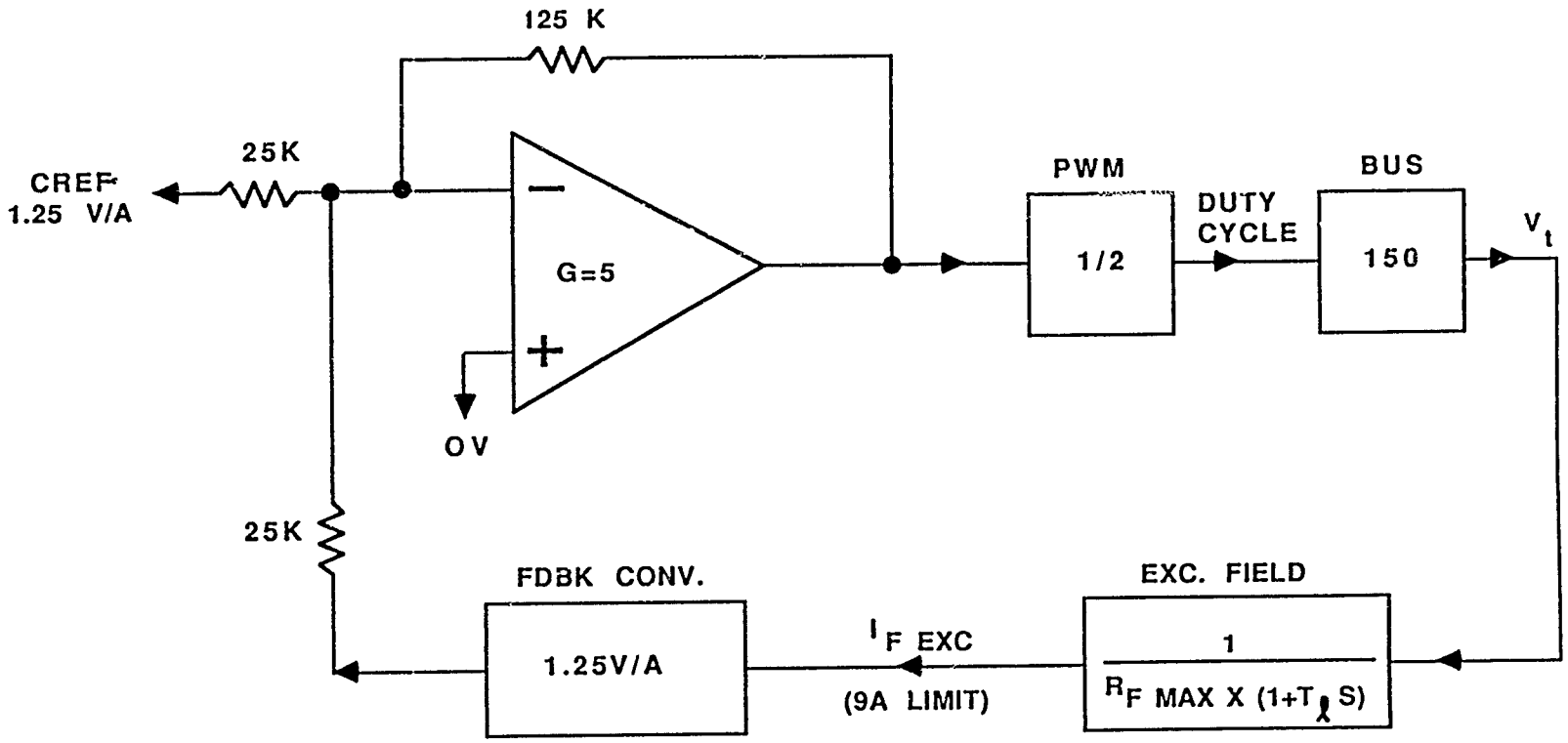


$$TF_{O.L.} = 5 \text{ X1/2 X150 X 1/9}\Omega\text{X 1.25 X } \frac{1}{R + S/8}$$

$$= \boxed{\frac{52}{(1 + S/8}} \qquad (8 \frac{RAD}{SEC} = 1.27 \text{ Hz}$$

$$F_{co} \simeq 66 \text{ Hz}$$

Figure 63. Current Loop (Inner Loop) Control Diagram

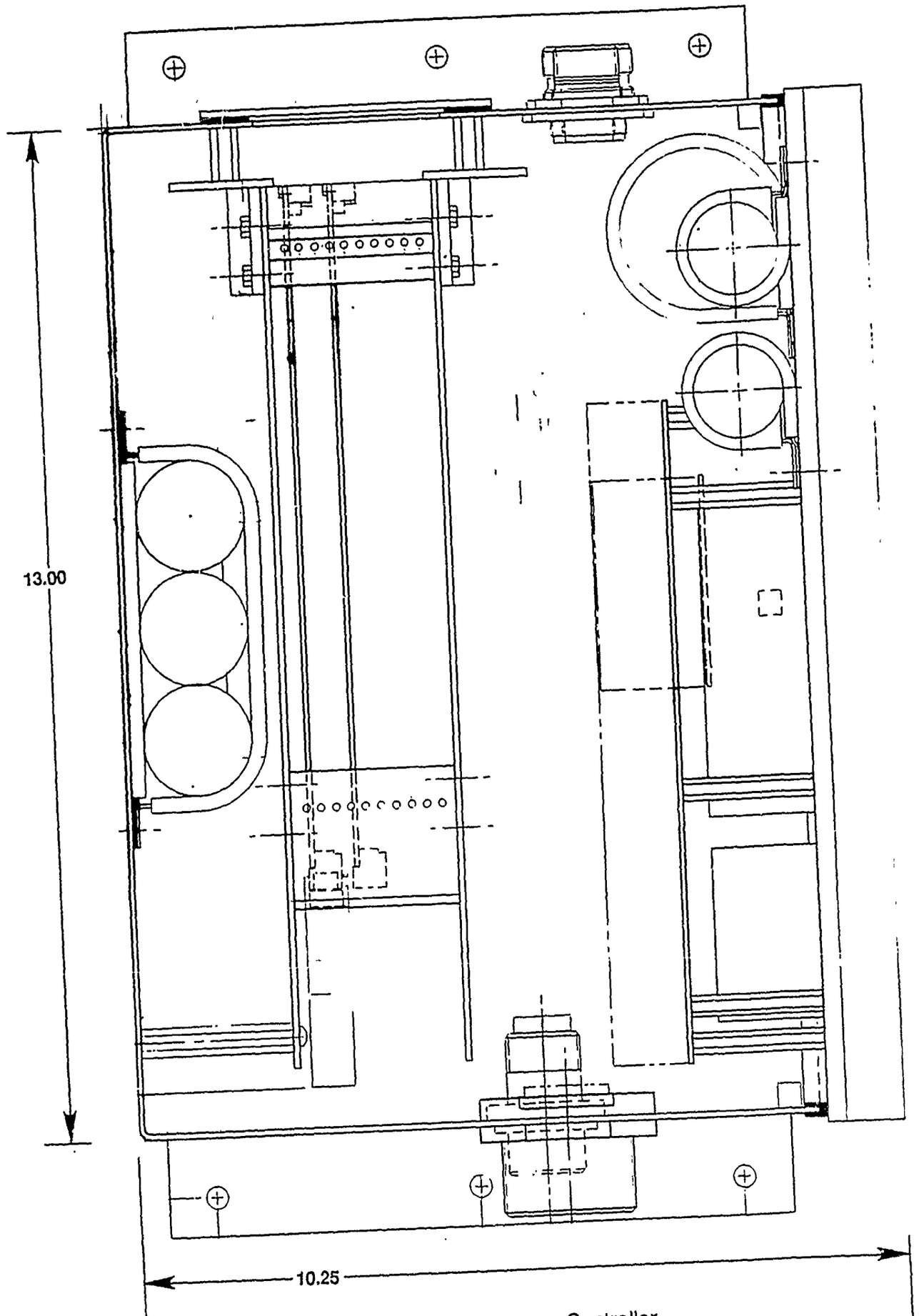


Figure 64. Propulsion System Controller



05/204/88/079a

The signal conditioning card and logic card are mounted in a standardized aluminum/plastic card rack which is mounted inside the box. This gives the PWB's adequate support for the shock loads. A removable cover over the card rack makes it possible to instack extender cards for testing purposes. The rack has one spare card slot.

The box has been fabricated from aluminum to minimize weight. Commercially available boxes were investigated but could not meet the requirements for volume. The cover and heat sink are sealed to keep out dust and fluids.

### 2.5.11 Thermal Analysis

A thermal analysis was performed on the power circuitry located on the extruded heatsink. This consists of the boost converter power bridge and the field regulator power bridge. One computer program calculates the power losses of the power components for the inputted operating conditions and a second program calculates the junction temperatures of the power semiconductors. Two conditions were examined; steady state operation at top speed was looked at (2-3 amps exciter field current), and a restart condition where the system was restarted (9 amps exciter current for 3 seconds) after steady state temperatures had been reached. All semiconductor junctions were well below 125 degrees C (150 degree C rated) for the worst case condition of restart. The details of the analysis and the actual temperatures are included in Appendix 7.

In the thermal analysis of the system, all the heat generated remotely from the heat sink was treated as flowing through the top and bottom and two sides of the PSC box. With a total heat load of 26 watts the wall temperature was calculated to be 66°C (in a 50°C environment). This is well below the 85°C rating of the electronic components. Based on this result more complex analysis of the heat transfer process inside the box was considered unnecessary.

### 2.5.12 Power Sensing Box (PSB)

The Power Sensing Box, see Figure 65, contains the hardware for sensing the alternator phase current for both load and fault monitoring and the hardware for sensing the terminal voltage (feedback voltage) for the volts/hertz regulator. The PSB is located on top of the alternator and is mounted to the power terminal board. The electrical schematic of the current sensing hardware is shown in Figure 66. The stepdown current transformers are custom designed and fabricated to fit within the PSB. The transformers are wound with a 2000:1 turns ratio. The output of each is connected to a burden resistor whose signal goes to the Propulsion System Controller (PSC). Since a three wire system is used between the alternator and the induction motor, only two current transformers are required to monitor the three phase power (the vector summation of the phase currents is zero).

The electrical schematic of the voltage feedback signal that is sent to the volts/hertz regulator is shown in Figure 67. The three phase voltage transformer, a full wave bridge rectifier and the burden resistor are also mounted in the PSB. The transformer has a 50:1 stepdown ratio. The rectifier and burden resistor convert the transformer output to a DC signal which goes to the volts/hertz regulator.

The power cables connecting the alternator to the motor are fed through grommets located on the PSB. The input and output wires for the current and the voltage sensing circuits are soldered to connector receptacles mounted on the PSB wall. The RTD (Resistance Temperature Detector) probes that sense alternator temperatures are held in place by compression fittings on the PSB. The RTD output wires are soldered to a second connector receptacle also on the PSB.

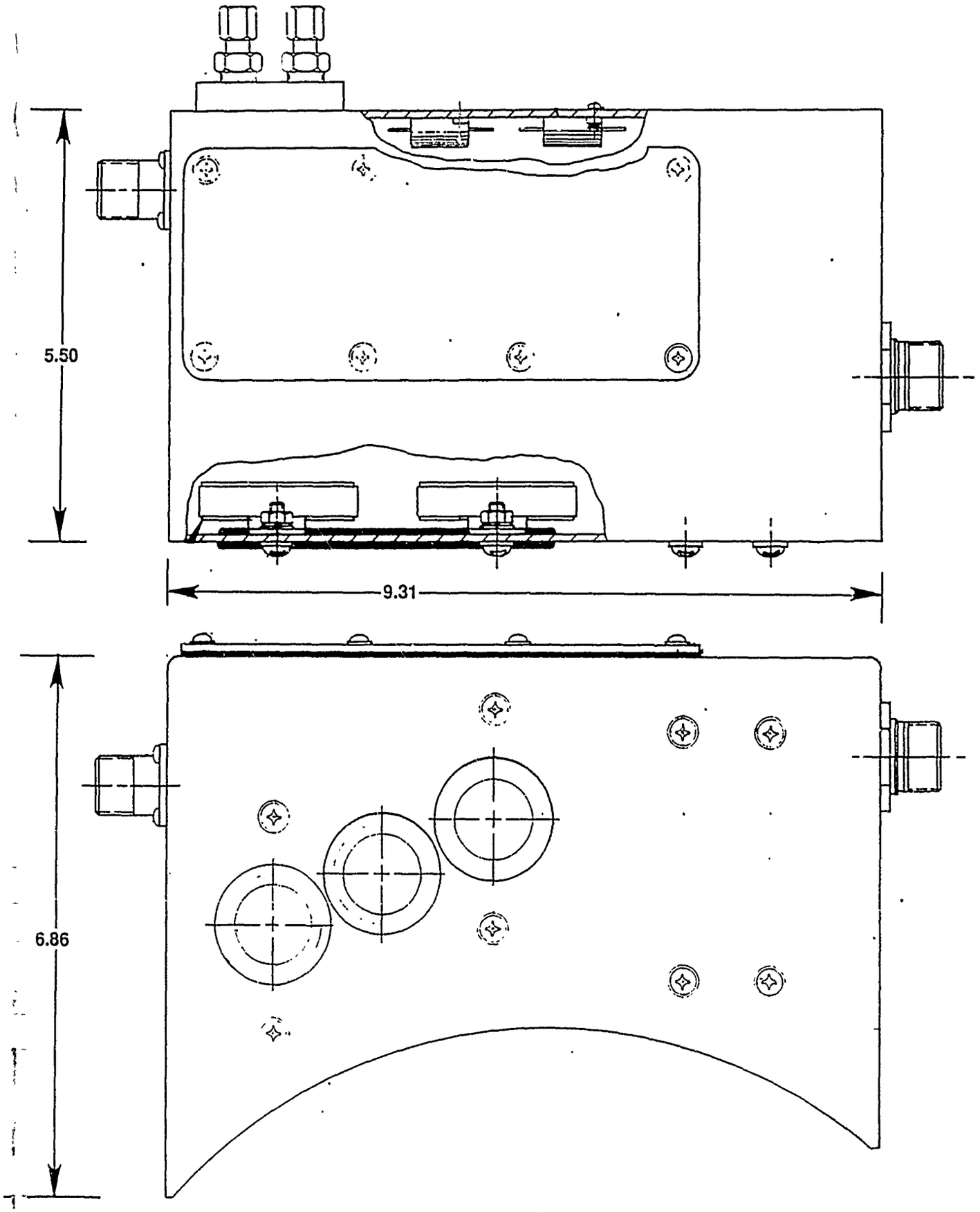


05/204/88/079

Figure 65. Power Sensing Box

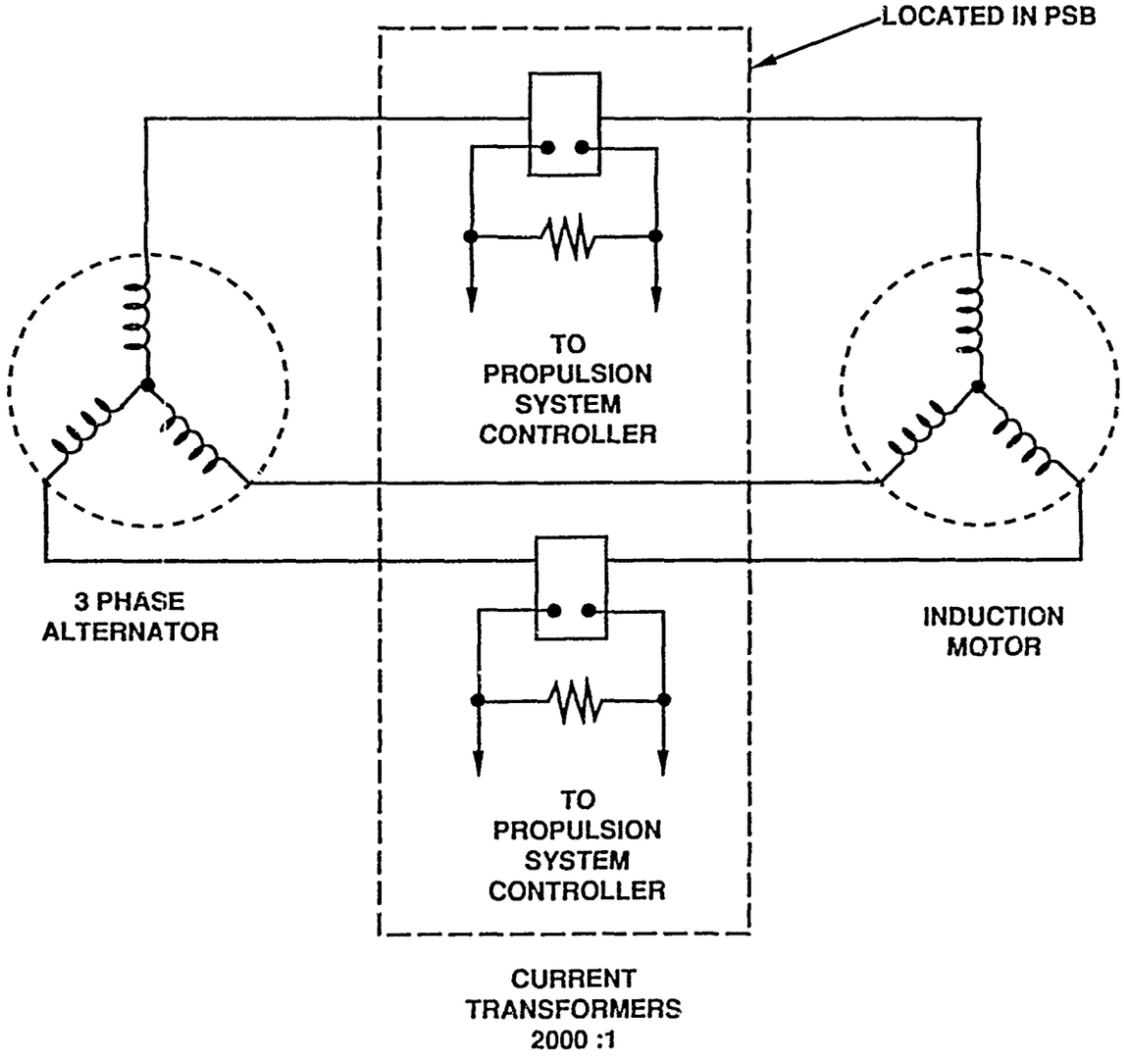


Figure 66. Power Sensing Box (PSB) - Current Sensing

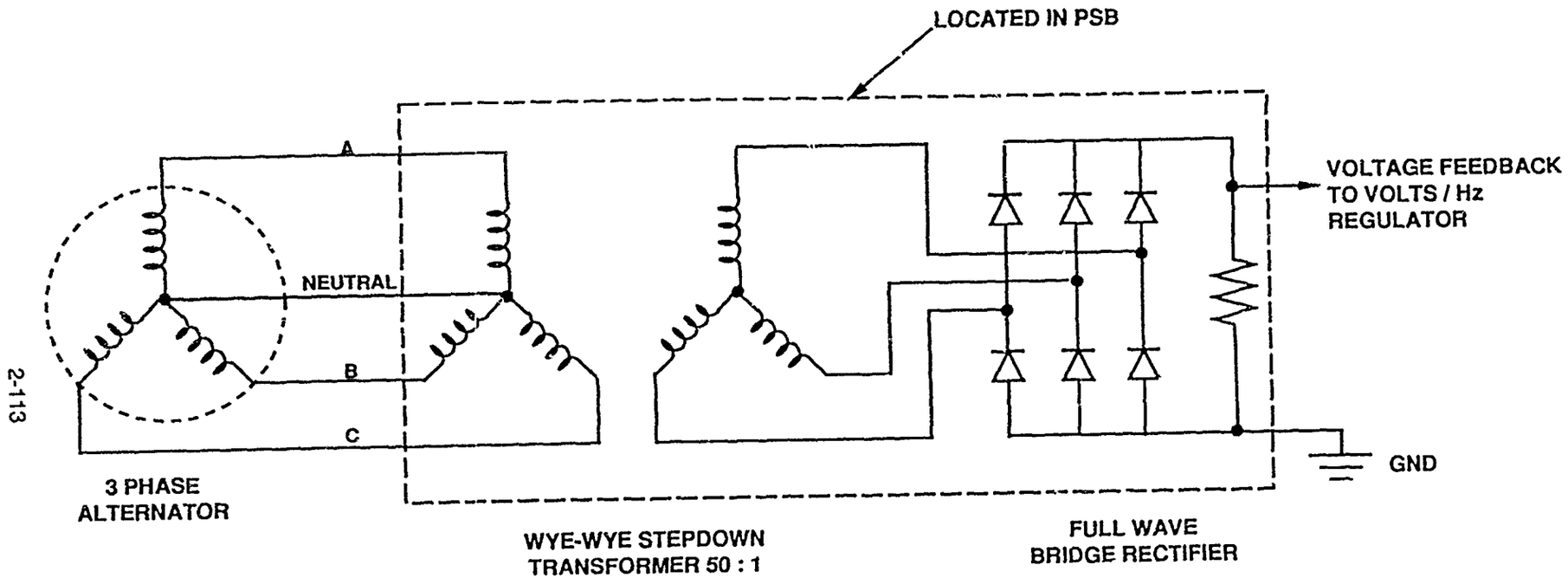


Figure 67. Power Sensing Box (PSB) - Voltage Feedback

## 2.5.13 PSC External Cable Interconnections

The external cables required for the propulsion system are shown in the cable interconnect diagram Figure 68. The diagram shows the interconnection of power, instrumentation, and vehicle interfaces.

The motor will be connected to the alternator using the 4/0 cable shown in Figure 52, two phases of which are routed through the current transformers located in the power sensing box. The instrumentation cable (W2) from the motor and the instrumentation cables (W5, W4) and the power sense cable (W3) from the alternator are connected to the PSC. Cable W1 connects the vehicle 28 VDC power to the PSC. The console in the vehicle is connected to the PSC via cable W6 and the keyboard and CRT with cable W7. For detailed PSC signal interface description see ICD, Drawing No. E77857.

The criteria for selection of connectors was based on the following specifications:

- Motor connectors and their cable mates must be immersible in sea water to a depth of 20 ft.
- Alternator, power sense box, and propulsion system controller connectors must be moisture resistant.

The motor connectors were selected from the Glenair Geo-Marine Series. These are of a hermetic design and are capable of greater than the design pressure. The other connectors in the system were selected from the military qualified D38999 series. These feature resilient seals between pins/sockets and insulators, which make them impervious to condensing moisture and sea water spray.

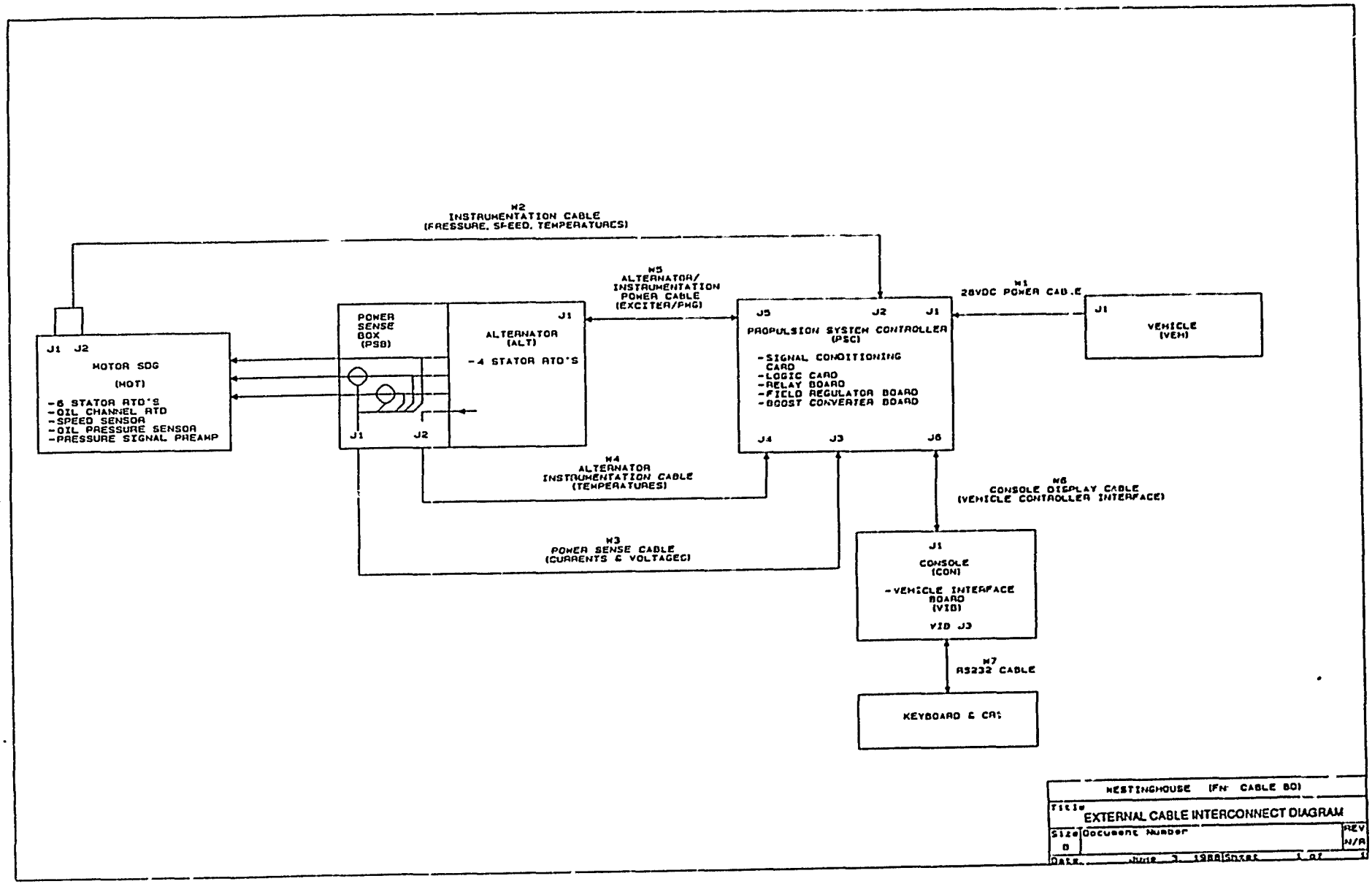


05/204/88/86

Figure 68. Cable Interconnect Diagram

## 2.6 System Performance Modeling

### 2.6.1 System Model

The system provides a speed at the load that is directly proportional to the speed of the prime mover for steady-state conditions. The speed of the load is always impelled toward a value that is directly proportional to the speed of the prime mover under dynamic conditions.

Figure 69 shows a general block diagram of the model of the system.

The model represents the characteristics of the actual system hardware with sufficient detail to provide simulation results that accurately predict the steady-state and dynamic behavior of the system.

Each portion or block of the model will be discussed separately in the following, starting from the prime mover and moving through the model to the load.

Prime Mover:

The prime mover is taken to be an ideal mechanical power source. In the model, the prime mover can deliver any needed amount of power at any speed and the speed is not affected by the mechanical load.

Permanent Magnet Generator:

The permanent magnet generator is, in effect, a tachometer that produces an output voltage that is directly proportional to the speed of the prime mover. The output voltage of the permanent magnet generator is the input to the dynamic control system. The terminal voltage of the main alternator is controlled to be directly proportional to the output voltage of the permanent magnet generator.

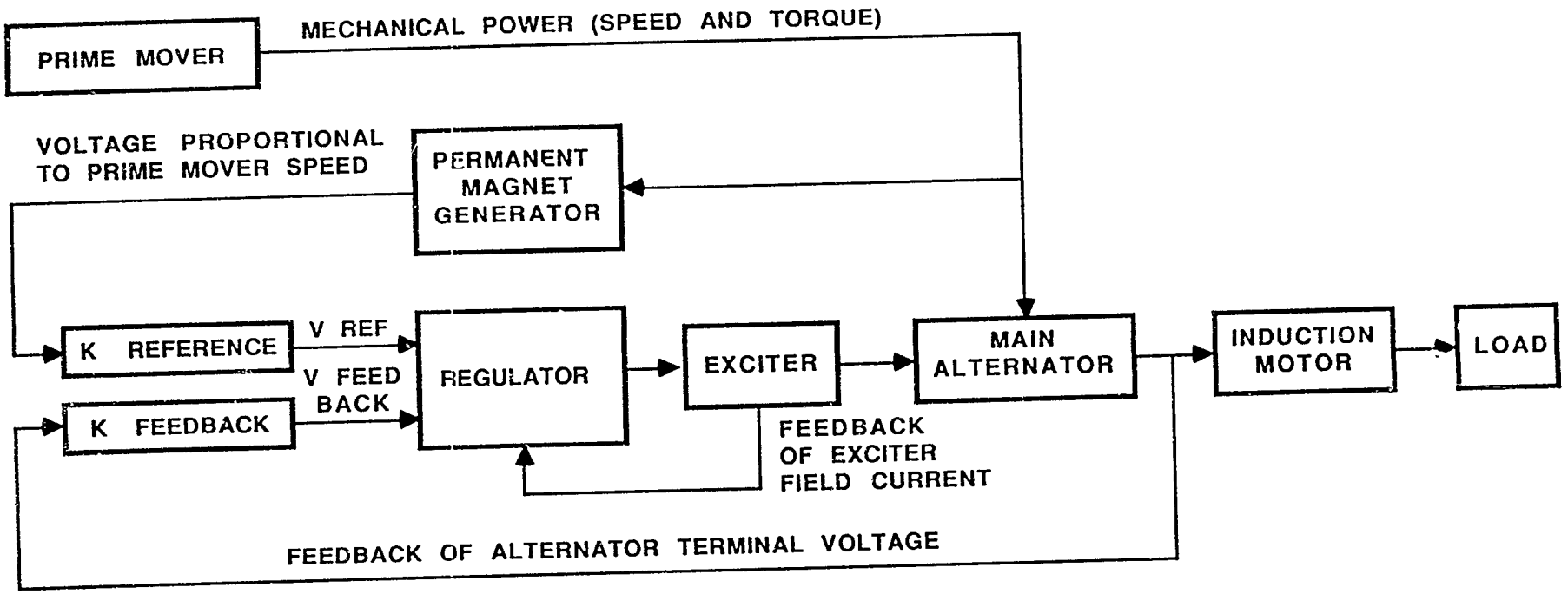




05/204/88/036-F

Figure 69. Block Diagram of System Model

Regulator:

Figure 70 shows a simplified block diagram of the regulator.

In the model, the reference voltage input to the regulator is calculated as a simple constant times the speed of the prime mover. The feedback of the alternator terminal voltage is also calculated by means of a simple constant that takes into account the three phase rectification and attenuation of the system hardware.

The model represents the proportional-integral feedback control method of the regulator, the pulse width modulation drive of the exciter field current, and the inner loop of feedback of the exciter field current that is used to limit the current to the 9 ampere thermal capability of the hardware.

A boost converter is used to obtain 150 volts DC from a 28 volt DC source. The 150 volts is needed to provide sufficient drive with the pulse width modulation to change the exciter field current fast enough to maintain stability during dynamic system variations due to changes of prime mover speed, changes of system load, or combinations of speed and load change.

Exciter:

Figure 71 shows a schematic representation of the exciter model.

The output of the regulator is represented in the model as a voltage input to the terminals of the exciter field winding. This voltage may be - DC bus voltage (-150 volts) or any value within the range of 0 to + DC bus voltage (0 volts to +150 volts). At each time step of the model execution, the differential equation of the exciter field circuit with this input voltage is solved by a fourth order Runge-Kutta numerical procedure to obtain a value for the exciter field current.

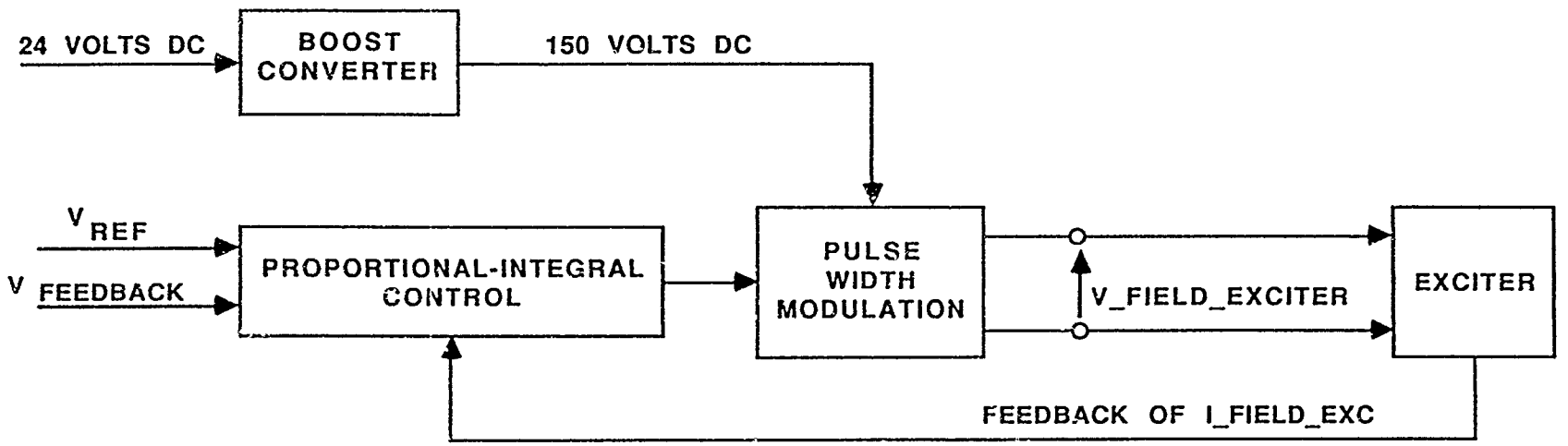




05/204/88/037-F

Figure 70. Regulator Model

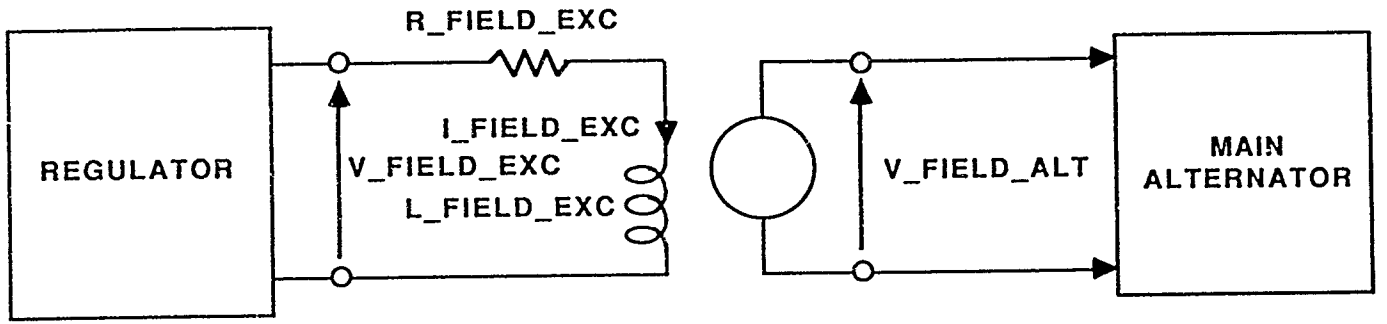


05/204/88/038-F

Figure 71. Exciter Model

The exciter field current is limited to a maximum positive value of 9 amperes. The input voltage to the exciter field is allowed to be equal to negative bus voltage to force the current toward zero, but the field current is not allowed to go negative.

The exciter field current is used as the input to a lookup table that is interpolated to obtain a value for the input voltage to the field of the main alternator. Since the exciter field current is allowed to have only positive values, the input voltage to the field of the main alternator can only have positive values. This simulates the operation of the rectifiers between the exciter output and the main alternator field winding of the actual hardware.

The lookup table has different sets of values for different system operating conditions. A different lookup table is used for each of three equivalent speeds of the prime mover and for the system cold or hot.

The lookup table values have been derived from the transfer curves shown in Figures 72 and 73. The curves show the steady-state relation between the current in the exciter field and the current in the main alternator field with magnetic saturation and machine temperatures taken into account. This information has been translated into curves of DC voltage input to the main alternator field winding versus exciter field current.

Main Alternator:

Figure 74 shows a schematic and block diagram representation of the model of the main alternator.

The calculation of the field current of the main alternator is done in the same way as the calculation of the exciter field current. At each time step of the model execution, the differential equation of the main alternator field circuit is solved by a fourth order Runge-Kutta numerical procedure. The input voltage in this equation is the output voltage of the exciter which is never negative; the main alternator field current can have only positive values and there is no upper limit imposed in the model.

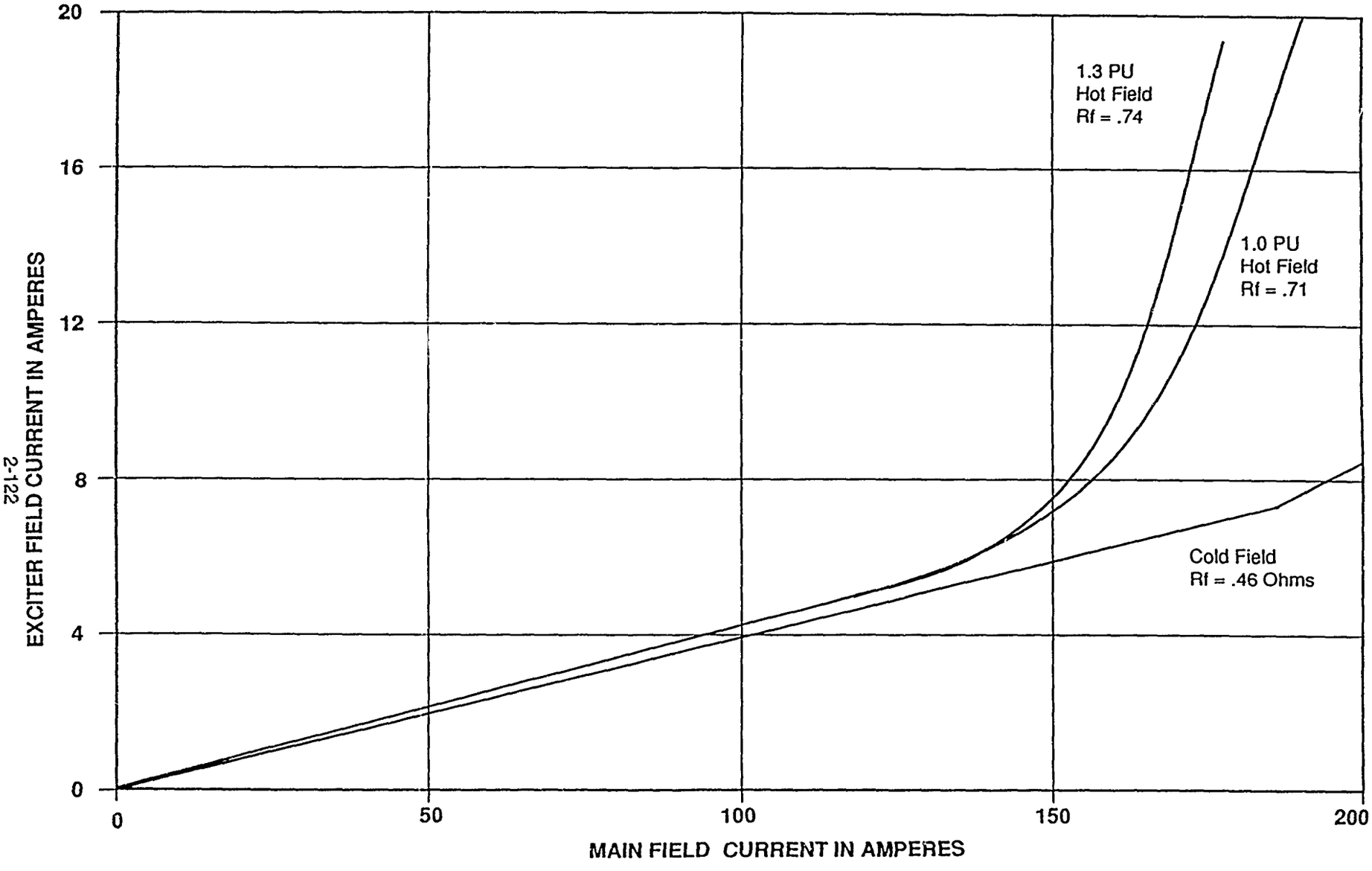




05/204/88/039-A

Figure 72. Exciter Field Current vs. Main Field Current (9000 RPM - Hiperco 50)

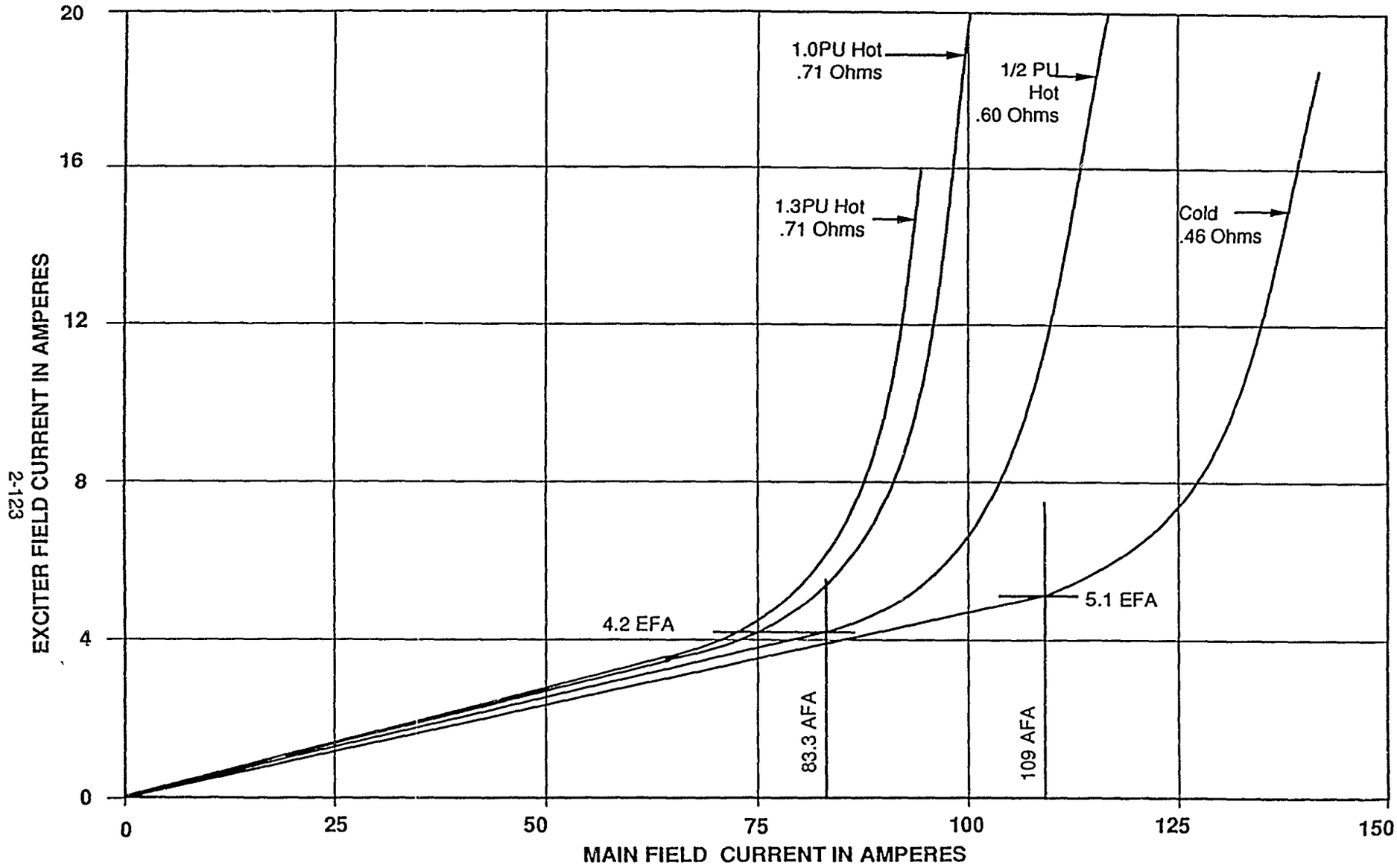


Figure 73. Exciter Field Current vs. Main Field Current (4306 RPM - Hiperco 50)

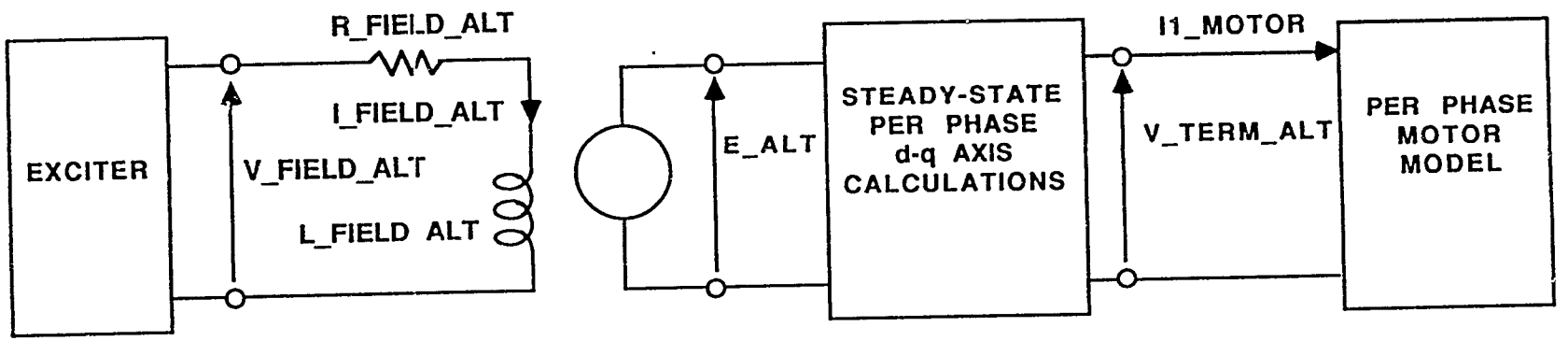


05/204/88/041-F



Figure 74. Main Alternator Model

An "effective" value of field current that is equal to the main alternator field current minus a demagnetizing component of the alternator load current is used as the input to a lookup table that is interpolated to obtain a value for the generated voltage within the main alternator. The lookup table values are multiplied by a constant factor and the prime mover speed to account for the variation of generated voltage with alternator speed. The values used in this lookup table have been derived from the curves shown in Figure 75. The curves show the steady-state relation between the current in the alternator field and the alternator terminal voltage for various load conditions with magnetic saturation and machine temperatures taken into account. This information has been translated into curves of generated voltage versus field current.

A steady-state d-q axis model is used in conjunction with the alternator load current (induction motor input current) to calculate the terminal voltage of the alternator. Figure 76 shows a curve that is used to account for saturation of the leakage inductance of the main alternator versus the load current. This curve is translated into a lookup table that is interpolated in the model. The d-q axis calculations also provide the value of the demagnetizing component of the load current that is subtracted from the field current to obtain the "effective" field current that is used with the lookup table.

Induction Motor:

Figure 77 shows the usual steady-state per phase equivalent circuit representation of the induction motor plus the resistance and inductance of the connecting cable from the main alternator to the induction motor.

The induction motor simulation calculations start from an initial value of motor speed which determines the slip at that moment in time. The voltages and currents in the equivalent circuit of the induction motor are calculated for the particular values of terminal voltage of the main alternator and the motor slip.

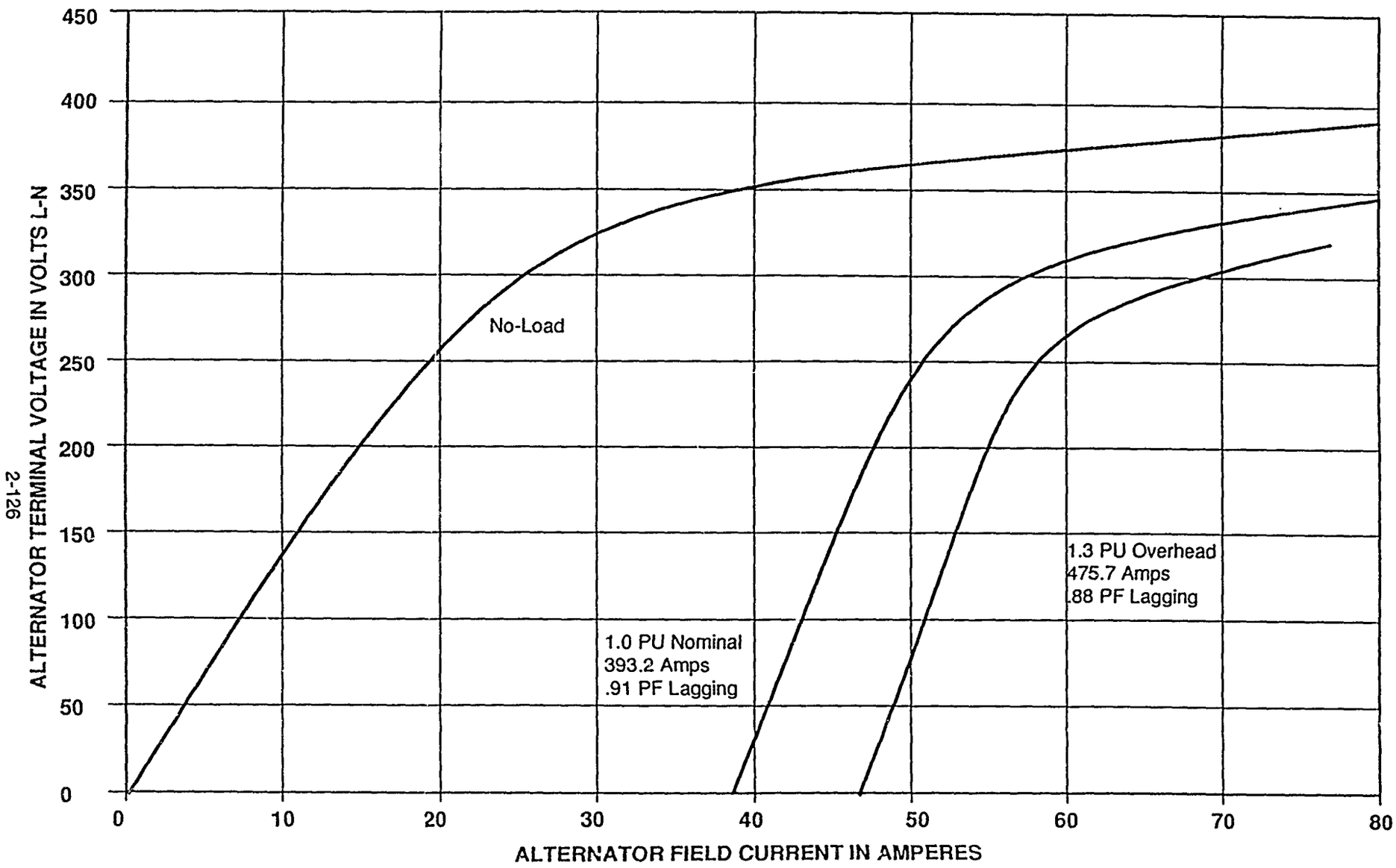


05/204/88/042-A

Figure 75. Load Saturation Curves for Main Alternator - - 9000 RPM

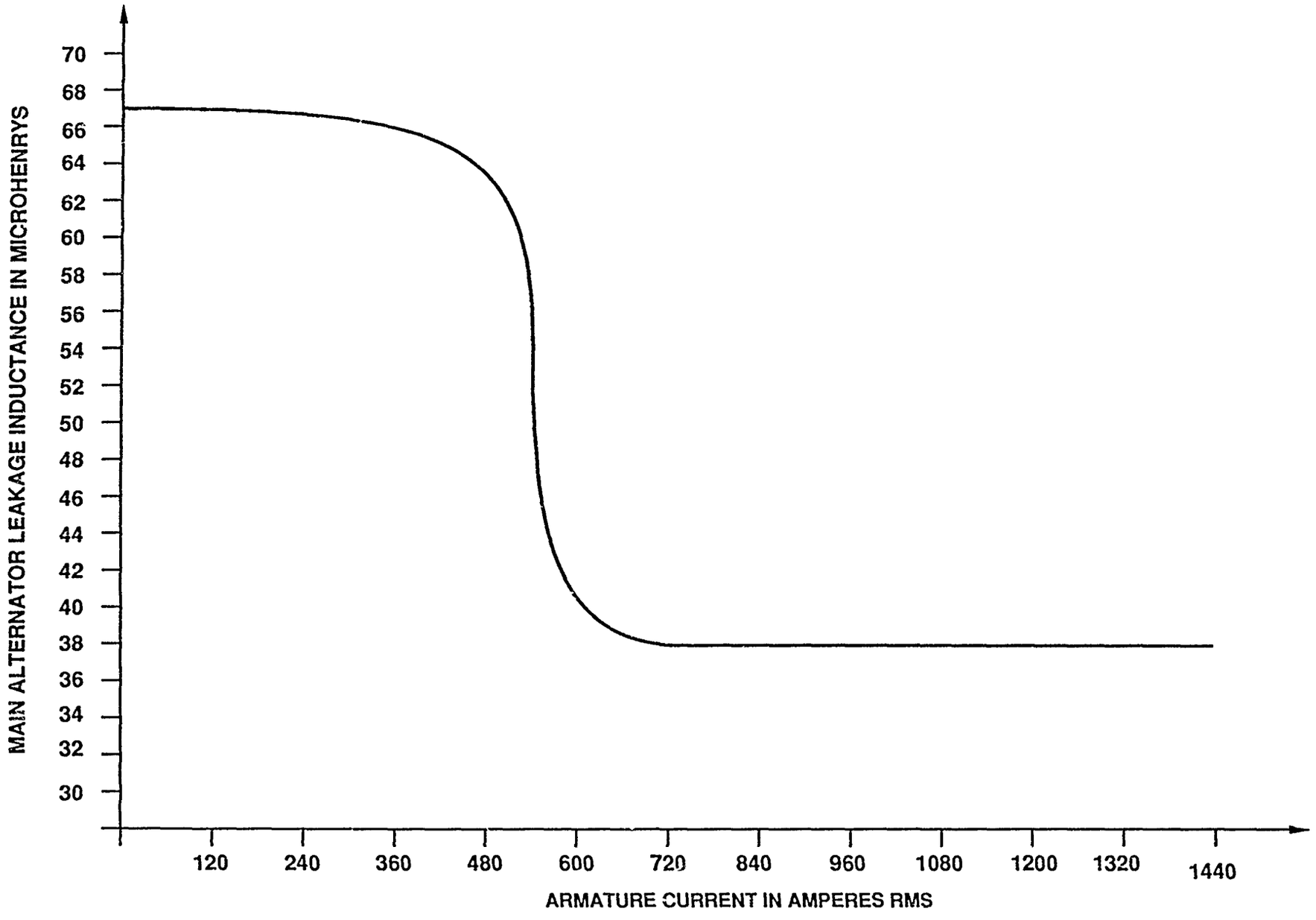


05/204/88/043-A

Figure 76. Main Alternator Leakage Inductance vs. Armature Current

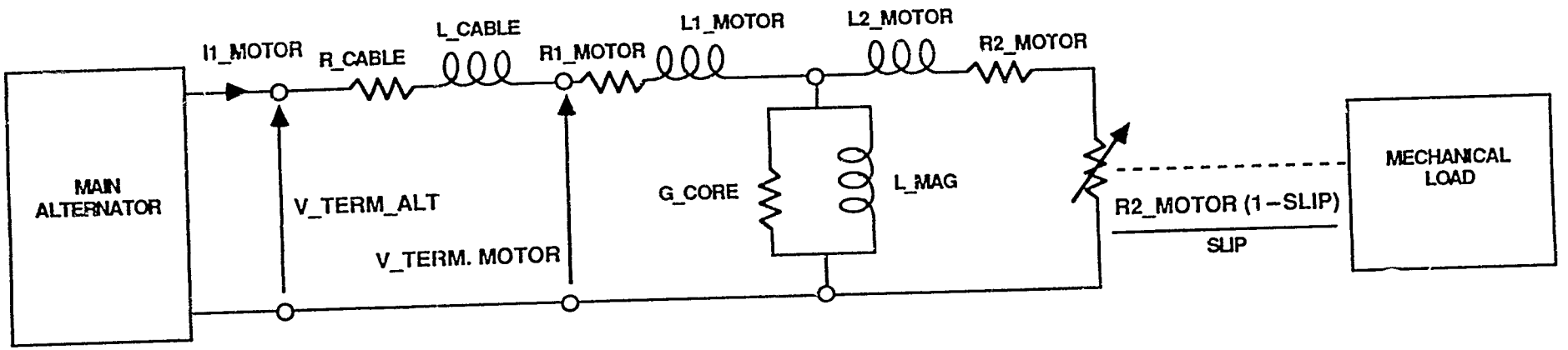


Figure 77. Induction Motor Model



05/204/88/044-F

Figure 78 shows the magnetic saturation of the magnetizing inductance of the motor versus the value of the volts per hertz at an operating point. Figures 79 and 80 show variation of R2_MOTOR and L2_MOTOR versus slip. These curves are used in the model as interpolated lookup tables.

The torque produced in the motor is calculated from the equivalent circuit and is used with the model of the load to calculate the speed of the motor.

Load:

The model of the load is represented by the block diagram of Figure 81 and the torque versus speed curve of Figure 82.

In the model, all load effects are referred to the motor side of the speed reduction gear and the combined equivalent friction and moment of inertia values of the motor, reduction gear, and load are treated as parts of the load. The torque versus speed curve of Figure 82 is represented in the model as torque equals a constant times speed squared. To account for the efficiency of the speed reduction gear, the constant has been chosen so that the nominal steady-state output power of the motor is 310.3 kilowatts (416 horsepower) at an equivalent alternator speed of 9000 rpm.

### 2.6.2 Results of Simulations Using Non-Linear System Model

#### 2.6.2.1 Starting Simulation

Due to thermal limitations in the alternator, the starting line current must be limited to about 900A for three seconds maximum duration. Figure 83 shows a "cold" start at an ambient temperature of 10 degrees C with all nominal system parameters. The motor started in 2.2 seconds with a peak line current of about 1000A.

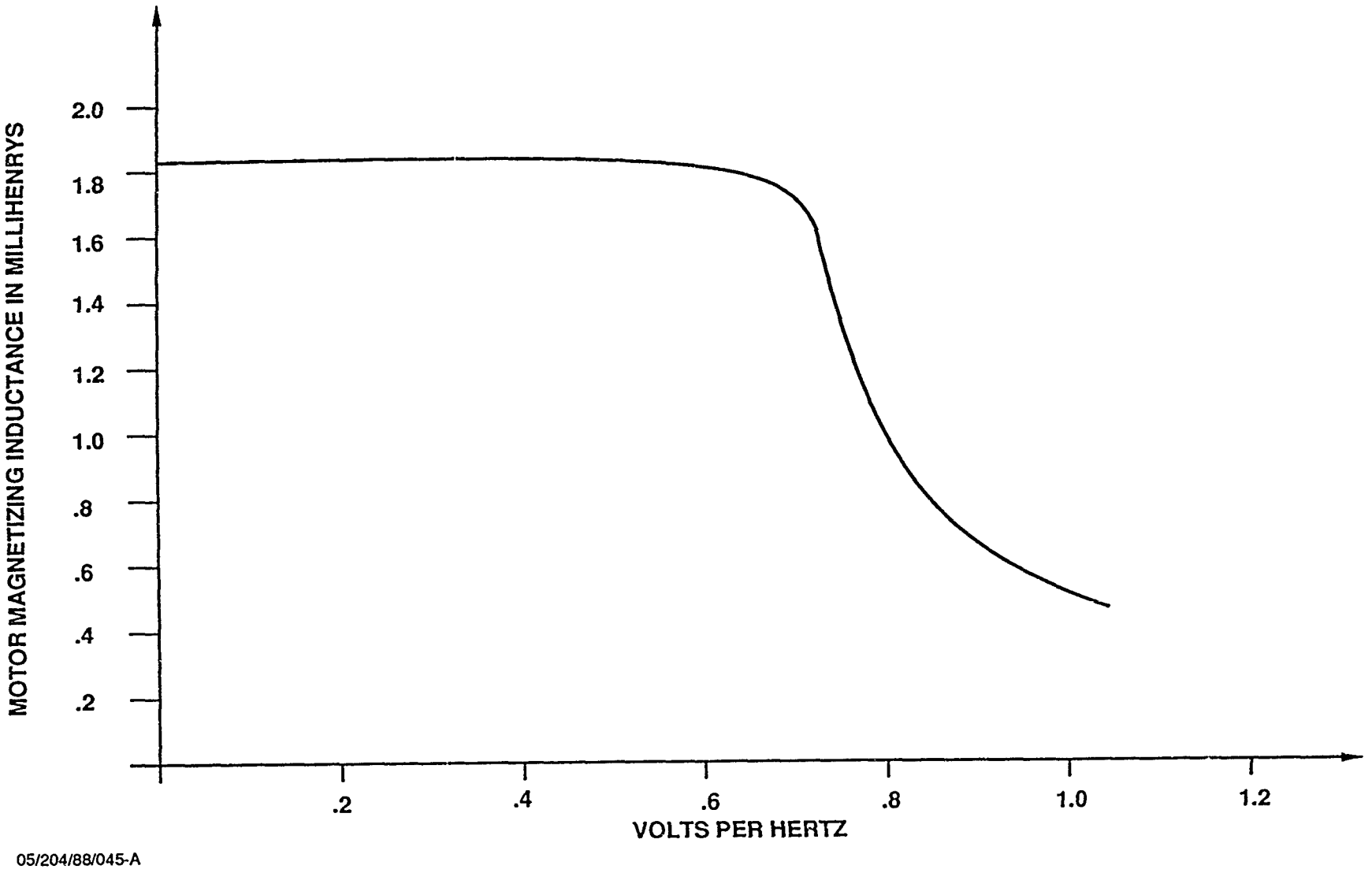




Figure 78. Motor Magnetizing Inductance vs. Volts Per Hertz

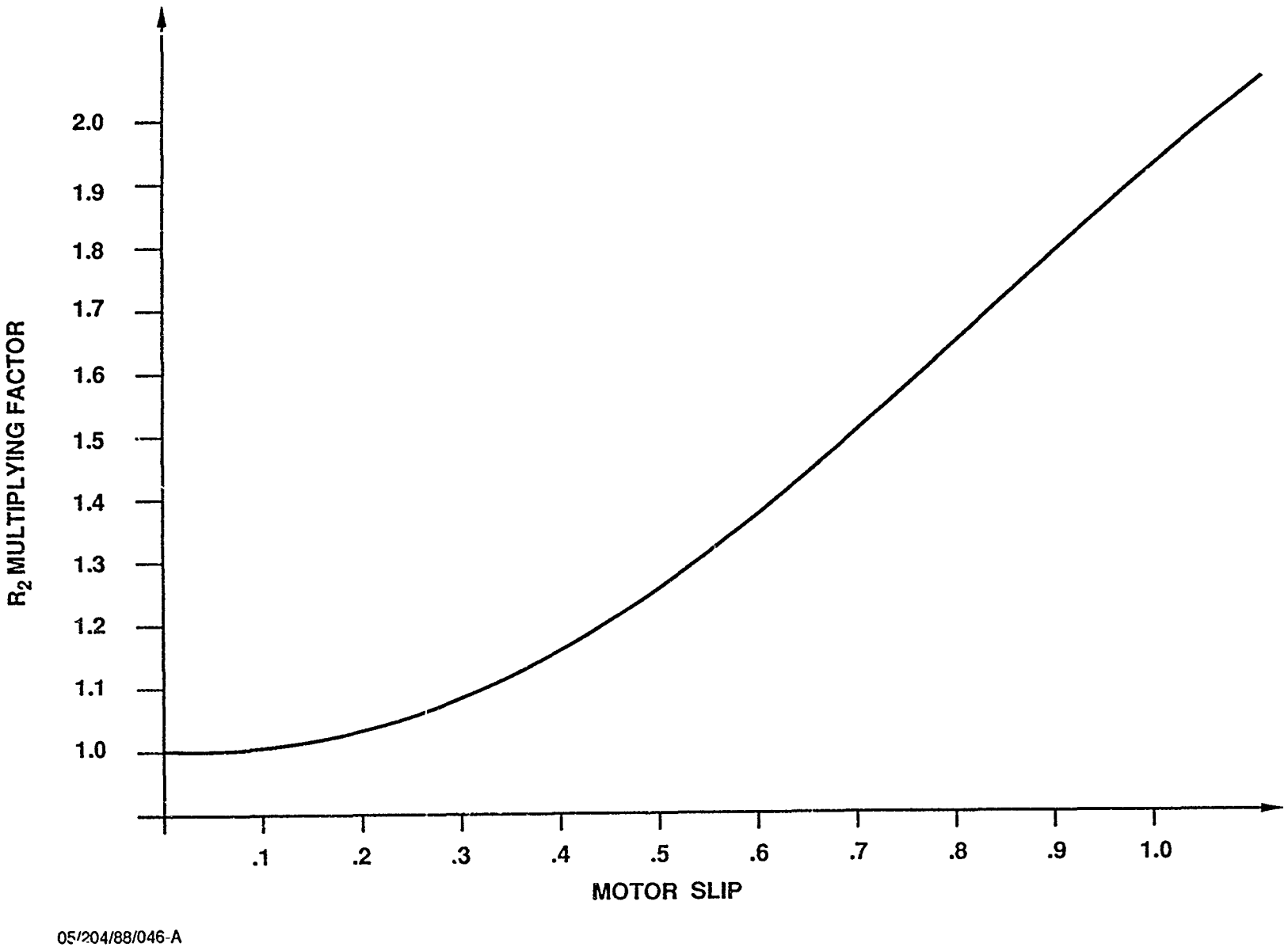


Figure 79. Motor Rotor Resistance Variation with Slip

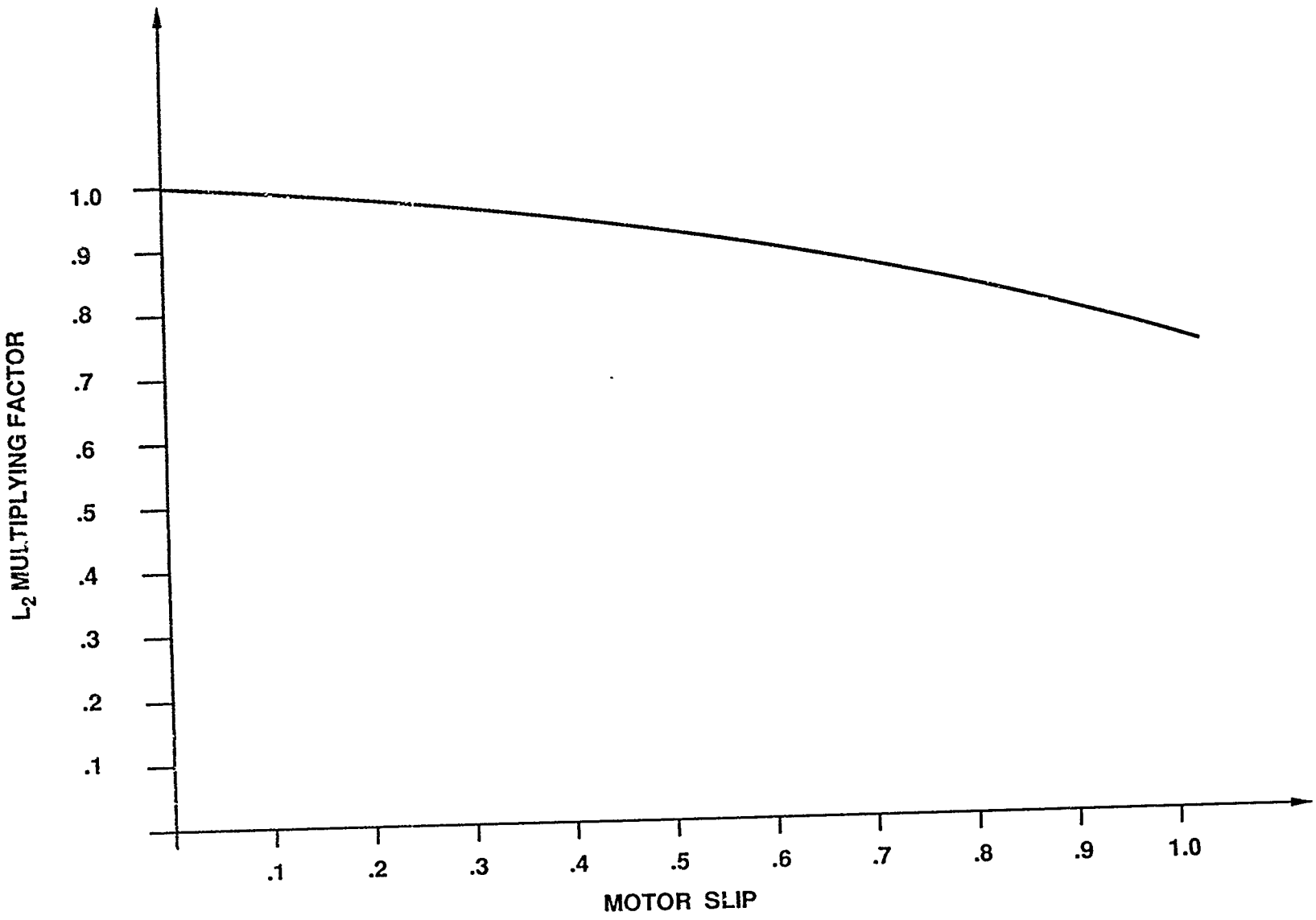


Figure 80. Motor Rotor Inductance Variation with Slip

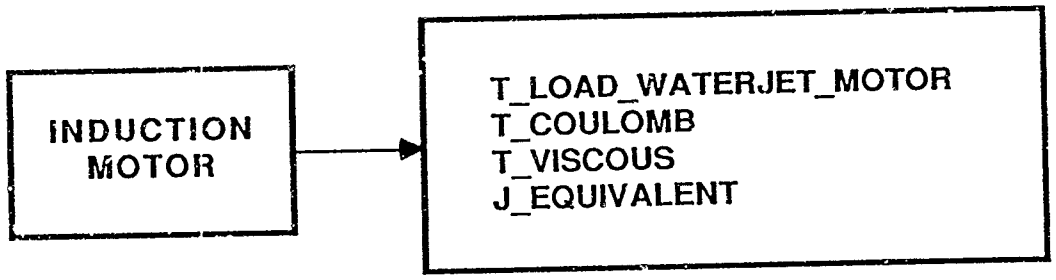






Figure 81. Load Model

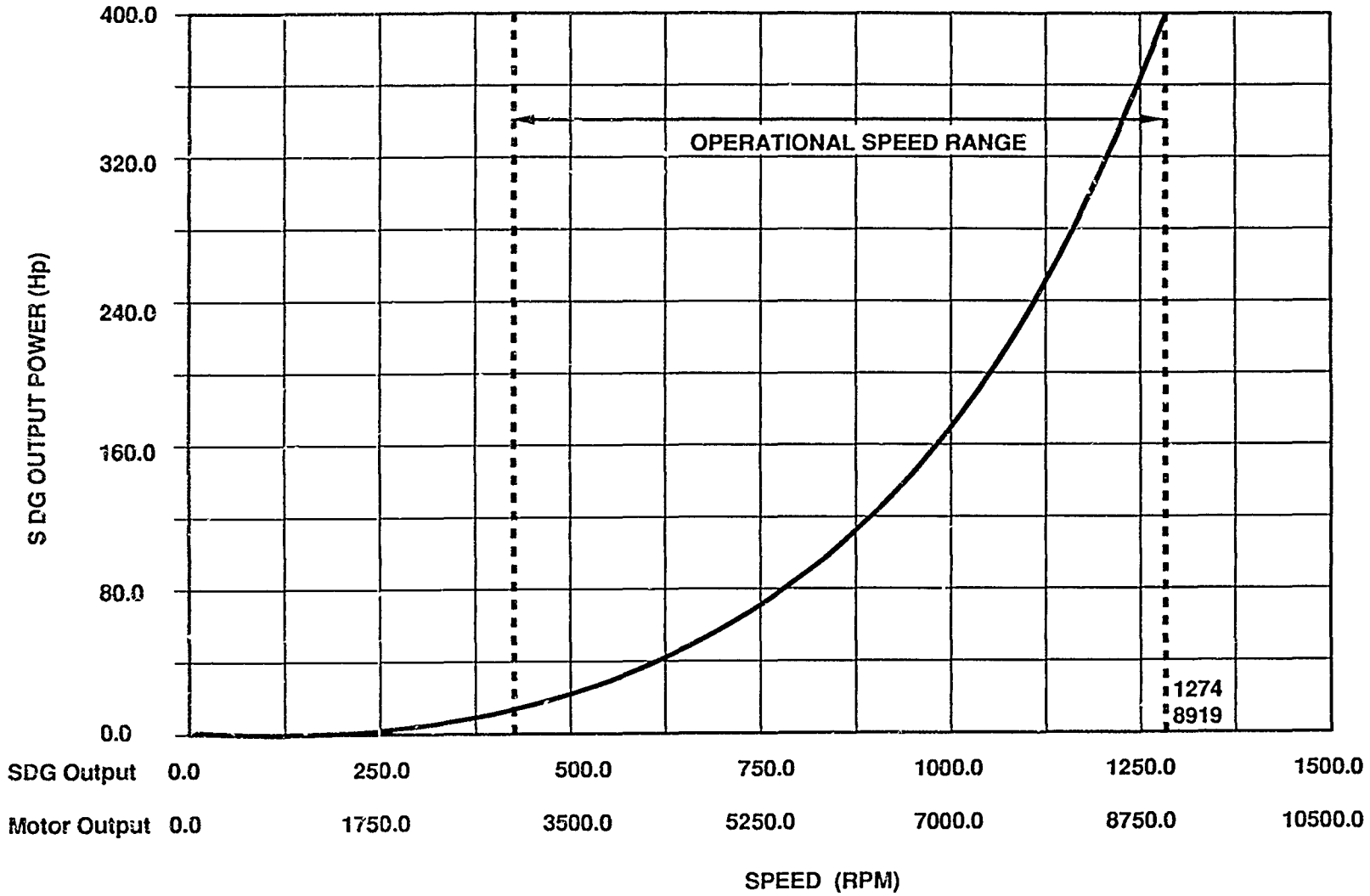


Figure 82. System Power Versus Speed

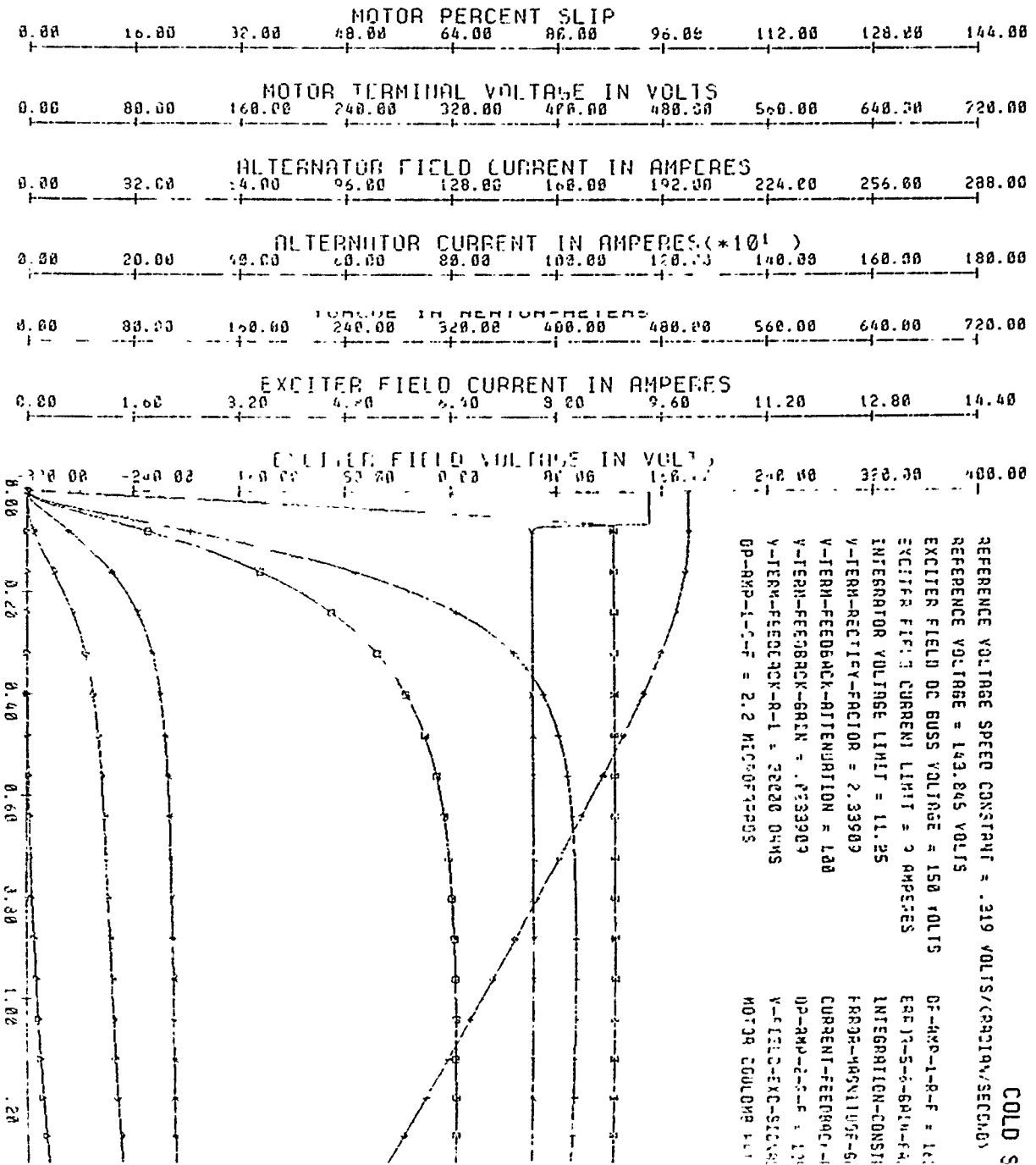
MOTOR PERCENT SLIP
0.00 16.00 32.00 48.00 64.00 80.00 96.00 112.00 128.00 144.00
MOTOR TERMINAL VOLTAGE IN VOLTS
0.00 80.00 160.00 240.00 320.00 400.00 480.00 560.00 640.00 720.00
ALTERNATOR FIELD CURRENT IN AMPERES
0.00 32.00 64.00 96.00 128.00 160.00 192.00 224.00 256.00 288.00
ALTERNATOR CURRENT IN AMPERES(*10¹ )
0.00 20.00 40.00 60.00 80.00 100.00 120.00 140.00 160.00 180.00
TORQUE IN NEWTON-METERS
0.00 80.00 160.00 240.00 320.00 400.00 480.00 560.00 640.00 720.00
EXCITER FIELD CURRENT IN AMPERES
0.00 1.60 3.20 4.80 6.40 8.00 9.60 11.20 12.80 14.40
EXCITER FIELD VOLTAGE IN VOLTS
-320.00 -240.00 -160.00 -80.00 0.00 80.00 160.00 240.00 320.00 400.00
0.00
0.20
0.40
0.60
0.80
1.00
.20
REFERENCE VOLTAGE SPEED CONSTANT = .319 VOLTS/(RADIAN/SECOND)
REFERENCE VOLTAGE = 143.845 VOLTS
EXCITER FIELD DC BUSS VOLTAGE = 150 VOLTS
EXCITER FIELD CURRENT LIMIT = 9 AMPERES
INTEGRATOR VOLTAGE LIMIT = 11.25
V-TERM-RECTIFY-FACTOR = 2.33909
V-TERM-FEEDBACK-ATTENUATION = 100
V-TERM-FEEDBACK-GAIN = .0233909
V-TERM-FEEDBACK-R-1 = 32220 OHMS
OP-AMP-1-C-F = 2.2 MICROFARADS
COLD S

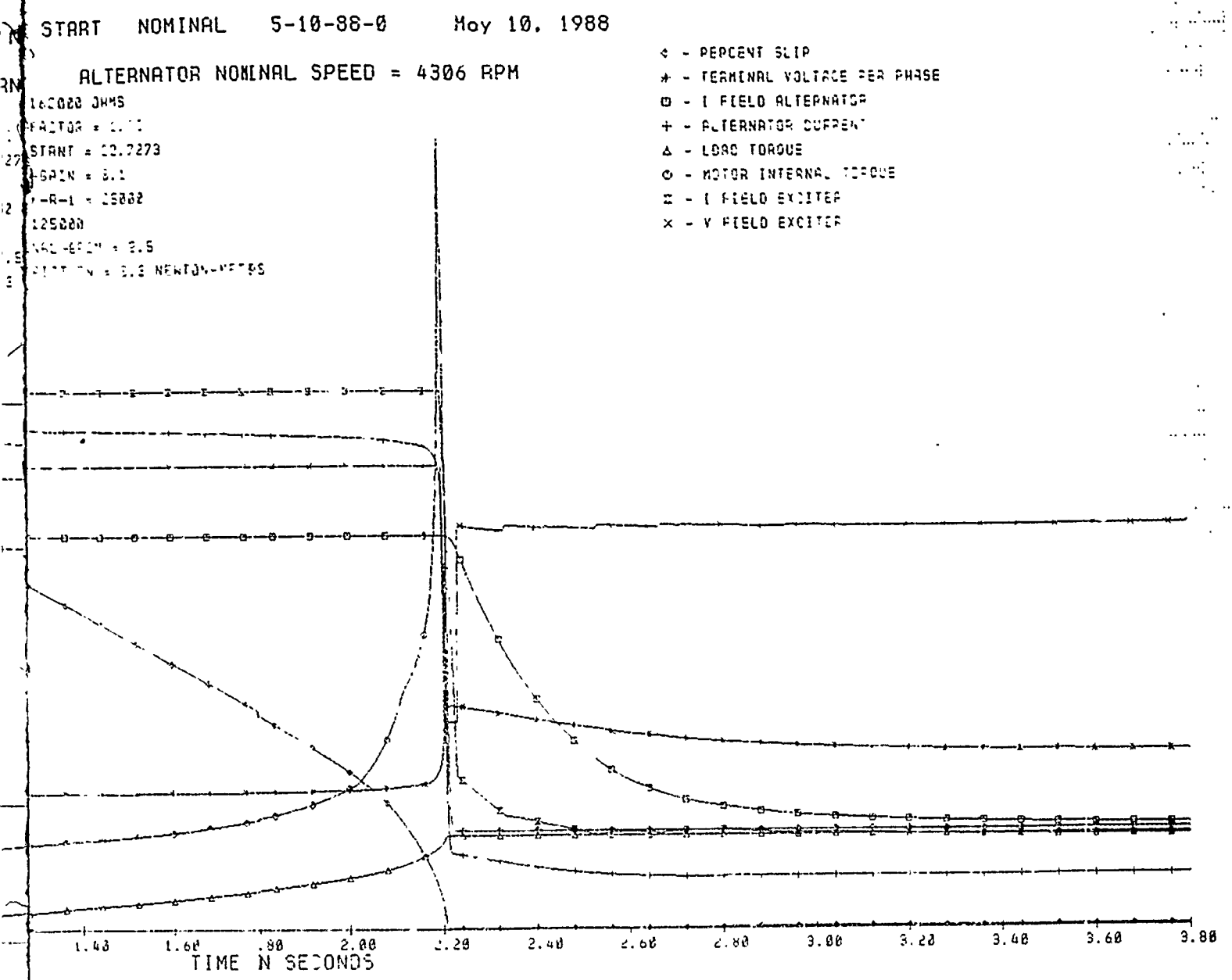


Figure 83. Cold Start - Nominal

292

Figure 84 shows another "cold" start but with the main alternator field resistance 20% high. The peak line current is about 900A but the duration has increased to 2.5 seconds. This resistance is the most sensitive parameter with regards to starting performance. The sensitivity analysis is included in Appendix VI.

Figure 85 shows a "hot" start at elevated temperatures (150 Deg C Motor) with nominal system parameters. Notice the current is reduced (800A) and the duration is slightly longer. Figure 86 shows another "hot" start but with only 100V bus and 7A current limit. The system still started acceptably.

2.6.2.2 Load Transient Simulation

Figures 87 and 88 show simulations of a hypothesized worst case load transient; the waterjet is pulled out of the water, removing the load, and after settling, is ramped into the water at a .1 second ramp rate. The system easily responds to the transient under nominal conditions and with reduced bus voltage and current limit of 100V and 5A respectively.

05/20/88/87b

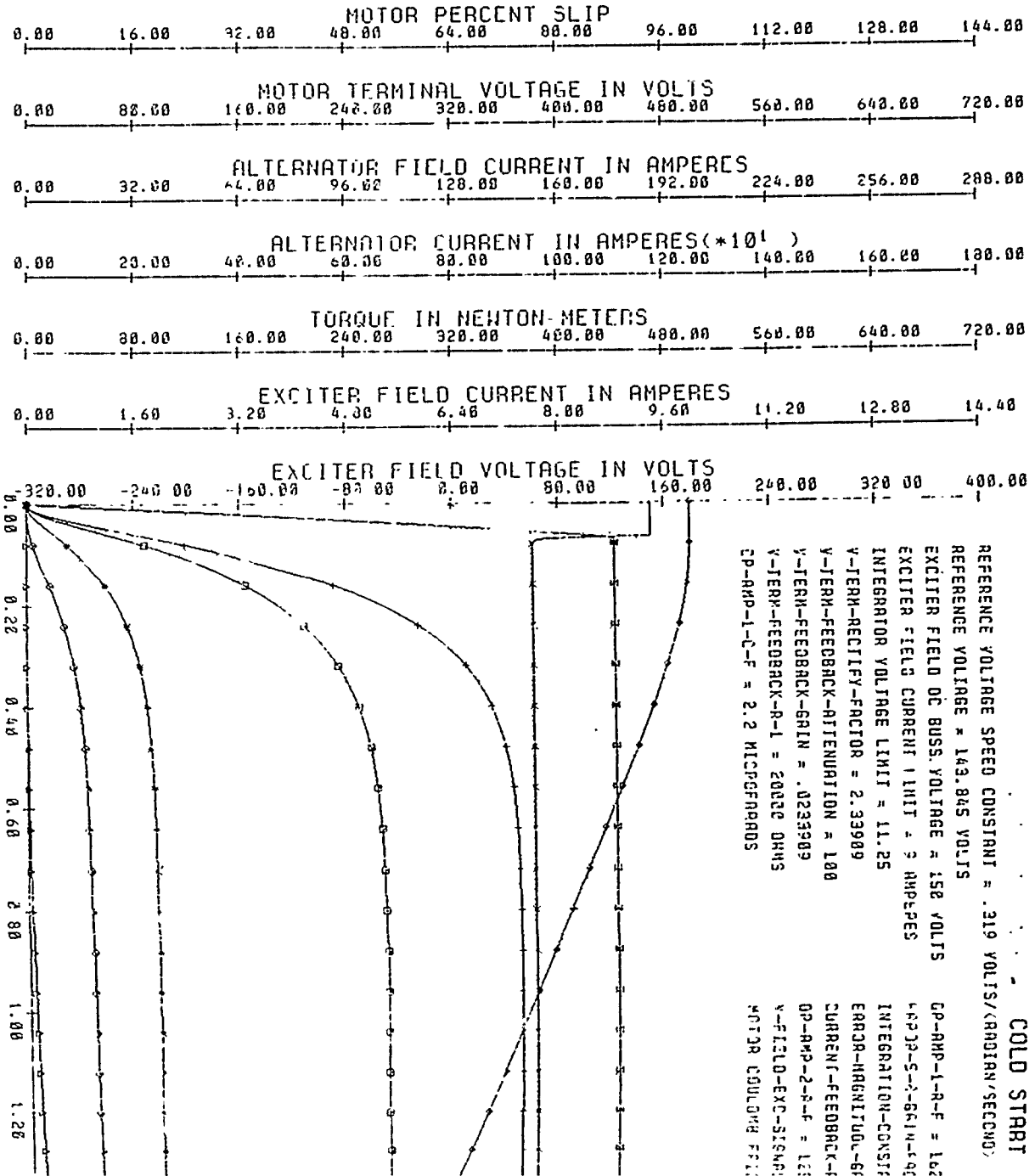
MOTOR PERCENT SLIP
0.00 16.00 32.00 48.00 64.00 80.00 96.00 112.00 128.00 144.00
MOTOR TERMINAL VOLTAGE IN VOLTS
0.00 80.00 160.00 240.00 320.00 400.00 480.00 560.00 640.00 720.00
ALTERNATOR FIELD CURRENT IN AMPERES
0.00 32.00 64.00 96.00 128.00 160.00 192.00 224.00 256.00 288.00
ALTERNATOR CURRENT IN AMPERES(*10¹ )
0.00 20.00 40.00 60.00 80.00 100.00 120.00 140.00 160.00 180.00
TORQUE IN NEWTON-METERS
0.00 80.00 160.00 240.00 320.00 400.00 480.00 560.00 640.00 720.00
EXCITER FIELD CURRENT IN AMPERES
0.00 1.60 3.20 4.80 6.40 8.00 9.60 11.20 12.80 14.40
EXCITER FIELD VOLTAGE IN VOLTS
-320.00 -240.00 -160.00 -80.00 0.00 80.00 160.00 240.00 320.00 400.00
0.00 0.20 0.40 0.60 0.80 1.00 1.20
REFERENCE VOLTAGE SPEED CONSTANT = .319 VOLTS/(RADIAN/SECOND)
REFERENCE VOLTAGE = 143.845 VOLTS
EXCITER FIELD DC BUS VOLTAGE = 150 VOLTS
EXCITER FIELD CURRENT LIMIT = 5 AMPERES
INTEGRATOR VOLTAGE LIMIT = 11.25
Y-TERM-RECTIFY-FACTOR = 2.33909
Y-TERM-FEEDBACK-ATTENUATION = 1.00
Y-TERM-FEEDBACK-GAIN = .0233909
Y-TERM-FEEDBACK-R-L = 20000 OHMS
OP-AMP-1-C-F = 2.2 MICROFARADS
OP-AMP-1-R-F = 143
OP-AMP-2-R-F = 133
Y-FIELD-EXC-SENSE
MOTOR COULOMB FRI
COLD START

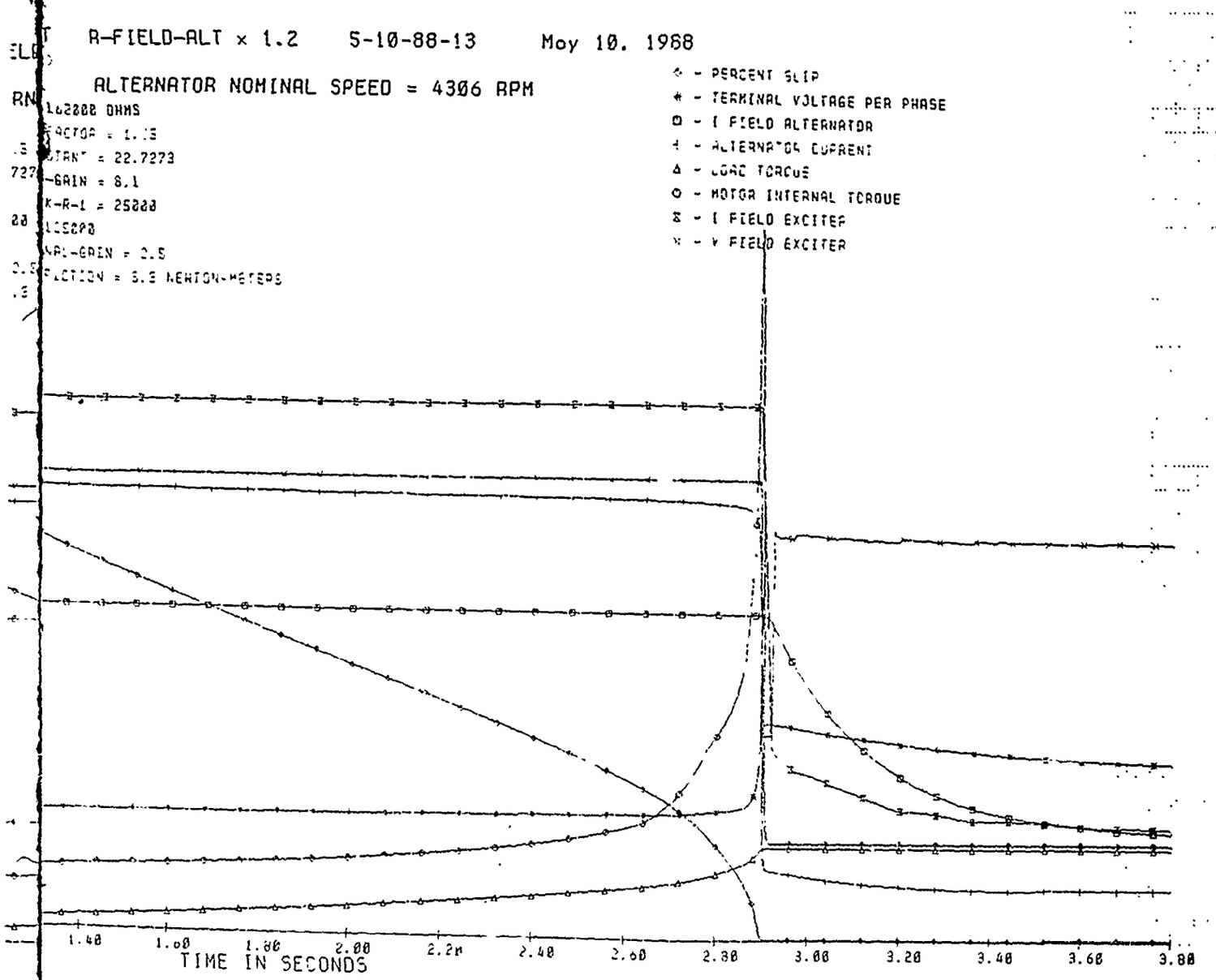


Figure 84. Cold Start - R-JField-Alt x 1.2



292

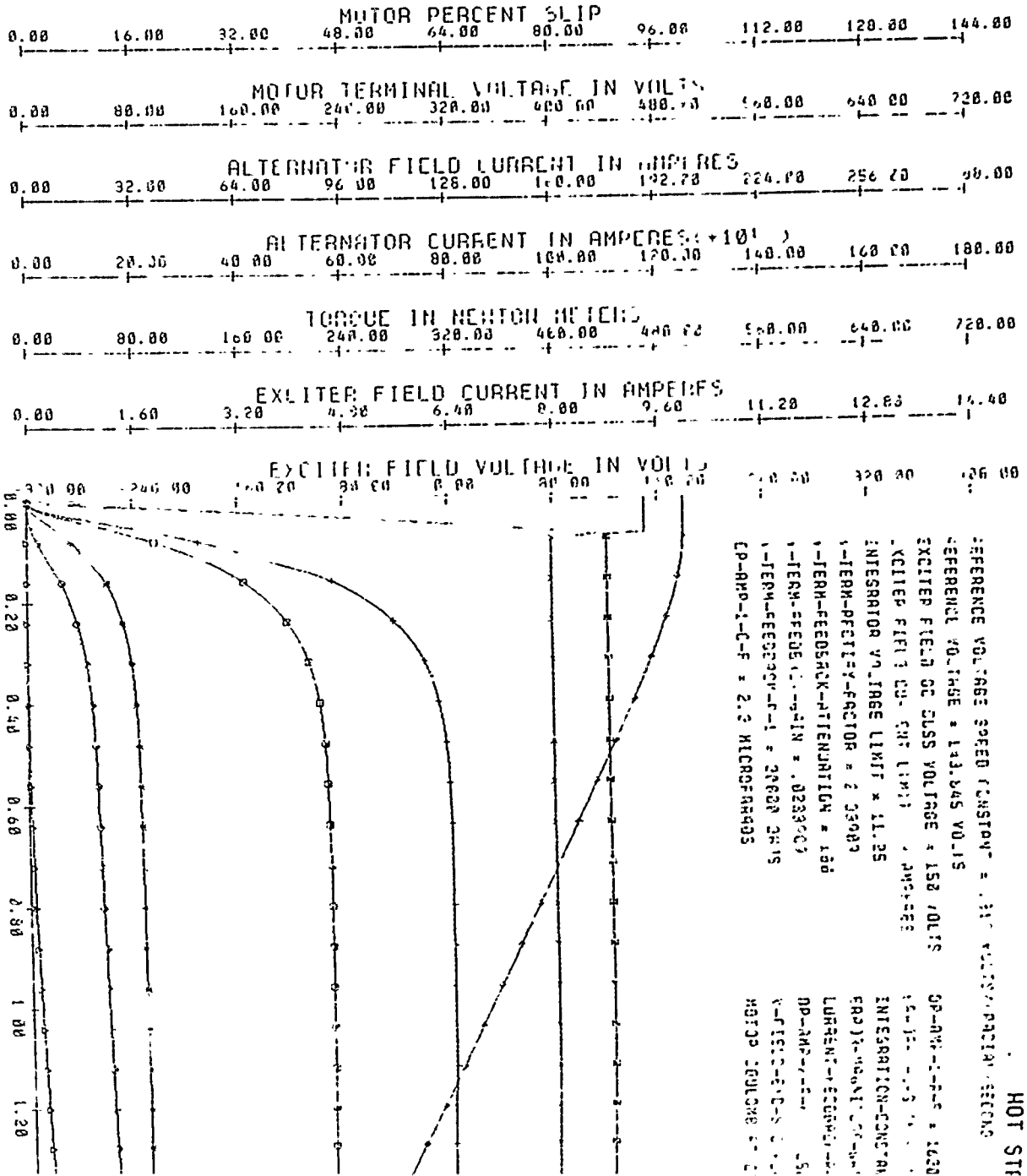
MOTOR PERCENT SLIP
0.00
16.00
32.00
48.00
64.00
80.00
96.00
112.00
120.00
144.00
MOTOR TERMINAL VOLTAGE IN VOLTS
0.00
80.00
160.00
240.00
320.00
400.00
480.00
560.00
640.00
720.00
ALTERNATOR FIELD CURRENT IN AMPERES
0.00
32.00
64.00
96.00
128.00
160.00
192.00
224.00
256.00
288.00
ALTERNATOR CURRENT IN AMPERES (*10^1)
0.00
20.00
40.00
60.00
80.00
100.00
120.00
140.00
160.00
180.00
TORQUE IN NEWTON METERS
0.00
80.00
160.00
240.00
320.00
400.00
480.00
560.00
640.00
720.00
EXCITER FIELD CURRENT IN AMPERES
0.00
1.60
3.20
4.80
6.40
8.00
9.60
11.20
12.80
14.40
EXCITER FIELD VOLTAGE IN VOLTS
0.00
0.20
0.40
0.60
0.80
1.00
1.20
REFERENCE VOLTAGE SPEED CONSTANT = 1.5
REFERENCE VOLTAGE = 143.845 VOLTS
EXCITER FIELD DC LOSS VOLTAGE = 158 VOLTS
EXCITER FIELD CURRENT LIMIT = AMPERES
INTEGRATOR VOLTAGE LIMIT = 11.25
1-TERM-DERIVATIVE-FACTOR = 2.53003
1-TERM-FEEDBACK-ATTENUATION = 100
1-TERM-FEEDBACK-GAIN = .0233003
1-TERM-FEEDBACK-T-1 = 2000 OHMS
EP-AMP-1-C-F = 2.2 MICROFARADS
HOT STA

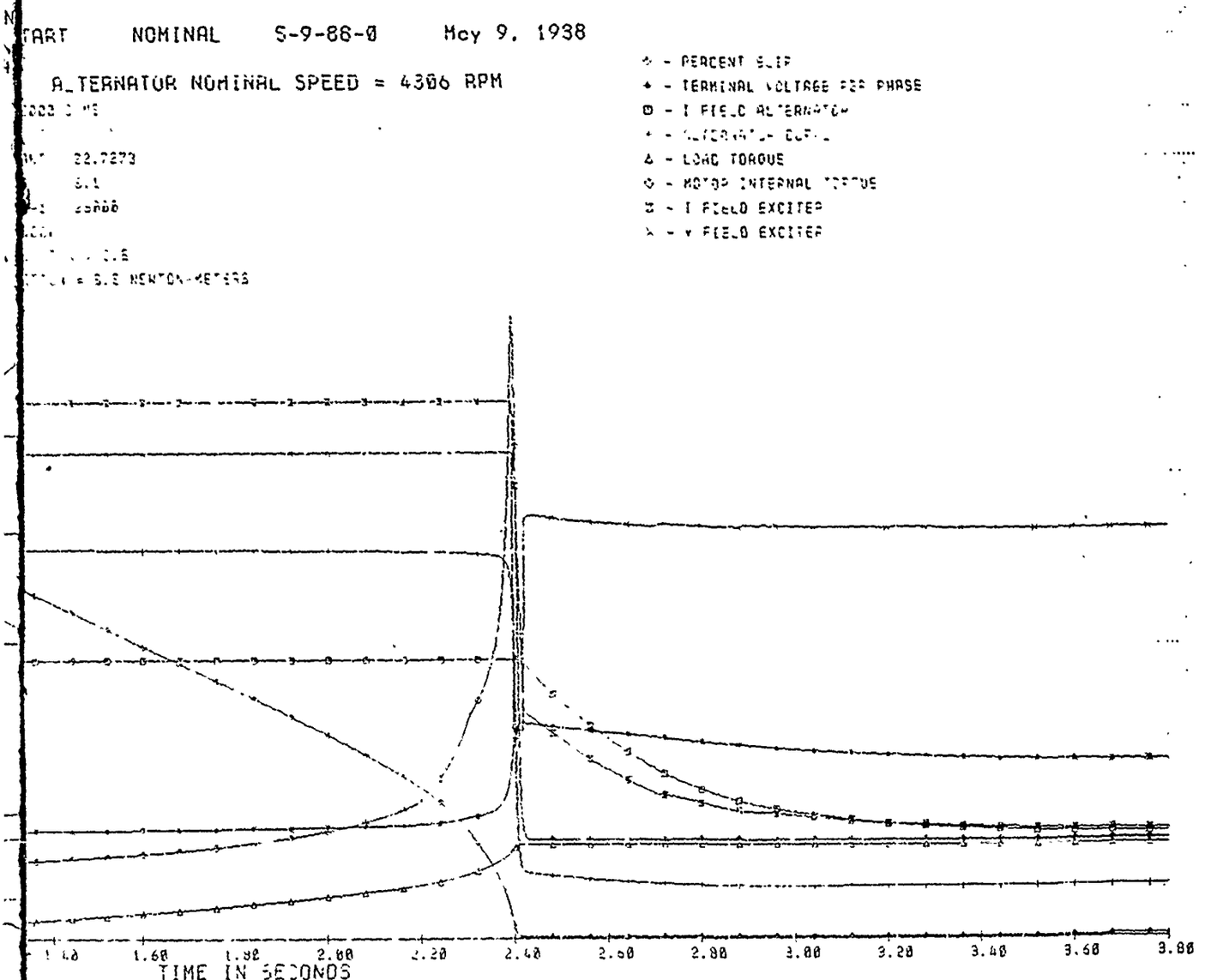


Figure 85. Hot Start - Nominal

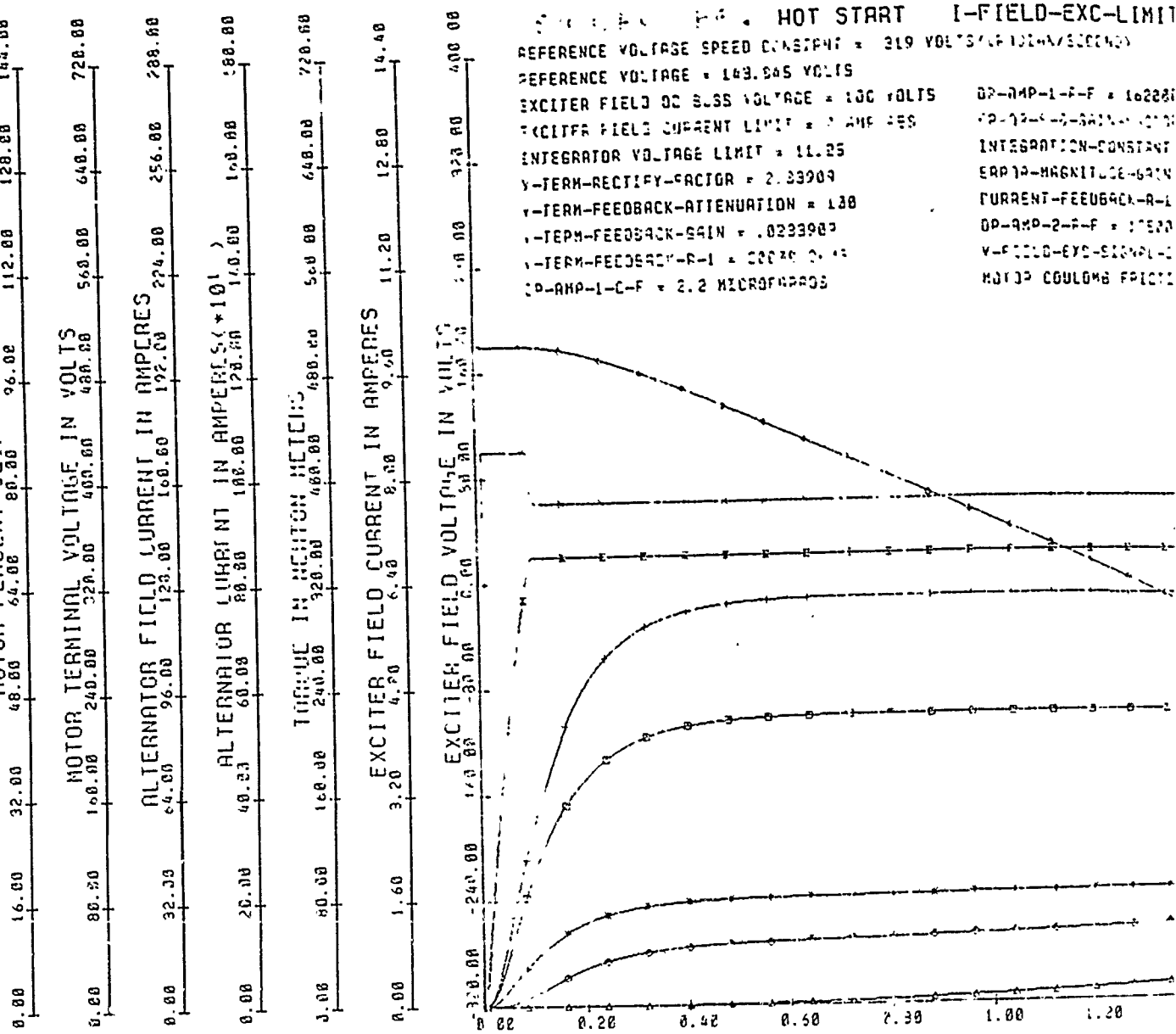


05/204/88/87d

182

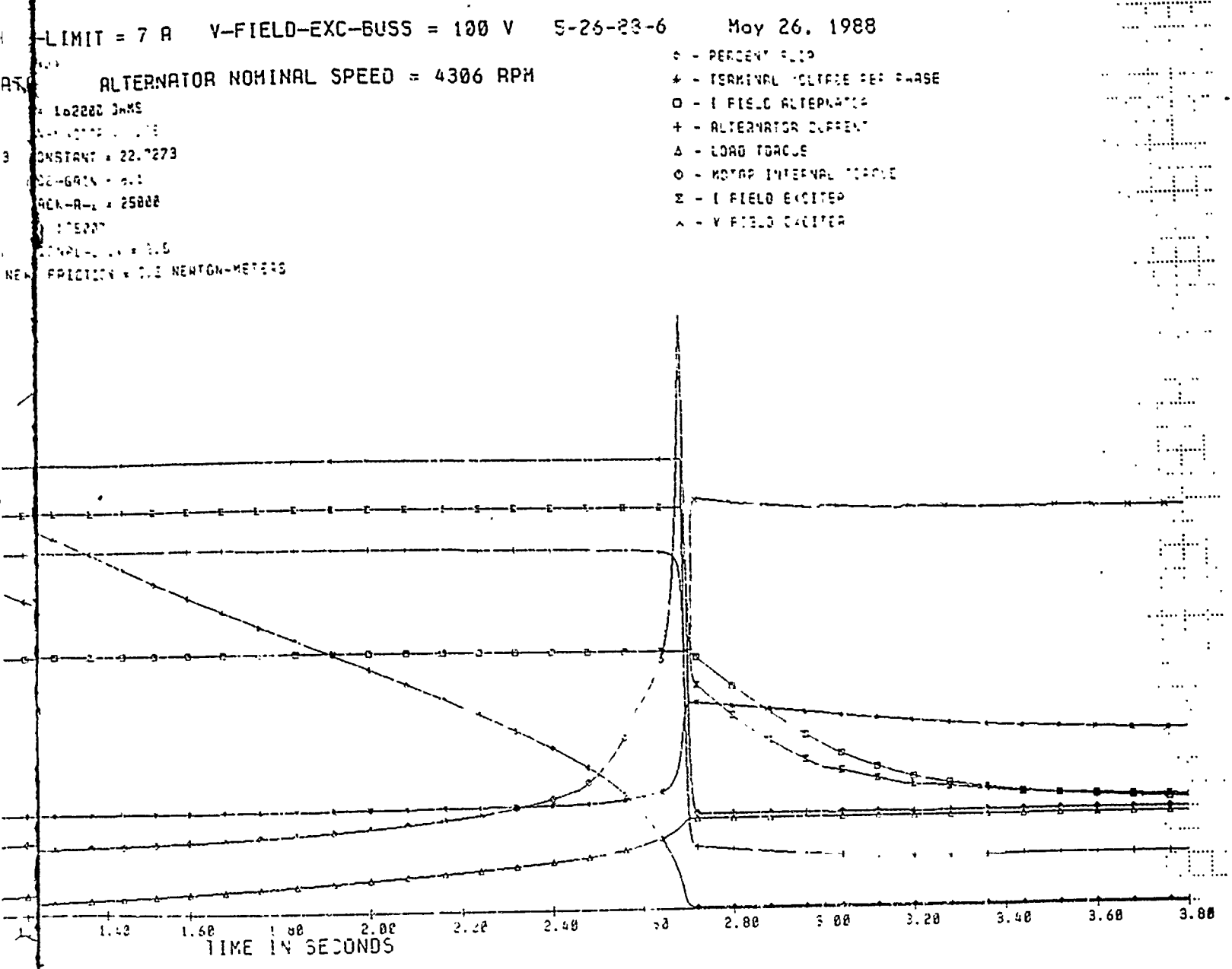


Figure 86. Hot Start - I-Field-EX -Limit = 7A

05/204/88/87d

137

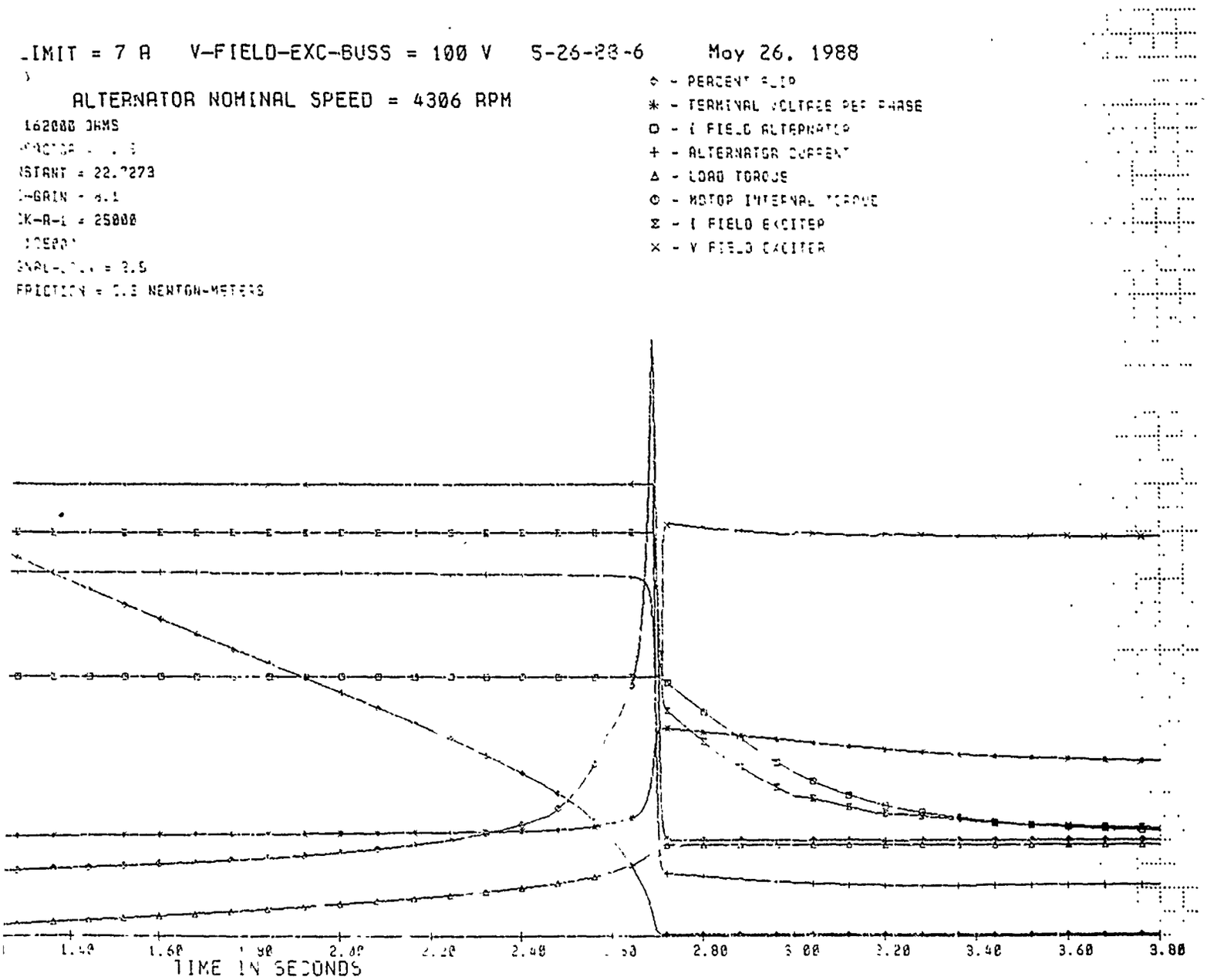


Figure 86. Hot Start - I-Field-EX -Limit = 7A



292

05/204/88/87e

152

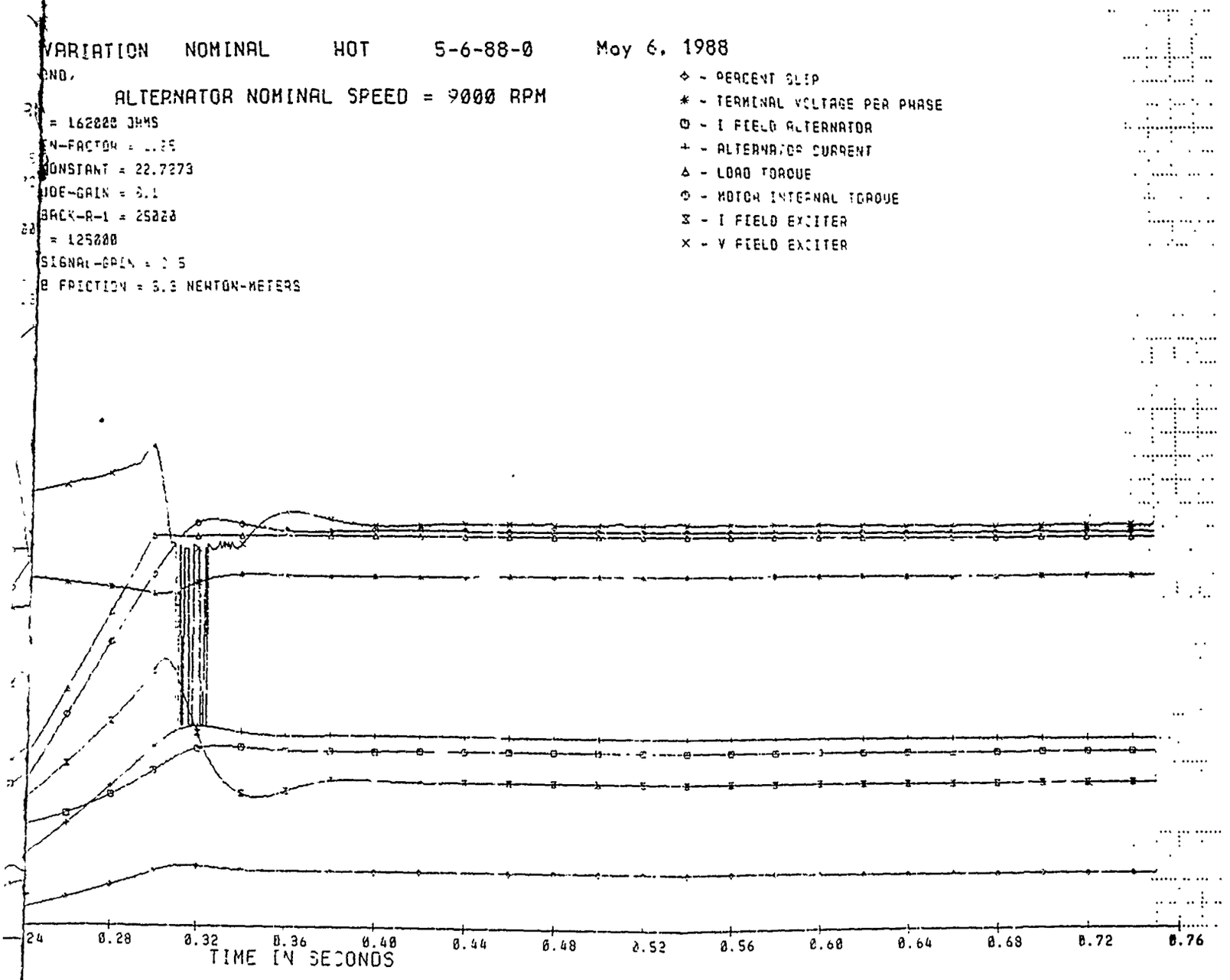


Figure 87. Ramp Load Variation - Nominal - Hot

2-140

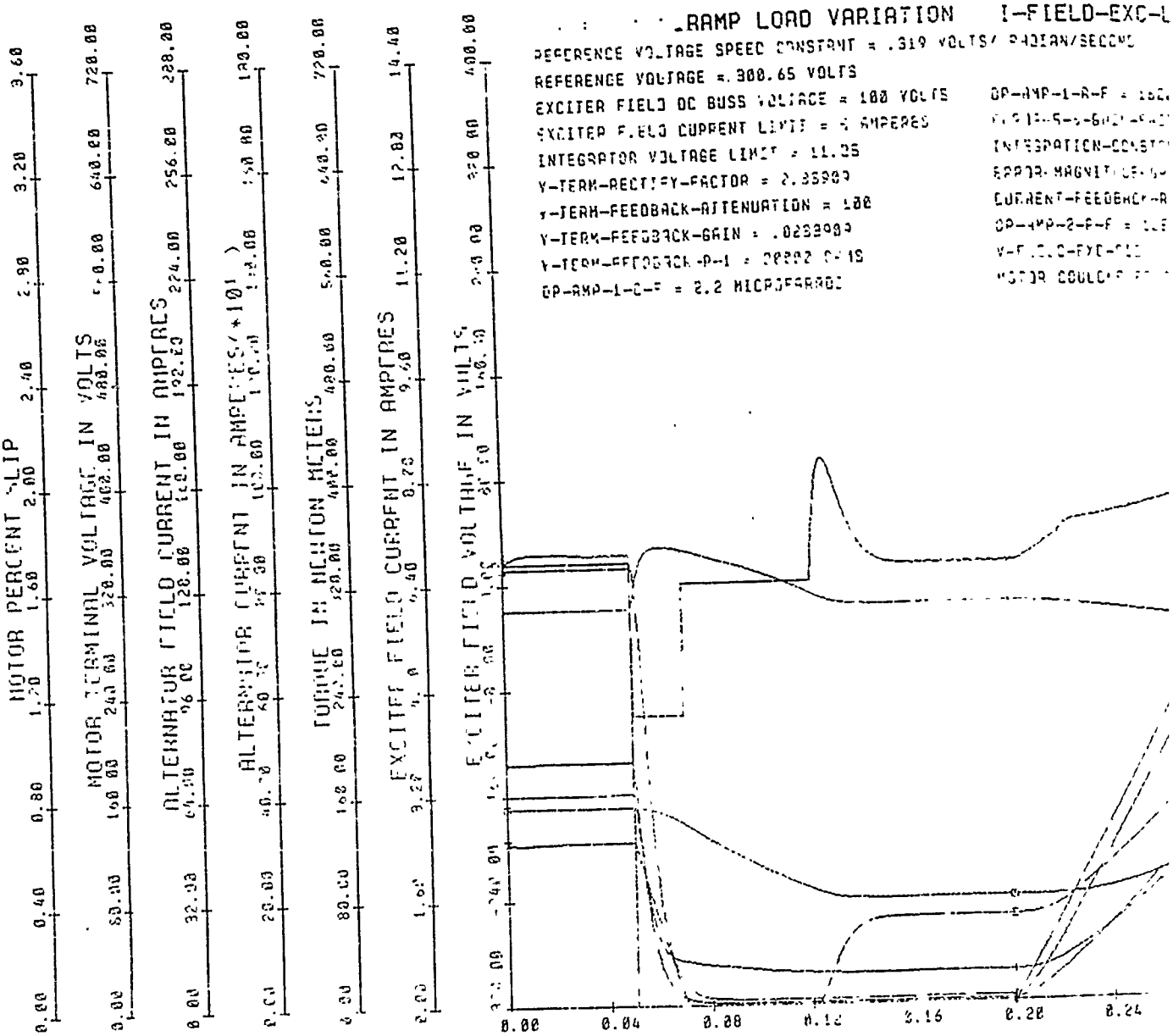


05/204/88/87f

197

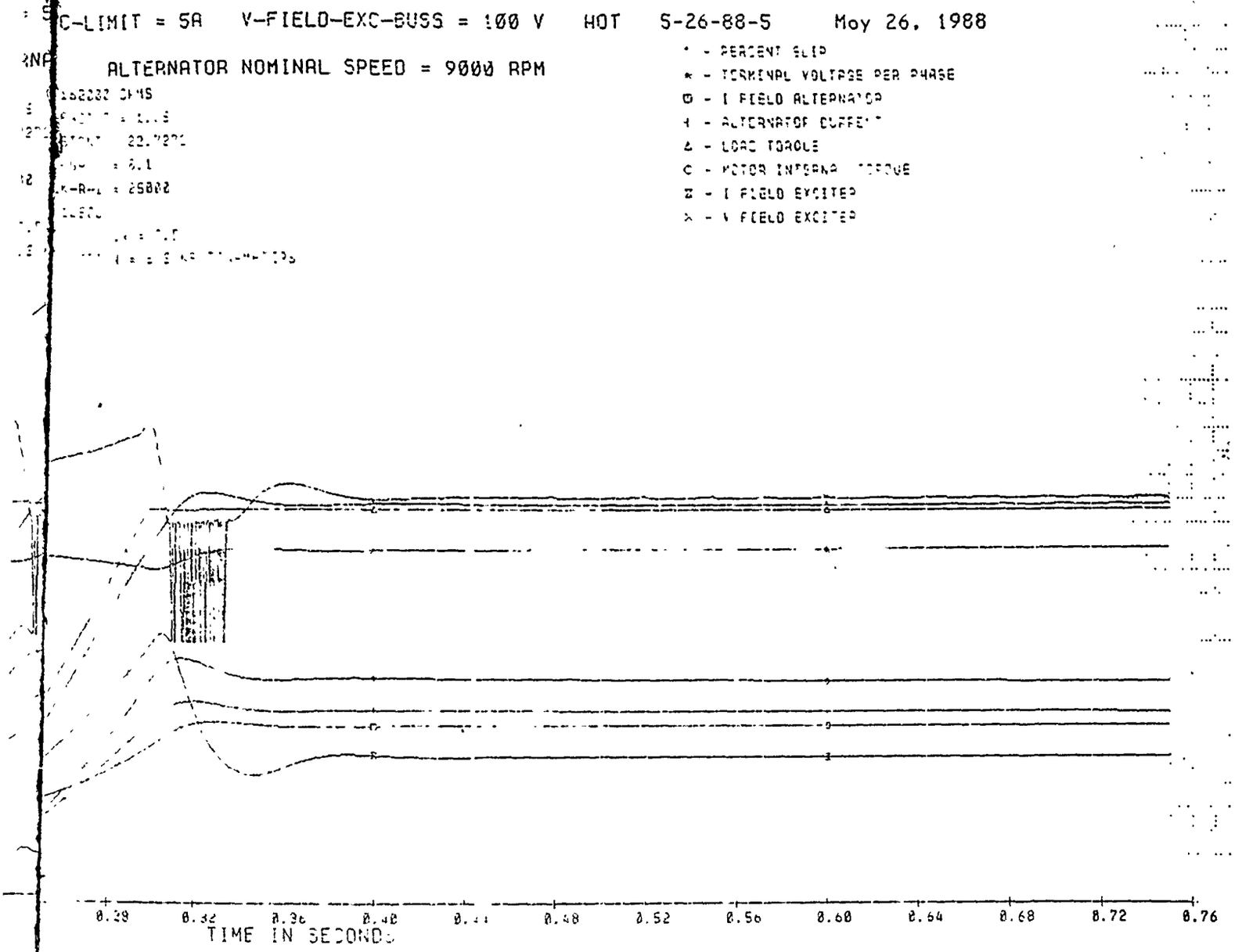


Figure 88. Ramp Load Variation - I-Field-EXC-Limit = 5A

292

20L(27)-5434z

Revision: 3
Date: 1 March 1988

PRELIMINARY

# INTERFACE SPECIFICATION

FOR

# ELECTRIC WATER PROPULSION SYSTEM FOR A HIGH SPEED TRACKED AMPHIBIOUS VEHICLE

BY

WESTINGHOUSE OCEANIC DIVISION-
Cleveland Operation
18901 Euclid Avenue
Cleveland, OH 44117

Prepared by: J. Witkowski 3/10/88
J. Witkowski Date
Technical Director

Approved: J. Triner 3/16/88
J. Triner Date
Program Manager

# APPENDIX I

## Interface Specification

INTERFACE SPECIFICATION
MARCH 1, 1988
(REVISION 3)

FOR
ELECTRIC WATER PROPULSION SYSTEM
FOR A HIGH SPEED TRACKED AMPHIBIOUS VEHICLE

TABLE OF CONTENTS

INTERFACE SPECIFICATION
MARCH 1, 1988
(REVISION 3)

FOR
ELECTRIC WATER PROPULSION SYSTEM
FOR A HIGH SPEED TRACKED AMPHIBIOUS VEHICLE
(Continued)

TABLE OF CONTENTS

INTERFACE SPECIFICATION
MARCH 1, 1988
(REVISION 3)

FOR
ELECTRIC WATER PROPULSION SYSTEM
FOR A HIGH SPEED TRACKED AMPHIBIOUS VEHICLE
(Continued)

TABLE OF CONTENTS

INTERFACE SPECIFICATION
MARCH 1, 1988
(REVISION 3)

FOR
ELECTRIC WATER PROPULSION SYSTEM
FOR A HIGH SPEED TRACKED AMPHIBIOUS VEHICLE

## TABLE OF FIGURES

REVISION STATUS SHEET
FOR
INTERFACE SPECIFICATION

REVISION 1
9 MARCH 1987

| SECTION | DESCRIPTION |
|---|---|
| 1.1 | Change - 28 Ton |
| 2.4.3 | Change - 28 Ton |
| | Clarify - "which includes" additional margin of 20% |
| 2.4.3.2 | Change - TBD to Section 2.4.3.3 Ref. |
| | Add - Coupling shear failure 2.5 times rated torque |
| 2.4.3.3 | Change - Shaft torsional shock load to "1.3" x |
| 2.4.4 | Change - Power source to 2.0 kW at 28 Volt |
| | Change - Gearbox to "2500" rpm |
| 2.5 | Change - "TBD" to "2.5 step-up" |
| 2.7 | Change - "420" volts to "520" volts |
| | Change - "140" to "-40" degrees celcius |
| 2.7.3 | Change - "motor" to "alternator" |
| 2.7.9 | Add - 130% load for 1 minute at 9000 rpm |
| | Change - "1.5" to "1.3" ft-lb |
| 2.7.10 | Change - "TBD" to "5000 - 7000" |
| 2.8.1 | Change - Remote location of controller |
| 2.9 | Change - "468" to "520" volts |
| 2.94 | Change - 15 to 27 degrees "F" to "C" |
| 2.98 | Clarify - Power-up regime and 100.1 volts |
| 2.9.9 | Add - "or configurable as such" |
| 2.9.13 | Add - "of seawater at 59°F" |
| 2.9.15 | Add - "or corrosion resistant stainless steel" |
| 3.0 | Add - "option" |

REVISION STATUS SHEET
FOR
INTERFACE SPECIFICATION

REVISION 2
4 DECEMBER 1987

| SECTION | RENUMBERED | DESCRIPTION |
|---|---|---|
| 2.4.1.1 | | Clarify - Oil Lubrication Interface Details Added |
| 2.4.2 | | Clarify - Envelope Added |
| | | Delete - "19 Inch Overall Length" |
| 2.4.2.2 | | Clarify - Motor Mounting Description |
| 2.4.2.3 | | Delete - Shock Loads Described in Motor Section |
| 2.4.3 | | Change - "1,250" to "1,274" RPM |
| 2.4.3.3b | | Change - "1,680" to "1,649" FT LB |
| 2.4.3.3c | | Change - "1,680" to "1,649" FT LB |
| 2.4.3.3g | | Change - "Figures 7, 8, 9" to "TBD"; Available Figures Do Not Adequately Describe Design Requirement |
| 2.4.3.3k | | Change - "1.0" to ".010" Inches |
| 2.4.3.4 | 2.4.4 | Change - "25" to "10" Feet/Second |
| 2.4.4 | 2.5 | Add "$\pm$4" to "28" Volts |
| | | Change - "TBD" to "RS232 Serial Link" |
| | | Add - Power Cable Description |
| 2.5 | 2.6 | Change - "1,000" to "1,100 $\pm$ 100" RPM |
| 2.6 | 2.7 | Add - "Maximum" Operational Speed Range, Etc. |
| 2.7 | 2.8 | Change - "A Brushless PMG Type" to "Equipped with a Brushless PMG" |
| | | Change - "550" to "450" Hertz |
| 2.7.1 | 2.8.1 | Add - "Maximum" Operational Speed Range, Etc. |
| 2.7.2 | 2.8.2 | Clarify - Reworded |
| 2.7.3 | 2.8.3 | Change - "375" to "380" |
| | | Add - "And the Terminal Cover/Power Sensing Box" |

REVISION STATUS SHEET
FOR
INTERFACE SPECIFICATION

REVISION 2
4 DECEMBER 1987
(Continued)

| SECTION | RENUMBERED | DESCRIPTION |
|---|---|---|
| 2.7.4 | 2.8.4 | Change - Specified Dimensions to "Outline Dimensions shall be in accordance with ICD "TBD"" |
| 2.7.5 | 2.8.5 | Clarify - Add Reference for Cooling Air Requirements |
| 2.7.6 | 2.8.6 | |
| 2.7.7 | 2.8.7 | Add - "Measured Free Field" |
| 2.7.8 | 2.8.8 | Add - "The Description of this shock load is "TBD"" |
| 2.7.9 | 2.8.9 | Change - "Shock Load of 1,680" to "Overload of 1,649" |
| 2.7.10 | 2.8.10 | |
| 2.7.11 | 2.8.11 | |
| 2.7.12 | 2.8.12 | |
| 2.7.13 | 2.8.13 | Change - "In Figure 10" to "On Westinghouse Outline Drawing No. 947F038" |
| 2.8 | 2.9 | |
| 2.8.1 | 2.9.1 | Add - Controller Volume & Outline Dimension Information |
| | 2.9.2 | Add - New Section Entitled "Weight" |
| 2.8.2 | 2.9.3 | |
| 2.8.3 | 2.9.4 | |
| 2.8.4 | 2.9.5 | Add - "The Description of this Shock Load is TBD |
| 2.8.5 | 2.9.6 | |
| 2.8.6 | 2.9.7 | Change - "Operate From" to "Not Exceed" |
| 2.8.7 | 2.9.8 | |

REVISION STATUS SHEET
FOR
INTERFACE SPECIFICATION

REVISION 2
4 DECEMBER 1987
(Continued)

| SECTION | RENUMBERED | DESCRIPTION |
|---|---|---|
| 2.8.8 | 2.9.9 | Add - "For both the Alternator and the Motor" |
| 2.8.9 | | Delete |
| 2.9 | 2.10 | Change - "400 HP ..... 9.90PF" to "400 HP Nominal Continuous SDG Output Power Rating at 0.90PF as a Design Goal" |
| | | Change - "8910 RPM" to "8919 RPM SDG Input Speed" |
| | 2.10.1 | Add - New Section Entitled "Shaft Speed" |
| | 2.10.2 | Add - New Section Entitled "Efficiency" |
| 2.9.1 | 2.10.3 | Change - "Refer to Para" to "In Accordance with ICD "TBD"" |
| 2.9.2 | 2.10.4 | Add - "The Description of the Shock Load is "TBD"" |
| 2.9.3 | 2.10.5 | Change - "Refer to Para" to "The Description of the Vibration Requirements is "TBD"" |
| 2.9.4 | 2.10.6 | |
| 2.9.5 | 2.10.7 | Clarify - Add Seawater Flow Information |
| 2.9.6 | 2.10.8 | Change - "300" to "TBD" |
| | | Add - "Calculated Weight is 329 LB" |
| 2.9.7 | 2.10.9 | Clarify - Specified Internal Oil & Removed References to External Hoses |
| 2.9.8 | 2.10.10 | Change - "3,000 RPM, 100.1 Volts L-L RMS, 150 Hz" to "2,750 $\pm$ 250 RPM" |
| 2.9.9 | 2.10.11 | Delete - "(Or Configurable As Such)" |
| 2.9.10 | 2.10.12 | Delete - "Without Any Degradation in Performance at Maximum Speed" |

REVISION STATUS SHEET
FOR
INTERFACE SPECIFICATION

REVISION 2
4 DECEMBER 1987
(Continued)

| SECTION | RENUMBERED | DESCRIPTION |
|---|---|---|
| 2.9.11 | 2.10.13 | Change - "a." to "Class H or Better" |
| | | Add - "c." and "d". |
| 2.9.12 | 2.10.14 | Clarify - Delete and Rewrite per Updated Information |
| 2.9.13 | 2.10.15 | |
| 2.9.14 | 1.10.16 | Change - "Which could be Continuous or Intermittent |
| | | During" to "Distributed Randomly Over" |
| 2.9.15 | 2.10.17 | Add - "External and" Internal Etc. |
| 2.10 | 2.11 | |
| 3.0 | | Delete - Not Applicable to Interface Document |

REVISION STATUS SHEET
FOR
INTERFACE SPECIFICATION

REVISION 3
1 MARCH 1988

| SECTION | DESCRIPTION |
|---|---|
| 2.2 | Change - "Diesel" to "Either a turbine or rotary" |
| 2.3 | Change - "TBD" to "Contractually Prescribed" |
| 2.4.1 | Change - "Westinghouse" reference to "Gould Interface Control Drawing (ICD), Drawing No. E77497" |
| | Change - "Diesel engine is" to "Prime movers are" |
| 2.4.2.1 | Add - "Or Composite Structure" |
| 2.4.2.2 | Change - "TBD" to "Drawing No. J77496" |
| 2.4.3.3.g. | Change - "DTNSRDC" to "DTRC" |
| 2.4.3.3.i. | Change - "25" to "2" |
| 2.4.3.3.j. | Add - "Motor/SDG including" |
| | Change - "25" to "1" |
| 2.5 | Clarify - Reworded |
| | Change - "25 feet ± 6 inches" to "Approximately 25 feet" |
| 2.6 | Change - "Diesel" to "Rotary and Turbine" and reword accordingly |
| | Change - "When the engine is at 1,100 ± 100 RPM" to "At 4,300 ± 100 RPM" |
| 2.7 | Change - "Diesel" to "Rotary" |
| | Add - "The turbine shall operate over a 2.09:1 speed range" |
| | Change - "2,500" and "125" to "4,300" and "215" |
| 2.8.1 | Change - "2,500" to "4,300" |
| | Reword for multiple prime movers |
| 2.8.4 | Change - "TBD" to "Drawing No. E77497" |
| 2.8.5 | Change - "Westinghouse" reference to "Drawing No. E77497" |
| 2.8.9 | Change - "A Diesel" to "Either a rotary or a turbine" |

REVISION STATUS SHEET
FOR
INTERFACE SPECIFICATION

REVISION 3
1 MARCH 1988
(continued)

| SECTION | DESCRIPTION |
|---|---|
| 2.8.13 | Change - "Westinghouse" ref to "Drawing No. E77497" |
| 2.9.8 | Clarify - Reworded to describe signals |
| 2.10.3 | Change - "TBD" to "Drawing No. J77496" |
| 2.10.9 | Change - "7078" to "7808" |
| 2.10.10 | Change - "2,750 ± 250" to "4,300 ± 100" |

| FIGURE | DESCRIPTION |
|---|---|
| 1 | Changed Diesel/Gearbox to reflect Rotary/Turbine/Gearboxes |

REV

## 1.0 SCOPE

### 1.1 Definition

1. This interface document establishes the requirements for the design, documentation, and fabrication of an electric water propulsion system for use in a 28 ton, high water speed, tracked amphibious vehicle.

## 2.0 REQUIREMENTS

### 2.1 Electric Water Propulsion Module (EWPM)

An electric water propulsion module includes a modified Westinghouse alternator, an alternator controller, power cabling, a propulsion drive unit (ac motor and speed decreasing gear), and a shaft coupling.

### 2.2 General Description

3. Four EWPMs are required to meet the water propulsion needs of the aforementioned Marine Corps amphibious vehicle. The alternator of the module will be directly coupled to a high speed splitter gearbox driven by either a turbine or rotary prime mover as shown in Figure 1. The mechanical power will be converted to electrical power by the three phase brushless alternator. This power will be supplied to the propulsion module where it will be converted to low speed mechanical power to direct drive a waterjet. The electrical system for the EWPM is shown in Figure 2. The alternator controller performs the control and protection function within the EWPM.

### 2.3 Electrical Power System Installation

3. The actual installation of the electric drive system components into the vehicle will be the responsibility of the vehicle integrator. The vendor shall provide the integrator with the assistance and support in the form of documentation of the hardware and a contractually prescribed amount of technical support at the vehicle integrator's facility.

### 2.4 Interface Requirements

#### 2.4.1 Splitter Gearbox

3. Each alternator shall be mounted to a splitter gear box per drawing TBD and shall have the spline and bolt circle details as shown on Gould Interface Control Drawing (ICD), Drawing No. E77497. The splitter gear box ratio shall be such to provide 9000 rpm at its output shaft (to each alternator) when the prime movers are at maximum operational speed.

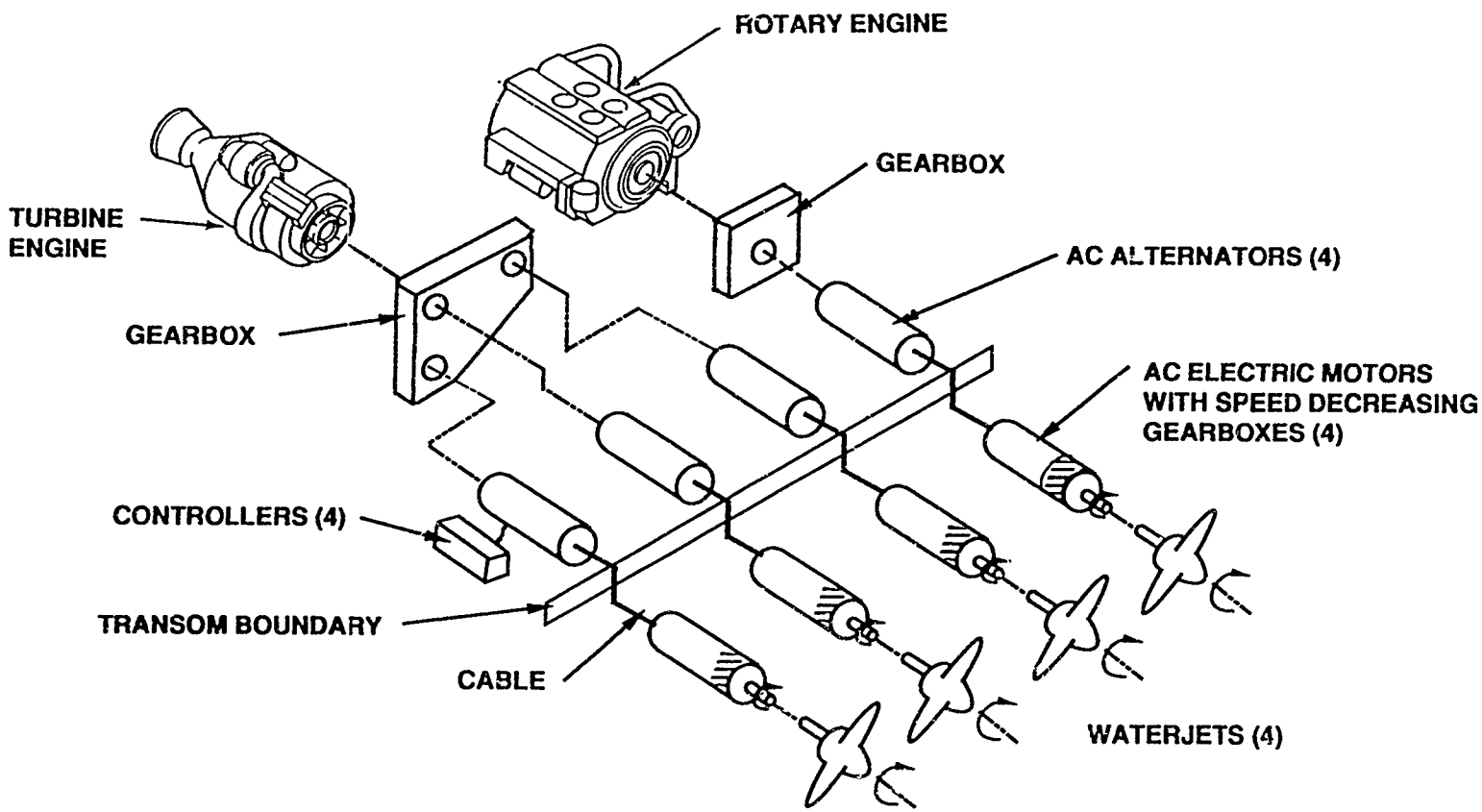


Figure 1. Propulsion System

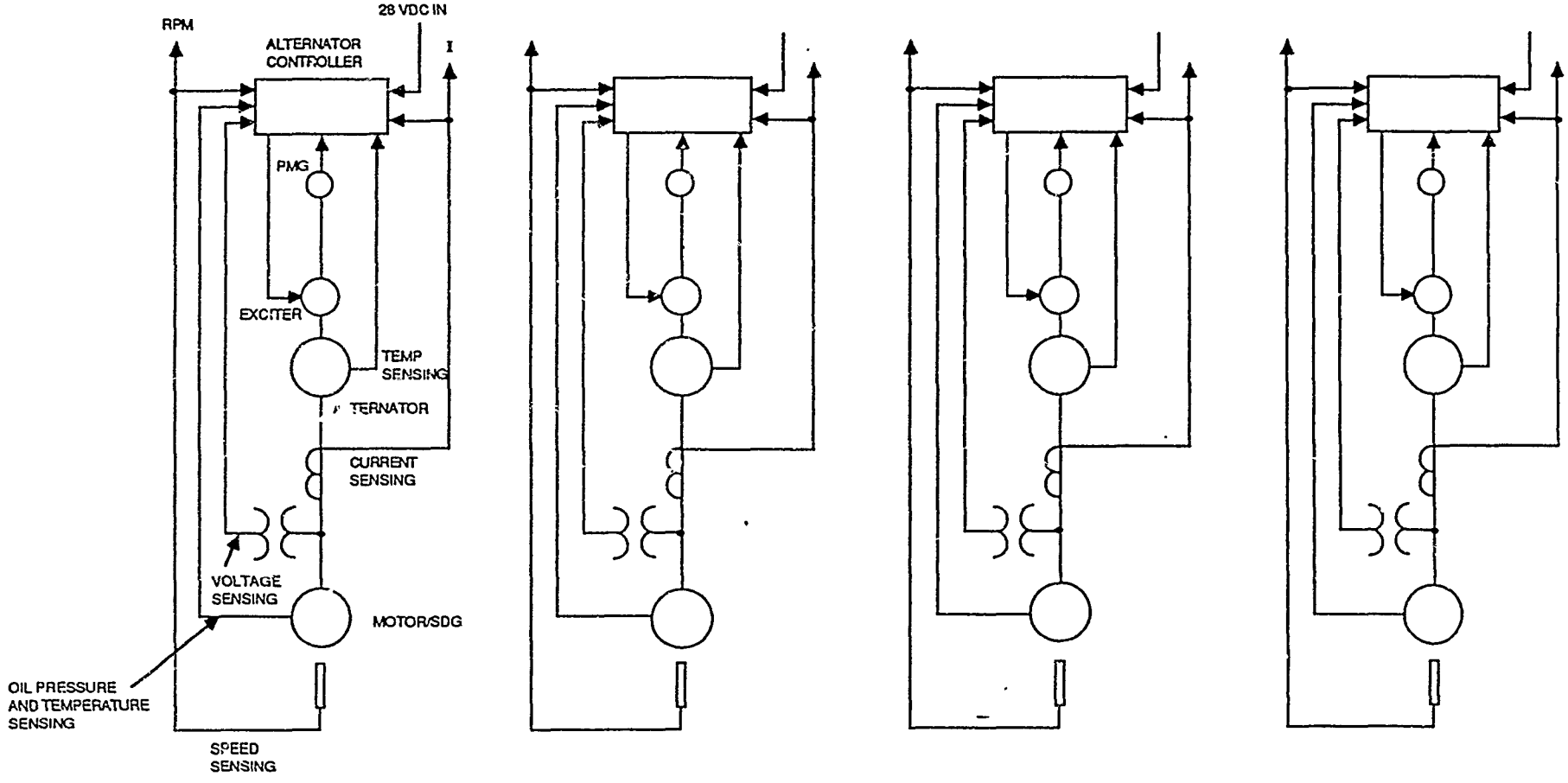


Figure 2. EWPM Electrical System

REV

2.4.1.1 Alternator Bearing Lubrication Oil

2. Figure 3 shows a portion of the alternator with an exhaust shroud and gearbox mounting added for reference.

In most applications, the engine, gearbox, and alternator share a common oil supply. A number of variations can be made to the oil system, however, without adversely affecting the alternator operation or requiring changes to the alternator design.

Oil to the alternator must be supplied at a pressure of 1 ± .5 psig (measured at reference ports "A" and "B" in Figure 3). Approximately 115 cc/minute is required for each bearing. Oil is typically supplied from a higher pressure line and regulated down to the 1 ± .5 psig pressure. The oil supply line for the drive-end bearing must be separate from the line for the fan-end bearing. If the two lines are common one bearing can be starved. The oil exits at the bottom of the alternator (reference ports "F" and "G").

The bearing cavities are enclosed by close-clearance seals. To prevent leakage the bearing cavity pressure must be lower than the surrounding ambient pressure. On the fan end, the pressure head developed by the fan is sufficient and this cavity may be gravity drained back to the supply reservoir or gearbox provided they are vented to atmospheric pressure.

The drive-end bearing lubricating oil flows into the cavity between the alternator and gearbox (reference location "J"). An exhaust shroud (reference "H") is required to provide a back pressure of approximately 3 inches of water. If the cavity between the gearbox and alternator is sealed, the oil must be evacuated thru port "F". The recommended sump line pressure is 1.0 ± .5 psig vacuum measured at port "F".

An alternate method is to provide a drain directly back into the gearbox through port "E" in conjunction with a gearbox pad vent "C". The exhaust shroud is still required but the drive-end bearing drain port "F" can be plugged.

Spline lubricant is typically provided from the gearbox through a hold "D" in the drive shaft.

2.4.2 Transom

2. The motor/speed decreaser and coupling envelope shall not be greater than 16.0" in diameter and be within the envelope as shown in Figure 4. The coupling can be in the transition area. The motor/speed decreaser shall be on the same center line as the waterjet drive shaft.

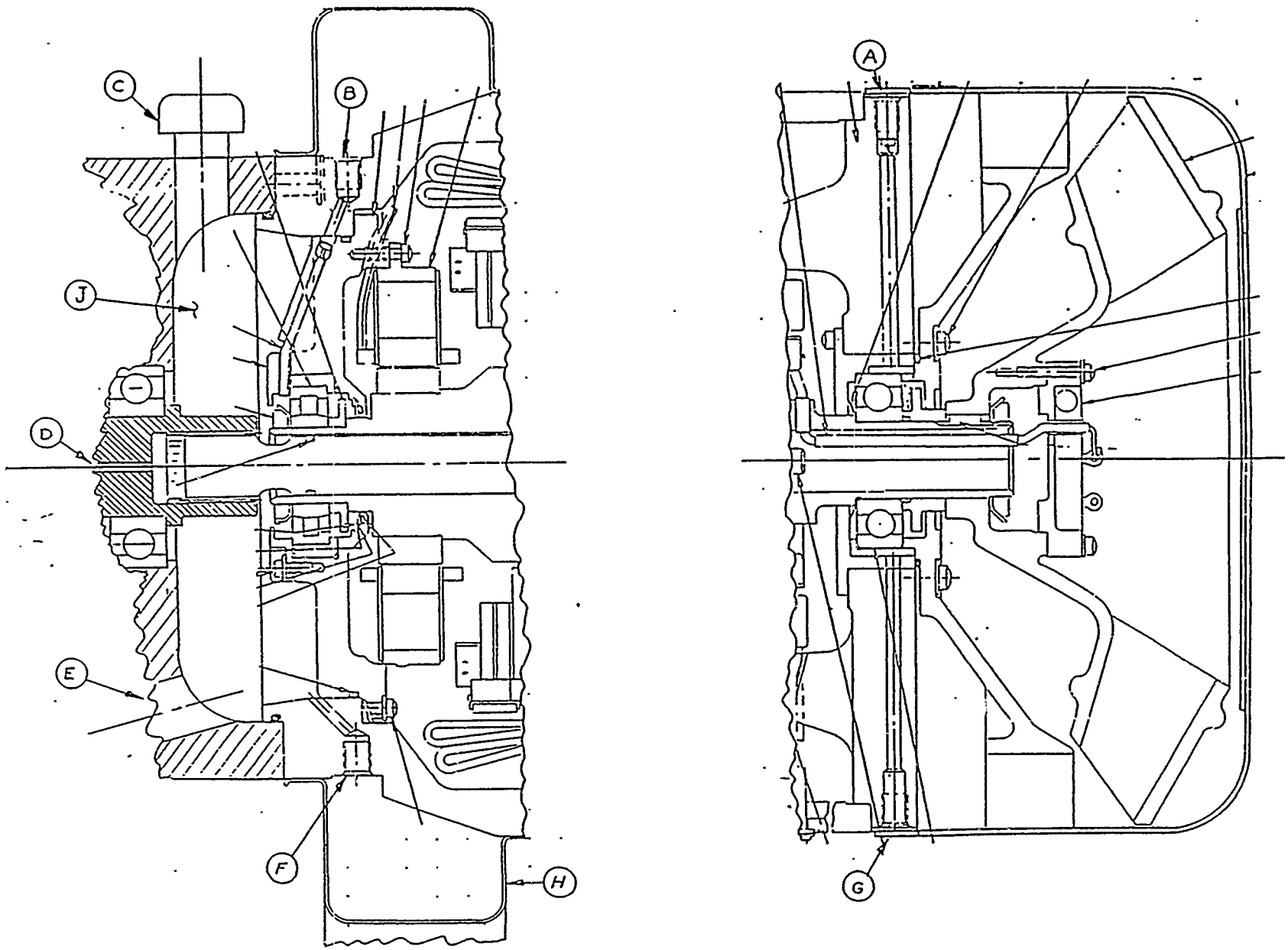


FIGURE 3. ALTERNATOR / GEARBOX / TYPICAL INSTALLATION

12/212/87J – 002

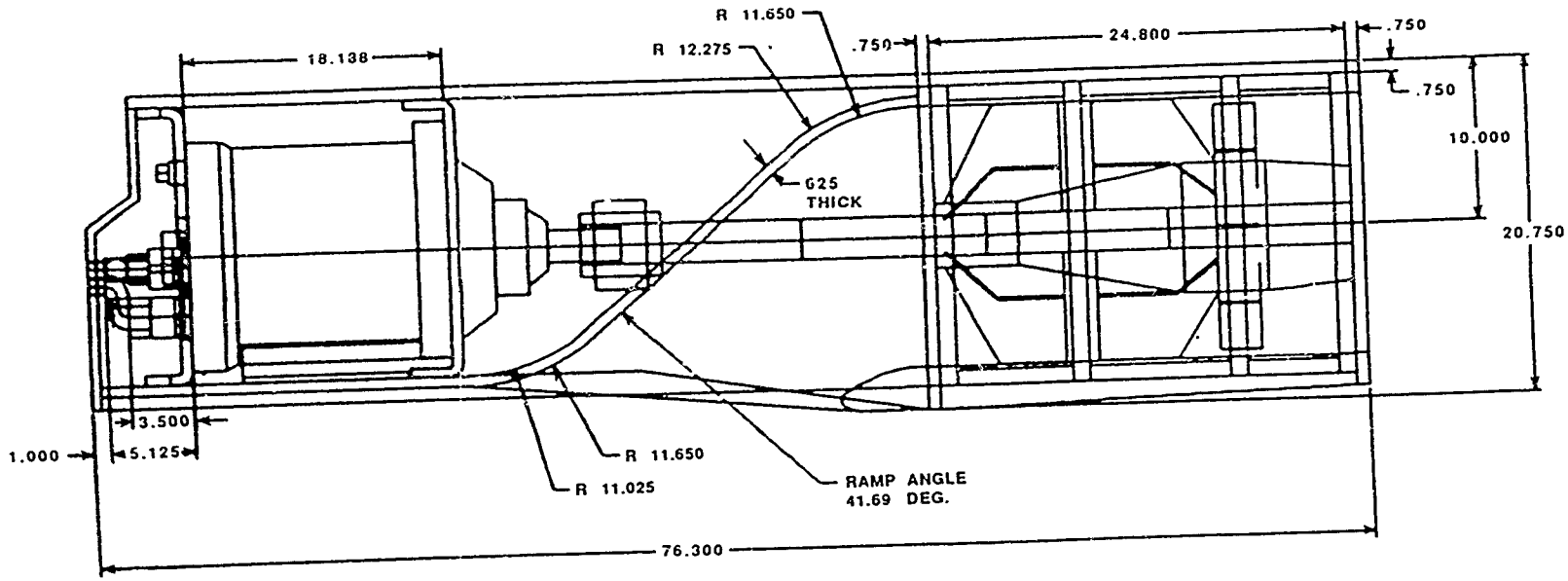


FIGURE 4. TRANSOM / MOTOR / SDG / COUPLING
INTERFACE ENVELOPE

REV

2.4.2.1 Transom Construction

3. The transom will be a welded truss or composite structure design for the sides and lateral bulkhead. The top, back, and bottom panels will be bolted to allow access to the motors. The bulkhead location is flexible.

2.4.2.2 Motor/SDG Installation

2., 3. The Motor/SDG shall be mounted rigidly within the transom as shown in Figure 4. The Motor/SDG shall be fastened to two brackets by a total of eight bolts, four each bracket. The Motor/SDG mounting features shall be in accordance with Gould ICD, Drawing No. J77496.

2.4.3 Waterjet

1., 2. Each waterjet for the 28 ton vehicle must produce 3900 pounds of thrust at nominally 1,274 rpm, producing a nominal 400 shp load on the motor. The waterjet will be rigidly mounted to the transom flap.

2.4.3.1 Waterjet Thrust

The thrust of the waterjet will be absorbed aft of the motor coupling in accordance with the vehicle integrator requirements.

2.4.3.2 Waterjet/SDG Coupling

1. The vendor shall provide a coupling between the motor/SDG and the waterjet. The coupling shall take up axial and radial misalignment as specified in Section 2.4.3.3. There shall be no thrust transmitted from the waterjet through the coupling. The coupling shall have a shear failure mode at 2.5 times rated torque.

2.4.3.3 Power Delivery to Waterjets

1.,2.,3.
a. Nominal Power delivered to the waterjet: 400 hp
b. Maximum shaft steady-state torsional load: 1649 ft-lbs.
c. Maximum shaft torsional overload: 1.3 x 1649 ft-lbs.
d. Repetition frequency of torsional overload: 100 events/hour
f. Flooded waterjet rotational inertia: 21 lb-ft$^2$
g. Speed-Torque characteristics: DTRC Figures "TBD"
h. Waterjet breakaway torque: 7-14 lb-ft.
i Breakaway torque of system thrust bearing: 2 lb-ft. max.
j. Breakaway torque of motor/SDG including shaft seals: 1 lb-ft. max.
k. Maximum shaft off-set misalignment: .010 inches
l. Maximum shaft angular misalignment: 0.2 degrees

REV

2.4.4 Thermal Management

2. The seawater flowrate past the motor housing shall be directly proportional to vehicle speed. At full vehicle speed the flow rate shall be 10 feet/second minimum. The temperature of the seawater shall be 80 °F maximum.

2.5 Electrical

1., 2.,3. A separate on-board power source shall provide 28 ± 4 volts dc to each alternator regulator; a total of 2.0 KW of power shall be available. From each alternator/motor module, data will be transmitted to the vehicle controller via RS232 serial link.

Each alternator shall be hard wired to each motor with flexible cable and be rated for the proper voltages and currents. The cables, three per motor, shall be sealed and capable of withstanding long term exposure to seawater and limited exposure to hydraulic oil and battery acid. The motor cables shall be of the construction shown in Figure 5, and shall be approximately 25 feet long. The cables shall exit the motor axially from the forward end and shall be capable of a one foot bend radius. The installation and termination of the cables shall be the responsibility of the vehicle integrator.

2.6 Power-Up Regime

1., 2.,3. The rotary and turbine engines shall be coupled to splitter gearboxes that provide 9,000 RPM input to the alternators at full engine power. Both engine transient speed regulations shall be ± 2% at full speed.

Each alternator/motor module shall be started sequentially, one at a time. Each alternator will be brought on line at 4,300 ± 100 RPM.

2.7 Operating Regime

2.,3. The rotary engine shall operate over a 3.6:1 speed range. The turbine shall operate over a 2.09:1 speed range. The alternator shall have a maximum operational speed range of 4,300 - 9000 rpm (215 - 450 hertz).

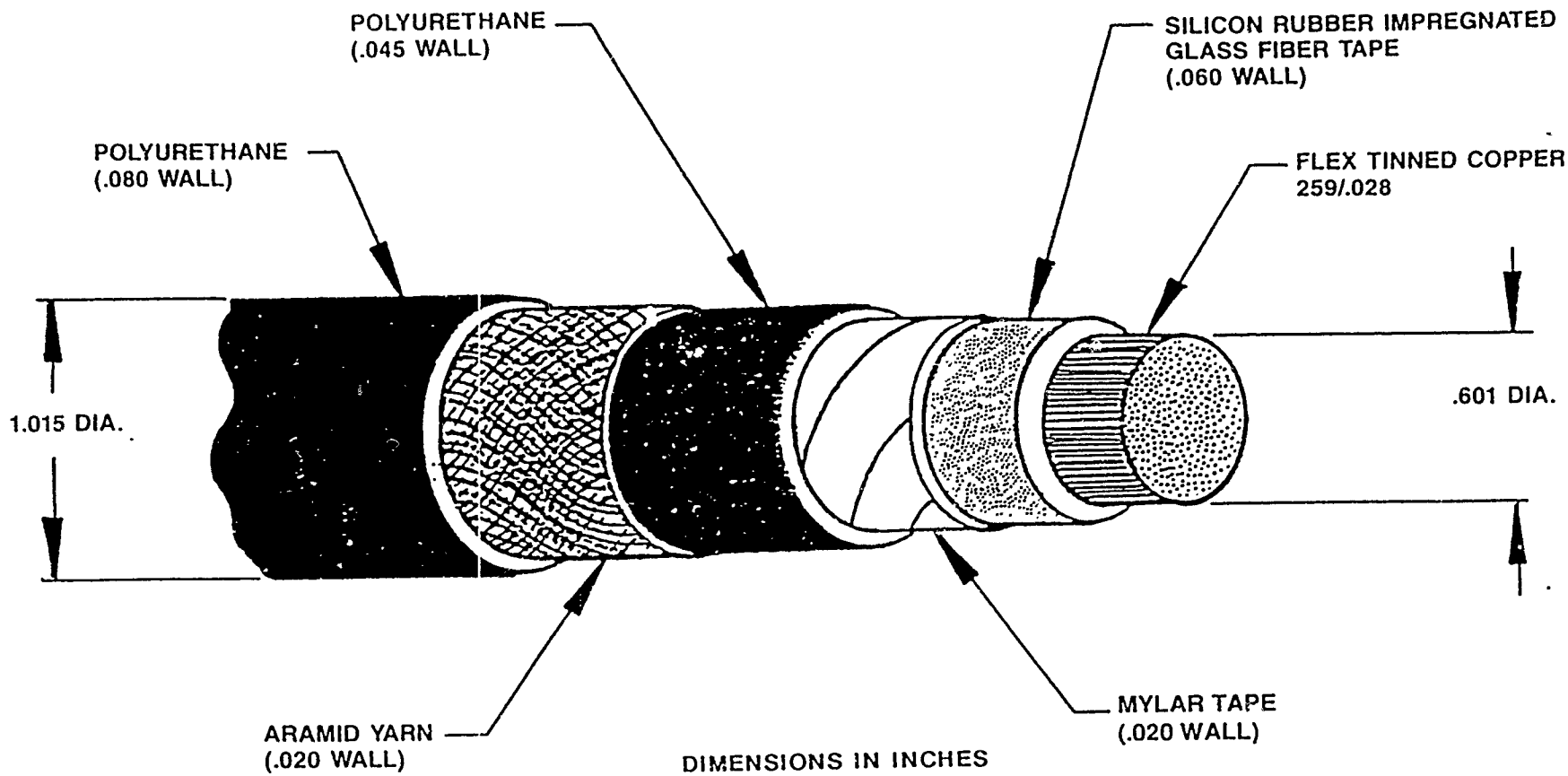


CABLE SIZE: 4/0 AWG
BEND RADIUS: 6 INCHES MIN.
NOMINAL WEIGHT: .944 POUNDS PER LINEAR FOOT

FIGURE 5. MOTOR / ALTERNATOR CABLE

12/212/87J – 004

REV

## 2.8 Alternator

1., 2. The vendor shall design, fabricate, and acceptance test alternators that meet the specifications listed below. The alternator shall be equipped with a brushless PMG and provide the following output characteristics at nominal conditions:

322 kW Nominal Continuous Power Rating at 0.85 PF
520 Volts L-L RMS, 3 Phase
450 Hertz

The alternator shall have an overload capability of at least 1.3 times 322 kW for a period of one minute at the maximum speed and an ambient air temperature of 38 degrees Celsius. The storage and transportation temperature will be -40 to 125 degrees Fahrenheit (-40 to 51.5 degrees celsius).

### 2.8.1 Shaft Speed

2., 3 The maximum speed of the alternator shall be 9000 rpm. The maximum operational speed range shall be 4300 - 9000 rpm. The splitter gearboxes between the alternators (four) and the engines shall be properly sized and geared to provide 9000 rpm input to the alternators at full engine speed.

### 2.8.2 Efficiency

2. The efficiency of the alternator shall be at least 88 percent at 322 kW, 9000 RPM (100% electrical power). This value shall be computed from the ratio of alternator output power divided by shaft input power. The efficiency calculation shall include the excitation power required for the rotating exciter.

### 2.8.3 Weight

1., 2. Each alternator shall weigh less than 380 pounds. This weight shall include all oil normally contained within the alternator and the terminal cover/power sensing box.

### 2.8.4 Dimensional Constraints

2., 3. The alternator shall be designed for minimum volume without compromising the other specified design criteria. Greater emphasis shall be placed on reducing length versus diameter. The alternator/power sensing box outline dimensions shall be in accordance with Gould ICD, Drawing No. E77497.

REV

2.8.11 Drive Shaft Bearing

2. The alternators shall be a two-bearing design and shall not depend on a driving gear for support of its drive shaft. Bearings shall be sized to support the specified shock loads as well as the specified torsional loads.

2.8.12 Insulation

2. Insulation of the alternator windings shall be selected to meet the following criteria:

a. The design limits and over temperature limits resulting from the offeror's cooling calculations.

b. Storage of the vehicle in damp salt air environments for extended periods of time.

c. An alternator shelf life of 10 years with intermittent use (to 1500 hours) spaced randomly through the 10 year period.

2.8.13 Alternator Mounting

2., 3. Each alternator shall be directly bolted to the speed increasing gearbox. The bolt hole pattern for the alternator mounting flange is shown on Gould ICD, Drawing No. E77497.

2.9 Alternator Controller

2. The alternator controller will provide protection and control capability for the electric water propulsion system. A bus compatible interface will be supplied for transfer of data to and from the propulsion system. The alternator controller will allow transparent control of the propulsion system over the entire operating range of the propulsion system. The controller will be designed to the operational requirements outlined below.

2.9.1 Dimensional Constraints

1., 2. The Contractor shall strive to minimize the size of the controller. The Contractor shall locate the controller remote to the alternator. The controller shall be less than one cubic foot volume. Controller outline dimensions shall be in accordance with ICD "TBD".

2.9.2 Weight

2. The controller, less cables, shall weigh less than 20 pounds.

REV

2.9.3 Cooling

2. The controller shall be cooled by natural convection. No source of forced air cooling shall be required.

2.9.4 Auxiliary Power

2. An auxiliary power source of 28 Vdc is available onboard the vehicle. A total of 2 kW is available for all vehicle controllers.

2.9.5 Shock Loads

2. The controller shall be designed to withstand 10G shock loads in all axes. The description of this shock load (G Force vs. Time) is "TBD".

2.9.6 Temperature

2. The compartment temperature limits for the alternator controller shall be between 0°C (32°F) and 50°C (122°F).

2.9.7 Data Bus Compatibility

2. All digital signals will be compatible with TTL logic, analog signals will not exceed -10V to +10V.

2.9.8 Data Required

2., 3 A single, V/Hz speed control signal will be supplied to the alternator controller by the alternator PMG. An output signal, proportional to motor speed, will be supplied by the alternator controller.

2.9.9 Protection

2. Electrical overload protection will be provided by the alternator controller for both the alternator and the motor.

2.10 Motor/SDG

2. The vendor shall design, fabricate, and acceptance test motors that meet the specifications listed below. The motor shall be a liquid cooled, 6 pole ac induction motor with a cage rotor construction and have the following output characteristics:

1. 400 HP Nominal Continuous SDG Output Power Rating at 0.90 PF as a design goal
520 Volts L-L RMS, 3-phase
8919 RPM SDG Input Speed (450 Hz)

REV

The motor must have a single output shaft that is to be mated with an integrally mounted speed decreasing gear (SDG). The Motor/SDG shall be capable of being mounted to the transom forward and aft bulkhead. Refer to Section 2.4.2.2, Motor/SDG Installation.

2.10.1 Shaft Speed

2. Synchronous motor speed at nominal conditions is 9000 rpm (450 Hz). The induction motor rotor slip under these conditions is calculated to be 0.9% which results in an SDG input shaft speed of 8919 rpm. The SDG speed reduction ratio is 7:1 which produces an output speed of 1274 rpm and a delivered torque of 1649 lb-ft.

2.10.2 Efficiency

2. The Motor/SDG shall have a minimum combined efficiency of 92% at nominal conditions (400 hp SDG output power, 520 volts L-L RMS, 1274 RPM SDG output speed, 450 Hz). The calculated efficiency of the motor alone is 96.2% at nominal conditions. The calculated SDG minimum efficiency is 96.0%.

2.10.3 Size

2., 3. The Motor/SDG outline dimensions shall be in accordance with Gould ICD, Drawing No. J77496.

2.10.4 Environmental

2. The motor/SDG, in any operational position shall sustain a shock load of 7.0 G in all axes at full power without any adverse impact. The motor/SDG shall operate in salt water without any degradation of structural members, seals, terminations, insulation system or motor performance. The description of the shock load (G Force vs. Time) is "TBD".

2.10.5 Transportation Vibration

2. The description of the vibration requirements is "TBD".

2.10.6 Operating Temperature

1., 2. The operating temperatures are as follows: Water temperature of 59 to 80 degrees F (15 to 27 degrees C). Transportation temperature of -40 to 125 degrees F (-40 to 51.5 degrees C).

2.10.7 Flooded Motor Area

2. The motor/SDG shall operate with the transom motor compartment flooded with seawater at a maximum temperature of 80 degrees fahrenheit. The water inlet size is 18 square inches/motor. Seawater shall flow axially past all external surfaces of the motor housing at the rate of 10 feet per second minimum at full vehicle speed. The seawater flow rate is proportional to the vehicle speed.

REV

2.10.8 Weight

2. The entire drive unit, motor, SDG, and coupling, shall not exceed "TBD" pounds. The calculated weight of the motor, SDG and coupling is 329 pounds.

2.10.9 Cooling/Lubrication

2., 3 The motor/SDG shall be self cooled using an integral heat exchanger with a maximum seawater temperature of 80 degrees fahrenheit. The same fluid, MIL-L-7808 turbine oil, shall be used for both cooling and lubrication in the gearbox and the motor. The oil circulation pump inlet and discharge ports shall remain constant with bi-directional drive. Oil passages from the gearbox to the motor shall be internal (no external hoses).

2.10.10 Power-Up Regime

1. 2.,3. The motor will be brought on line when the alternator is at 4,300 ± 100 RPM.

2.10.11 Operating Regime/Motor Reversing

1.,2. Refer to paragraph 2.7, Operating Regime. The requirement for the motors to be operated in reverse rotation after initial installation is not necessary. The possibility for half of the motors to operate clockwise and half to operate counterclockwise exists, so the oil circulation pump shall be bi-directional.

2.10.12 Overload Torque

2. The motor/SDG shall be capable of developing an overload torque of 130% of full load torque for one minute.

2.10.13 Motor Insulation

2. The insulation of the motor windings shall be selected to meet the following criteria:

a. Materials selected will be temperature class H (180°C) or better and consistent with the required Motor/SDG life requirements.

b. Storage of the vehicle in damp salt air environments for extended periods of time.

c. 500 hour operating life distributed randomly over a 10 year period.

d. Compatible with MIL-L-7808 internal cooling oil.

REV

2.10.14 Drive Unit Sensors

2. The motor shall have the following devices to provide data about its operating condition:

1) A magnetic-type speed sensor which has an output voltage rating of 28 V peak-to-peak minimum @ 1000 IPS with a 20 DP gear and a .005" air gap into 100,000 ohms. The coil resistance of the sensor is 850 ohms maximum. The full scale frequency is 1050 Hz.

2) An oil pressure transducer which has a .1 millivolt/psi outlet at 5 VDC excitation and has a bridge resistance of 350 Ω. The full scale range is 25 psi.

3) An oil temperature transducer; which is a platinum RTD with a resistance of 100 Ω at 0°C and a nominal temperature coefficient of resistance of .385 Ω/°C. The transducer is rated at 200°C maximum.

4) 6 Stator winding temperature transducers, each being a platinum RTD with a resistance of 100 Ω at 0°C and a nominal temperature coefficient of resistance of .385 Ω/°C. The transducer is rated at 200°C maximum.

* The selection of these components is by Gould. The instrumentation should be durable and put as far forward as possible if there is a need to access them. Routing of sensor leads and wiring will be the responsibility of the vehicle integrator.

2.10.15 Hydrostatic Head

1., 2. The motor shall withstand a hydrostatic head of 20 feet of seawater at 59°F.

2.10.16 Service Lifecycle

2. The motor shall have a service life of 500 hours distributed randomly over a period of 10 years.

2.10.17 Corrosion Protection

1., 2. The motor shall be completely sealed and the external and internal components protected from corrosive environments encountered during both operation and storage. All exposed fasteners shall be plated or corrosion resistant stainless steel.

REV

## 2.11 Vehicle Pitch Angle Data

2. From the enclosed pitch numbers, the absolute pitch angle that the motors could see is the sum of the vehicle pitch angle (worst case for either calm water or sea state 2) and the relative flap angle.

| Speed MPH | Vehicle Pitch Angle Calm Water | Vehicle Pitch Angle Sea State 2 | Flap Angle | Total Flap Angle |
|---|---|---|---|---|
| 8 | 5.1 | ~ 10 | 0.5-2.5 | 5.6-12.5 |
| 10 | 7.0 | 10.4 | .6-3.4 | 7.6-13.8 |
| 12 * | 11.1 | 10.2 | .8-4.4 | 11.0-15.5 |
| 14 | 8.9 | 10.2 | 1.0-5.4 | 9.9-15.6 |
| 16 | 8.5 | 10.3 | 1.3-6.5 | 9.8-16.8 |
| 18 | 8.9 | 10.5 | 1.5-8.0 | 10.4-18.5 |
| 20 | 9.1 | 10.3 | 1.7-7.7 | 10.8-18.0 |
| 22 | 8.8 | 9.1 | 2.2-7.3 | 11.0-16.4 |
| 24 | 7.8 | 8.2 | 2.5-7.0 | 10.3-15.2 |
| 26 | 6.9 | 7.4 | 3.2-6.8 | 10.1-14.2 |
| 28 | ~ 7 | ~ 7 | | |

* This is Model Data Scaled up to full size and ~12 mph was where hump was reached on the model. This condition is only momentary.

# APPENDIX II

## Alternator Vendor Survey

# APPENDIX II

## Alternator Vendor Survey

Prior to selecting the Westinghouse Electric Corporation (Lima Facility) as the supplier of the alternator, an alternator vendor survey was conducted and is summarized in Figure II.1. The preliminary technical data was based upon the dedicated alternator/motor configuration. Requests were sent to six vendors of which three responded with proposals.

The Westinghouse alternator came closest to meeting the performance and weight requirements for the electric propulsion system. It has been in service for over ten years and is in current production. The alternator was originally designed for the U.S. Navy's Pegasus Program.

The Niehoff alternator would have required a new electromagnetic and cooling system design to meet the electrical system requirements. Approximately 200 pounds of auxiliary hardware would be required to support 24 GPM of cooling oil for each alternator. This would have added 800 pounds to the electric propulsion system with its attendant penality on vehicle performance.

The alternator proposed by Garrett would have required a major development effort on their part since they did not have anything in their current product inventory to meet the electric system requirements. Their alternator was significantly heavier and would not have met the program delivery schedule.

| Vendor | Dimensions | Wt | Volts | Freq | Speed | Eff | Advantages | Disadvantages |
|---|---|---|---|---|---|---|---|---|
| Westinghouse | 25.9"x 13.4" | 373# | 520 | 500 | 10KRPM | 90.1 | a. Air Cooled<br>b. Existing design<br>c. Extensive design experience | 36 lbs. heavier than spec |
| Niehoff | 22"x17" | 374# | 500 | 800 | 12KRPM | 88.8 | | a. 37 lbs heavier than spec<br>b. 300# of hardware to support 24 GPM/ Alt for ea. alt.<br>c. New design effort<br>d. Eff less than 90% |
| Garrett | 21.5"x20" | 1200# | 800 | 250 | 15KRPM | 92 | a. Eff > 90% | a. Wt. 860 lb. heavier<br>b. New product - major development effort required |
| Bendix | No Bid | | | | | | | |
| Lear Siegler | No Bid | | | | | | | |
| Sundstrand | No Bid | | | | | | | |



Figure II-1. Alternator Vendor Summary

The remaining vendors, who build military alternators, declined to bid based primarily because of the 322 kW power requirements. Their alternator power ratings were in the range of 70 - 100 kW.

# APPENDIX III

## Alternator Description

# APPENDIX III

## 322 kW Brushless Alternator

The power source for each induction motor is a commercially available air-cooled 322 kW brushless alternator. The alternator is being purchased from the Westinghouse Electric Company, Lima Facility, part number 977J031-6. The alternator was originally designed for the U.S. Navy for use in the Pegasus program in 1972 and as such is a proven design.

The internal features of the alternator are shown in Figure III.1. The alternator is made up of three major elements as follows:

a. Permanent Magnet Generator (PMG)

b. Exciter with rotating rectifier bridge

c. Main alternator

The PMG provides voltage information for the system controller. The PMG is located at the drive end of the alternator. The permanent magnet rotor is assembled on a common shaft with the main field assembly. The single phase stator winding assembly is attached to the alternator housing.

The rotating exciter armature and rectifier bridge provide excitation to the main field windings. The exciter field winding is attached to the anti-drive end bearing housing. The exciter field winding which provides excitation for the exciter armature gets its power from the PMG. This

transfer of power is accomplished without the use of brushes or slip rings. The output of the rectifiers are hard wired to the main field winding which is assembled on a common shaft. The field coil end turns are supported and banded to withstand the centrifugal forces encountered during operation. The alternator three phase output is brought out just inboard of the anti-drive end bearing support to an external terminal board.

The alternator is air cooled requiring 1100 cfm of air. Air is brought into the machine at the anti-drive end and is exhausted at the drive end. A separate oil source is required for bearing lubrication.

The propulsion alternator technical specifications are summarized in Table III.1.

Table III.1 - Propulsion Alternator Technical Specifications

| | |
|---|---|
| Nominal Power Rating (Continuous) KW<br>Power Factor | 332 + 3% - 0%<br>.85 |
| Overload Capability - 1 Minute Duration, 9000 RPM | 419 kW |
| Minimum Starting Current @ 215.3 Hz | 900 Amps for 3 Sec |
| Nominal Voltage L-L VRMS @ 450 Hz | 520 ± 5% |
| Nominal Frequency Hz | 450 Hz |
| Nominal Shaft Speed | 9000 RPM |
| Number of Phases | 3 |
| Efficiency at Nominal Rating | 88% Minimum |
| Operating Speed Range (Max./Min.) | 4300 - 9000 RPM |
| Weight Limit (Lbs.) | >337* |
| Voltage Control Method | Constant Volt/Hz over speed range |
| Volts/Hz (Ratio) Regulation | 1% for a 0-100% Current Load |
| Excitation Type | Brushless PMG |
| Shock & Vibration | 10 g - all axes |
| Mounting Envelope | 15" dia. x 17" long |
| Service Life | 1500 hrs. dist. evenly over 10 years |
| Noise Level | 93 DBA at 3 ft. |
| Method of Cooling | Air Cooled, 1100 CFM @ 9000 RPM |
| Lubrication - Each Bearing | MIL-L-7808 Oil, 115 cc/min @ .5-1.5 psi |
| Electrical Load Type | Induction Motor |
| Prime Mover Power | Diesel Engine Via Gear Box |

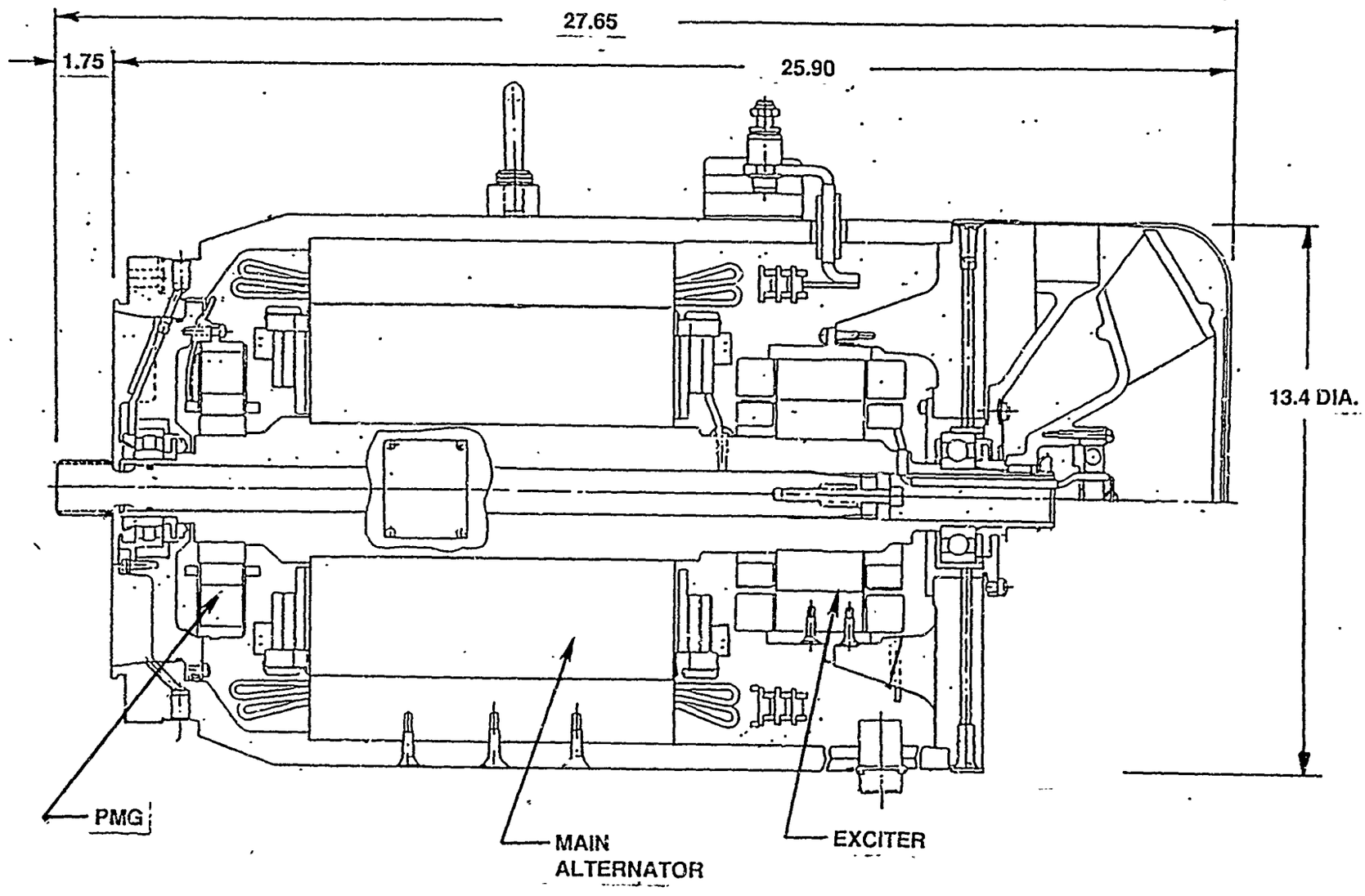


05/204/88/022

Figure III-1. Alternator, Westinghouse Model 977J031-6

# APPENDIX IV

## Stress Calculations

# SHAFT BENDING STRESS - 7g SHOCK LOAD

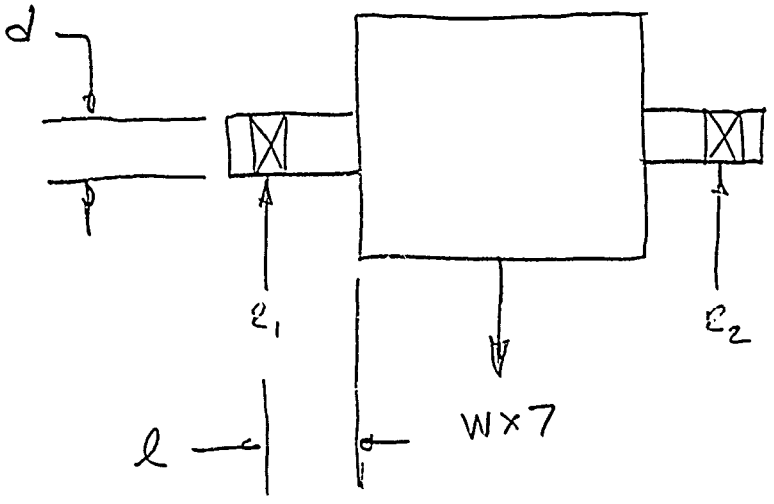


DUE TO SYMETRY $R_1 = R_2 = \frac{W \times 7}{2}$ lb

$W = .76$ lb. WEIGHT

$R_1 = 266$ Lb. REACTION FORCE

BENDING MOMENT $M = R_1 l$ in-Lb

$l = .875$ in. LENGTH

$M = 232$ in Lb. MOMENT

$S_b = \frac{M}{Z}$ PSI BENDING STRESS

$Z = \frac{\pi d^3}{32}$ $in^3$ SECTION MODULUS

$d = 1.25$ DIAMETER

$Z = .1917 \ in^3$

$S_b = 1214$ PSI

MATERIAL: PH13-8 MO

SAFE WORKING STRESS: 190,500 PSI BENDING

FACTOR OF SAFETY = 157

SHAFT TORSIONAL SHEAR STRESS - 1.3 OVERLOAD

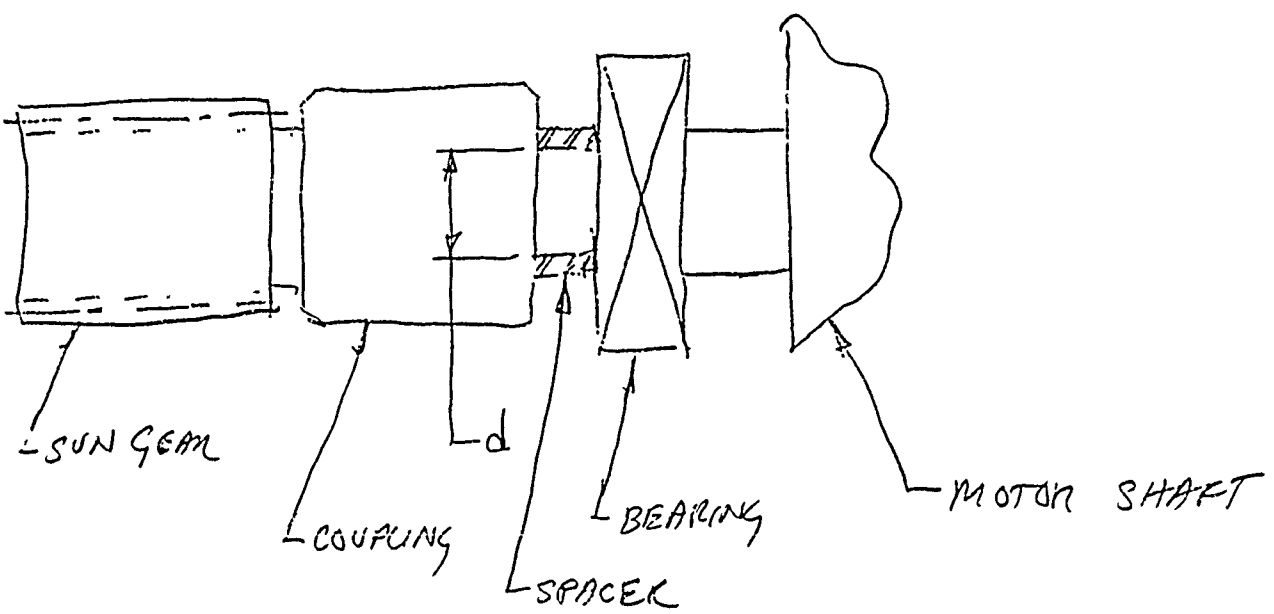


$S_s = \frac{Tr}{J}$ PSI — SHEAR STRESS

$J = \frac{\pi d^4}{32}$ $IN.^4$ — POLAR MOMENT OF INERTIA

$d = .95$ IN — DIAMETER

$r = d/2$ — RADIUS

$T = 1.3 \times 2917 = 5795$ IN-LB TORQUE

$J = .0799$

$S_s = 22,600$ PSI

MATERIAL: PH 13-8 Mo

SAFE WORKING STRESS: 75000 PSI SHEAR

FACTOR OF SAFETY = 3.32

ASSEMBLY STRESS OF ROTOR LAMINATION ON SHAFT

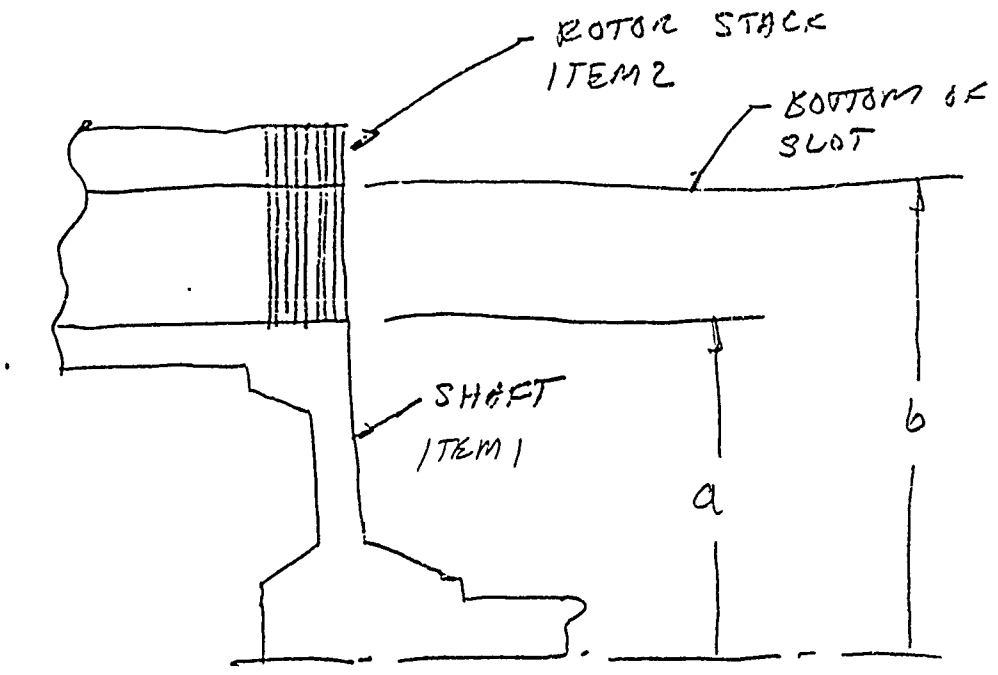

$$\Delta_1 = p_1 \cdot \frac{a}{E_1}(1-\nu_1)$$ ROARK, FORMULAS FOR STRESS AND STRAIN 4TH EDITION P308, CASE 34

$$\Delta_2 = p_2 \frac{a}{E_2}\left(\frac{b^2+a^2}{b^2-a^2}+\nu_2\right)$$ ROARK P308, CASE 33

$p_1 = p_2 = p$ = PRESSURE AT INTERFACE

$\Delta = \Delta_1 + \Delta_2$ = TOTAL INTERFERENCE BETWEEN IRIS

REARRANGING:

$$\frac{1}{p} = \frac{1}{\Delta}\left[\frac{a}{E_1}(1-\nu_1) + \frac{a}{E_2}\left(\frac{b^2+a^2}{b^2-a^2}+\nu_2\right)\right]$$

$\Delta$ = .0015 IN MAX RADIAL INT.

$E_1 = E_2 = 30 \times 10^6$ PSI ELASTIC MODULUS

$\nu_1 = \nu_2 = .3$ POISSON'S RATIO

$a$ = 2.875 IN. $b$ = 3.887 IN.

$p$ = 3550 PSI

$$S_t = p\frac{b^2+a^2}{b^2-a^2}$$ ROARK P308, CASE 33

$S_t$ = 12000 PSI TANGENTIAL STRESS

MATERIAL PERMENDUR V SPECIFIED MIN. Y.P = 30,000 PSI

FACTOR OF SAFETY = 2.5.

EQUIVALENT ROTOR CONFIG. TO SHOCK

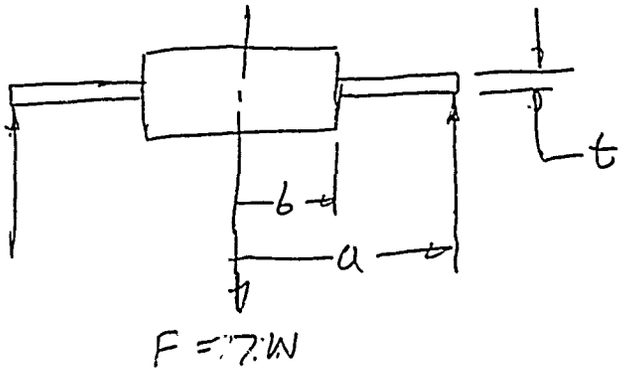


INNER EDGE FIXED, OUTER EDGE SIMPLY SUPPORTED

ROARK P. 222 CASE 22

$S_{MAX} = \frac{\beta F}{t^2}$ $y_{max} = \frac{\alpha F a^2}{E t^3}$ ROARK P242

$a = 6.5$ in INSIDE RADIUS

$b = 1.625$ in OUTSIDE RADIUS

$E = 10 \times 10^6$ PSI ELASTIC MODULUS

$t = .688$ in THICKNESS

$\alpha = .293$ $\beta = 1.514$ ROARK P. 241

$W = 76$ 16 ROTOR WEIGHT

$F = 532$ 16 FORCE DUE TO SHOCK LOAD

$S_{MAX} = 1700$ PSI BENDING STRESS

$y_{MAX} = .0020$ IN. DEFLECTION

MAT'L 6061-T6 ALUMINUM - SAFE BENDING STRESS: 40,00

S. F. = 23.5

HOUSING AND STATOR FIT, CIT

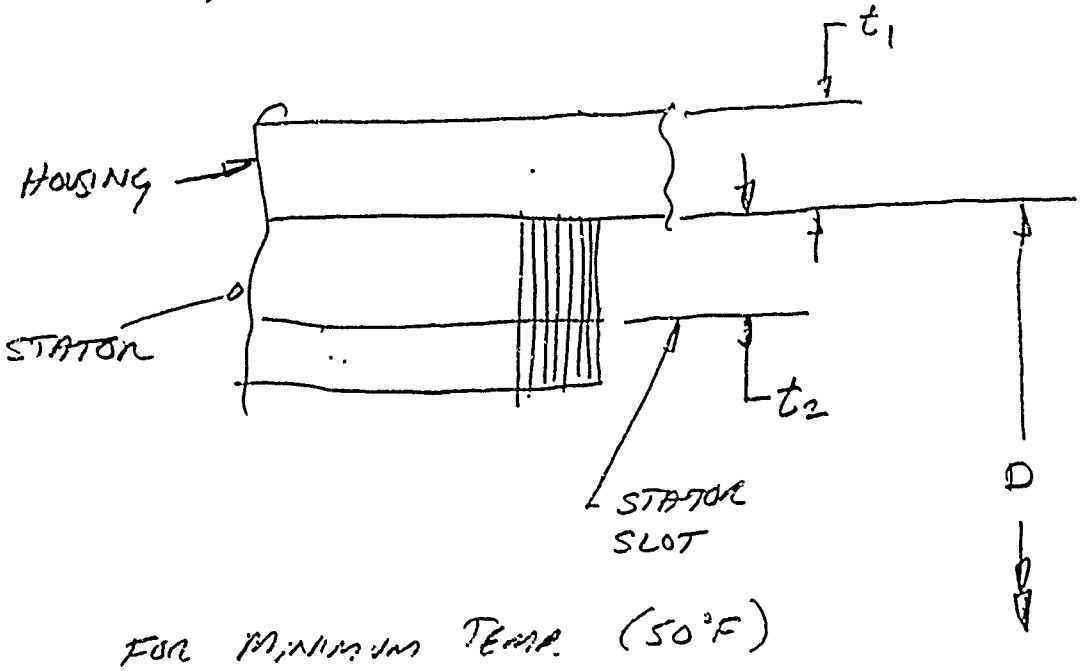


FOR MINIMUM TEMP (50°F)

$\Delta_{T_1} = K_1 D(T_1 - T_{RT})$ = THERMAL GROWTH OF HOUSING

$\Delta_{T_2} = K_2 D(T_2 - T_{RT})$ = THERMAL GROWTH OF STATOR

$\Delta m = .014$ IN. MECHANICAL INTERFERENCE AT ROOM TEMP ($T_{RT} = 72°F$)

$T_1 = T_2 = 50°F$

$\Delta = \Delta_m + \Delta_{T2} - \Delta_{T1}$ NET INTERFERENCE

$K_1 = 13.6 \times 10^{-6} / °F$

$K_2 = 5.44 \times 10^{-6} / °F$

$D = 11.625$

$\Delta = .0161$ in.

ASSEMBLY PRESSURE

$$\Delta_1 = \frac{P_1}{E_1}\frac{D^2}{2t_1} \qquad \Delta_2 = \frac{P_2}{E_2}\frac{D^2}{2t_2}$$

THIN WALL PIPE

$$\Delta = \Delta_1 + \Delta_2 \qquad P = P_1 = P_2$$

COMBINING ABOVE EQUATIONS

$$\frac{1}{P} = \frac{D^2}{2\Delta}\left(\frac{1}{E_1 t_1} + \frac{1}{E_2 t_2}\right)$$

$E_1 = 10 \times 10^6$ PSI ELASTIC MODULUS

$E_2 = 30 \times 10^6$ PSI " "

$t_1 = .625$ IN. WALL THICKNESS

$t_2 = .625$ in. " "

$D = 11.625$ IN. DIAMETER

$P = 1120$ PSI ASSEMBLY PRESSURE

$$S_1 = \frac{PD}{2t_1} = 10,400 \text{ PSI}$$

$$S_2 = \frac{PD}{2t_2} = 10,400 \text{ PSI}$$

MATERIAL:

ITEM 1 6061-T6 SAFE STRESS 40,000 PSI

FACTOR OF SAFETY 3.84

ITEM 2 PERMENDUR V SPECIFIED MINIMUM Y.P = 30,000 PSI

FACTOR OF SAFETY 2.88

MINIMUM INTERFERENCE AT OPERATING TEMPERATURE

$$\Delta = \Delta_m + \Delta_{T_2} - \Delta_{T_3}$$

$T_1 = 136\ ^\circ F$ AVG HOUSING TEMPERATURE

$T_2 = 170^\circ F$ AVG STATOR TEMPERATURE

$\Delta_m = .008$ IN. MINIMUM MECHANICAL INTERFERENCE

$\Delta = .0041$ IN. I.E. INTERFERENCE MAINTAINED.

BEARING LIFE

$T = 39$ LB THRUST LOAD

$nd^2 = .8789$ BEARING CONSTANT BARDEN CAT P. 88

$T/nd^2 = 44.4$

$\phi = 9.6^\circ$ CONTACT ANGLE BARDEN CAT. P. 98

$P = XR + YT$, BARDEN CAT. P. 88

$R = 37.5$ LB = RADIAL LOAD

$X = f(\phi, T/nd^2) = .46$ BARDEN CAT. P. 89

$Y = f(\phi) = 1.70 = 1.70$ " " P. 89

$P = 83.55$

$L_{10} = \left(\frac{C}{P}\right)^{3}$ [illegible] INDEX CAT. P. 88

$C = 2320$ LB DYNAMIC CAPACITY " " P. 98

$L_{10} = 2.311 \times 10^{13}$ REVOLUTIONS (MINIMUM LIFE OF 90% OF BEARINGS)

@ 9000 RPM

LIFE = 42810 HRS

REQUIRED LIFE 500 HRS

FACTOR OF SAFETY 85.6

SHOCK LOADS

$C_0 = 1,136$ 16 STATIC RADIAL CAPACITY BARDEN P. 98

$R = 7 \times 375 = 2625$ RADIAL LOAD WITH SHOCK

FACTOR OF SAFETY : 4.33

$T_0 = 1,772$ 16 STATIC THRUST CAPACITY BARDEN P. 98

$T = 7 \times 75 = 525$ LB THRUST LOAD WITH SHOCK

FACTOR OF SAFETY : 3.375

# Engineering

## Bearing Performance

### Bearing Life

The useful life of a ball bearing has historically been considered to be limited by the onset of fatigue or spalling of the raceways and balls, assuming that the bearing was properly selected and mounted, effectively lubricated and protected against contaminants.

This basic concept is still valid, but refinements have been introduced as a result of intensive study of bearing failure modes. Useful bearing life may be limited by reasons other than the onset of fatigue.

#### Service life

When a bearing no longer fulfills minimum performance requirements in such categories as restraining torque, vibration or elastic yield, its service life may be effectively ended.

If the bearing remains in operation, its performance is likely to decline for some time before fatigue spalling takes place. In such circumstances, bearing performance is properly used as the governing factor in determining bearing life.

Lubrication can be an important factor influencing service life. Many bearings are prelubricated by the bearing manufacturer with an appropriate quantity of lubricant. They will reach the end of their useful life when the lubricant either migrates away from the bearing parts, oxidizes or suffers some other degradation. At that point, the lubricant is no longer effective and surface distress of the operating surfaces, rather than fatigue, is the cause of failure. Bearing life is thus very dependent upon characteristics of specific lubricants, operating temperature and atmospheric environment.

Specific determination of bearing life under unfavorable conditions can be difficult, but experience offers the following guidelines to achieve better life.

1. Reduce load—particularly minimize applied axial preload.
2. Decrease speed to reduce the duty upon the lubricant and reduce churning.
3. Lower the temperature. This is important if lubricants are adversely affected by oxidation, which is accelerated at high temperatures.
4. Increase lubricant supply by improving reservoir provisions.
5. Increase viscosity of the lubricant, but not to the point where the bearing torque is adversely affected.
6. To reduce introduction of contaminants, substitute sealed or shielded bearings for open bearings and use extra care in installation.
7. Improve alignment and fitting practice, both of which will reduce duty on the lubricant and tend to minimize wear of bearing cages.

The most reliable bearing service life predictions are those based on field experience under comparable operating and environmental conditions.

#### Fatigue life

The concept that bearing life is limited by the onset of fatigue is generally accurate for bearings operating at normal speeds in general machinery applications. The basic relationship between bearing capacity, imposed loading and expected fatigue life is:

$$L_{10} = \left(\frac{C}{P}\right)^3 \times 10^6 \text{ revolutions.}^* \qquad \text{(Formula 1)}$$

In the above expression:

- $L_{10}$ = Minimum life in revolutions for 90% of a typical group of apparently identical bearings.
- C = Basic Load Rating.
- P = Equivalent Radial Load, computed as follows:

$$P = XR + YT \qquad \text{(Formula 2)}$$

or

$$P = R \qquad \text{(Formula 2)}$$

whichever is greater.

In the preceding equation:

- R = Radial load.
- T = Thrust load.
- X = Radial load factor relating to contact angle.
- Y = Axial load factor depending upon contact angle, T and ball complement.

For Basic Load Ratings, see Data Reference Tables starting on page 95. For X and Y factors, see Tables 19 and 20.

*See AFBMA Standard 9 for more complete discussion of bearing life in terms of usual industry concepts.

# Engineering

## Bearing Performance

Tabular engineering data listed for miniature and instrument bearings are for bearings with rings and balls of AISI 440C stainless steel. Data for spindle and turbine bearings are for bearings of SAE 52100. See page 67 for definitions of static and dynamic load ratings. Static capacities for deep groove bearings are based on Code 5 radial play.

**Data Reference Numbers — 200 cont. and 300**

| Data Reference Number | Load Factor Table | Initial Contact Angle, degrees — Radial Play Range — Code 3 | Code 5 | Code 6 | Std. | Ball Complement — Number n | Diameter d | Value nd² | Static Capacity — Radial $C_o$ (lbs.) | Thrust $T_o$ (lbs.) | Basic Dynamic Load Rating C (lbs.) |
|---|---|---|---|---|---|---|---|---|---|---|---|
| 201HJB | 20 | | 12.6 | 16.4 | 15.3 | 10 | 13/64" | .5493 | 661 | 876 | 1,432 |
| 202 | 20 | 10.7 | 15.2 | 19.5 | | 7 | 1/4" | .4375 | 510 | 701 | 1,306 |
| 202H | 20 | | 12.4 | 15.9 | 14.8 | 10 | 1/4" | .6250 | 769 | 1,093 | 1,622 |
| 203 | 20 | 10.4 | 14.8 | 18.9 | | 8 | 17/64" | .5645 | 692 | 1,094 | 1,614 |
| 203H | 20 | | 12.0 | 15.4 | 14.4 | 10 | 17/64" | .7056 | 894 | 1,885 | 1,825 |
| 203HJB | 20 | | 12.0 | 15.4 | 14.4 | 11 | 17/64" | .7761 | 983 | 1,626 | 1,945 |
| 203HX37 | 20 | | 12.0 | 15.4 | 12.9 | 10 | 17/64" | .7056 | 903 | 1,503 | 1,839 |
| 204 | 20 | 9.6 | 13.6 | 17.5 | | 8 | 9/32" | .7813 | 969 | 1,537 | 2,173 |
| 204H | 20 | | 11.1 | 14.2 | 15.1 | 10 | 9/32" | .9766 | 1,241 | 2,034 | 2,440 |
| 204HJB | 20 | | 11.1 | 14.2 | 15.1 | 11 | 9/32" | 1.074 | 1,370 | 2,237 | 2,601 |
| 205 | 20 | 9.6 | 13.6 | 17.5 | | 9 | 9/32" | .8789 | 1,136 | 1,772 | 2,380 |
| 205H | 20 | | 11.1 | 14.2 | 15.1 | 11 | 9/32" | 1.074 | 1,440 | 2,295 | 2,607 |
| 205HJB | 20 | | 11.1 | 14.2 | 15.1 | 13 | 9/32" | 1.270 | 1,698 | 2,712 | 2,914 |
| 206 | 20 | 8.8 | 14.5 | 17.9 | | 9 | 5/16" | 1.270 | 1,627 | 2,525 | 3,295 |
| 206H | 20 | | | | 15.1 | 11 | 19/64" | 1.820 | 2,364 | 5,295 | 4,248 |
| 207 | 20 | 8.1 | 13.4 | 16.6 | | 9 | 5/16" | 1.723 | 2,228 | 4,056 | 4,363 |
| 207H | 20 | | 12.0 | | 14.8 | 12 | 5/16" | 2.297 | 3,079 | 5,554 | 5,165 |
| 208 | 20 | 7.8 | 12.9 | 15.9 | | 9 | 19/64" | 1.978 | 2,600 | 6,182 | 4,954 |
| 208H | 20 | | | | 15.0 | 12 | 19/64" | 2.637 | 3,580 | 8,076 | 5,843 |
| 209 | 20 | 7.8 | 12.9 | 16.0 | | 10 | 19/64" | 2.197 | 3,071 | 5,327 | 5,318 |
| 209H | 20 | | | | 15.0 | 13 | 19/64" | 2.856 | 3,973 | 7,071 | 6,145 |
| 210H | 20 | | | | 15.0 | 14 | 1/2" | 3.500 | 4,879 | 8,713 | 7,250 |
| 211H | 20 | | | | 14.9 | 14 | 9/16" | 4.430 | 6,140 | 13,923 | 8,973 |
| 212H | 20 | | | | 14.9 | 14 | 5/8" | 5.469 | 7,569 | 13,579 | 10,870 |
| 213H | 20 | | | | 15.2 | 14 | 11/16" | 6.617 | 9,104 | 20,706 | 12,880 |
| 214H | 20 | | | | 15.2 | 15 | 11/16" | 7.090 | 9,921 | 22,613 | 13,447 |
| 215H | 20 | | | | 15.2 | 17 | 11/16" | 8.035 | 11,396 | 26,070 | 14,558 |
| 216H | 20 | | | | 15.1 | 15 | 3/4" | 8.440 | 11,920 | 27,195 | 15,691 |
| 218H | 20 | | | | 15.3 | 15 | 7/8" | 11.48 | 16,098 | 36,781 | 20,739 |
| 220H | 20 | | | | 15.2 | 15 | 1" | 15.00 | 20,909 | 47,637 | 26,417 |
| 304H | 20 | | | | 15.1 | 9 | 13/32" | 1.485 | 1,720 | 3,786 | 3,567 |
| 305H | 20 | | | | 15.0 | 10 | 13/32" | 2.197 | 2,606 | 5,747 | 5,007 |
| 306H | 20 | | | | 15.0 | 10 | 17/32" | 2.822 | 3,412 | 7,544 | 6,326 |
| 307H | 20 | | | | 15.0 | 11 | 9/16" | 3.480 | 4,339 | 9,607 | 7,549 |
| 308H | 20 | | | | 14.9 | 11 | 5/8" | 4.297 | 5,427 | 12,010 | 9,164 |
| 309H | 20 | | | | 15.2 | 11 | 11/16" | 5.199 | 6,561 | 14,679 | 10,864 |
| 310H | 20 | | | | 15.1 | 11 | 3/4" | 6.188 | 7,850 | 17,510 | 12,732 |

Table 19. Load Factors for Miniature and Instrument Bearings

| T/nd² | Contact Angle, degrees | | | |
|---|---|---|---|---|
| | 5 | 10 | 15 | 20 |
| | Values of Axial Load Factor Y | | | |
| 25 | 3.23 | 2.23 | 1.60 | 1.18 |
| 50 | 2.77 | 2.09 | 1.56 | 1.18 |
| 100 | 2.41 | 1.93 | 1.51 | 1.18 |
| 150 | 2.22 | 1.83 | 1.46 | 1.18 |
| 200 | 2.10 | 1.76 | 1.43 | 1.18 |
| 300 | 1.92 | 1.66 | 1.38 | 1.18 |
| 500 | 1.71 | 1.53 | 1.31 | 1.18 |
| 750 | 1.55 | 1.43 | 1.25 | 1.18 |
| 1000 | 1.43 | 1.35 | 1.21 | 1.18 |
| | Values of Radial Load Factor X | | | |
| | 0 56 | 0.46 | 0.44 | 0.43 |

Table 20. Load Factors for Spindle and Turbine Bearings

| T/nd² | Contact Angle, degrees | | | | | | | | |
|---|---|---|---|---|---|---|---|---|---|
| | 5 | 6 | 7 | 8 | 9 | 10 | 15 | 20 | 25 |
| | Values of Axial Load Factor Y | | | | | | | | |
| 10 | — | — | — | 2.38 | 2.27 | 2.13 | 1.57 | 1.00 | 0.87 |
| 20 | 2.40 | 2.32 | 2.23 | 2.14 | 2.10 | 1.94 | 1.50 | 1.00 | 0.87 |
| 30 | 2.22 | 2.15 | 2.08 | 2.00 | 1.92 | 1.83 | 1.46 | 1.00 | 0.87 |
| 40 | 2 09 | 2 03 | 1 97 | 1 91 | 1.84 | 1 76 | 1.42 | 1.00 | 0.87 |
| 50 | 1.93 | 1.94 | 1.89 | 1.83 | 1.77 | 1 70 | 1.40 | 1.00 | 0.87 |
| 60 | 1.91 | 1.87 | 1.82 | 1.77 | 1.71 | 1 65 | 1.37 | 1.00 | 0.87 |
| 70 | 1.85 | 1.81 | 1.76 | 1.72 | 1.67 | 1.61 | 1.35 | 1.00 | 0.87 |
| 80 | 1 79 | 1.76 | 1.72 | 1.68 | 1.63 | 1.58 | 1.33 | 1.00 | 0.87 |
| 90 | 1.75 | 1.71 | 1.68 | 1.64 | 1.59 | 1.55 | 1.31 | 1.00 | 0 87 |
| 100 | 1.71 | 1.67 | 1.64 | 1 60 | 1.56 | 1.52 | 1 30 | 1 00 | 0.87 |
| 150 | 1.55 | 1.53 | 1.50 | 1.47 | 1.45 | 1.41 | 1.23 | 1.00 | 0.87 |
| 200 | 1 45 | 1 43 | 1 41 | 1.38 | 1.36 | 1.34 | 1.19 | 1.00 | 0.87 |
| 300 | 1.31 | 1.30 | 1.28 | 1.26 | 1.25 | 1.23 | 1.12 | 1.00 | 0.87 |
| 400 | 1.22 | 1.21 | 1.20 | 1.18 | 1.17 | 1.16 | 1.07 | 1.00 | 0.87 |
| 500 | 1.15 | 1.14 | 1.13 | 1.12 | 1.11 | 1.10 | 1 02 | 1 00 | 0 87 |
| 600 | 1.10 | 1 09 | 1 08 | 1.07 | 1.05 | 1.05 | 1.00 | 1.00 | 0.87 |
| 700 | 1.06 | 1.05 | 1.04 | 1.03 | 1.02 | 1.01 | 1.00 | 1 00 | 0.87 |
| 800 | 1.03 | 1.02 | 1.01 | 1.00 | 1.00 | 1.00 | 1.00 | 1.00 | 0.87 |
| 900 | 1.00 | 1.00 | 1.00 | 1.00 | 1.00 | 1.00 | 1.00 | 1.00 | 0.87 |
| 1000 | 1 00 | 1.00 | 1 00 | 1 00 | 1.00 | 1.00 | 1.00 | 1.00 | 0.87 |
| | Values of Radial Load Factor X | | | | | | | | |
| | 0 56 | 0 51 | 0.49 | 0.48 | 0.47 | 0.46 | 0.44 | 0.43 | 0.41 |

Note: Values of nd² are given in Data Reference Tables starting on page 95.

# SDG STRESS CALCULATIONS

## INPUT SHAFT KEY STRESS

TORQUE = 1.3 x 2943 IN.-LB.

SHAFT DIA = .984

KEY 1/4 x 1/4 x 1 1/4 LG

SHEAR AREA = .312 $in^2$

SHEAR FORCE = 1.3 x 2943 ÷ .492 = 7775 lb.

$S_s$ = 7775 ÷ .312 = 24920 PSI

ALLOWABLE SHEAR = 132000 ÷ 2 = 66,000 PSI
(BETHLEHEM STEEL: 4140 STL @ 311 BHN)

F.S. = 2.65

COMPRESSIVE STRESS

AREA = .156 $in^2$

S = 7775 ÷ .156 = 49,000 PSI

ALLOWABLE STRESS = 132000 PSI (4140 AS ABOVE)

F.S. = 2.69

COUPLING STRESSES

NECK

$d_o$ = 2.00 in.

$d_i$ = 1.625 in.

$R = \frac{d_i}{d_o} = .8125$

$d$ = EQUIV. SOLID. SHAFT = $d_o \sqrt[3]{1-R^4}$

$d = 1.652$

$S_s = \frac{5.093\,T}{d^3} = \frac{5.093 \times 2942 \times 1.3}{1.652^3} = 4321$ PSI

ALLOWABLE SHEAR STRESS = 145000 ÷ 2 = 72000 PSI
(J&L STEEL : 4150 STEEL @ 350 BHN)

S.F. = 16.7

SPLINE

$S_s = 1.2732 \frac{T}{LD^2}$

L = SPLINE LENGTH = .312 in.

D = PITCH DIAMETER = 1.392 in.

T = TORQUE = 2942 x 1.3 in. LB.

$S_s$ = 8020 PSI

S.F. = 8.98

COMPRESSIVE STRESS ON TEETH!

$A = .125$ in. ACTIVE PROFILE $\times .312$ FACE WIDTH $\times$ 12 TEETH $= .468$ in.$^2$

$F = 2942 \times 1.3 \div .781 = 4900$ LBS

$S = 4900 \div .468 = 10{,}100$ PSI

ALLOWABLE STRESS = 145000 PSI

S. F. = 14.4

RING GEAR TANG

TOTAL LOAD ON RING GEAR TANG = $4217 \times 1.3$ LB

BENDING STRESS = $\frac{WL}{Z}$

$L = .2$ in.

$Z = \frac{bd^2}{12}$

$b = .375$ in.

$d = .750$ in

$Z = .0176$

$S = 62{,}400$ PSI

SAFE BENDING STRESS = 145,000 PSI (4150 STL AS ABOVE

S.F. = 2.32

COMPRESSIVE STRESS OF DOWEL ON ALUMINUM BULKHEAD

$$\text{AREA} = .62 \times .8 = .5 \text{ in}^2$$

$$S = \frac{4217 \times 1.3}{.5} = 11{,}000 \text{ PSI}$$

SAFE COMPRESSIVE STRESS = 22,000 PSI
(A356 CAST ALUMINUM)

S.F. = 2.00

# APPENDIX V

## Thermal Calculations

REQUIRED OIL FLOW RATE

$$\dot{m} = \frac{q}{\Delta T C_p 3600}$$

$q = 50400$ Btu/Hr. TOTAL HEAT FLOW INTO OIL

$T_H = 215°F$ HOT OIL TEMP

$T_C = 155°F$ COLD OIL TEMP

$\Delta T = 60°F$

$C_p = .514$ Btu/lbm °F

$\dot{m} = .4543$ lbm/sec FLOW RATE

$$Q = \frac{1728 \times 60}{231} \frac{\dot{m}}{\rho}$$

$\rho = 58.28$ lbm/ft³ DENSITY OF OIL

$Q = 3.5$ GPM FLOW RATE

# HEAT EXCHANGER RESISTANCES

NOTE: HEAT EXCHANGER TREATED AS TWO SEPARATE UNITS - UNIT 1 OVER STATOR CARRIES HEAT FROM THE STATOR AS WELL AS THE OIL AND UNIT 2 ADJACENT TO THE STATOR CARRIES HEAT FROM THE OIL ONLY

## COVECTION TO OUTER WALL

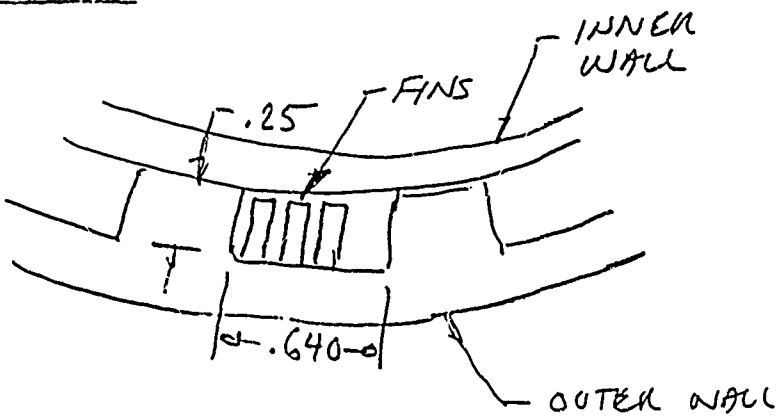


FINS:

28 FINS/IN.
.240 IN. HIGH
.005 THICH
3003 ALUMINUM

$P = .6414$ IN, PERIMETER
$A_p = .007368\ IN^2$ AREA OF ONE PASSAGE
$4r_h = .0544$ IN HYDRAULIC DIAMETER
$A/V = 715\ ft^2/ft^3$ HEAT TRANSFER AREA PER UNIT OF FIN VOLUME
$A_f/A = .9399$ FIN AREA PER UNIT OF HEAT TRANSFER AREA

$$R_E = \frac{12}{g_c}\frac{\dot{m}D}{A\mu}$$

$\dot{m} = .223$ lbm/sec (FLOW SPLIT INTO 2 PARALLEL PATHS)

$D = 4r_h = .0544$ in,

$A = .1289\ in^2$ AREA OF TOTAL PASSAGE

$\mu = 7.032 \times 10^{-5}$ lbf-sec/ft$^2$ VISCOSITY OF OIL

$R_e = 499.1$

$P_r = 3600 \times 32.2 \times \frac{C_p \mu}{K}$

$C_p = .514$ Btu/lbm °F — SPECIFIC HEAT OF OIL

$K = .07$ Btu/Hr · Ft · °F — THERMAL CONDUCTIVITY OF OIL

$P_r = 59.86$

$N_u = f\left(\frac{Re\ Pr\ D}{L}\right)$ — KEITH, PRINCIPLES OF HEAT TRANSFER, 2ND ED. P. 590

$D = 4r_h = .0544$ IN. — HYDRAULIC DIAMETER

$L = 139.9$ IN. — TOTAL LENGTH OF ONE BANK OF HEAT EXCHANGER

$\frac{Re\ Pr\ D}{L} = 11.63$

$N_u = 4.2$ — KEITH P. 590

$h_c = \frac{12\ Nu\ k}{D} = 64.8$ Btu/Hr-Ft²-°F — HEAT TRANSFER COEFFICIENT

FIN EFFICIENCY

$m = \sqrt{\frac{2h_c}{K\delta}}$ — KAYS & LONDON, COMPACT HEAT EXCHANGERS 2ND ED., P. 14

$K = 100$ Btu/Hr · Ft · °F — THERMAL CONDUCTIVITY OF FIN

$\delta = .005$ IN — FIN THICKNESS

$m = 55.77\ ft^{-1}$

$\eta_f = f(ml)$ — KAYS & LONDON P50

$l = .240$ IN. — LENGTH OF FIN

$ml = 1.116$

used directly in the log-mean-rate equations for heat exchangers presented in Chapter 11.

The mean Nusselt numbers for laminar flow in tubes at a uniform wall temperature have been calculated analytically by various investigators. Their results are shown in Fig. 8–12 for several velocity distributions. All of these solutions are based on the idealizations of a constant tube-wall temperature and a uniform temperature distribution at the tube inlet and apply strictly only when the physical properties are independent of temperature. The abscissa is the dimensionless quantity $\mathrm{Re}_D \mathrm{Pr} D/L$, usually

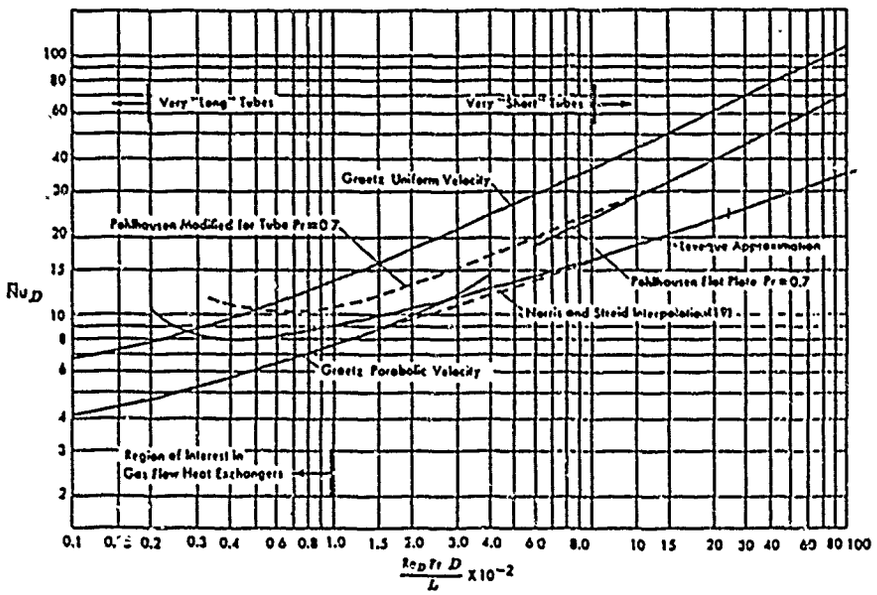


FIG. 8–12. Curves illustrating solutions for laminar-flow heat transfer at constant wall temperature. (Extracted from "Numerical Solutions for Laminar Flow Heat Transfer in Circular Tubes," by W. M. Kays, published in *Trans. ASME*, Vol. 77, 1955, with permission of the publishers, The American Society of Mechanical Engineers)

called the Graetz number Gz. To determine the mean value of the Nusselt number for a given tube of length $L$ and diameter $D$, one evaluates the Reynolds number $\mathrm{Re}_D$, the Prandtl number Pr, forms the dimensionless parameter $\mathrm{Re}_D \mathrm{Pr} D/L$, and enters the curve of Fig. 8–12. The selection of the curve representing the conditions which most nearly correspond to the physical conditions depends on the nature of the fluid and the geometry of the system. For high-Prandtl-number fluids, such as oils, the velocity profile is established much more rapidly than the temperature profile. Consequently the application of the curve labeled "parabolic velocity" does not lead to a serious error in long tubes when $\mathrm{Re}_D \mathrm{Pr} D/L$ is less than 100.

Fig. 2-11. Heat transfer effectiveness of straight and circular fins.

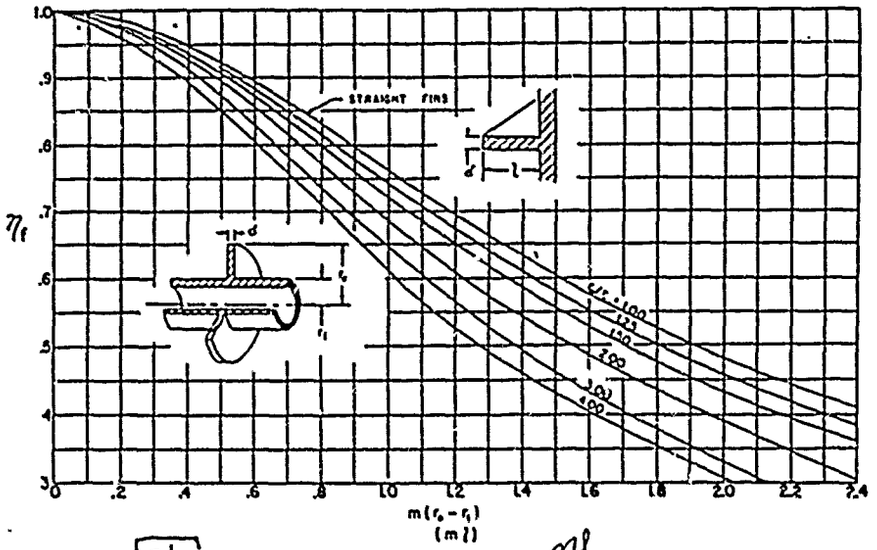


$m = \sqrt{\frac{2h}{k\delta}}$ circ. fins

$= \sqrt{\frac{4h}{kd}}$ rods

Fig. 2-12. Heat transfer effectiveness as a function of number of transfer units and capacity rate ratio; counterflow exchanger.

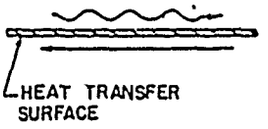


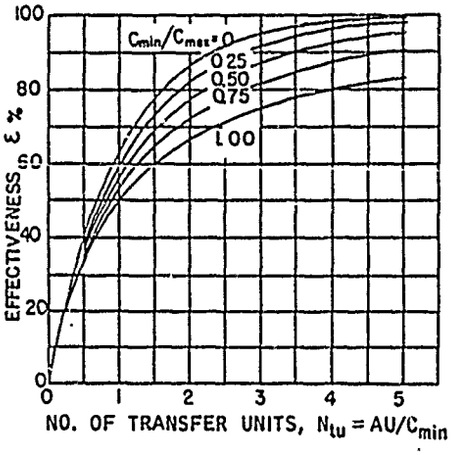


Fig. 2-13. Heat transfer effectiveness as a function of number of transfer units and capacity rate ratio; parallel-flow exchanger.

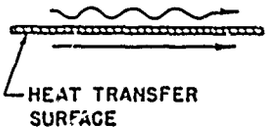


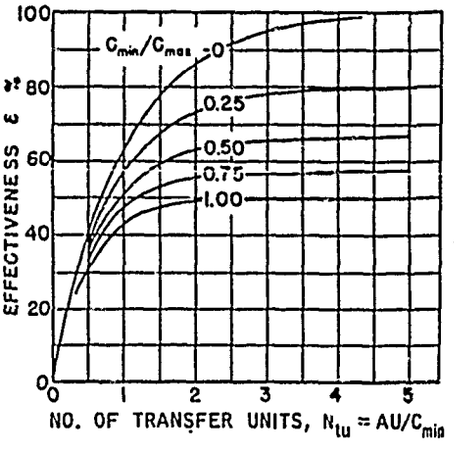

$\eta_f = .73$ FIN EFFICIENCY

$\eta_0 = 1 - Af/A(1-\eta_f)$ KAYS & LONDON P 14

$\eta_0 = .7462$ OVERALL EFFICIENCY

$$R = \frac{1}{\eta_0 h_c (A/V) V}$$ RESISTANCE

$V_1 = .01789\ ft^3$ VOLUME OF HEAT EXCHANGER OVER STATOR

$V_2 = .006388\ ft^3$ VOLUME OF HEAT EXCHANGER ADJACENT TO STATOR

$R_1 = .001617$ HR-°F/BTU

$R_2 = .004526$ HR-°F/BTU

CONVECTION TO INNER SHELL

$$R = \frac{1}{h_c A}$$ RESISTANCE

$A_1 = .7670\ ft^2$ AREA OF INNER SHELL OVER STATOR

$A_2 = .4474\ ft^2$ AREA OF INNER SHELL ADJACENT TO STATOR

$h_c = 64.8$ BTU/HR-FT²-°F

$R_1 = .02011$ HR-°F/BTU

$R_2 = .03448$ HR °F/BTU

INNER SHELL TO OUTER SHELL

$R = \frac{1}{h_c A}$ RESISTANCE

$A_1 = .4602\ ft^2$ AREA OF INNER SHELL & OUTER SHELL CONTACT CONE OVER STRUT

$A_2 = .2684\ ft^2$ AREA ADJACENT TO STRUT

$1/h_c = .0002\ \frac{Hr\text{-}Ft^2\text{-}°F}{BTU}$ GENERAL ELECTRIC, HEAT TRANSFER DATA BOOK, SECT 502.5 P 13

$R_1 = .0004346\ Hr\text{-}°F/BTU$

$R_2 = .0007452\ Hr\text{-}°F/BTU$

OUTER WALL

$R = \frac{t}{KA}$ RESISTANCE

$t = .375$ IN. WALL THICKNESS

$K = 119\ BTU/Hr\text{-}Ft\text{-}°F$ THERMAL CONDUCTIVITY OF ALUMINUM

$A_1 = 1.432\ ft^2$ AREA OVER STRUT

$A_2 = .3183\ ft^2$ AREA ADJACENT TO STRUT

$R_1 = .0001834\ Hr\text{-}°F/BTU$

$R_2 = .0003209\ Hr\text{-}°F/BTU$

8.

## ALUMINUM, BARE SURFACES (200 to 6000 psi) - Solid blocks in air at reduced pressure ($p < 0.1$ atm)

For aluminum in air at 1 atm absolute pressure, see pages 10-11.
For aluminum at lower contact pressures and at reduced air pressure ($p < 0.1$ atm), see page 12.
For aluminum in other gases, see page 14.
For aluminum with sandwich material in air, see page 15; at reduced pressure ($p < 0.1$ atm), see page 16.
For aluminum with dissimilar metal in air, see page 20; at reduced pressure ($p < 0.1$ atm), see page 21.
For other metals in air, see pages 5-6, 17; at reduced pressure ($p < 0.1$ atm), see pages 18-19.
For aluminum with riveted joints in air, see page 22.

| Curve | Material[4] | Finish | Roughness Rms (μ in.) Block 1 | Roughness Rms (μ in.) Block 2 | Fluid in Gap | Temp (°F) | Condition | Ref. No.[3] |
|---|---|---|---|---|---|---|---|---|
| d | Aluminum[9] | Ground | 53 | 53 | Air | R.T. | Clean, 4.5 mm Hg abs | 10 |
| e | Aluminum 6061-T6 | Milled | 8-16 | 8-16 | Air | 83 | Clean, $10^{-4}$ mm Hg abs | 45 |
| f | Aluminum 6061-T6 | Milled | 50-60 | 50-60 | Air | 112 | Clean, $10^{-4}$ mm Hg abs | 45 |

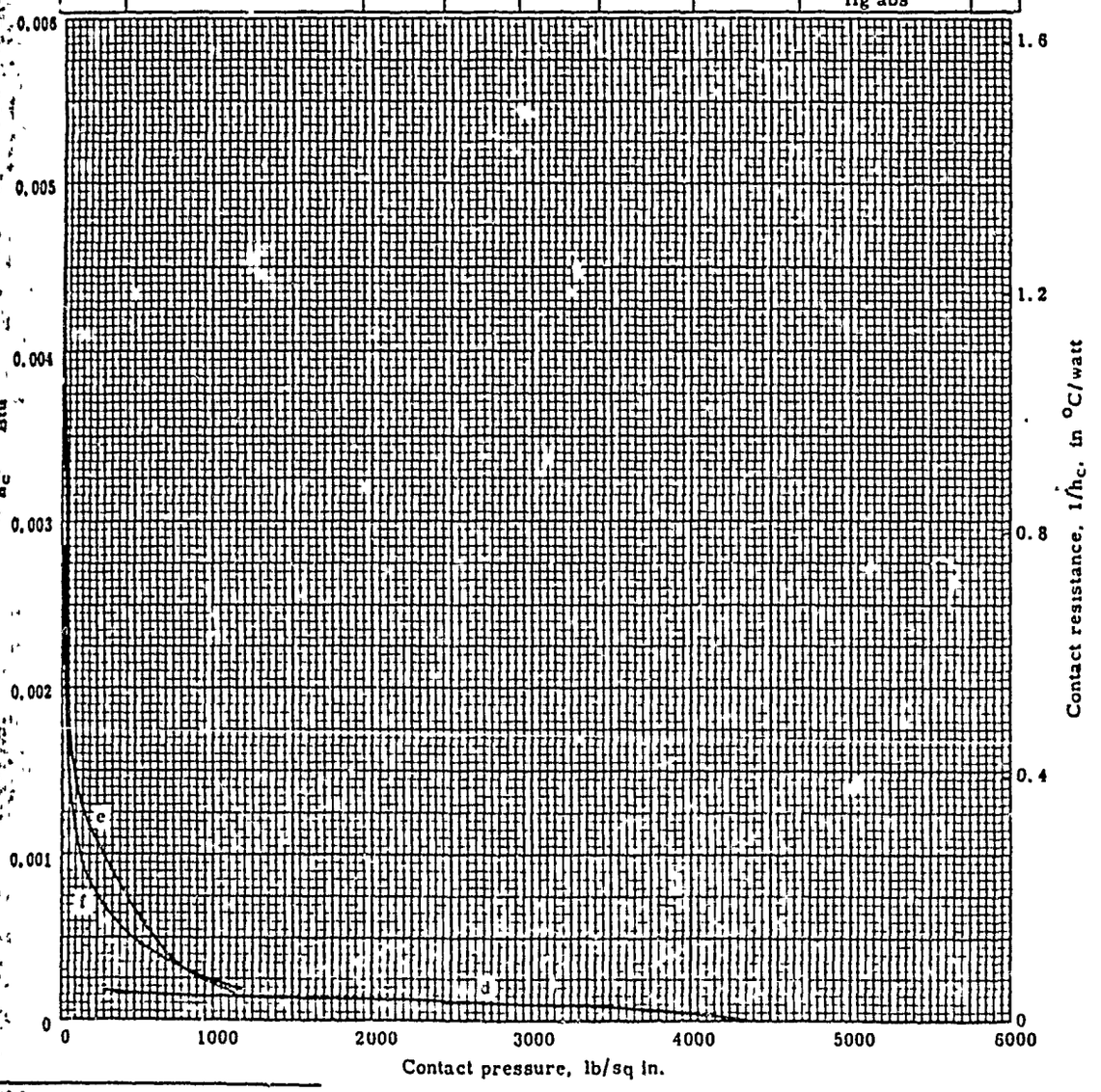


See page 24

FOULING FACTOR

$$R = \frac{1}{h_c A}$$

$h_c = 2000$ KREITH P505

$A_1 = 1.432 ft^2$ AREA OUTER STATOR

$A_2 = .8183 ft^2$ AREA ADJACENT TO STATOR

$R_1 = .0003492$ $HR-{}^\circ F/BTU$

$R_2 = .0006110$ $HR-{}^\circ F/BTU$

CONVECTION TO WATER

$$Re = \frac{1}{12 g_c} \frac{\rho V \ell}{\mu}$$

$\rho = 62.4$ $lbm/ft^3$ DENSITY OF WATER

$V = 10$ ft/sec. WATER VELOCITY

$\ell = 11$ in. LENGTH OF SHELL

$\mu = 1.5 \times 10^{-5}$ lbf-sec/ft² VISCOSITY OF WATER

$Re = 1.184 \times 10^6$

$$h_c = .036 \frac{k}{\ell} Pr^{\frac{1}{3}} Re^{.8}$$ KREITH P 314

$Pr = 5.07$ PRANDTL NO OF WATER

$k = .353$ BTU/HR-FT-°F THERMAL CONDUCTIVITY OF WATER

$h_c = 18.56$ BTU/HR-ft²-°F

$R = \frac{1}{h_c A}$ RESISTANCE

$A_1 = 1.432$ $ft^2$ AREA OVER STATOR

$A_2 = .8185$ $ft^2$ AREA ADJACENT TO STATOR

$R_1 = .0003763$ $Hr\text{-}^\circ F/BTU$

$R_2 = .0006584$ $Hr\text{-}^\circ F/BTU$

PRESSURE DROP THROUGH ~~HEAT~~ EXCHANGER

$f = 64/Re$

$Re = 499.1$ REYNOLDS NUMBER OF OIL

$f = .1282$ FRICTION FACTOR

$\Delta P = \frac{144}{2g_c} f\left(\frac{l}{D}\right)\frac{1}{\rho}\left(\frac{\dot{m}}{A}\right)^2$

$l = 139.9$ in. LENGTH OF PASSAGE

$D = 4r_h = .0544$ in. HYDRAULIC DIAMETER OF PASSAGE

$\rho = 58.28$ lbm/ft$^3$ DENSITY OF OIL

$\dot{m} = .223$ lbm/sec FLOW RATE OF OIL

$A = .1289$ in$^2$ AREA OF TOTAL PASSAGE

$\Delta P = 37.8$ PSI

## THERMAL ANALYSIS OF HEATSINK ASSEMBLY (ALTERNATOR VOLTAGE CONTROLLER)

THE HEATSINK ASSEMBLY CONTAINS THE POWER SEMICONDUCTORS FOR BOTH THE BOOST CONVERTER AND THE FIELD REGULATOR, WHICH IT POWERS. THESE COMPONENTS ALL CONDUCT HEAT TO A COMMON EXTRUDED HEATSINK. THE INTENT OF THIS ANALYSIS IS TO DETERMINE THE JUNCTION TEMPERATURES OF BOOST CONVERTER POWER CUBES (2) AND THE FIELD REGULATOR POWER MOSFETS (2) AND BACK DIODES (2) AT MAXIMUM AMBIENT OF 50 DEGREES C.

SINCE THE FIELD REGULATOR GETS ITS POWER FROM THE BOOST CONVERTER, THE OPERATING POINTS OF THE TWO ARE RELATED. SYSTEMS MODELING SHOWS A STEADY STATE FIELD CURRENT NEAR 2.5 AMPS AND STARTING CURRENT OF 9 AMPS (CURRET LIMIT) FOR 3 SECONDS MAXIMUM. THE STEADY STATE THERMAL ANALYSIS USED 3 AMPS FIELD CURRENT. THE BOOST CONVERTER SUPPLIES 150V AT ABOUT 0.6 AMPS AT THIS OPERATING POINT.

AFTER DETERMINING THE STEADY STATE TEMPERATURES OF THE JUNCTIONS AND THE HEATSINK, A RE-START IS ASSUMED TO OCCUR. THE START TAKES A MAXIMUM OF 3 SECONDS WITH FIELD CURRNT OF 9 AMPS AND BOOST CONVERTER CURRENT OF 5.5 AMPS. SINCE THE HEATSINK HAS A THERMAL TIME CONSTANT OF ABOUT 20 MINUTES, IT WILL NOT CHANGE TEMPERATURE SIGNIFICANTLY DURING THE 3 SECOND START. THE JUNCTION TEMPERATURE IS TAKEN AS THE STEADY STATE HEATSINK TEMPERATURE PLUS THE DELTA T FROM JUNCTION TO SINK CALCULATED DURING START.

THREE BASIC PROGRAMS AND ONE SPICE PROGRAN ARE USED TO DO THE THERMAL ANALYSIS. THE FIRST ONE CALCULATES THE DUTY CYCLE OF THE BOOST CONVERTER FOR A GIVEN OUTPUT CURRENT. THIS IS NEEDED BY THE SECOND PROGRAM TO CALCULATE LOSSES. THE LISTINGS OF THESE TWO BOOST CONVERTER PROGRAMS FOLLOWS:

PROGRAM #1

```
5 REM PGM TO CALCULATE DUTY CYCLE AS FN OF VBUS,TR,VIN,IPEAK
6 REM NAME OF PGM IS DTBOOSTDC.BAS
10 INPUT 'VBUS(OUTPUT),VSOURCE(IN),ISEC=';VB,VS,ISEC
15 INPUT 'VDIODE,RDS(AT 150C),RSOURCE,RPRIM,RSEC=';VD,RDS,RIN,RTF,RSEC
20 INPUT 'TURNS RATIO=';TR
25 OPEN "DC.DAT" FOR OUTPUT AS FILE #2%, ACCESS WRITE, &
   SEQUENTIAL VARIABLE
30 VPRIM= (VS-2*RDS*IP-RIN*IP*DC-RTF*IP)
35 DC=(VB + 2*VD + ISEC*RSEC)/(TR*VPRIM)
26 IP= ISEC*TR
36 PRINT #2%,'INPUTS'
37 PRINT #2%
40 PRINT 'VBUS,VSOURCE,IPEAK,ISEC=';VB,VS,IP,ISEC
45 PRINT #2%,'VBUS,VSOURCE,IPEAK,ISEC=';VB,VS,IP,ISEC
50 PRINT 'VDIODE,RDS,RSOURCE,RPRIM,RSEC=';VD,RDS,RIN,RTF,RSEC
55 PRINT #2%,'VDIODE,RDS,RSOURCE,RPRIM,RSEC=';VD,RDS,RIN,RTF,RSEC
66 PRINT #2%
67 PRINT #2%
68 PRINT #2%,'OUTPUTS'
69 PRINT #2%
80 PRINT 'DUTY CYCLE=';DC
85 PRINT #2%,'DUTY CYCLE=';DC
70 PRINT 'VPRIMARY=';VPRIM
75 PRINT #2%,'VPRIMARY=';VPRIM
60 PRINT 'TURNS RATIO(STEP-UP)=';TR
65 PRINT #2%,'TURNS RATIO(STEP-UP)=';TR
90 CLOSE #2%
100 END
```

PROGRAM #2

```
10 REM THIS PGM CALCULATES LOSSES IN DT BOOST CONVERTER
12 REM AND CALULATES TRANSIENT DELTA T FROM CASE TO JUNCTION
13 REM THIS PGM CALLED DTBOOSTDIS.BAS
15 OPEN "DIS.DAT" FOR OUTPUT AS FILE #2%, ACCESS WRITE, &
   SEQUENTIAL VARIABLE
20 INPUT 'VBUS,VS,DUTY,TR=';VB,VS,DC,TR
30 INPUT 'FREQ,LFILT,IPEAKPRIM=';FREQ,LFILT,IP
40 INPUT 'RDS(FET),VDIODE=';RDS,VD
50 INPUT 'QGATE,IQGATE=';QG,IQG
60 INPUT 'QMILLER,VQMILLER=';QM,VQM
70 INPUT 'VGATE TO SWITCH ID=';VID
80 INPUT 'VGATE PS,RGATE=';VG,RG
85 INPUT 'TRANSIENT THERM Z FOR FET MODULE=';ZTMOD
86 INPUT 'TCASE OR TSINK BEFORE TRANSIENT=';TCASE
90 VL=(VB/DC)-VB
100 DT=DC/(2*FREQ)
110 DISEC=(VL*DT)/LFILT
120 DIPRIM=DISEC*TR
130 IA=IP-(DIPRIM/2)
140 IB=IP+(DIPRIM/2)
150 DCFET=DC/2
160 IRMSSQ=DCFET*(IA*IA + IA*(IB-IA) + ((IB-IA)*(IB-IA))/3)
170 PCOND=IRMSSQ*RDS
180 DCDIODE=(1-DC)/2
190 PDIODE=VD*DCDIODE*((IA+IB)/2)
200 TIR= (QG*(IP/IQG))/(.75*(VG/RG))
210 TVF= (QM*(VS/VQM))/((VG-VID)/RG)
220 PSWON= .5*VS*IA*FREQ*(TIR+TVF)
230 PSWOFF= .5*VS*IB*FREQ*(TIR+TVF)
240 PSW= PSWON+PSWOFF
250 PTOT=PSW + PCOND + PDIODE
251 PMOD= PTOT*2
252 PBOOST=2*PMOD
270 DELT_T= PMOD*ZTMOD
280 TJ= TCASE+DELT_T
281 PIN=VS*IP*DC
282 POUT=VB*IP/TR
283 EFF1=POUT/PIN
284 EFF2=POUT/(POUT+PBOOST)
300 PRINT 'INPUTS'
310 PRINT #2%,'INPUTS'
320 PRINT
321 PRINT #2%
330 PRINT 'VBUS,VS,DUTY,TR=';VB,VS,DC,TR
331 PRINT 'FREQ,LFILT,IPEAKPRIM=';FREQ,LFILT,IP
332 PRINT 'RDS(FET),VDIODE=';RDS,VD
333 PRINT 'QGATE,IQGATE=';QG,IQG
334 PRINT 'QMILLER,VQMILLER=';QM,VQM
335 PRINT 'VGATE TO SWITCH ID=';VID
336 PRINT 'VGATE PS,RGATE=';VG,RG
337 PRINT 'TRANSIENT THERM Z FOR FET MODULE=';ZTMOD
338 PRINT 'TCASE OR TSINK BEFORE TRANSIENT=';TCASE
430 PRINT #2%,'VBUS,VS,DUTY,TR=';VB,VS,DC,TR
431 PRINT #2%,'FREQ,LFILT,IPEAKPRIM=';FREQ.LFILT,IP
432 PRINT #2%,'RDS(FET),VDIODE=';RDS,VD
433 PRINT #2%,'QGATE,IQGATE=';QG,IQG
434 PRINT #2%,'QMILLER,VQMILLER=';QM,VQM
435 PRINT #2%,'VGATE TO SWITCH ID=';VID
```

```
436 PRINT #2%,'VGATE PS,RGATE=';VG,RG
437 PRINT #2%,'TRANSIENT THERM Z FOR FET MODULE=';ZTMOD
438 PRINT #2%,'TCASE OR TSINK BEFORE TRANSIENT=';TCASE
450 PRINT
451 PRINT
452 PRINT #2%
453 PRINT #2%
454 PRINT 'OUTPUTS'
455 PRINT #2%,'OUTPUTS'
456 PRINT
457 PRINT #2%
500 PRINT 'SEC RIPPLE IP-P,PRIM RIPPLE IP-P=';DISEC,DIPRIM
501 PRINT 'I TURN ON TIME,I TURN OFF TIME=';TIR,TVF
502 PRINT 'PCOND,PSW,PDIODE=';PCOND,PSW,PDIODE
503 PRINT 'POWER MODULE,POWER BOOST=';PMOD,PBOOST
504 PRINT 'DELT_T,JUNCTION T=';DELT_T,TJ
505 PRINT 'EFF1,EFF2=';EFF1,EFF2
600 PRINT #2%,'SEC RIPPLE IP-P,PRIM RIPPLE IP-P=';DISEC,DIPRIM
601 PRINT #2%,'I TURN ON TIME,I TURN OFF TIME=';TIR,TVF
602 PRINT #2%,'PCOND,PSW,PDIODE=';PCOND,PSW,PDIODE
603 PRINT #2%,'POWER MODULE,POWER BOOST=';PMOD,PBOOST
604 PRINT #2%,'DELT_T,JUNCTION T=';DELT_T,TJ
605 PRINT #2%,'EFF1,EFF2=';EFF1,EFF2
620 CLOSE #2%
630 END
```

THE THIRD BASIC PROGRAM CALCULTES POWER LOSSES IN THE FIELD REGULATOR FOR A GIVEN FIELD CURRENT.THE LISTING IS GIVEN BELOW:

PROGRAM #3

```
10 REM PGM IS CALLED DTFREG.BAS
20 REM IT CALCULATES DUTY CYCLE,POWERS,SW TIMES,CAP I,BOOST I
30 REM INPUTS ARE FLD I,BUS V,FREQ,RFLD,RDS,VGATE,RGATE &
35 REM QGATE,QMIL,IQ,VQ,VID,VD
40 INPUT 'FIELD I, BUS V=';IFD,VB
50 INPUT 'FLD REG FREQ=';FREQ
60 INPUT 'EXC RESISTANCE=';RFLD
70 INPUT 'BACK DIODE V=';VD
80 RDS=.72
85 VG=15
90 RG=100
95 QG=17E-9
100 IQ=13
105 QMILL=64E-9
110 VQ=360
115 VID=5
120 OPEN "FREG.DAT" FOR OUTPUT AS FILE #2%, ACCESS WRITE, &
    SEQUENTIAL VARIABLE
130 DC=(IFD*RFLD + VB - 2*VD)/(2*VB -2*IFD*RDS - 2*VD)
140 ISEC=(2*DC - 1)*IFD
150 REM BELOW CALCULATES POWER
155 REM ****************************************
160 IRMSSQ=IFD*IFD*DC
161 PCON=IRMSSQ*RDS
170 TIR=(QG*(IFD/IQ))/(.75*VG/RG)
180 TVF=(QMILL*(VB/VQ))/((VG-VID)/RG)
190 PSW = VB*IFD*FREQ*(TIR+TVF)
200 PDIODE=VD*IFD*(1-DC)
210 PTOT=(PCON + PSW + PDIODE)*2
220 PFLD=IFD*IFD*RFLD
225 REM OUTPUT
230 REM ************************************
240 PRINT 'IFLD,VBUS,FREQ=';IFD,VB,FREQ
245 PRINT #2%,'IFLD,VBUS,FREQ=';IFD,VB,FREQ
250 PRINT 'FIELD RES, VDIODE=';RFLD,VD
255 PRINT #2%,'FIELD RES, VDIODE=';RFLD,VD
260 PRINT
265 PRINT #2%
270 PRINT 'OUTPUTS'
275 PRINT #2%,'OUTPUTS'
280 PRINT 'BOOST OUTPUT I=';ISEC
285 PRINT #2%,'BOOST OUTPUT I=';ISEC
290 PRINT 'FLD REG DUTY CYCLE=';DC
295 PRINT #2%,'FLD REG DUTY CYCLE=';DC
300 PRINT 'PCON,PDIODE=';PCON,PDIODE
305 PRINT #2%,'PCON,PDIODE=';PCON,PDIODE
310 PRINT 'TIR,TVF,PSW=';TIR,TVF,PSW
315 PRINT #2%,'TIR,TVF,PSW=';TIR,TVF,PSW
320 PRINT 'PTOTAL FLD REG=';PTOT
325 PRINT #2%,'PTOTAL FLD REG=';PTOT
326 PRINT 'POWER IN FLD=';PFLD
327 PRINT #2%,'POWER IN FLD=';PFLD
330 CLOSE #2%
340 END
```

AFTER ALL OF THE POWER LOSSES WERE CALCULATED USING THE ABOVE THREE PROGRAMS, A SPICE NETWORK MODEL WAS USED TO DETERMINE THE JUNCTION TEMPERATURES OF THE SEMICONDUCTORS. THE THERMAL RESISTANCES WERE OBTAINED FROM DATA SHEETS OF THE DEVICES. THE SPICE LISTING IS GIVEN BELOW:

SPICE MODEL

```
DAVID TAYLOR SS THERMAL MODEL,BOOST AND FIELD REG
***NAME OF PGM IS DTTEMP.IGS
********* ENTER TOTAL POWER LOSS FIELD REG DIODES
IPD2 0 1 2.2
*********************************
******** ENTER 1/2 ZJC AND ZCS,FIELD REG DIDOE
RJCD2 1 4 .4
RCSD2 4 7 .2
*********************************
********** ENTER TOTAL POWER LOSS FIELD REG FETS
IPFET2 0 2 13.14
*****************************
********** ENTER 1/2 ZJC AND ZCS FOR FIELD REG FETS
RJCFET2 2 5 .4
RCSFET2 5 7 .2
***********************************
************ ENTER TOTAL BOOST CONVERTER LOSS
IPBOOST 0 3 18.4
*******************************
*********** ENTER 1/2 ZJC AND ZCS FOR BOOST MODULES
RJCMOD2 3 6 .125
RCSMOD2 6 7 .05
***********************************
*********** ENTER HEAT SINK ZSA
RSA 7 0 .3
.END
```

FIGURES A5-1 AND A5-2 SUMMARIZE THE STEADY STATE ANALYSIS AND TRANSIENT (STARTING) ANALYSIS, RESPECTIVELY. IN ALL CASES, THE JUNCTION TEMPERATURES ARE BELOW 150 DEGREE C, THE MAXIMUM ALLOWED JUNCTION TEMPERATURE. UNDER STEADY STATE CONDITIONS, THE JUNCTIONS ARE ONLY BETWEEN 60 AND 70 DEGREES C, RESULTING IN HIGH RELIABILITY.

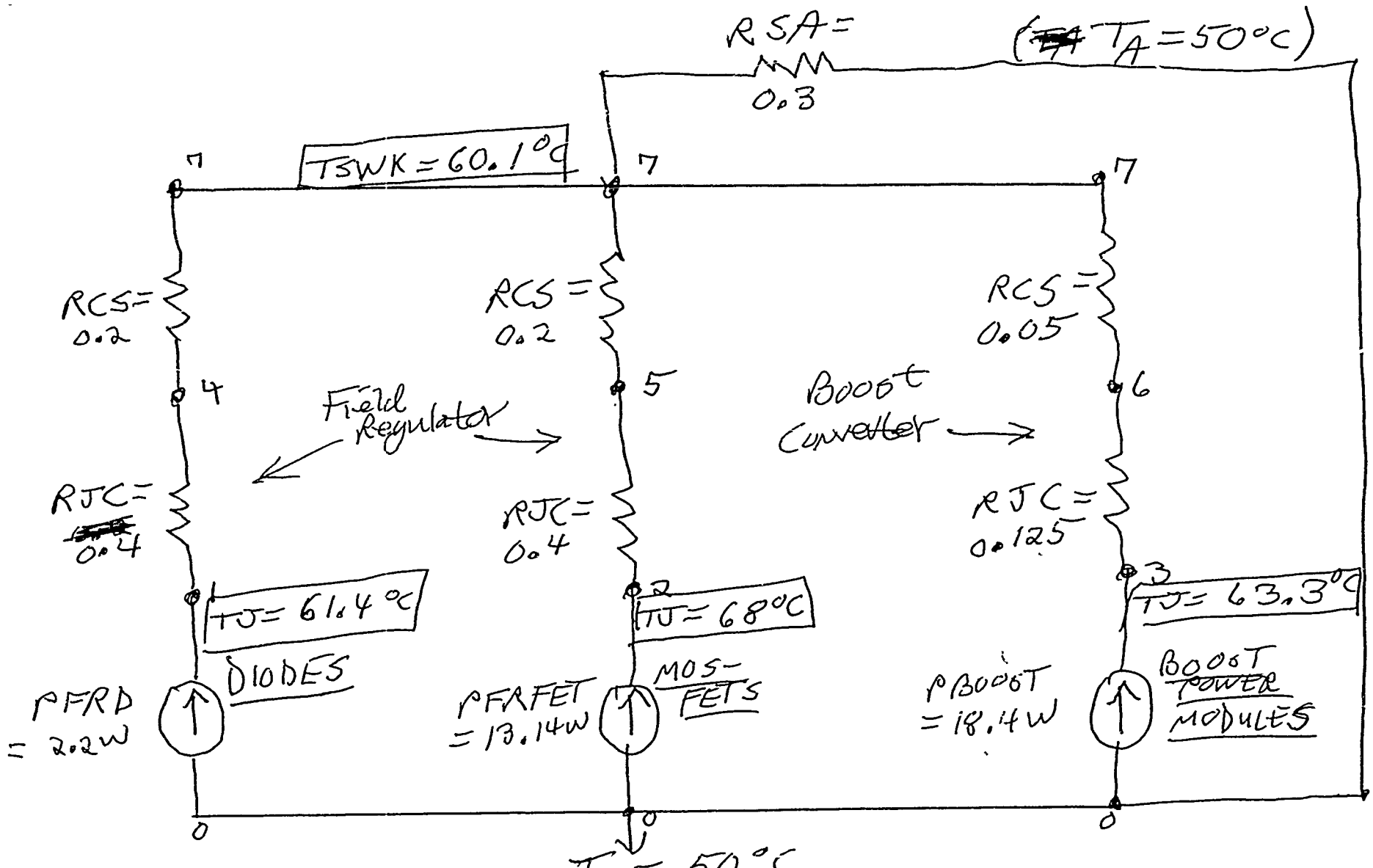


Figure A5-1, Steady State Thermal Profile

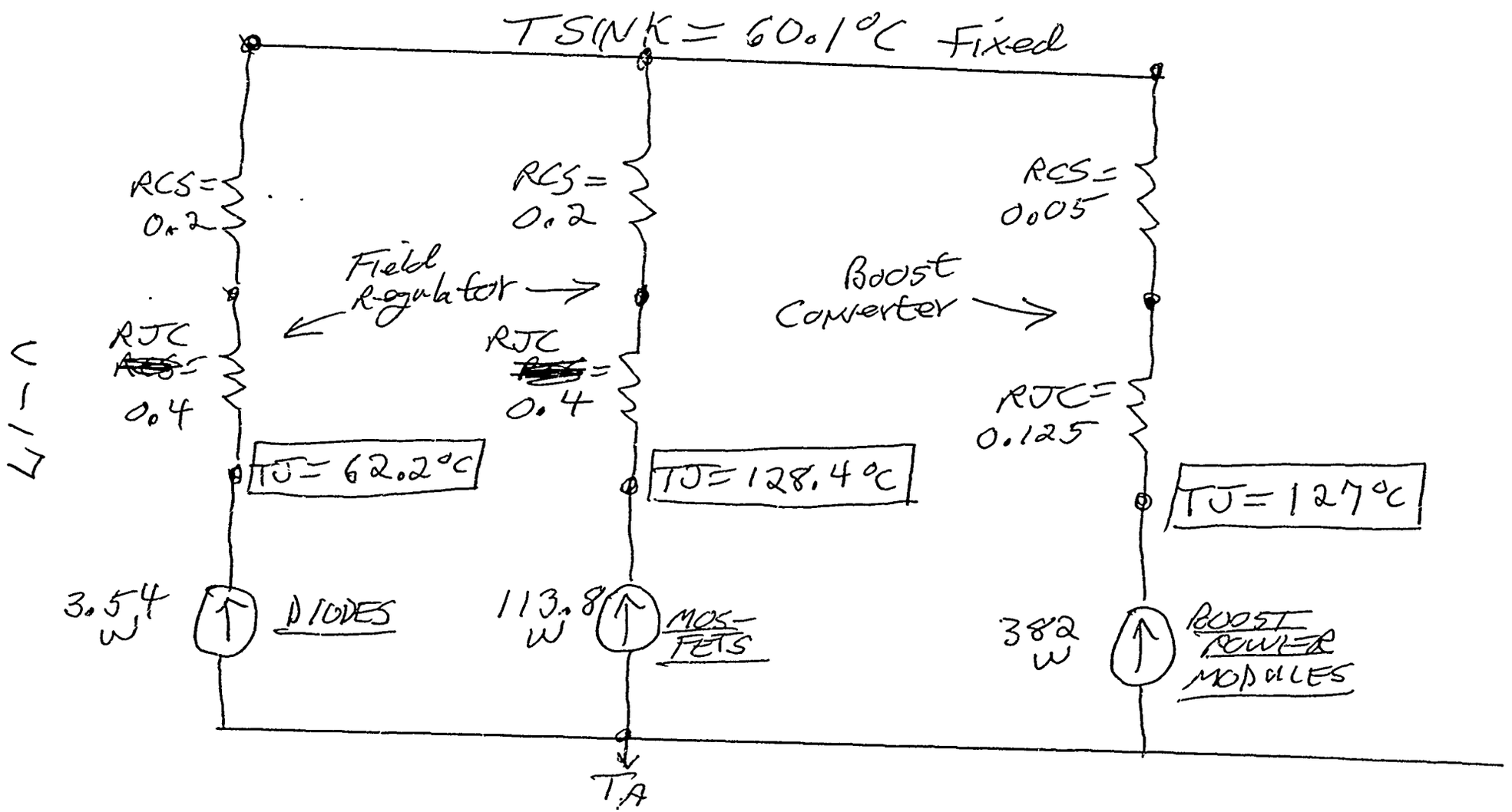


Figure A5-2 . Re-Start Thermal Profile.

# APPENDIX VI

## Sensitivity Analysis

## APPENDIX VI SENSITIVITY ANALYSIS

A digital computer model was used to investigate the sensitivity of dynamic performance to variations of the parameters of the David Taylor amphibious vehicle electric propulsion system.

The model is described in Appendix VI-A. The results of the simulation runs using the model are shown in 56 computer plots that are included in a separate Appendix VI-B available on request.

The effects of varying the parameters were found to be small or negligible for all but one type of case.

The only significant sensitivity to variation of the system parameters was found for the case of starting the motor with an increased value of the resistance of the field winding of the main alternator. The results for these cases raise the concern that a small difference between the predicted value and the actual resistance of the alternator field winding could cause motor starting times to be too long so that thermal limits are exceeded. A summary of these results is shown in Tables VI-I and VI-II

Table VI-I

COLD START TIME VERSUS ALTERNATOR FIELD WINDING RESISTANCE

| Field winding resistance (at base temperature of 25 deg C) | Time to start |
|---|---|
| Nominal R_FIELD_ALT = .455 ohm | 2.2 seconds |
| R_FIELD_ALT x 1.2 = .546 ohm | 2.9 seconds |
| R_FIELD_ALT x 1.3 = .5915 ohm | 3.45 seconds |
| R_FIELD_ALT x 1.5 = .6825 ohm (Slip = 39 % at 3.8 seconds) | more than 3.8 seconds 6 seconds estimated |
| R_FIELD_ALT x 0.5 = .2275 ohm | 1.5 seconds |

Table VI-II

HOT START TIME VERSUS ALTERNATOR FIELD WINDING RESISTANCE

| Field winding resistance (at base temperature of 25 deg C) | Time to start |
|---|---|
| Nominal R_FIELD_ALT = .455 ohm | 2.4 seconds |
| R_FIELD_ALT x 1.1 = .5005 ohm | 3.05 seconds |
| R_FIELD_ALT x 1.2 = .546 ohm (Slip = 19 % at 3.8 seconds) | more than 3.8 seconds 4 seconds estimated |
| R_FIELD_ALT x 1.5 = .6825 ohm (Slip = 56 % at 3.8 seconds) | more than 3.8 seconds 8 seconds estimated |
| R_FIELD_ALT x 0.5 = .2275 ohm | 1.1 seconds |

Sensitivity to parameter variation was studied for three cases of dynamic performance :

1. Load variation at 9000 rpm nominal speed with system hot.
2. Motor start at 4306 rpm alternator speed with system cold.
3. Motor start at 4306 rpm alternator speed with system hot.

Case 1

With the system operating in a steady-state condition at a main alternator speed of 9000 rpm with a motor output power of 310 kilowatts (416 horsepower), the load was reduced to zero and then returned to normal value to simulate the case where the propellor might be out of the water momentarily. It is believed that the load variation for an actual case that might occur would probably have a pattern that would be somewhat similar to a parabola. A ramp variation of the load was selected as an easily implemented approximation since the actual curve is not known.

The load torque was instantly reduced to zero and remained at zero for 150 milliseconds which is a sufficient time for the system to reach a steady-state no load condition. The load torque was then increased from zero to the normal value along a linear ramp over a time period of 100 milliseconds.

One simulation was run for this case with the nominal values for all parameters except that the propellor torque was increased by a factor of 1.3, i.e. the same nominal speed, but a motor output power of 400 kilowatts (535 horsepower).

Table VI-III shows a summary of the parameter variations that were simulated for case 1.

The first column in each of the tables shows the identification number for each simulation run.

Case 2

Starting of the motor from zero speed was simulated for the condition of a main alternator speed of 4306 rpm with all parts of the system cold at a temperature of 20 degrees Celsius. The simulated time duration was chosen to be 3.8 seconds for convenience; the nominal time to start is 2.2 seconds when cold and 2.4 seconds when hot.

Table VI-IV shows a summary of the parameter variations that were simulated for case 2.

Case 3

Starting of the motor from zero speed was simulated for the condition of a main alternator speed of 4306 rpm with all parts of the system at temperatures the same as for the case of nominal 9000 rpm steady-state operation. (Temperatures the same as for case 1 above.)

Table VI-V shows a summary of the parameter variations that were simulated for case 3.

For those simulation runs that have a condition of EXC_SAT_CURVE x 0.90, (run numbers 5_24_88_2, 5_24_88_3, 5_24_88_4) the magnetic saturation curves of the exciter were modified as shown in Figures VI-1, VI-2, and VI-3. The magnetic saturation effect in the exciter was made more severe by making a ten percent reduction of the exciter output voltage to be applied to the input to the field of the main alternator for values of the exciter field current that are in the saturation region. This was not a very significant change in the simulated system because the exciter field current was limited to a maximum value of 9 amperes which is not very far into saturation (Figures VI-1, VI-2, and VI-3). In the steady-state operating condition at 9000 rpm, the exciter field current is about 2.5 amperes; the exciter field current is at or near the limit only during transient conditions of starting or dynamic load variations.

Table VI-III

LOAD VARIATION AT NOMINAL 9000 RPM HOT WITH 100 MILLISECOND LOAD RAMP

| RUN NUMBER | CONDITIONS | |
|---|---|---|
| 5_6_88_0 | Nominal | |
| 5_6_88_1 | L_FIELD_ALT x 1.5 | |
| 5_6_88_2 | L_FIELD_ALT x 0.5 | |
| 5_6_88_3 | R_FIELD_ALT x 0.5 | |
| 5_6_88_4 | R_FIELD_ALT x 1.5 | |
| 5_6_88_5 | L_FIELD_ALT x 1.5 | R_FIELD_ALT x 1.5 |
| 5_6_88_6 | L_FIELD_ALT x 1.5 | R_FIELD_ALT / 1.5 |
| 5_6_88_7 | L_FIELD_EXC x 1.5 | |
| 5_6_88_8 | L_FIELD_EXC x 0.5 | |
| 5_6_88_9 | R_FIELD_EXC x 1.5 | |
| 5_6_88_10 | L_FIELD_EXC x 1.5 | R_FIELD_EXC / 1.5 |
| 5_6_88_11 | T_COULOMB_MOTOR x 2 | |
| 5_6_88_12 | R_2_MOTOR x 1.5 | |
| 5_24_88_2 | EXC_SAT_CURVE x 0.90 | |
| 5_26_88_3 | I_FIELD_EXC_LIMIT = 7 A | |
| 5_26_88_4 | I_FIELD_EXC_LIMIT = 7 A | V_FIELD_EXC_BUSS = 100 V |
| 5_26_88_5 | I_FIELD_EXC_LIMIT = 5 A | V_FIELD_EXC_BUSS = 100 V |
| 5_24_88_1 | K_LOAD_PROP_MOTOR x 1.3 | |

Table VI-IV

COLD START AT NOMINAL 4306 RPM

| RUN NUMBER | CONDITIONS | |
|---|---|---|
| 5_10_88_0 | Nominal | |
| 5_10_88_1 | L_FIELD_ALT x 1.5 | |
| 5_10_88_2 | L_FIELD_ALT x 0.5 | |
| 5_10_88_3 | R_FIELD_ALT x 0.5 | |
| 5_10_88_4 | R_FIELD_ALT x 1.5 | |
| 5_10_88_5 | L_FIELD_ALT x 1.5 | R_FIELD_ALT x 1.5 |
| 5_10_88_6 | L_FIELD_ALT x 1.5 | R_FIELD_ALT / 1.5 |
| 5_10_88_7 | L_FIELD_EXC x 1.5 | |
| 5_10_88_8 | L_FIELD_EXC x 0.5 | |
| 5_10_88_9 | R_FIELD_EXC x 1.5 | |
| 5_10_88_10 | L_FIELD_EXC x 1.5 | R_FIELD_EXC / 1.5 |
| 5_10_88_11 | T_COULOMB_MOTOR x 2 | |
| 5_10_88_12 | R_2_MOTOR x 1.5 | |
| 5_10_88_13 | R_FIELD_ALT x 1.2 | |
| 5_10_88_14 | R_FIELD_ALT x 1.3 | |
| 5_24_88_3 | EXC_SAT_CURVE x 0.90 | |
| 5_26_88_2 | I_FIELD_EXC_LIMIT = 7 A | |
| 5_26_88_8 | I_FIELD_EXC_LIMIT = 7 A | V_FIELD_EXC_BUSS = 100 V |
| 5_26_88_9 | I_FIELD_EXC_LIMIT = 5 A | V_FIELD_EXC_BUSS = 100 V |

Table VI-V

HOT START AT NOMINAL 4306 RPM

| RUN NUMBER | CONDITIONS | |
|---|---|---|
| 5_9_88_0 | Nominal | |
| 5_9_88_1 | L_FIELD_ALT x 1.5 | |
| 5_9_88_2 | L_FIELD_ALT x 0.5 | |
| 5_9_88_3 | R_FIELD_ALT x 0.5 | |
| 5_9_88_4 | R_FIELD_ALT x 1.5 | |
| 5_9_88_5 | L_FIELD_ALT x 1.5 | R_FIELD_ALT x 1.5 |
| 5_9_88_6 | L_FIELD_ALT x 1.5 | R_FIELD_ALT / 1.5 |
| 5_9_88_7 | L_FIELD_EXC x 1.5 | |
| 5_9_88_8 | L_FIELD_EXC x 0.5 | |
| 5_9_88_9 | R_FIELD_EXC x 1.5 | |
| 5_9_88_10 | L_FIELD_EXC x 1.5 | R_FIELD_EXC / 1.5 |
| 5_9_88_11 | T_COULOMB_MOTOR x 2 | |
| 5_9_88_12 | R_2_MOTOR x 1.5 | |
| 5_9_88_13 | R_FIELD_ALT x 1.2 | |
| 5_9_88_14 | R_FIELD_ALT x 1.1 | |
| 5_24_88_4 | EXC_SAT_CURVE x 0.90 | |
| 5_26_88_1 | I_FIELD_EXC_LIMIT = 7 A | |
| 5_26_88_6 | I_FIELD_EXC_LIMIT = 7 A | V_FIELD_EXC_BUSS = 100 V |
| 5_26_88_7 | I_FIELD_EXC_LIMIT = 5 A | V_FIELD_EXC_BUSS = 100 V |

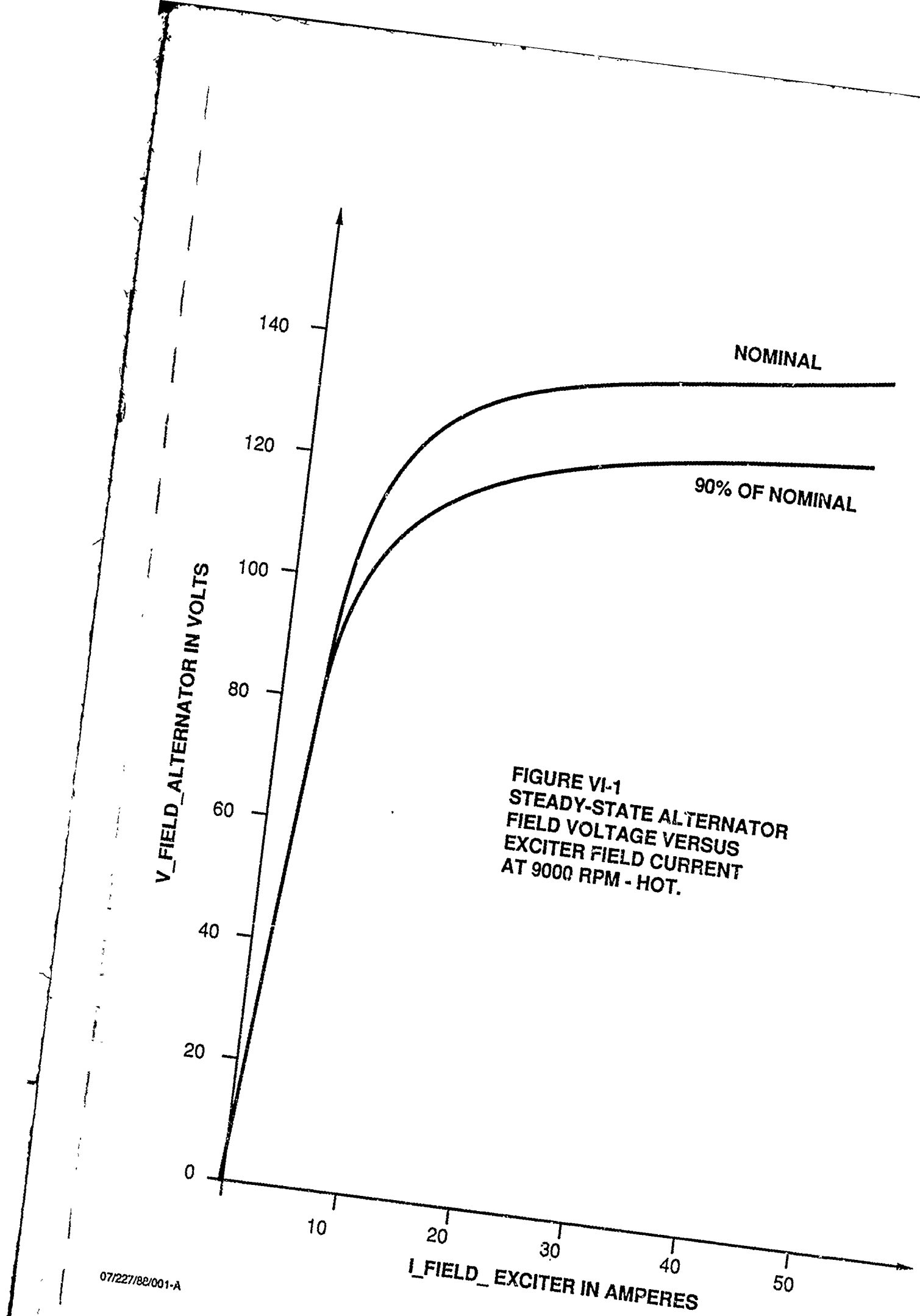


FIGURE VI-1
STEADY-STATE ALTERNATOR
FIELD VOLTAGE VERSUS
EXCITER FIELD CURRENT
AT 9000 RPM - HOT.

07/227/88/001-A

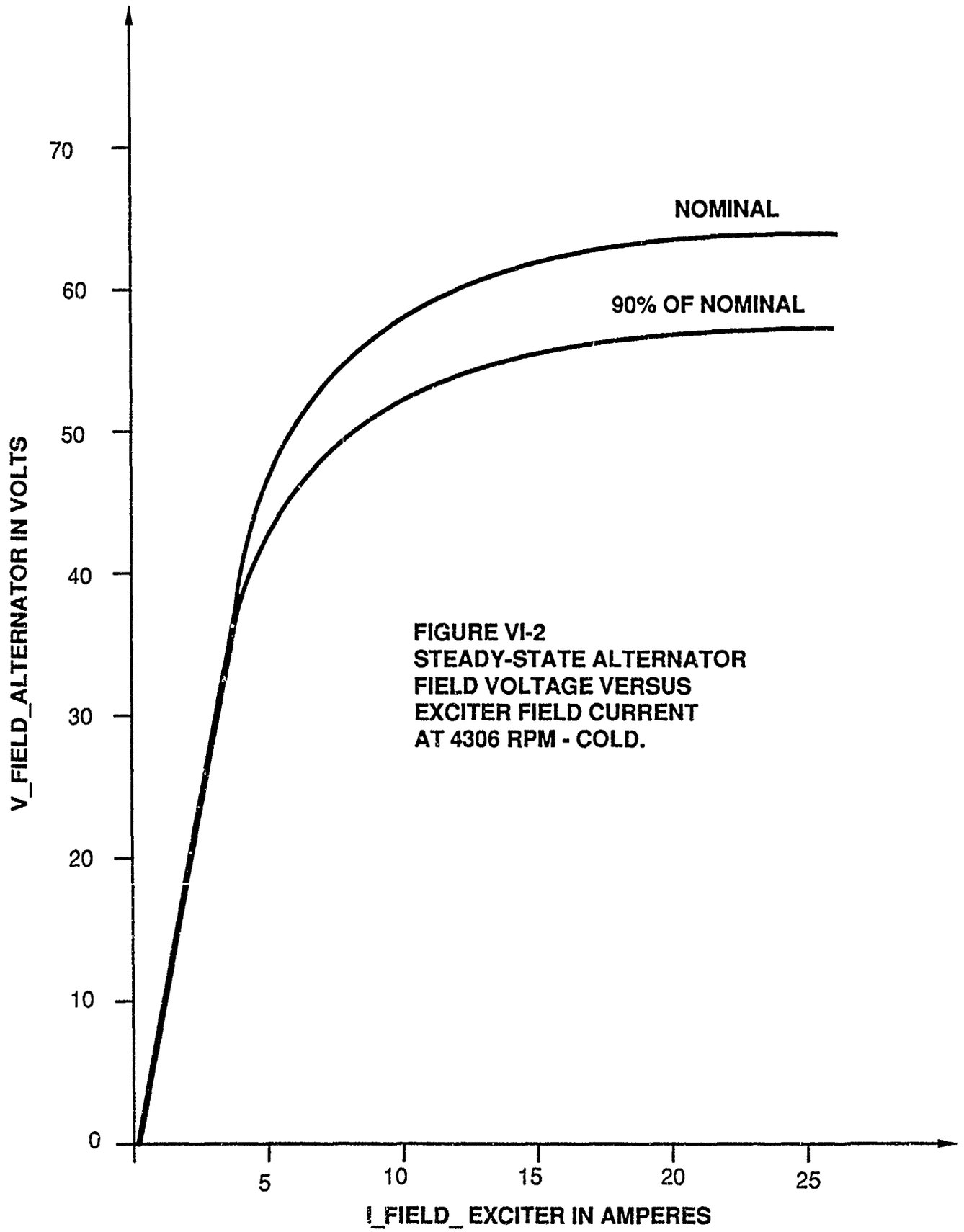


**FIGURE VI-2**
**STEADY-STATE ALTERNATOR FIELD VOLTAGE VERSUS EXCITER FIELD CURRENT AT 4306 RPM - COLD.**

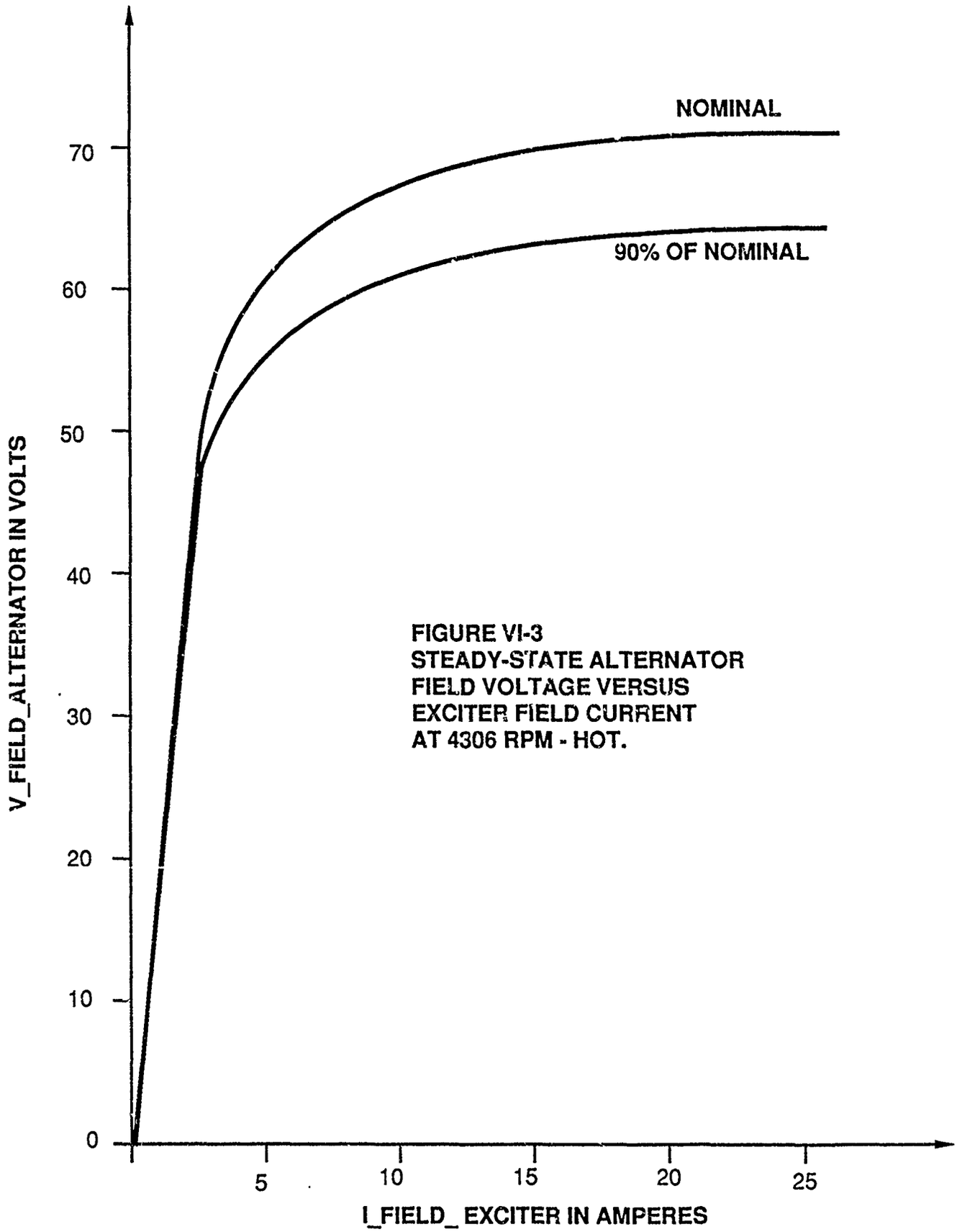


**FIGURE VI-3**
**STEADY-STATE ALTERNATOR FIELD VOLTAGE VERSUS EXCITER FIELD CURRENT AT 4306 RPM - HOT.**

# APPENDIX VI-A

Appendix VI-A contains a description of the digital computer model that has been used to simulate the dynamic performance of the electric propulsion system of the David Taylor amphibious vehicle.

## SYSTEM MODEL

The system provides a speed at the load that is directly proportional to the speed of the prime mover for steady-state conditions. The speed of the load is always impelled toward a value that is directly proportional to the speed of the prime mover under dynamic conditions.

Figure VI-A-1 shows a general block diagram of the model of the system.

The model represents the characteristics of the actual system hardware with sufficient detail to provide simulation results that accurately predict the steady-state and dynamic behavior of the system.

Each portion or block of the model will be discussed separately in the following, starting from the prime mover and moving through the model to the load.

### Prime Mover

The prime mover is taken to be an ideal mechanical power source. In the model, the prime mover can deliver any needed amount of power at any speed and the speed is not affected by the mechanical load.

### Permanent Magnet Generator

The permanent magnet generator is in effect a tachometer that produces an output voltage that is directly proportional to the speed of the prime mover. The output voltage of the permanent magnet generator is the input to the dynamic control system. The terminal voltage of the main alternator is controlled to be directly proportional to the output voltage of the permanent magnet generator.

### Regulator

Figure VI-A-2 shows a simplified block diagram of the regulator.

In the model, the reference voltage input to the regulator is calculated as a simple constant times the speed of the prime mover. The feedback of the alternator terminal voltage is also calculated by means of a simple constant that takes into account the three phase rectification and attenuation of the system hardware.

The model represents the proportional-integral feedback control method of the regulator, the pulse width modulation drive of the exciter field current, and the inner loop of feedback of the exciter field current that is used to limit the current to the 9 ampere thermal capability of the hardware.

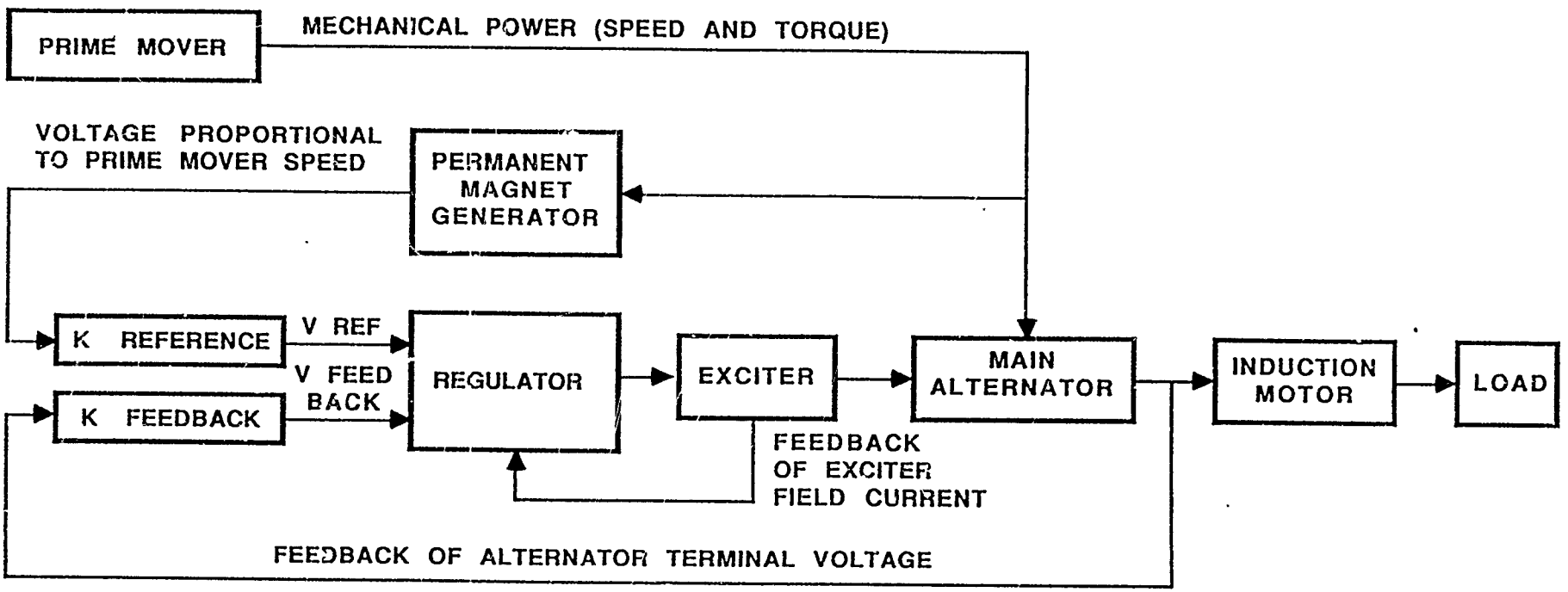




7/227/88/4

Figure VI-A-1. Block Diagram System Model

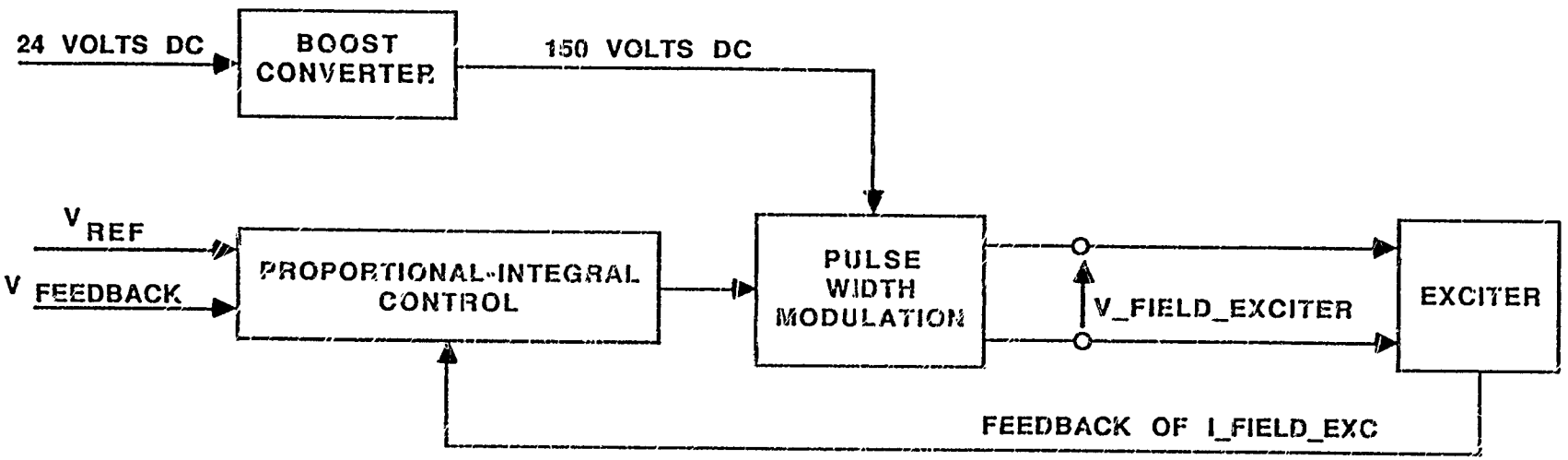


7/27/88/5



Figure VI-A-2. Regulator Model

A boost converter is used to obtain 150 volts DC from a 24 volt DC source. The 150 volts is needed to provide sufficient drive with the pulse width modulation to change the exciter field current fast enough to maintain stability during dynamic system variations due to changes of prime mover speed, changes of system load, or combinations of speed and load change.

## Exciter

Figure VI-A-3 shows a schematic representation of the exciter model.

The output of the regulator is represented in the model as a voltage input to the terminals of the exciter field winding. This voltage may be - DC buss voltage (- 150 volts) or any value within the range of 0 to + DC buss voltage (0 volts to + 150 volts). At each time step of the model execution, the differential equation of the exciter field circuit with this input voltage is solved by a fourth order Runge-Kutta numerical procedure to obtain a value for the exciter field current.

The exciter field current is limited to a maximum positive value of 9 amperes. The input voltage to the exciter field is allowed to be equal to negative buss voltage to force the current toward zero, but the field current is not allowed to go negative.

The exciter field current is used as the input to a lookup table that is interpolated to obtain a value for the input voltage to the field of the main alternator. Since the exciter field current is allowed to have only positive values, the input voltage to the field of the main alternator can only have positive values. This simulates the operation of the rectifiers between the exciter output and the main alternator field winding of the actual hardware.

The lookup table has different sets of values for different system operating conditions. A different lookup table is used for each of three equivalent speeds of the prime mover and for the system cold or hot.

The lookup table values have been derived from the transfer curves shown in Figures VI-A-4, and VI-A-5. The curves show the steady-state relation between the current in the exciter field and the current in the main alternator field with magnetic saturation and machine temperatures taken into account. This information has been translated into curves of DC voltage input to the main alternator field winding versus exciter field current.

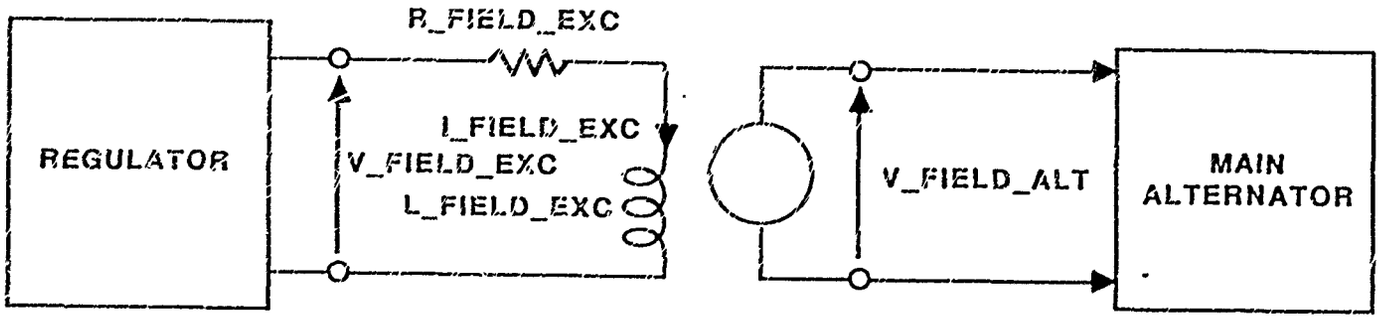


7/227/88/C6



Figure VI-A-3. Exciter Model

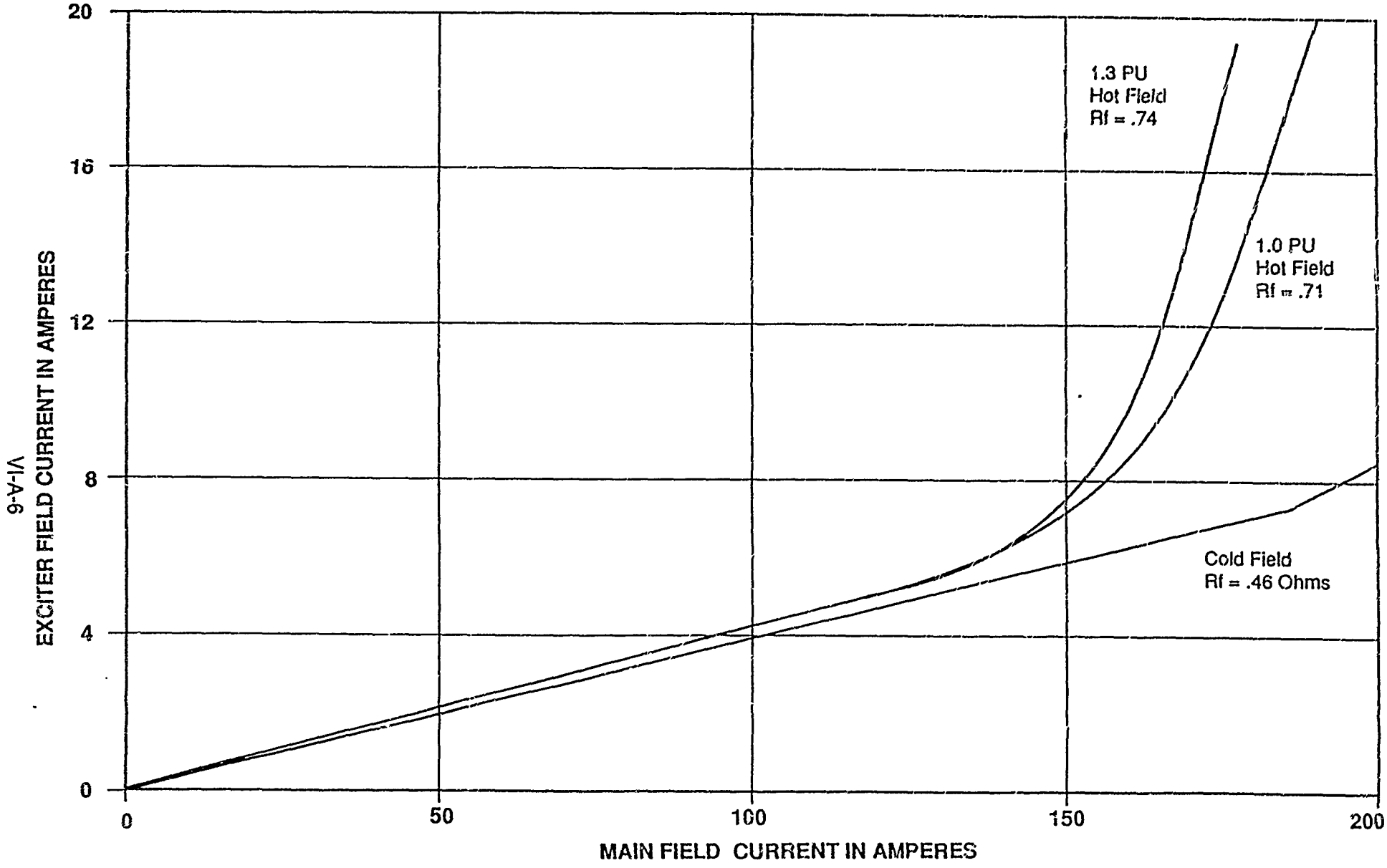




7/227/88/07

Figure VI-A-4. Exciter Field Current vs. Main Field Current (9000 RPM - Hipersco 50)

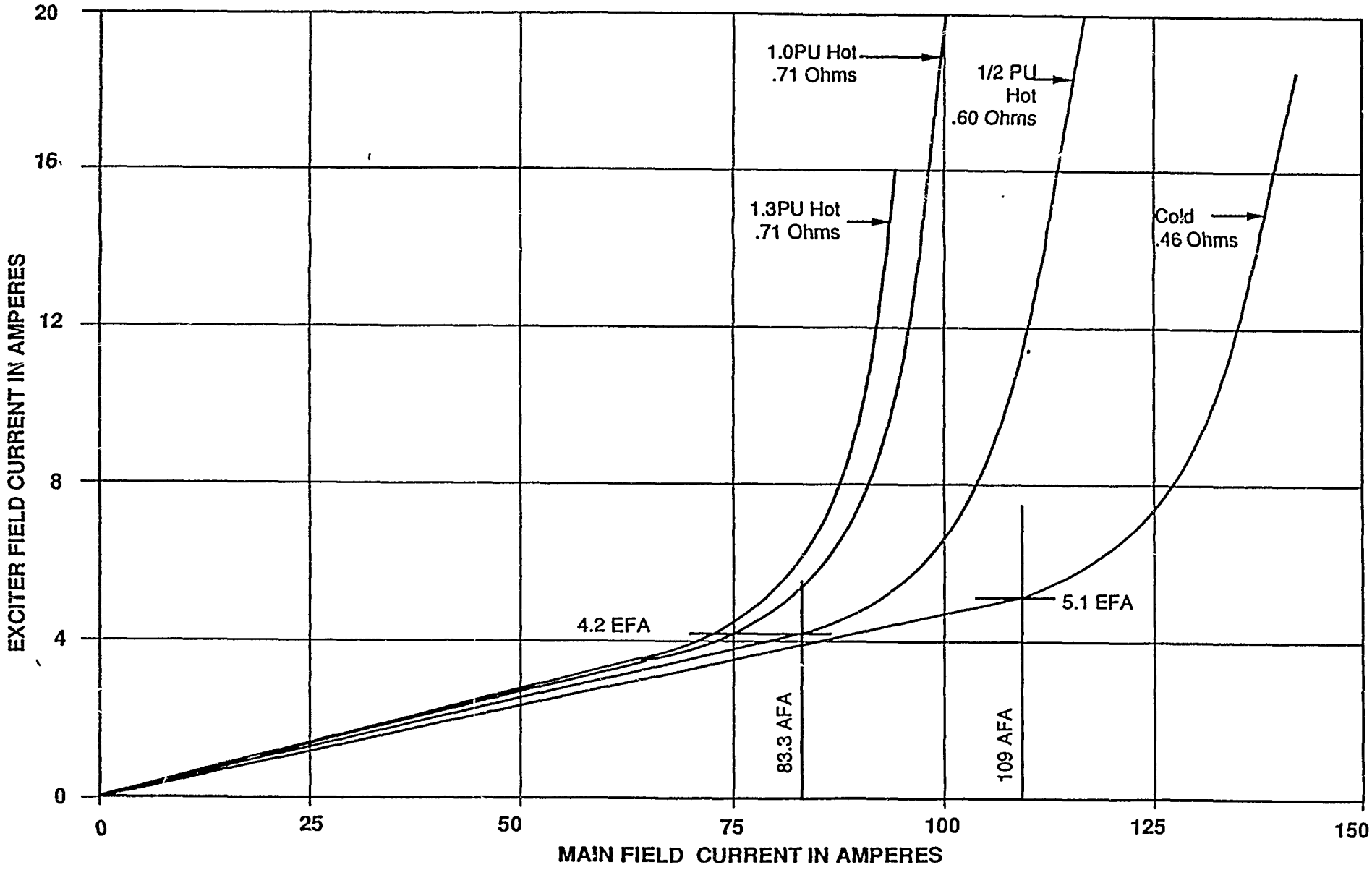


7/227/88/08

Figure VI-A-5. Exciter Field Current vs. Main Field Current (4306 RPM - Hipersco 50)

## Main Alternator

Figure VI-A-6 shows a schematic and block diagram representation of the model of the main alternator.

The calculation of the field current of the main alternator is done in the same way as the calculation of the exciter field current. At each time step of the model execution, the differential equation of the main alternator field circuit is solved by a fourth order Runge-Kutta numerical procedure. The input voltage in this equation is the output voltage of the exciter which is never negative. The main alternator field current can have only positive values and there is no upper limit imposed in the model.

An "effective" value field current that is equal to the main alternator field current minus a demagnetizing component of the alternator load current is used as the input to a lookup table that is interpolated to obtain a value for the generated voltage within the main alternator. The lookup table values are multiplied by a constant factor and the prime mover speed to account for the variation of generated voltage with alternator speed. The values used in this lookup table have been derived from the curves shown in Figure VI-A-7. The curves show the steady-state relation between the current in the alternator field and the alternator terminal voltage for various load conditions with magnetic saturation and machine temperatures taken into account. This information has been translated into curves of generated voltage versus field current.

A steady-state d-q axis model is used in conjunction with the alternator load current (induction motor input current) to calculate the terminal voltage of the alternator. Figure VI-A-8 shows a curve that is used to account for saturation of the leakage inductance of the main alternator versus the load current. This curve is translated into a lookup table that is interpolated in the model. The d-q axis calculations also provide the value of the demagnetizing component of the load current that is subtracted from the field current to obtain the "effective" field current that is used with the lookup table.

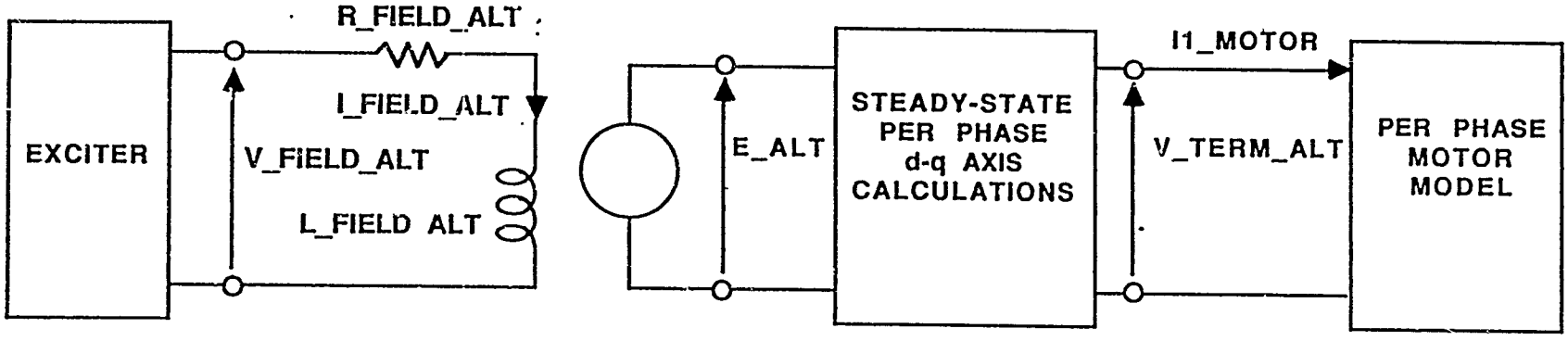




7/227/88/09

Figure VI-A-6. Main Alternator Model

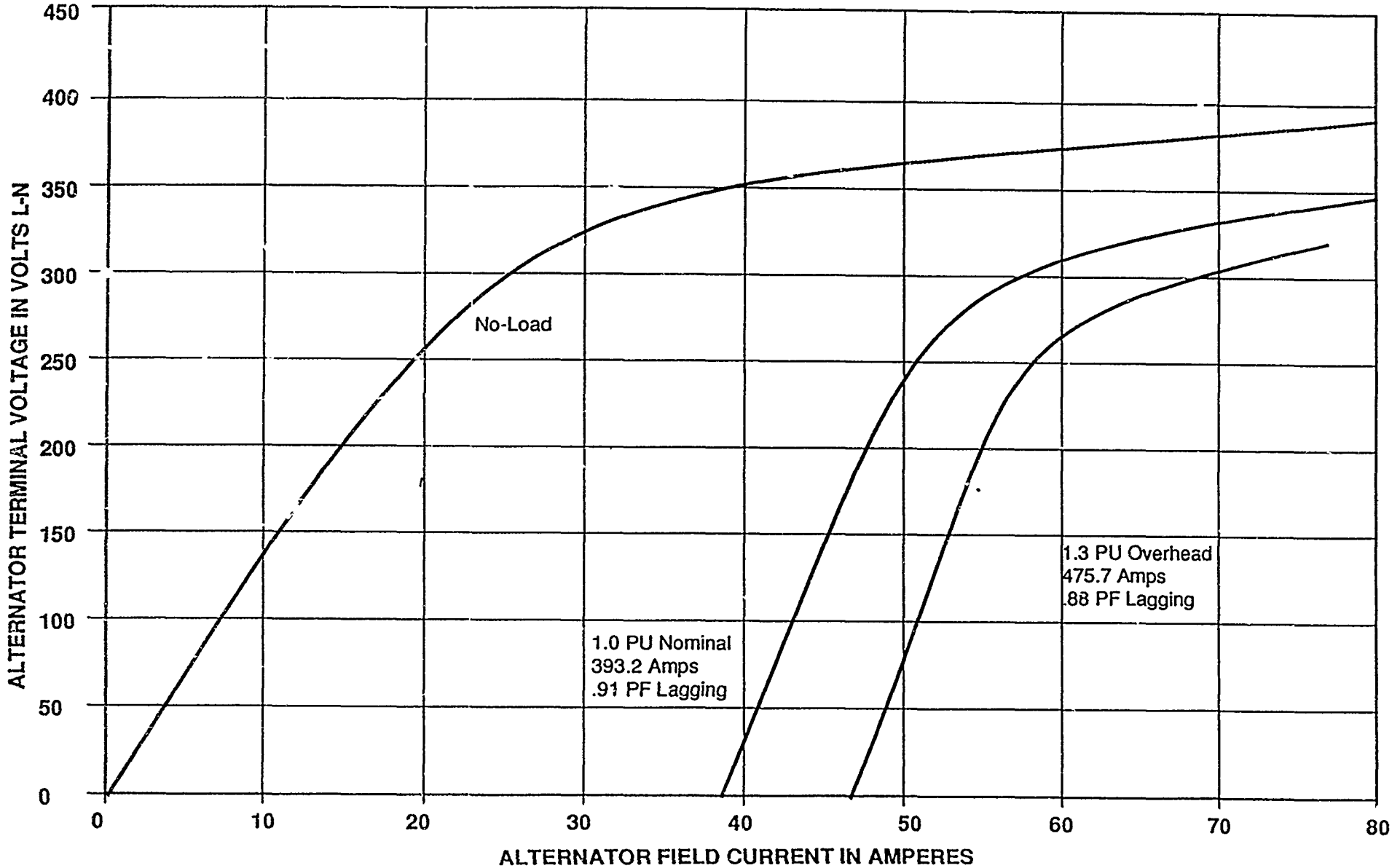


Figure VI-A-7. Load Saturation Curvers for Main Alternator – 9000 RPM

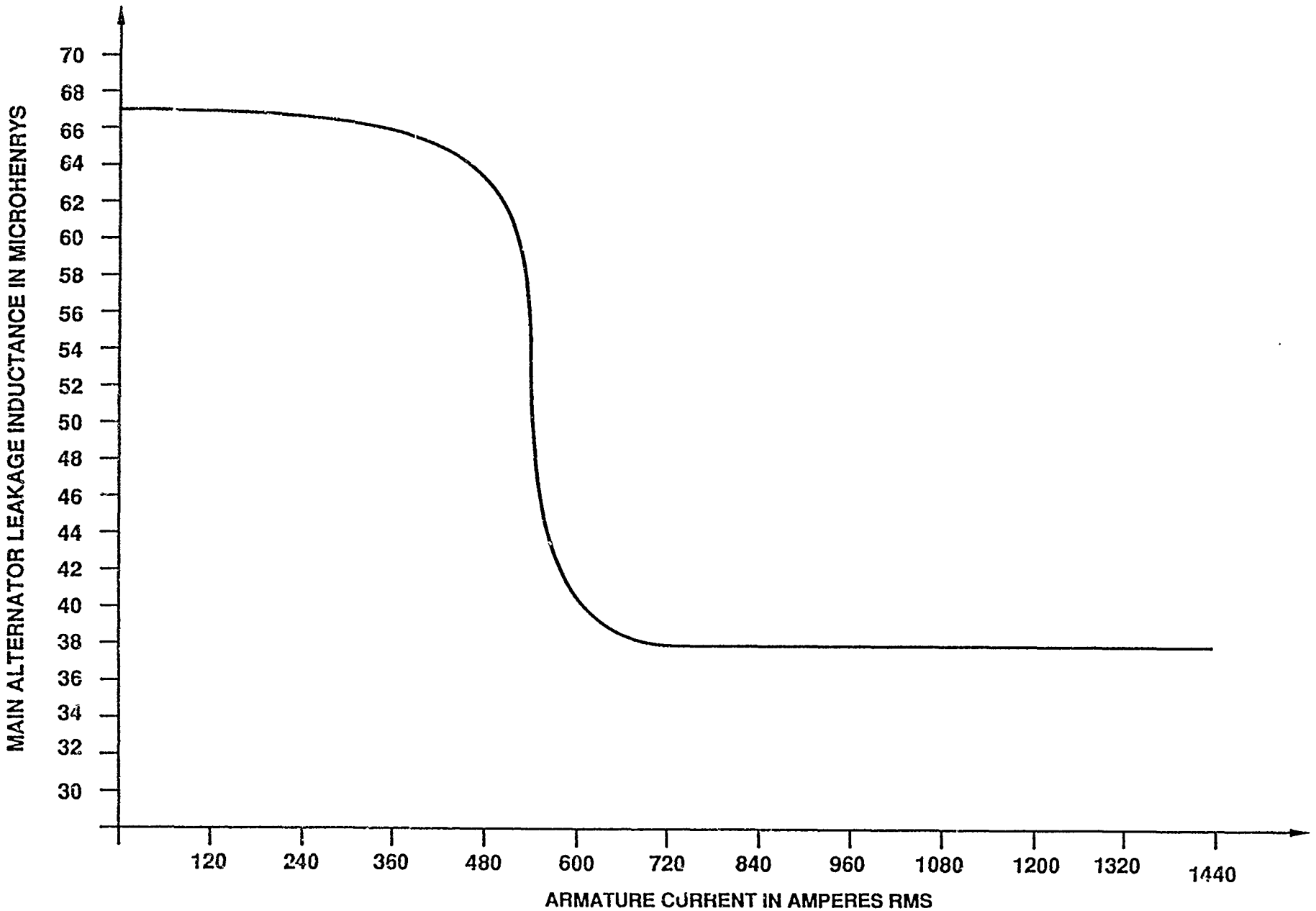




05/20 7/227/88/11

Figure VI-A-8. Main Alternator Leakage Inductance vs. Armature Current

## Induction Motor

Figure VI-A-9 shows the usual steady-state per phase equivalent circuit representation of the induction motor plus the resistance and inductance of the connecting cable from the main alternator to the induction motor.

The induction motor simulation calculations start from an initial value of motor speed which determines the slip at that moment in time. The voltages and currents in the equivalent circuit of the induction motor are calculated for the particular values of terminal voltage of the main alternator and the motor slip.

Figure VI-A-10 shows the magnetic saturation of the magnetizing inductance of the motor versus the value of the volts per hertz at an operating point. Figures VI-A-11 and VI-A-12 show variation of R2_MOTOR and L2_MOTOR versus slip. These curves are used in the model as interpolated lookup tables.

The torque produced in the motor is calculated from the equivalent circuit and is used with the model of the load to calculate the speed of the motor.

## Load

The model of the load is represented by the block diagram of Figure VI-A-13 and the torque versus speed curve of Figure VI-A-14.

In the model, all load effects are referred to the motor side of the speed reduction gear and the combined equivalent friction and moment of inertia values of the motor, reduction gear, and load are treated as parts of the load. The torque versus speed curve of Figure VI-A-14 is represented as torque equals a constant times speed squared. To account for the efficiency of the speed reduction gear, the constant has been chosen so that the nominal steady-state output power of the motor is 310.3 kilowatts (416 horsepower) at an equivalent prime mover speed of 9000 rpm.

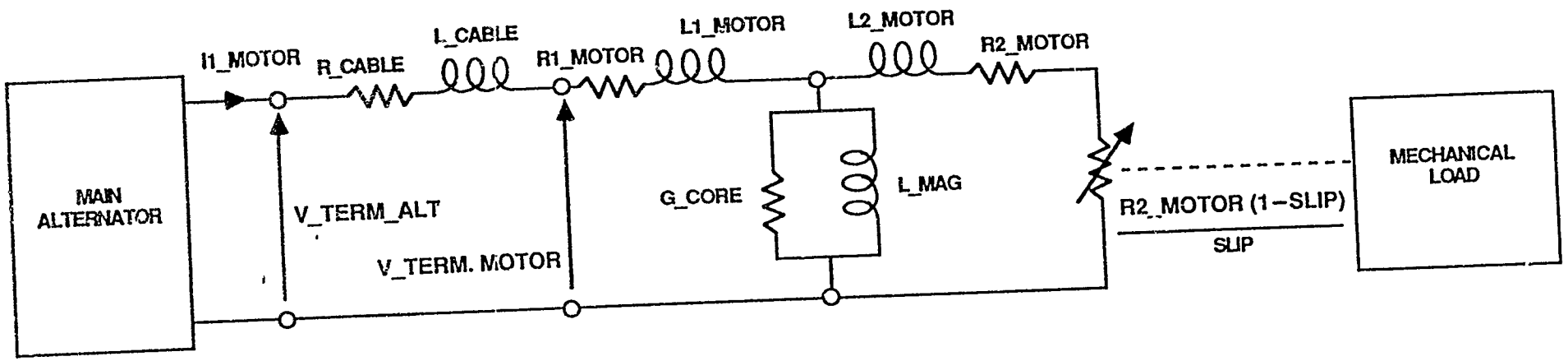


Figure VI-A-9. Induction Motor Model

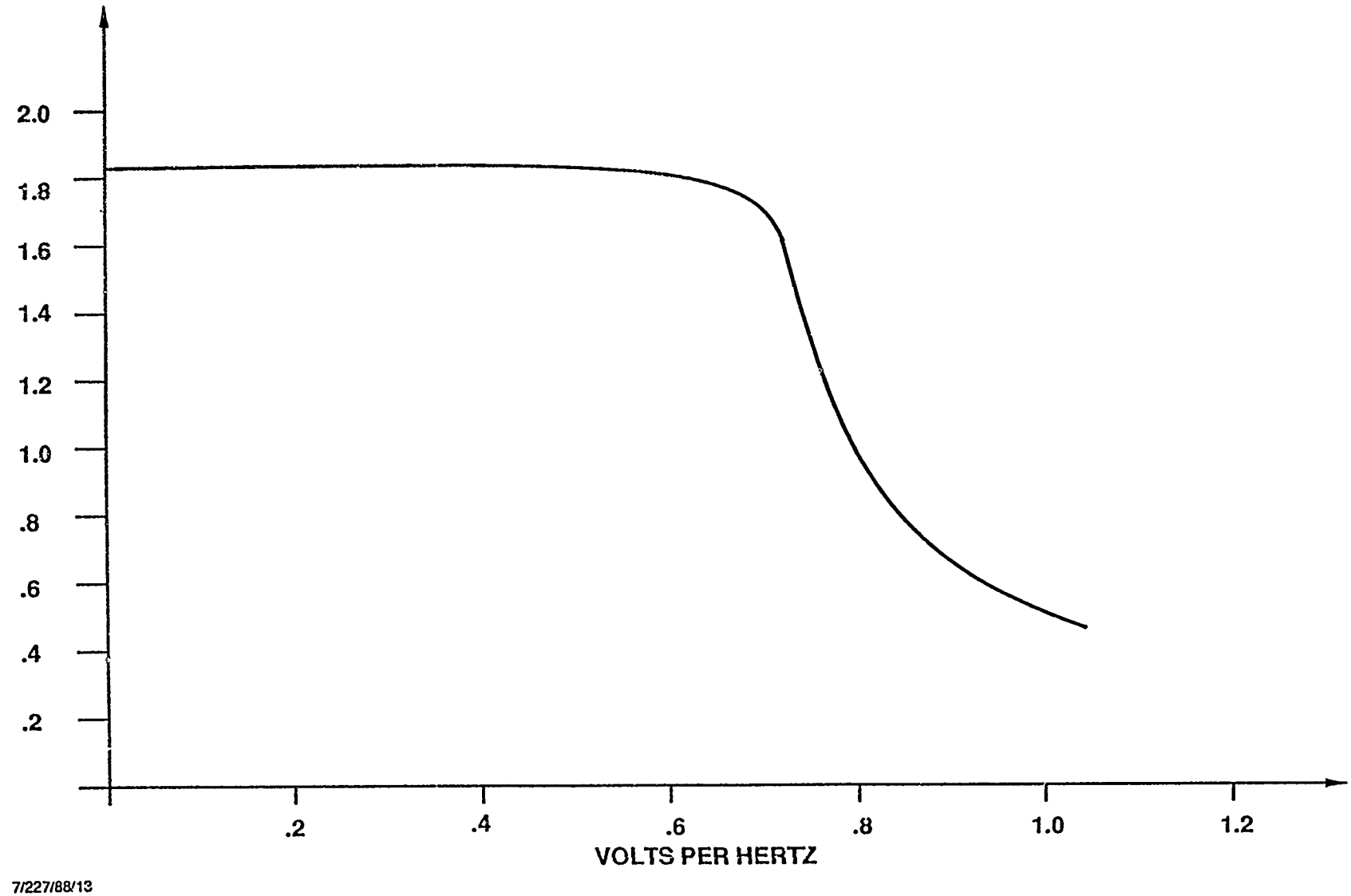


Figure VI-A-10. Motor Magnetizing Inductance vs. Volts Per Hertz

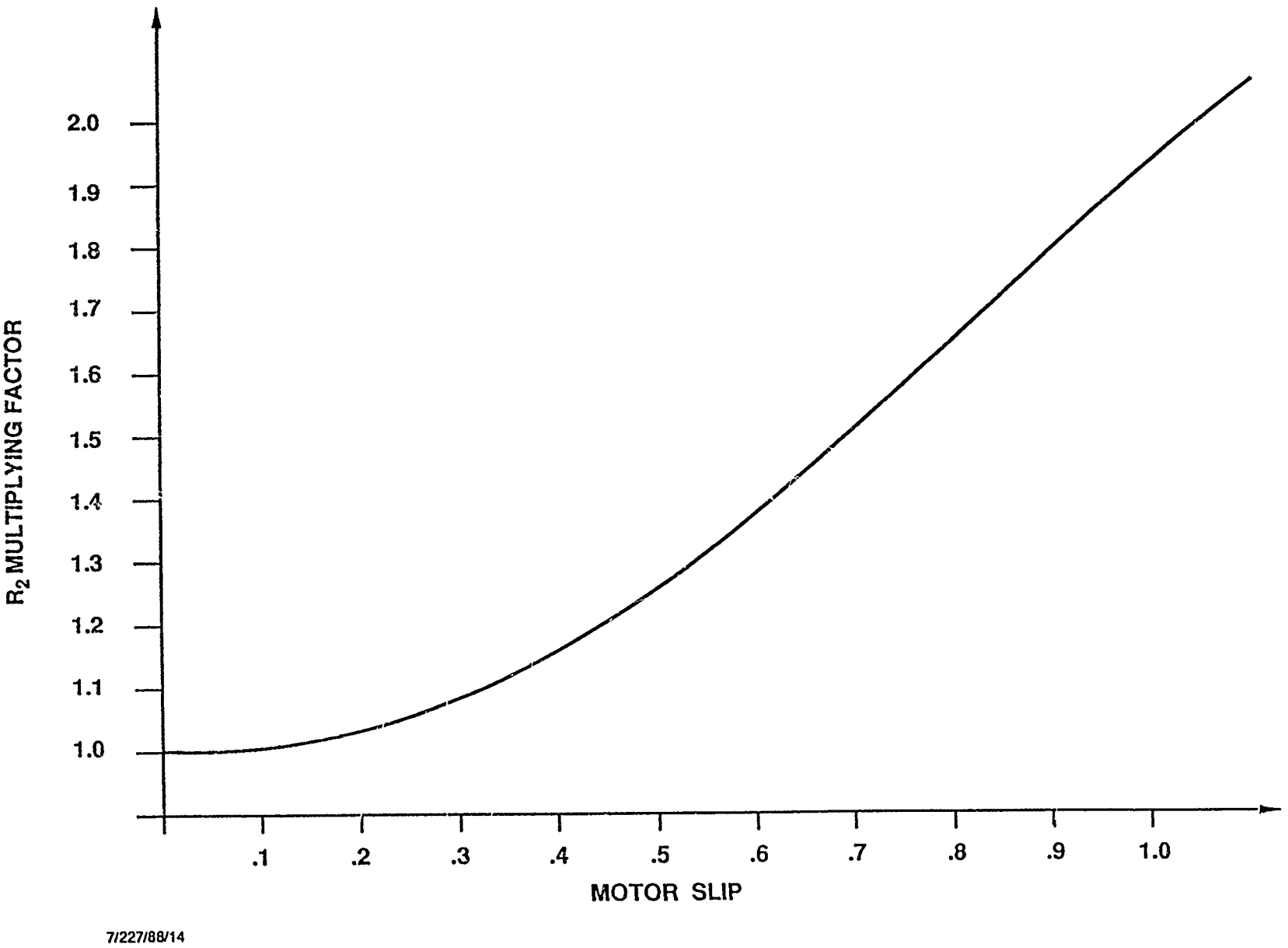


Figure VI-A-11. Motor Rotor Resistance Variation with Slip

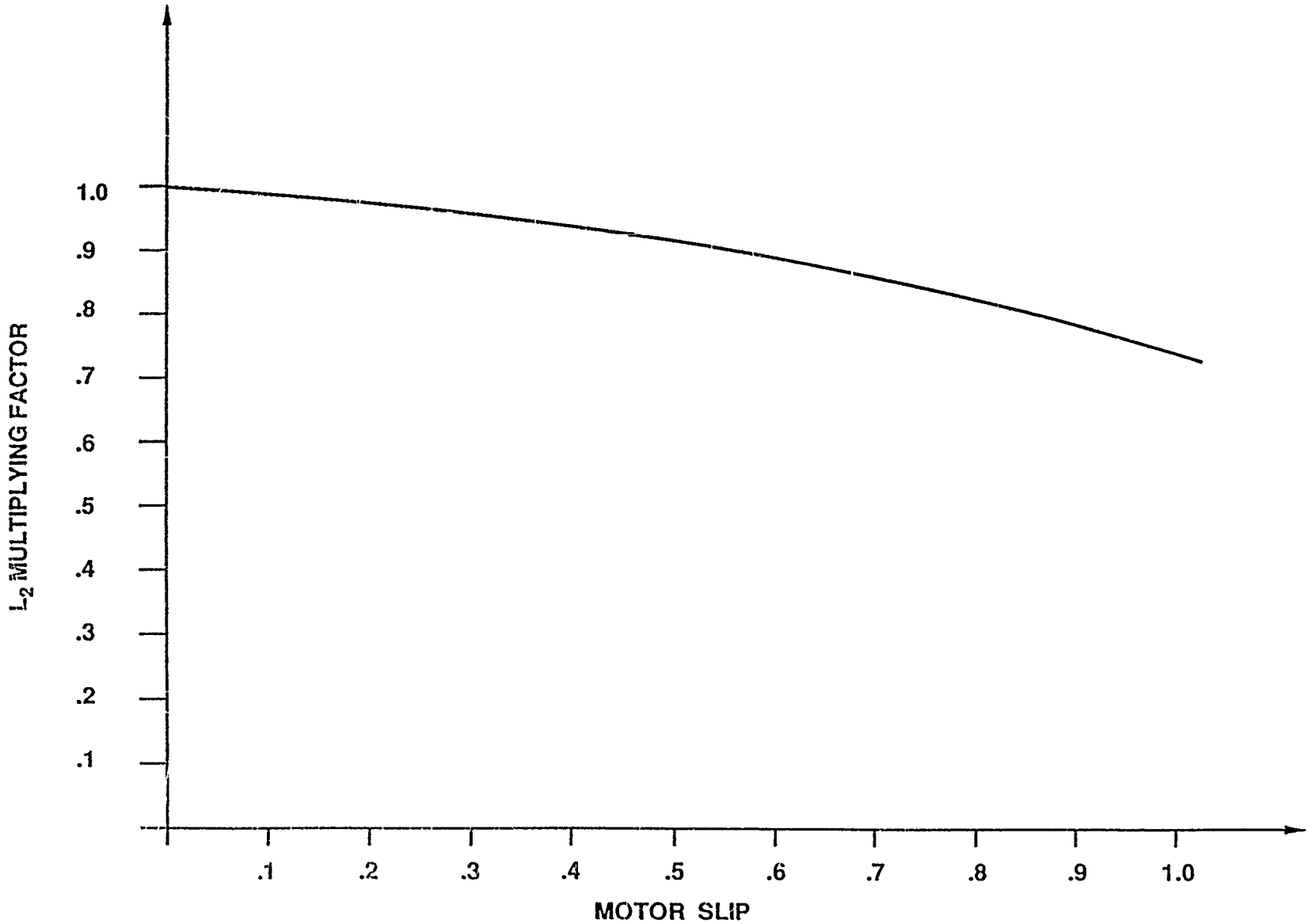


Figure VI-A-12. Motor Rotor Inductance Variation with Slip

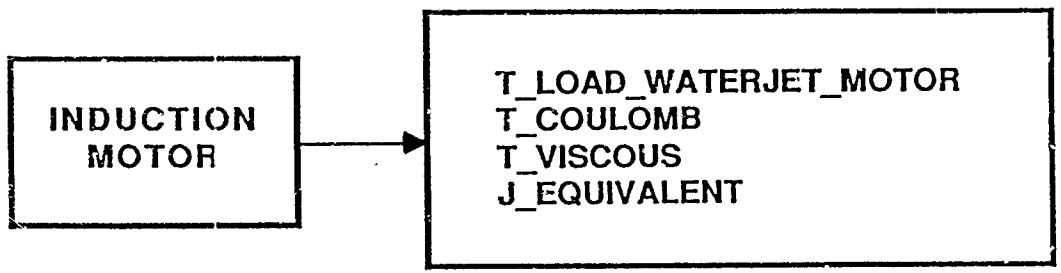




7/227/88/16

Figure VI-A-13. Load Model

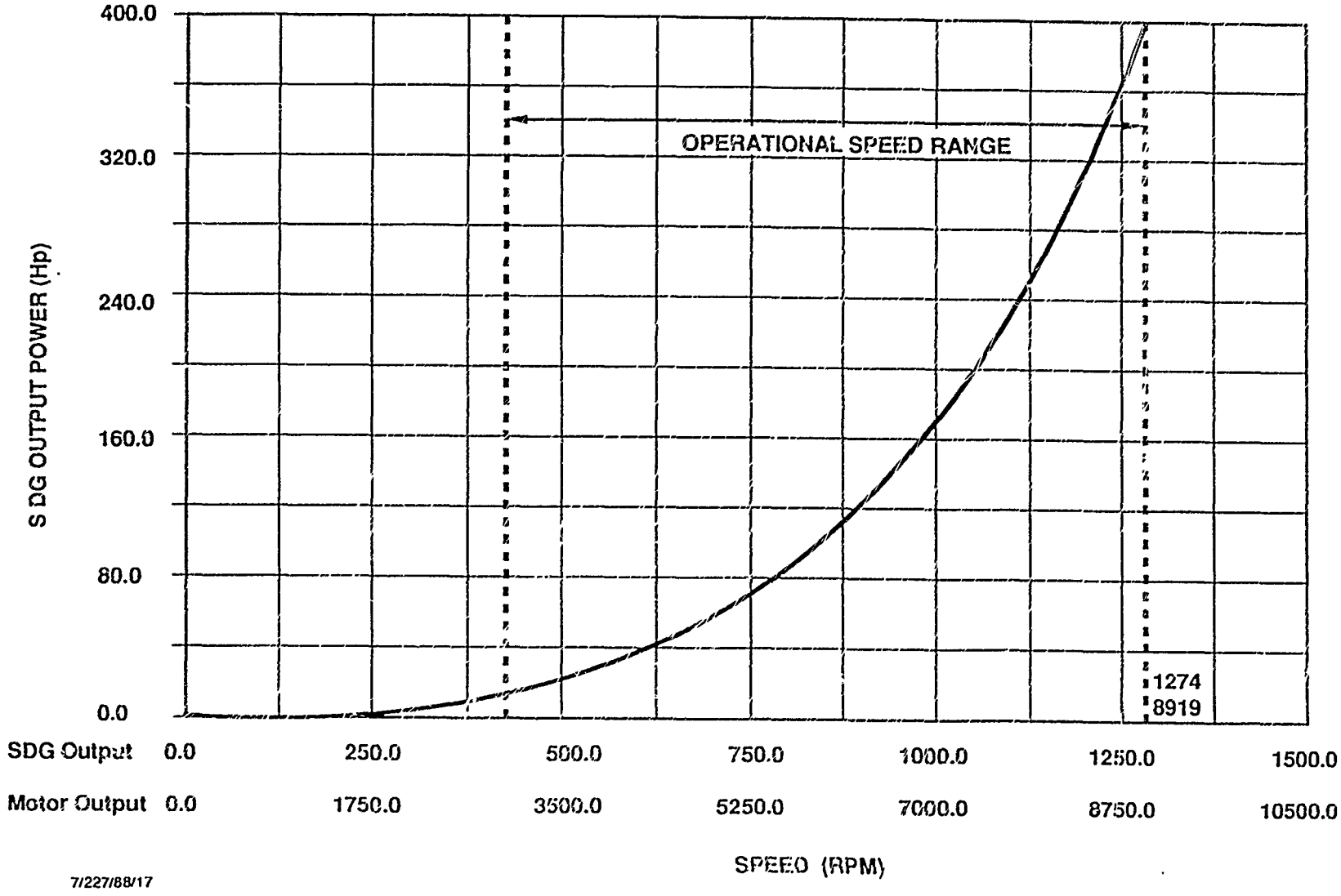


Figure VI-A-14. System Power Versus Speed .

# APPENDIX VI-B

The main body of Appendix VI-B is available on request.

Appendix VI-B contains 56 computer plots of the simulation results that were used to investigate the sensitivity of dynamic performance of the David Taylor amphibious vehicle electric propulsion system to variations of the system parameters. Each plot is 11 x 25 inches.

Curves of the following system variables are shown on each plot :

- PERCENT SLIP
  The percent slip of the propulsion motor with respect to the synchronous speed determined by the main alternator speed.

- TERMINAL VOLTAGE PER PHASE
  The rms line to neutral voltage per phase of the main alternator.

- I FIELD ALTERNATOR
  The current supplied by the exciter to the field winding of the main alternator.

- ALTERNATOR CURRENT
  The rms current per phase supplied by the main alternator to the propulsion motor.

- LOAD TORQUE
  The propellor load torque as seen at the motor.

- MOTOR INTERNAL TORQUE
  The torque developed inside the motor at the airgap; equal to the propellor load torque as seen at the motor plus friction torques plus torque to accelerate the moment of inertia.

- I FIELD EXCITER
  The current supplied by the regulator to the field winding of the exciter.

- V FIELD EXCITER
  The voltage supplied by the regulator to the terminals of the field winding of the exciter.